Jordanides, Niove E. (2008) *Expression and function of drug transporters in primitive CML cells.* PhD thesis.

http://theses.gla.ac.uk/604/

Expression and function of drug transporters

in primitive CML cells

by

Niove E. Jordanides

A thesis submitted for the degree of Doctor of Philosophy to the

University of Glasgow

March 2008

Section of Experimental Haematology and haemopoietic stem

cells

Division of Cancer Sciences and Molecular Pathology

Faculty of Medicine

Abstract

Chronic myeloid leukaemia (CML) is a stem cell (SC) disorder initiated by the reciprocal translocation between chromosome 9 and 22, giving rise to the Philadelphia (Ph) chromosome and the resulting expression of the oncogenic fusion protein BCR-ABL. The current first line of treatment is imatinib mesylate (IM), a tyrosine kinase inhibitor (TKI) that competes with ATP to block ABL kinase activity, which in turn prevents tyrosine phosphorylation of downstream molecules and selectively induces apoptosis of BCR-ABL cells. However, despite excellent cytogenetic responses, only a minority of patients achieve complete molecular response (CMR). We have previously identified a population of quiescent (q) Ph$^+$ SC found in chronic phase (CP) CML that are relatively insensitive to IM and other TKIs and which may be responsible for the molecular persistence of this disease. This population may be insensitive because TKIs do not reach therapeutic concentrations within the cell. Such resistance to classical chemotherapeutic drugs, the phenomenon of multidrug resistance (MDR), is mediated by ABC transporters. In this study we have investigated whether CML SC express the clinically relevant ABC transporters and determine their interaction with TKIs. In addition, we determined whether the inhibition of these transporters increased the efficacy of TKI against CML SC.

Using CML CD34$^+$ cells isolated from newly diagnosed patients, normal CD34$^+$ cells and cell lines transduced with specific transporters as controls, the relative expression of drug transporters were determined in CML CD34$^+$ cells and intracellular staining confirmed protein expression. The interaction of drug transporters with TKIs was assessed using a combination of substrate displacement assays and radiolabelled assays. The effect of transporter inhibitors

with TKIs on the growth and differentiation of q34$^+$ and more mature CD34$^+$ cells from CML patients in CP were assessed with regard to cell division, apoptosis and BCR-ABL kinase activity.

When compared to normal CD34$^+$ cells, CML CD34$^+$ cells over-expressed *ABCG2* mRNA. In contrast *MDR1* expression was reduced in CML CD34$^+$ cells and *MRP1* was detected at similar expression levels in both populations. All three drug transporters were expressed at the protein levels in CML CD34$^+$ cells. It was determined that at therapeutic concentrations (5µM) IM and nilotinib both inhibited ABCG2 and MDR1 and nilotinib also inhibited MRP1. Neither drug was a substrate for any of the transporters. In contrast, dasatinib was shown to be a substrate for ABCG2 and MRP1, but had no effect on MDR1. Therefore activity and concentration of dasatinib but not IM or nilotinib may be altered by the activity of these proteins. In keeping with their inhibitory activity, neither IM nor nilotinib demonstrated significantly increased efficacy when combined with specific ABC transporter inhibitors (FTC or PSC 833). Surprisingly, although dasatinib was a substrate for ABCG2 and MRP1, dasatinib did not further increase apoptosis, or reduce the qSC population.

Therefore, although MDR1, MRP1 and ABCG2 were found to be expressed and functional in CML CD34$^+$ cells and to interact with TKI, the co-treatment of TKIs with drug transporter inhibitors did not further increase apoptosis, reduce BCR-ABL kinase activity or reduce the qSC population. Therefore, modulation of individual transporter activity is unlikely to reverse the resistance of this population of cells to TKI and will not improve the clinical response to these drugs.

Table of Contents

List of Tables

List of Figures

Related Publications

Copland M, Hamilton A, Elrick LJ, Baird JW, Alllan EK, **Jordanides N**, Barow M, Mountford JC, Holyoake TL. Dasatinib (BMS-354825) targets an earlier progenitor population than imatinib in primary CML but does not eliminate the quiescent fraction. *Blood*, 2006; 107(11), 4532-9.

Jordanides N, Jørgensen HG, Holyoake TL, Mountford JC. Functional ABCG2 is over-expressed on primary CML CD34$^+$ cells and is inhibited by imatinib mesylate. *Blood*, 2006; 108(4), 1370-3.

Jørgensen HG, Alllan EK, **Jordanides NE**, Mountford JC Holyoake TL. Nilotinib exerts equipotent anti-proliferative effects to imatinib and does not induce apoptosis in CD34$^+$ CML cells. *Blood*. 2007 May 1;109(9):4016-9. Epub 2007 Jan 9.

In preparation

N.E Jordanides, H.G Jørgensen, T.L Holyoake, J. C Mountford. Efflux transporters limit the concentration of new generation tyrosine kinase inhibitor dasatinib, yet modulation of these transporters does not reverse the resistance in CML CD34$^+$ cells. *In preparation*

J. C Mountford*, N.E Jordanides*, A. Davies*, A. Giannoudis, S. Hatziieremia, H.G Jørgensen, T.L Holyoake, M. Pirmohamed, R.E Clark. Nilotinib concentration in CML CD34$^+$ cells is not mediated by active uptake or efflux by major drug transporters. *In preparation*

N.E Jordanides, S. Hatziieremia, T.L Holyoake, J. C Mountford. Drug transporters do not mediate the resistance of Imatinib in CML CD34+ cells. *In preparation*

Acknowledgements

I would like to thank a number of people who, without their help, would have made this undertaking far more arduous. Firstly, I am indebted to my supervisors Jo Mountford and Tessa Holyoake, who have given me invaluable guidance and encouragement both during and prior to the PhD. I would also like to thank all my colleagues at the lab who have helped to make this experience enjoyable. Special thanks to Nick for making the "admin" days fun.

I would especially like to thank my family who have also experienced the trials and tribulations of the PhD with me and gave me the confidence to succeed. I promise, no more studying! Finally, I would like to give a special thanks to Mr. Rodney Uppamoon, for his constant support and encouragement.

Author's Declaration

Unless otherwise stated, I declare that all the work presented in this thesis is my own.

Definitions and Abbreviations

^{3}H	Tritiated
^{14}C	Carbonated
5GF	Serum free medium supplemented with a 5 growth factor cocktail
aa	Amino acid
ABC	ATP binding cassette
ABCG2	ATP binding cassette subfamily member 2 protein
ABL	Abelson proto-oncogene
AML	Acute myeloid leukaemia
AP	Accelerated phase
APML	Acute promyelocytic leukaemia
Ara-C	Cytosine arabinoside
ATP	Adenine tri-phosphate
BC	Blast crisis
BCR	Breakpoint-cluster region gene
BCR-ABL	The breakpoint cluster region-abelson protein tyrosine kinase
BCR-ABL	The BCR-ABL fusion gene
BCRP	Breast cancer related protein (ABCG2)
BIT	Bovine serum albumin/insulin/transferrin
BM	Bone marrow
BSA	Bovine serum albumin
°C	Degrees centigrade
CCR	Complete cytogenetic remission
cDNA	Complimentary DNA
CFC	Colony forming cell
CFSE	Carboxy-fluorescein diacetate succinimidyl ester
CHR	Complete haematological response
CLP	Common lymphoid progenitor
CML	Chronic myeloid leukaemia
CMP	Common myeloid progenitor
CMR	Complete molecular response
CP	Chronic phase
CrkL	CT10 regulator of kinase-like protein
CSC	Cancer stem cell
Das	Dasatinib
dH$_2$0	Distilled water
DMEM	Dulbecco's modified eagle's medium
DMSO	Di-methyl sulphoxide
DNA	Deoxyribonucleic acid
EDTA	Ethylenediamine tetra-acetic acid
FACS	Fluorescence-assisted cell sorting
FCS	Foetal calf serum
FISH	Fluorescence *in situ* hybridisation
FITC	Fluoroscein isothiocyanate
FL	Fluorescence channel
FSC	Forward Scatter
FTC	Fumitremorgin-C
FTI	Farnesyl transferase inhibitor
G$_0$	Gap-phase 0 (of cell cycle)
G$_1$	Gap-phase 1 (of cell cycle)

GAPDH	Glyceraldehyde-3-phosphate dehydrogenase
G-CSF	Granulocyte-colony stimulating factor
GM	Geometric mean
GM-CSF	Granulocyte macrophage-colony stimulating factor
hr(s)	Hour(s)
HSC	Haemopoietic stem cell
HSA	Human serum albumin
Hst	Hoechst 33342
IC_{50}	Inhibitory concentration $_{50}$
IFNα	Interferon α
IM	Imatinib mesylate
IMDM	Iscove's modified dulbecco's medium
IRIS	International study of interferon versus STI571
JAK	Janus kinase
kD	kilodalton
LDL	Low density lipoprotein
lin$^-$	Lineage negative
LSC	Leukaemic stem cell
LTC-IC	Long term culture-initiating cell assay
LT-HSC	Long-term HSC
M	Molar concentration
MDR	Multidrug Resistance protein
MDR1	Multidrug resistance 1 protein
min(s)	minute(s)
ml	Milliliter
MCR	Major cytogenetic response
MNC	Mononuclear cell
mPB	Mobilised peripheral blood
MRD	Minimal residual disease
mRNA	messenger ribonucleic acid
MRP1	Multidrug resistance-associated protein
MW	Molecular weight
µCi	Micro curie
µg	Micrograms
µl	Microlitre
µM	Micromolar
nd	Not determined
ng	Nanogram
NOD-SCID	Non obese-severe combined immunodeficiency
ns	Not significant
p	Phosphorylated
PB	Peripheral blood
PBS	Phosphate buffered saline
PCR	Polymerase Chain Reaction
PE	Phycoerythrin
Ph	Philadelphia Chromosome
PI	Propidium Iodide
Py	Pyronin
q	Quiescent
qPCR	Quantitative PCR
RT-PCR	Real Time RT-PCR
rHu-G-CSF	Recombinant Human Granulocyte Colony Stimulating Factor

RNA	Ribonucleic acid
rpm	Revolutions per minute
RT	Room Temperature
RT-PCR	Reverse Transcriptase Polymerase Chain Reaction
SC	Stem cell
SCF	Stem cell factor
SDS	Sodium Dodecyl Sulphate
SD	Standard deviation
S.E	Standard Error
SFM	Serum free medium
SL-IC	SCID leukaemia intiating cell
SNBTS	Scottish National Blood Transfusion Service
SP	Side Population
SSC	Side Scatter
ST-HSC	Short-term HSC
TKI	Tyrosine Kinase Inhibitor
UCB	Umbilical Cord Blood
WBC	White Blood Cell
WT	Wild type

1 Introduction

1.1 Normal haemopoietic stem cell (HSC) and haemopoiesis

Haemopoiesis is a carefully regulated process which results in the production of $\sim 10^{11}$ erythrocytes, leukocytes and platelets each day. All of the formed blood cell lineages arise from a multi-potent HSC population, which may differentiate through a series of intermediate lineage, committed progenitor cells.

The HSC is a rare cell located in the bone marrow (BM). Based on limiting dilution studies in non-obese diabetic-severe combined immune deficient (NOD-SCID) mice, it has been estimated that there are approximately 3×10^6 HSCs in humans (Wang *et al.* 1997). The HSC has two key identifying properties; its ability to differentiate into multiple cell types and to self-renew (Shizuru *et al.* 2005). Self-renewal may be symmetrical, resulting in two daughter HSCs, or asymmetrical, producing an identical copy of itself and a downstream progenitor. Studies carried out on mouse BM cells have identified three distinct HSC populations that constitute 0.05% of mouse BM cells; long-term HSCs (LT-HSC) which are capable of indefinite self-renewal, short-term HSCs (ST-HSC) which have a limited time span for self-renewal, and multi-potent progenitors that have little or no detectable self-renewal capacity (Morrison *et al.* 1997). These populations form a hierarchy in which the LT-HSC gives rise to ST-HSC, which forms the multi-potent progenitor, which then leads to either a lymphoid or myeloid lineage progenitor (Figure 1-1).
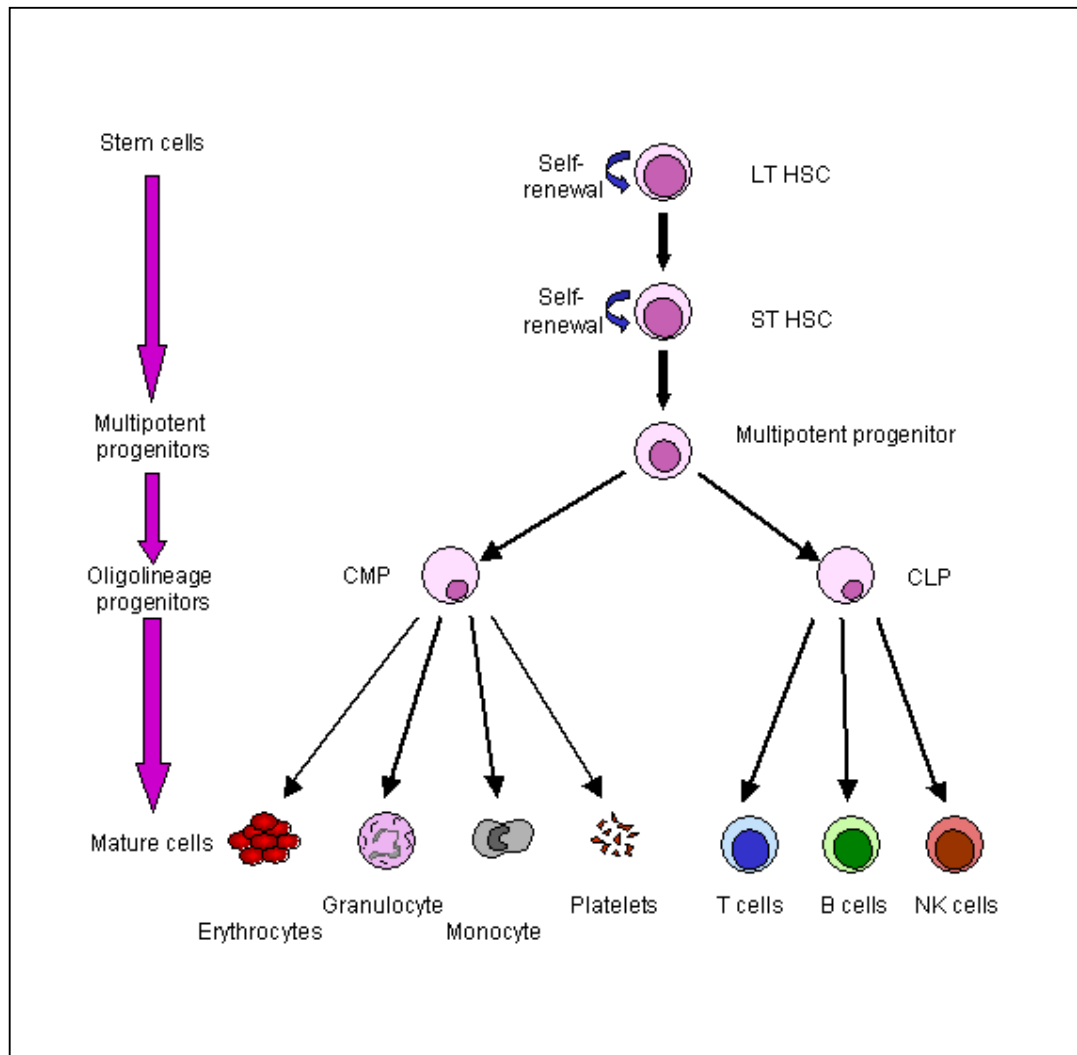
Figure 1-1 Schematic diagram of the haemopoietic cell hierarchy

Only LT-HSC and ST-HSC have the capacity for self-renewal, which is lost once the cell has become a multi-potent progenitor. These give rise to the CLP and CMP, which undergo several proliferation and differentiation steps to give rise to mature, terminally differentiated progeny. [LT- long term, ST- short term, HSC- haemopoietic stem cell, CMP- common myeloid progenitor, CLP- common lymphoid progenitor]

For clinical and laboratory purposes, HSCs may be isolated by immunophenotyping using CD34, a surface glycoprotein involved in cell adhesion, as the surrogate marker (Berenson *et al.* 1988). However, the isolated CD34$^+$ population is heterogeneous and only a small minority are true HSCs with multi-lineage potential that have indefinite self-renewal. These are characterised as

CD34$^+$/lin$^-$/38$^{low/-}$ (Miller *et al.* 1999) and are predominantly in the quiescent state (i.e. in G$_0$), maintained so by their microenvironment. Another method for obtaining enriched HSC populations is by exploiting their ability to efflux Hoechst 33342 (Hst). Goodell *et al* (Goodell *et al.* 1997) identified the small side population (SP) of cells that are Hst low which have the same immature phenotype as the HSC. *In vitro* studies of these primitive cells however, are difficult due to their rarity but also due to the unclear mechanism of self-renewal and differentiation which, in culture conditions, results in loss of stem cell phenotype with the acquisition of lineage-specific markers (Weissman 2000).

1.2 Cancer stem cell (CSC)

The original hypothesis, known as the "clonal genetic model", defined cancer as a proliferative disease that originated from mutated tumour cells that contributed equally to the tumourigenic activity. However, the identification of normal HSCs and an improved understanding of haemopoiesis, led to the suggestion that the cancer cells may be organised as a similar hierarchy, with tumours originating from a rare population of functionally distinct CSC. The first definitive evidence for the CSC hypothesis and the identification of the leukaemic stem cell (LSC) was reported by Bonnet and Dick (Bonnet and Dick 1997). They found that only a small defined subset of cells were capable of initiating acute myeloid leukaemia (AML) in NOD-SCID mice. These cells, termed SL-IC (SCID leukaemia-initiating cell) were identified as CD34$^+$CD38$^-$, which confirmed that primitive cells rather than committed progenitor cells represented the cell of origin for leukaemic transformation (Bonnet and Dick 1997).

To date, the origin of LSCs is controversial (Figure 1-2). One view is that the LSCs are HSCs that have become leukaemic as a result of accumulated mutations. The reasoning for this theory is that as HSCs already possess the machinery for self-renewal as well as various developmental pathways, they may require fewer mutations to maintain the ability for self-renewal than the activation of these pathways in a more differentiated cell. Secondly, the nature of HSCs to persist for long periods of time increases the opportunity for mutations to accumulate in these stem cells (as shown by the atomic bomb survivors who developed cancer several years post exposure). Evidence for this view is supported by the cells with the CD34$^+$CD38$^-$ phenotype which resembles that of the normal HSC, initiating most AML subtypes in NOD/SCID mice (Bonnet and Dick 1997).

In contrast, LSCs may also be a more restricted or differentiated mature cell that has transformed and acquired the stem cell capability of self-renewal. Cozzio *et al* (Cozzio *et al.* 2003) demonstrated that retroviral transduction of the potent leukaemic fusion gene *MLL-ENL* can give rise to self-renewal properties in the CMP and induce AML when transplanted into irradiated mice. Similarly, progenitors transduced with *MOZ-TIF2* resulted in leukaemia, yet in contrast progenitors transduced with *BCR-ABL* did not (Huntly *et al.* 2004). This suggests that only some leukaemia oncogenes can confer self-renewing properties to haemopoietic progenitors.

Following documentation of the LSC, recent studies have now suggested that the CSC concept may also be relevant in solid tumours. Similar to the study by Bonnet and Dick (Bonnet and Dick 1997), breast cancer in NOD-SCID mice was initiated by the isolation of a phenotypically distinct subset of breast cancer cells (Al-Hajj *et*

al. 2003) and brain cancer stem cells were able to generate new tumours *in vivo*

(Singh *et al.* 2004); this field is ever expanding.
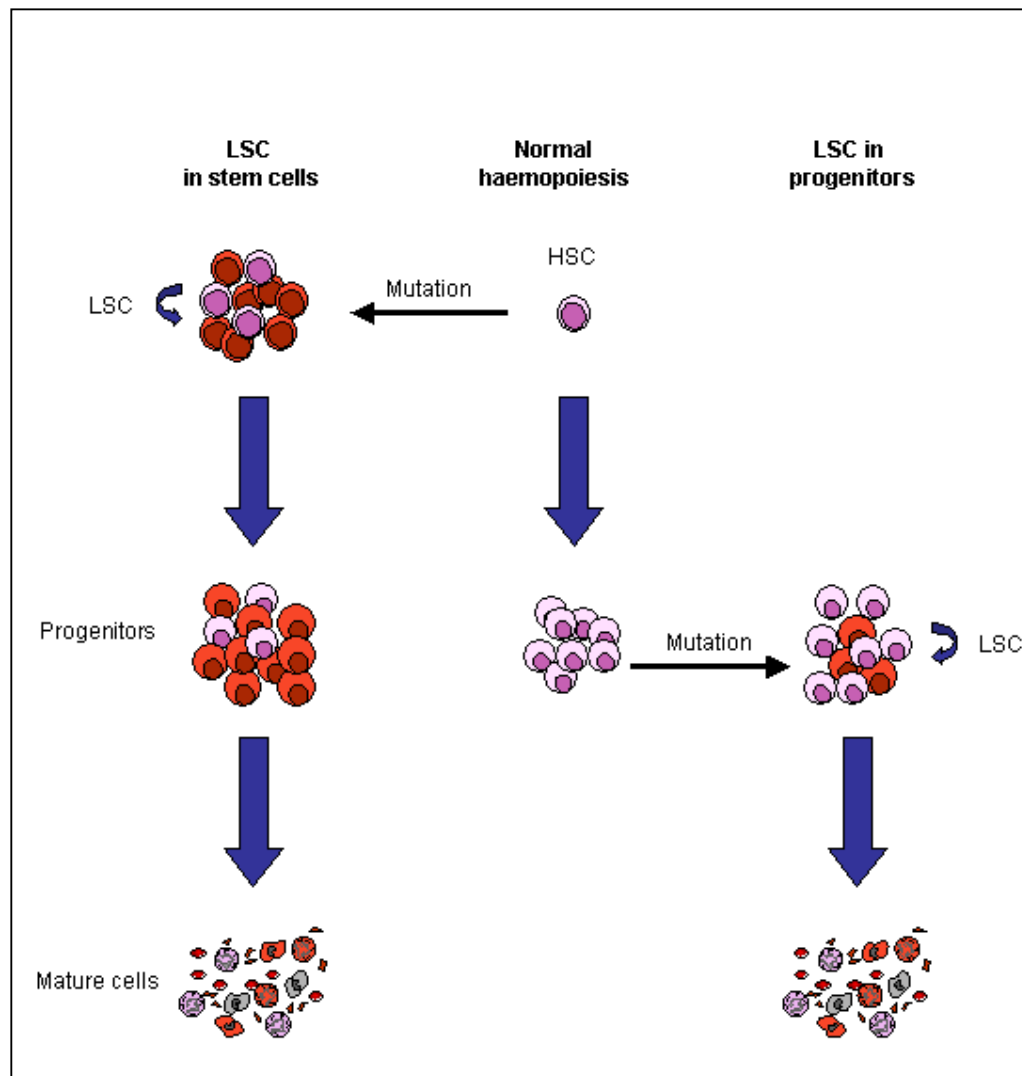
Figure 1-2 Origin of LSC

The LSC may arise by transformation events occurring in the HSC which disrupts the normal development and gives rise to the self-renewing LSC. In contrast the transformation may occur in the restricted progenitors. The mutations in these cells must reactivate the self-renewal properties in order to generate the LSC. [LSC-leukaemic stem cell, HSC-haemopoietic stem cell]

1.3 Chronic myeloid leukaemia (CML)

One disease that has been established as a CSC driven disease is CML. CML is a clonal myeloproliferative disorder that is initiated by the reciprocal translocation between the 3' end of the *C-ABL* (Abelson) gene from chromosome 9 and the 3' end of the *BCR* (Breakpoint Cluster Region) gene on chromosome 22 (t(9;22)(q34;q11)), giving rise to the abnormally small chromosome 22 (also termed Philadelphia (Ph) chromosome, named so after the city in which it was discovered) (Rowley 1973). The molecular consequence of this translocation is the expression of the fusion gene *BCR-ABL*. Depending upon the site of the breakpoint in BCR, two fusion proteins can be produced, one of 185kD (p185, seen in B cell-acute lymphoblastic leukaemia (B-ALL) and one of 210kD (p210). The latter constitutively active tyrosine kinase oncoprotein is seen in >95% of patients with CML (Druker *et al.* 2001).

CML accounts for 15-20% of all leukaemias in adults with an incidence of approximately 1 in 100,000. CML may be diagnosed in all age groups, although the median age of onset is 40-60 years, with a slight male predominance of 1.4:1 (Faderl *et al.* 1999). The principal cause is unclear, although there is a clear link with exposure to ionising radiation, as demonstrated by the atomic bomb survivors. CML typically has three clinical stages, presenting in an initial chronic phase (CP), progressing to accelerated phase (AP) and reaching blast crisis (BC) in typically 3-5 years, although in some cases the CP transforms rapidly to BC. In over 90% of cases, CML is diagnosed in CP and is characterised by an abnormally high white blood cell count consisting mainly of mature and immature myeloid cells, increased megakaryocytes in BM and splenomegaly (Sawyers 1999). Detection of the Ph chromosome by cytogenetic analysis of BM cells,

however, continues to be the basis upon which CML is diagnosed. In many clinical centres, the development of highly sensitive quantitative PCR to detect *BCR-ABL* transcripts has become a valuable tool for monitoring responses to therapy (Lion *et al.* 1995). As the disease progresses, additional cytogenetic abnormalities arise. During AP there is an increase in immature cells with additional cytogenetic abnormalities and BC behaves like an acute leukaemia with a very poor prognosis.

1.3.1 Role of BCR, ABL and the fusion protein BCR-ABL

The proteins ABL1 and BCR are ubiquitously expressed in non-malignant cells and have many cellular regulatory functions (Laneuville 1995). BCR can modulate actin polymerisation through RAC (Diekmann *et al.* 1991), activate NF-κB (Montaner *et al.* 1998) and may influence the RAS pathway through interaction with the growth factor binding protein 2 (GRB2) (Goga *et al.* 1995; Ma *et al.* 1997). ABL1 protein is predominately nuclear, although it may also be present in the cytoplasm and modulates both cell cycle regulation and response to integrin signalling (Van Etten 1999). ABL1 also forms complexes with GRB2 and the CT10 regulator of kinase-like (CrkL) protein.

The role of BCR-ABL in the pathogenesis of CML was established in 1990, when murine BM cells transfected with the p210 oncoprotein (p210$^{\text{BCR-ABL}}$) were transplanted into irradiated recipients, causing them to develop a myeloproliferative disorder closely resembling CML (Daley *et al.* 1990). However, although necessary, BCR-ABL alone may not be sufficient to cause CML as low *BCR-ABL* transcripts have also been detected in the blood of healthy individuals, suggesting that other factors may contribute to the transformation of this disease (Biernaux *et al.* 1995; Bose *et al.* 1998).

A consequence of BCR-ABL however, is an increase in cell proliferation. Initially it was assumed this was due to the most mature proliferating cells in CP CML causing the expansion of Ph$^+$ cells, known as the "discordant maturation hypothesis". However, this was refuted with further studies demonstrating that the myeloid expansion is a result of increased numbers of primitive CML progenitor cells (Marley *et al.* 1996). Holyoake *et al* (Holyoake *et al.* 1999) have also demonstrated deregulated mechanisms in the quiescent population leading to an increase in cell cycling and contributing to increased proliferation.

BCR-ABL is exclusively localised to the cytoplasm (in contrast to ABL which shuttles between the nucleus and cytoplasm), resulting in the constitutive phosphorylation of several substrates and activation of a range of cytoplasmic and nuclear transduction pathways. The substrates include adaptor molecules such as CrkL (Oda *et al.* 1994; Sattler *et al.* 1996) and GRB2 (Pendergast *et al.* 1993), adhesion proteins and proteins with catalytic function (such as Ras-GAP). These in turn activate many pathways that regulate cell proliferation and apoptosis (Figure 1-3).

The anti-apoptotic phosphatidylinositol-3 kinase (PI3 kinase) pathway is activated when it forms a complex with BCR-ABL, Cbl and the adaptor molecules Crk and CrkL (Sattler and Salgia 1998). This in turn activates the downstream effector AKT kinase, which exerts its anti-apoptotic effects through phosphorylation of downstream target molecules. AKT can then phosphorylate IkB kinase, inducing the degradation of NF-κB inhibitor IkB. The released NF-κB then translocates to the nucleus allowing proliferation, inhibition of apoptosis and control of differentiation. In addition AKT can also phosphorylate BAD, which is a pro-apoptotic member of the BCL-2 family that binds to BCL$_{xL}$, inhibiting its function.

Phosphorylation of BAD by AKT releases BCL_{xL} to bind to BAX and hence neutralises the pro-apoptotic effects of BAX.
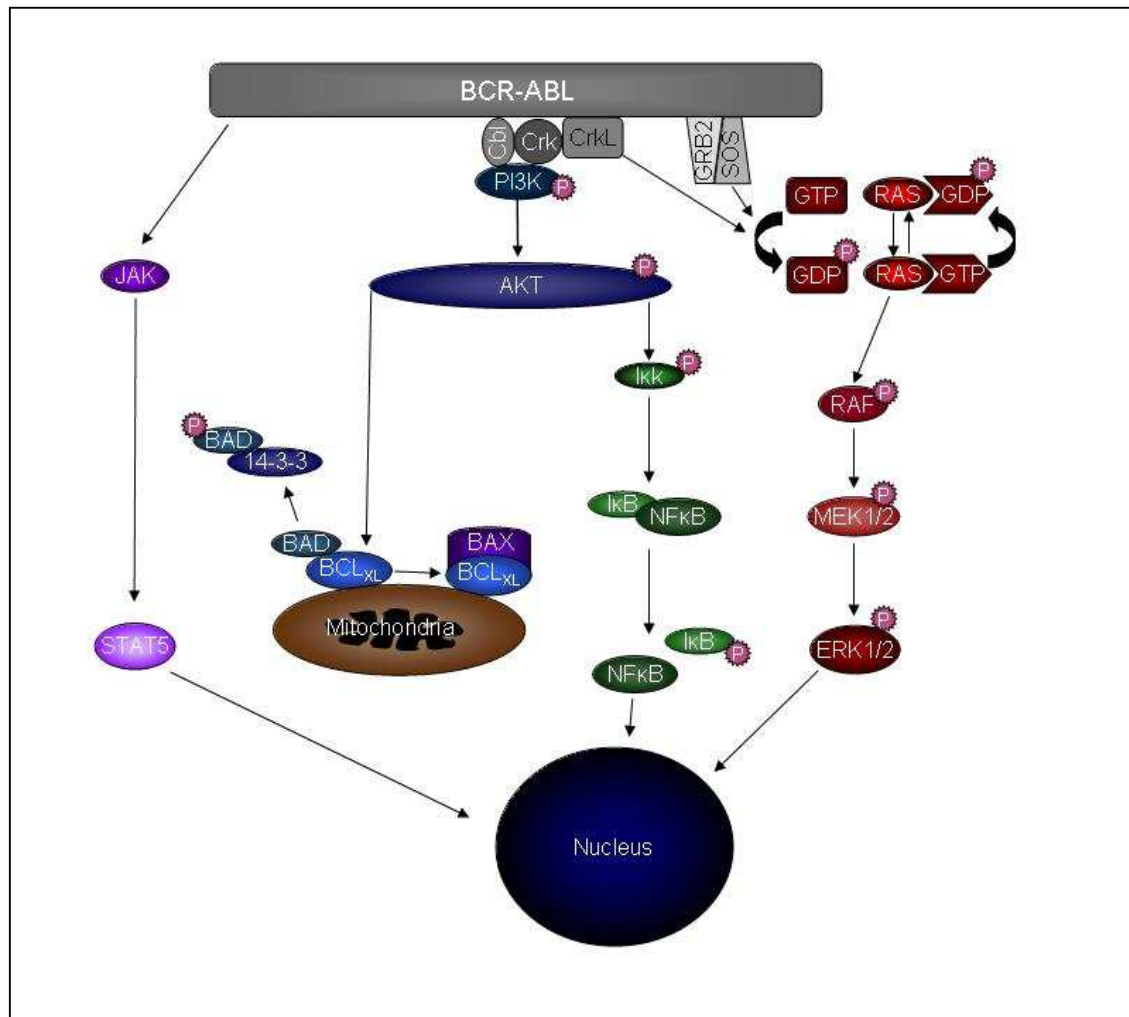
Figure 1-3 Schematic diagram of the main signalling pathways activated by BCR-ABL in CML cells

In normal HSCs, these pathways are normally activated by cytokines, promoting survival, differentiation and proliferation. In the absence of growth factors, BCR-ABL can bypass this requirement activating these pathways and prolonging survival by inhibiting apoptosis. The phosphorylation of substrates such as CrkL activates many pathways that regulate cell proliferation and promote cell survival. Indeed, the constitutive phosphorylation of CrkL may be used as a surrogate marker of BCR-ABL activity in the laboratory. Phosphorylation of AKT leads to cell survival. The phosphorylation of IκK results in the phosphorylation and degradation of IκB, releasing NF-κB to translocate to the nucleus where it can exert its anti-apoptotic and proliferative effect. Similarly BAD is phosphoryated to allow BCL_{XL} to bind to BAX, neutralising its pro-apoptotic effect. BCR-ABL also stabilises RAS in the active form, activating the RAF-MEK-ERK cascade pathway, resulting in transcriptional regulation.

Autophosphorylation of the BCR-ABL oncogene also leads to the constitutive activation of the RAS pathway via interaction with the small adapter protein GRB2 (Ma *et al.* 1997). RAS are a group of guanine nucleotide proteins (G-proteins) that can transduce external signals to transcription factors in the nucleus. Activation of RAS is achieved by farnesylation of RAS in the cytoplasm. Farnesylated RAS then translocates to the cell membrane and interacts with regulatory proteins, maintaining a balance between the active and inactive form of RAS. However, the association of BCR-ABL with the GRB2/SOS complex (son of sevenless) retains RAS in the active form. This results in stimulation of the RAF-MEK-ERK effector pathway and subsequent transcriptional control of cell growth, proliferation and differentiation (Sawyers *et al.* 1995).

Another mechanism that may cause deregulated turnover and anti-apoptotic phenotype is BCR-ABL induced growth factor independence, either through ligand-independent receptor activation, such as the JAK/STAT (JAK-Janus Kinases, STAT-Signal Transducer of Transcription) pathway or autocrine production of cytokines. Normally, cytokines such as interleukin-3 (IL-3) activate JAK, causing phosphorylation of STAT5 which then translocates to the nucleus and upregulates transcription genes such as BCL_{xL} which enhance cell survival, proliferation and differentiation (Horita *et al.* 2000). In the presence of BCR-ABL, however, the requirement of cytokines is bypassed such that JAK is activated in the absence of exogenous cytokines. In some cases, the constitutive activation of STAT5 is not always associated with activation of JAK, but activated via the SRC family haemopoietic cell kinase (HcK), hence bypassing the requirement of cytokines for translocation and activation of transcription genes (Klejman *et al.* 2002). Overall, the pathways activated by BCR-ABL lead to deregulated proliferation and are anti-apoptotic.

In addition to inducing cytokine independent activation of JAK/STAT5 mediated signalling mechanisms, BCR-ABL also activates the autocrine production of growth factors. Studies have conclusively confirmed an autocrine loop for IL-3, granulocyte-colony stimulating factor (G-CSF) and granulocyte macrophage-colony stimulating factor (GM-CSF), in mouse BM cells transduced with *bcr-abl* expressing retroviral vectors (Zhang and Ren 1998; Abolhoda *et al.* 1999) and in primitive human CML cells (Jiang *et al.* 1999), which in turn maintained cell survival and proliferation (Strife *et al.* 1988; Bedi *et al.* 1994; Maguer-Satta *et al.* 1998; Jiang *et al.* 1999; Fu *et al.* 2000; Jiang *et al.* 2002). The specific activation of IL-3 production following BCR-ABL transduction suggested that control of IL-3 expression was a direct consequence of BCR-ABL activation, as cells with an inactive BCR-ABL kinase did not express IL-3 (Anderson and Mladenovic 1996) and, further downstream, increased STAT5 phosphorylation was a direct function of IL-3 stimulation (Jiang *et al.* 1999).

1.3.2 Historic treatment of CML

Following the discovery of CML in the 19th century, initial therapeutic treatments included administering highly toxic arsenic or performing splenectomy, both of which had limited success. Subsequently, the introduction of radiotherapy provided a good control of symptoms but did not extend survival. However, this remained the standard treatment until the introduction of the oral alkylating agent busulphan in the 1950's, which showed a selective action on haemopoietic tissue despite being toxic to germinal epithelium, and the antimetabolite hydroxyurea. Neither, however, prevented disease progression.

In the 1980's the use of Interferon α (IFNα) was introduced for the treatment of CML. Although it restored normal haematological values in a lower proportion of patients compared to those treated with busulphan or hydroxyurea, IFNα was able to induce Ph$^+$ reduction in 5-15% cases (Talpaz *et al.* 1986) and when combined with arabinoside (Ara-C), induced a complete haematological response (CHR) of 66% and major cytogenetic response (MCR) of 41%, with a survival rate of 85.7% within three years (Guilhot *et al.* 1997). However, this treatment was associated with a number of side effects ranging from nausea and diarrhoea to thrombocytopenia and the majority of patients had minimal residual disease (MRD), which ultimately led to IFNα resistance.

In addition, allogeneic BM transplantation was introduced at the same time for younger patients (<50-55yrs). This procedure has a significant morbidity and mortality of between 20-40%, due to the associated graft-versus-host disease and frequent infections (Sawyers 1999). Yet post-transplant, there is up to a 70% leukaemia-free survival and to date this remains the only curative treatment (Clift and Anasetti 1997; Gratwohl *et al.* 1998). However, due to the nature of the transplant and the difficulty in obtaining HLA matched donors only a minority of patients are suitable for these transplants.

1.3.3 Development of a therapeutic drug for CML

The discovery that the abnormal tyrosine kinase activity of ABL is essential for BCR-ABL mediated transformation and pathogenesis of CML made this an ideal target for therapeutic intervention. The first demonstration that synthetic inhibitors could be engineered to possess selective activity came from the development of a series of low molecular weight compounds called tyrphostins (TYRosine

PHOSphorylaTion Inhibitors), the most potent of which were able to selectively inhibit epidermal growth factor (EGF) cell-dependent proliferation, whilst not affecting the EGF-independent proliferation. Further development led to the generation of AG 490, the first synthetic compound that could inhibit proliferation *in vivo* and *in vitro.* Working independently, Ciba-Geigy (now known as Novartis) identified the phenylamino-pyrimidine compounds as being selective inhibitors against the platelet derived growth factor-receptor (PDGF-R) tyrosine kinase and began high throughput screening. The compound CGP57148, later branded as STI 571 ((signal transduction inhibitor 571), imatinib mesylate (IM), Glivec[®], or Gleevec[®]), emerged as a potent inhibitor of PDGF-R, ABL, ARG and C-KIT (Druker *et al.* 1996; Heinrich *et al.* 2000; Okuda *et al.* 2001) (Figure 1-4).
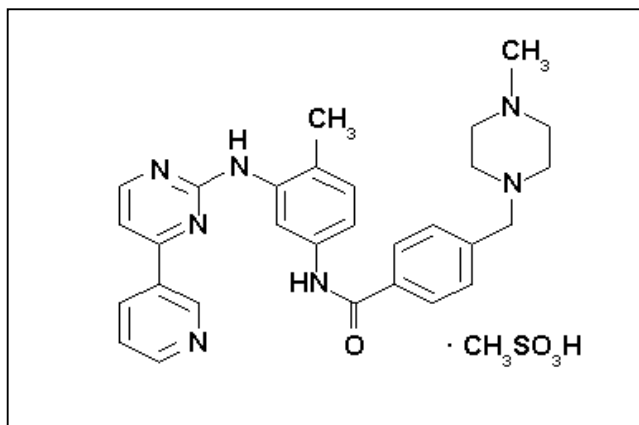
Figure 1-4 Structure of imatinib mesylate (IM)

IM exerts its effect on BCR-ABL by binding to only the highly conserved NH_2-terminal anchor region of the ATP binding pocket of the enzyme, known as the "activation loop", preventing phosphorylation of substrates and inhibiting intracellular signals (Figure 1-5). This region controls the catalytic activity of the kinase by switching between the active and inactive states. Crystallographic

studies show that IM binds to the ATP site only when the activation loop is closed,

thus stabilizing the inactive state (Schindler *et al.* 2000).
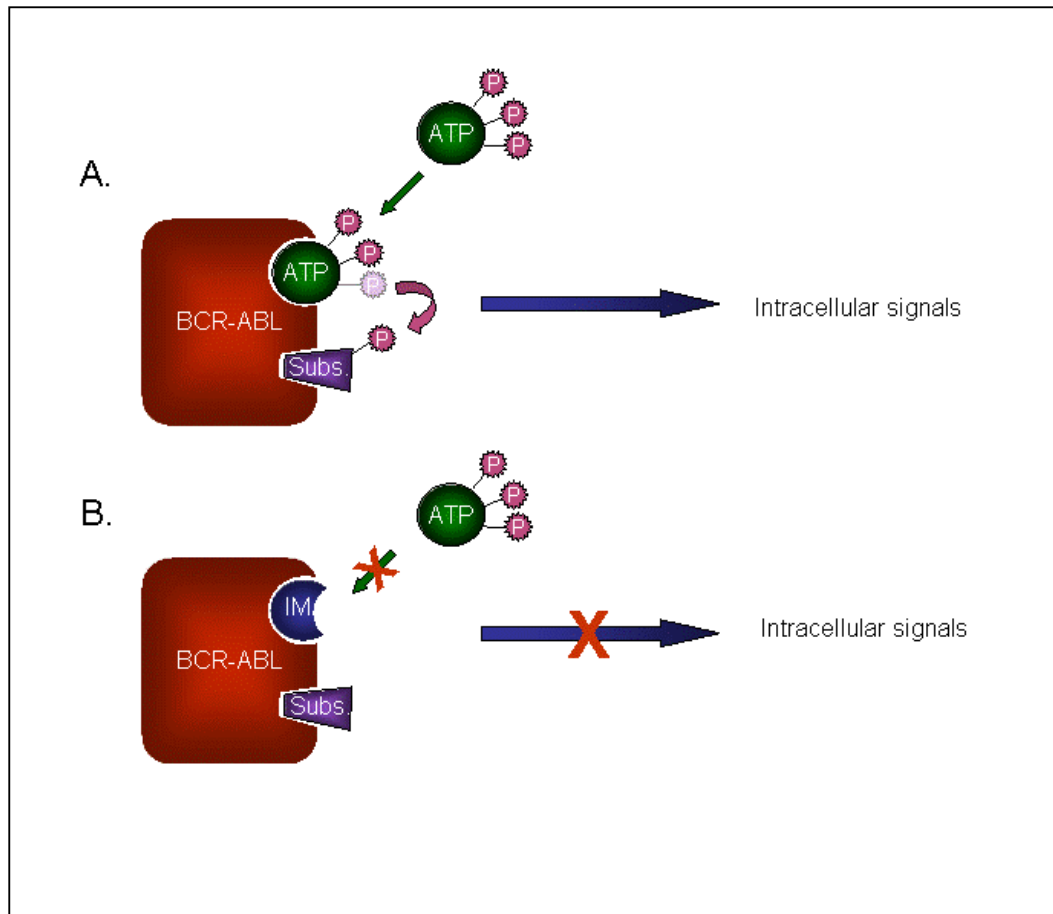
Figure 1-5 Mechanism of IM

BCR-ABL requires ATP binding for phosphorylation of substrates and subsequent activation of downstream pathways that promote cell survival, proliferation and regulation. IM can compete with ATP, binding to the inactive state of BCR-ABL, preventing the phosphorylation of substrates that would activate intracellular signals. [Subs. - substrate, p-phosphorylation]

The efficacy of this compound was validated in myeloid cell lines, demonstrating

inhibition of cell proliferation and tumour formation (Druker *et al.* 1996). Colony

forming cell (CFC) assays of peripheral blood (PB) or BM cells from CML patients

showed a 92-98% decrease in the number of BCR-ABL colonies formed compared

to no inhibition of normal colony formation at 1µM IM. At 10µM, normal BM colony formation was inhibited by 15-20%, with substantial loss at very high doses (50µM), suggesting that at this dosage there was loss of selectivity causing inhibition of other tyrosine kinases. Experimental data with thymidine assays that measure proliferation also correlated with CFC assays (Gambacorti-Passerini *et al.* 1997). Murine studies demonstrated inhibition of tumour growth in mice inoculated with *bcr-abl,* with no adverse effects in the control mice, confirming efficacy *in vivo* (Druker *et al.* 1996) and complete eradication of tumour was achieved with continuous administration of IM (le Coutre *et al.* 1999).

The high selectivity of this compound at suppressing BCR-ABL cell expansion in CML patient samples and eradicating bcr-abl tumours in mice led to its introduction to clinical trials. Phase I dose escalating studies were initially carried out in CP CML patients who had failed IFNα. Haematological and cytogenetic responses were observed in 98% and 53% respectively with side effects including nausea, myalgia, oedema and diarrhoea (Druker 2001). Phase II studies continued to show efficacy and low toxicity (Atallah *et al.* 2002), however IM resistance in some patients was starting to develop (Ottmann and Hoelzer 2002).

The success of the above phase I/II trials led to a multicentre phase III, randomised study (IRIS, International Randomised study of IFNα plus Ara-C versus STI571), comparing IM with IFNα + Ara-C in newly diagnosed CP CML patients. Within 18 months the superiority of IM over conventional IFNα treatment was evident. A MCR of 87.1% was observed in patients treated with IM, compared to 34.7% for those treated with IFNα + Ara-C. Furthermore, complete cytogenetic response (CCR) was observed in 76.2% of patients treated with IM versus 14.5% in those with IFNα + Ara-C. In addition, fewer patients progressed to AP or BC in

the IM group. The efficacy and tolerance quickly resulted in the approval of IM as the first line of treatment for patients with newly diagnosed CML in CP (O'Brien *et al.* 2003).

The study has now reached its sixth year with the most recent cumulative CCR and MCR rates at 57% and 67% respectively, and an overall survival rate of patients who have received IM as initial therapy of 76%. In addition, there has been no increase in rates of serious adverse effects with continued use of IM, demonstrating that it is an effective and safe therapy for CP CML patients (Hochhaus *et al.* 2007).

1.3.4 Molecular resistance

However, despite the efficacy of IM, molecular resistance has been noted. This is generally observed in CML patients at the advanced stage of disease, although it has also been seen in CP patients, resulting in IM being less successful (Talpaz *et al.* 2002). Resistance can be described either as primary, defined as failure to achieve CHR in 3 months or CCR in 12 months, or acquired, defined as loss of established IM response or progression to AP or BC.

It has been speculated that IM resistance may be either BCR-ABL independent or BCR-ABL dependent. Worryingly, BCR-ABL independence would suggest that the cells are no longer reliant upon BCR-ABL to drive proliferation, but have acquired other oncogenic mutations (Donato *et al.* 2004). This would mean that kinase inhibitors such as IM, that specifically target BCR-ABL, would never be able to kill the insensitive stem cell. There is also increasing evidence that SRC family kinases may reduce the BCR-ABL dependence of the leukaemic cell, as patients who have progressed whilst being treated with IM have an increased SRC kinase

activity, while the *BCR-ABL* transcripts and protein are reduced (Donato *et al.* 2003). This has led to the development of new agents that target the SRC kinase and inhibit other non-ATP binding sites.

In contrast, CSC resistance may be dependent upon BCR-ABL. Firstly, it has been hypothesised that Ph^{+} cells have various mechanisms to evade the pro-apoptotic effect of IM. These include the development of mutations within the IM binding domain (Gorre *et al.* 2001) with in excess of 40 mutations having been detected so far (Branford *et al.* 2002). These are found within the ATP binding site (P-loop), activation loop (A-loop) or the carboxy terminus. Some mutations only confer a moderate degree of resistance, however, the mutations that are found in the P-loop are associated with a poorer outcome (Branford *et al.* 2002). This is probably due to the mutations altering and destabilising the conformation of the ATP-binding site and restricting the binding of IM (Shah *et al.* 2002). In addition, the single nucleotide substitution of C to T at position 315, resulting in an isoleucine residue instead of a threonine remains the most clinically significant due to its resistance to high IM concentrations and poor prognosis in CML patients. Threonine is vital to IM inhibition as it forms critical hydrogen bonds and the replacement with isoleucine results in a steric clash, preventing IM binding (Gorre *et al.* 2001).

1.3.5 New therapeutic developments

In order to overcome these therapeutic shortfalls of IM in resistance, the quest for superior drugs has led to the assessment of many new antileukaemic agents that may be used alone or in combination to circumvent this (Table 1-1). These include selective ABL inhibitors, dual SRC/ABL kinase inhibitors and other non-ATP

competitive inhibitors. Two agents with promising results to date are nilotinib and

dasatinib.

Target	Mechanism	Agents
BCR-ABL activity	New TKIs - ABL kinase - ABL and SRC kinase	Nilotinib, ON012380 dasatinib, bosutinib PD166326
BCR-ABL stability	Heat shock protein 90 inhibitors	17-AAG
	Histone deacetylase inhibitors	Trichostatin A
BCR-ABL localisation	Nuclear trapping	Leptomycin B
Alternative targets	Aurora kinase inhibitors	MK-0457, PHA-739358
	Farnesyl transferase inhibitors (FTI)	Lonafarnib, SCH66336, L-744,832
	Induction of apoptosis	TRAIL
	PI3-kinase inhibitors	Wortmannin, LY294002
	Proteasome inhibitors	Bortezomib, PS341
	Protein kinase C	Bryostatin
	Reactive oxygen species	Adaphostin

Table 1-1. Summary of antileukaemic agents being evaluated in CML. Modified and adapted from (Heaney and Holyoake 2007)

1.3.5.1 Nilotinib (AMN107, Tasigna®)

In order to eliminate IM resistance, Novartis designed a new inhibitor based on the

crystal structure of the IM-ABL complex. The result was nilotinib (Figure 1-6), a

high affinity aminopyrimidine-based ATP competitive inhibitor with approximately

20x more potency than IM in killing BCR-ABL expressing cell lines (K562).

Nilotinib can also inhibit the activity of ARG, C-KIT, and PDGF receptor kinases. In

addition, nilotinib has shown effectiveness against all BCR-ABL mutations except

for T315I (Manley *et al.* 2002; Manley *et al.* 2005). The additional methyl group of

isoleucine restricts access to the drug and hence inhibits binding. In addition, nilotinib, as with IM, can only bind to the inactive conformation of BCR-ABL.
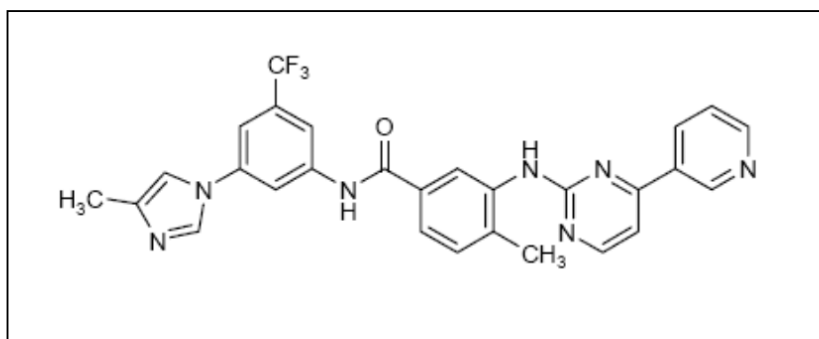
Figure 1-6 Structure of nilotinib

In a phase I dose-escalation study, IM-resistant CML patients treated with nilotinib showed haematological and cytogenetic responses of 92% and 53% respectively for CP and 72% and 48% respectively for AP patients, with a favourable safety and tolerability profile. Common side effects included myelosuppression, skin rash and hyperbilirubinaemia. Yet, in contrast to IM, nilotinib was not associated with oedema. Ongoing phase II studies in patients who have failed IM therapy also show favourable responses (Kantarjian *et al.* 2006).

1.3.5.2 Dasatinib (BMS-354825, Sprycel[®])

In addition to the requirement for more powerful BCR-ABL inhibitors, there has been a need to develop agents that can bind to the BCR-ABL complex regardless of the conformation status, thus reducing the likelihood of resistance. In addition, the development of new generation inhibitors that can simultaneously bind to ABL and SRC family kinases has been explored, as the overexpression of SRCs may mediate BCR-ABL independent IM resistance and may be associated with the

pathogenesis of the disease. One such agent is dasatinib (Figure 1-7), developed

by Bristol-Myers Squibb. Dasatinib is a highly potent active inhibitor of SRC and

SRC family kinases which also has inhibition against BCR-ABL, C-KIT, PDGF and

ephrin receptor tyrosine kinases (Lombardo *et al.* 2004; Nam *et al.* 2005;

Schittenhelm *et al.* 2006). Unlike IM and nilotinib, dasatinib can form a complex

with ABL both in the active and inactive conformation (Lombardo *et al.* 2004).

Dasatinib has a 325x greater potency than IM and, like nilotinib, can effectively

bind to all the mutations except for T315I (O'Hare *et al.* 2005) (Shah *et al.* 2004).
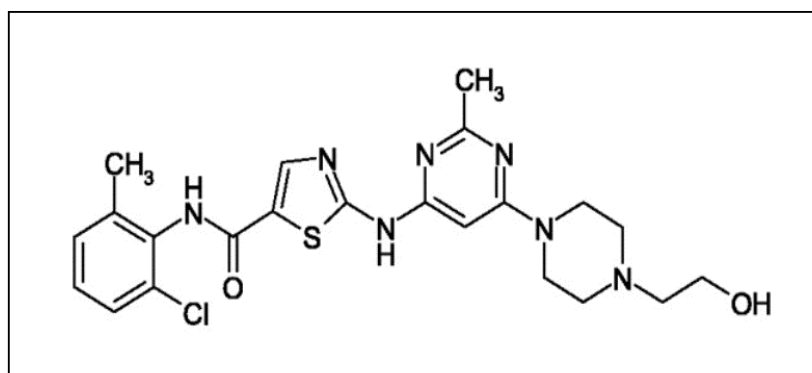
Figure 1-7 Structure of dasatinib

A phase I dose escalation study in IM resistant CML patients showed 92.5% of CP

patients and 70% of AP patients attained haematological response. The common

side effects included myelosuppression, pericardial effusion and oedema.

Completed phase II trials also show positive data with a CHR in 90%, instigating

the accelerated licence approval for use in CML patients in the U.S. and U.K.

(Talpaz *et al.* 2006; Guilhot *et al.* 2007).

1.3.6 Disease persistence

However, in addition to molecular resistance and despite effective CCR in CP with TKIs and other new agents, the majority of patients have persistent detectable disease by sensitive RT-PCR assay (Hughes and Branford 2003; Muller *et al.* 2003; Branford *et al.* 2004). Investigations have described two populations of primitive leukaemic cells. The first subset undergo cell cycle arrest and accumulate in the G_0/G_1 phase in the presence of anti-proliferative agents, including IM (Jorgensen *et al.* 2005b), which may be encouraged into cell cycle with sequential pulsed therapy. The second are a deeply quiescent Ph^+ stem cell population identified by their *in vitro* progenitor activity demonstrated by an LTC-IC assay and their ability to engraft immunodeficient mice (Holyoake *et al.* 1999). Further studies have demonstrated that these CML LSCs are insensitive to the pro-apoptotic effect of IM, even at concentrations 10x higher than those achievable *in vivo* (Holyoake *et al.* 1999; Graham *et al.* 2002). Even continued IM therapy does not eradicate these cells (Bhatia *et al.* 2003). In addition, these cells are resistant to nilotinib (Jorgensen *et al.* 2007a) and, although a little more responsive, persist in the presence of dasatinib (Copland *et al.* 2006). Furthermore, patients relapse rapidly following discontinuation with IM, further confirming that these cells persist. It is likely, therefore, that it is these BCR-ABL positive cells within the patient that are responsible for the MRD detected in the majority of IM treated patients and may be the cause for relapse at a later date.

1.3.7 Disease resistance by transport

One explanation for the failure of the TKIs to effectively eradicate the stem cell population is that the drug never reaches a therapeutic intracellular concentration.

This mechanism of drug resistance, termed multidrug resistance (MDR), is a common phenomenon and has been attributed to the broad specificity drug efflux pumps of the ATP binding cassette (ABC) family. These efflux proteins limit tumour kill by reducing the accumulation of cytotoxic agents to below therapeutic thresholds, either by limiting uptake, enhancing efflux or affecting membrane lipids (Yanovich and Taub 1983). Furthermore, they may alter the distribution within the cell and thus limit the exposure of the cytotoxic agents to the target (Kitazono *et al.* 1999) and may provide resistance by protecting the tumour cells from multiple forms of caspase-dependent apoptosis (Smyth *et al.* 1998).

In some cases, resistance may also be associated with progressive *BCR-ABL* gene amplification (Gorre *et al.* 2001), where multiple copies of the *BCR-ABL* gene can be detected in the interphase nuclei in patients who relapse after initially responding to IM. Characterisation by FISH (Fluorescence *In Situ* Hybridization) shows a unique inverted duplicate Ph chromosome with interstitial amplification of the *BCR-ABL* fusion gene, again suggesting that there may be insufficient IM present in the leukaemic cell to inhibit the increased level of oncogenic protein.

1.4 ABC transporters

The membrane of a living cell is mainly composed of a lipid bilayer that prevents the free flow of molecules across the membrane barrier and has transporters that actively pump solutes. Drug transporters have been classified into two major families: ABC transporters and solute carrier transporters (Choudhuri and Klaassen 2006).

ABC transporters were given their name in 1992 based on the most characteristic feature of this superfamily, namely the ATP binding cassette (Higgins 1992). These plasma membrane glycoproteins are present in most cells and mediate the transfer of a substrate across the membrane against a concentration gradient, using energy derived from ATP hydrolysis. In normal physiology there is uptake of substrates, including nutrients and biologically active substances, while toxic compounds are actively effluxed from tissues, secretory organs and blood-brain barrier, providing an important protective function (Sarkadi *et al.* 2004). These toxic compounds, however, also include specific chemotherapeutic compounds, which affect therapeutic intervention by lowering the effective drug concentration inside the cell.

Typically, an ABC transporter is composed of four parts; two hydrophobic transmembrane domains (TMD) and two ATP hydrolysing domains, bound by a flexible linker region (Figure 1-8). The membrane domains anchor the protein to the membrane and form pores that allow the substrate to cross the membrane and therefore determine the substrate specificity. The ATP binding domains, also known as nucleotide binding domains (NBDs) are located in the cytoplasm and provide the energy to transport the substrate across the membrane. Some transporters consist of only one membrane integral domain and one NBD; however these "half transporters" must form homodimers or heterodimers for active function.
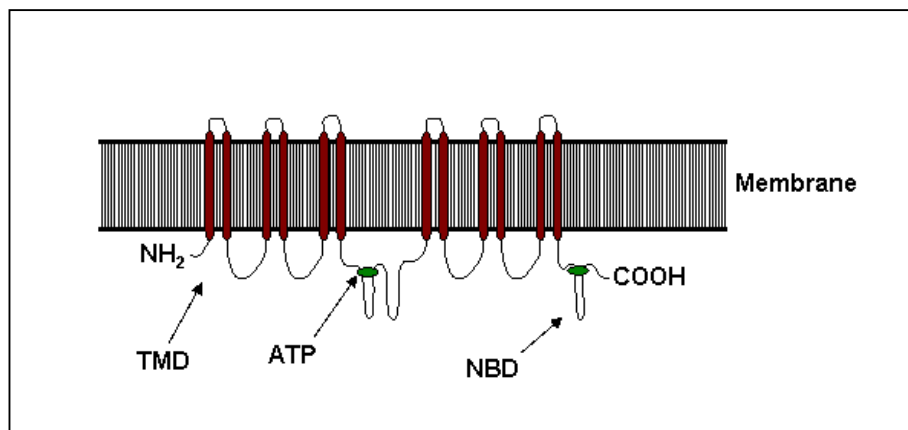
Figure 1-8 Schematic diagram of an ABC transporter

An ABC transporter typically consists of two hydrophilic cytosolic nucleotide binding domains (NBD) and two transmembrane domains (TMD), each of which spans the membrane six times. The binding of ATP at the NBD provides energy for transport of substrates across the membrane. Some transporters e.g. ABCG2 are half-transporters and composed of only one NBD and one TMD.

To date there are in excess of 50 members belonging to the ABC family, categorised into seven subfamilies. These are characterised by a high level of sequence homology and extensive conservation of the ATP-binding domains (Higgins 1995; Gottesman and Ambudkar 2001). Of these, 15 have been shown to have involvement in the extrusion of chemotherapeutic compounds, of which 3 have the greatest influence in malignant cells and account for nearly all of the MDR.

1.4.1 MDR1 (Multidrug resistance 1)

Initially discovered in 1976 (Juliano and Ling 1976) and most extensively studied, MDR1 (also known as p-glycoprotein or p-gp, ABCB1, gp170) was the first ABC transporter observed to modulate drug permeability in tumour cells. Located on chromosome 7 and encoded by the *ABCB1* gene, MDR1 is a 170kD glycoprotein

consisting of two 610aa half-transporters joined by a 60aa flexible linker. This transporter is normally expressed in the plasma membrane of the HSC (Chaudhary and Roninson 1991), colon, small intestine and kidney (Tan *et al.* 2000). It may also play a role in the blood-brain (Rao *et al.* 1999) and placental barriers (Smit *et al.* 1999) by removing toxic substances and protecting vital organs. The substrates of MDR1 range in size and chemical structure, yet the common denominator is their amphipathic nature, suggesting a mechanism in their drug translocation. The hydrophobic parts of the drug allow rapid insertion into the inner hemi-leaflet of the cell membrane, but the hydrophilic residues slow the entry into the inner-leaflet such that the pump is able to extrude the drug. As such, amphipathic anticancer agents are included in the active efflux of substrates, including anthracyclines, taxanes, anthracenes, epipodophyllotoxins and vinca alkaloids (Bates *et al.* 2001).

MDR1 overexpression has been shown in numerous tumour cells, including breast cancer (Trock *et al.* 1997), ovarian cancer (van der Zee *et al.* 1995), head and neck tumours (Ng *et al.* 1998) and non-Hodgkins lymphoma (Yuen and Sikic 1994). Furthermore, repeated courses of cytotoxic or radiation therapy may induce MDR1 overexpression, hence accounting for the increasing clinical resistance in these diseases (Ng *et al.* 1998). Indeed, the presence of MDR1 is so detrimental to patients that those with MDR1 positive tumours have poorer prognoses than those with MDR1 negative neoplasms. A meta-analysis of 31 studies of MDR in breast cancer observed that patients expressing MDR1 were three times more likely to fail chemotherapy than those that were MDR1 negative (Trock *et al.* 1997).

Some studies have also shown that MDR1 expression is associated with AML (Musto *et al.* 1991; Zhou *et al.* 1992). Zhou *et al* studied 126 adult AML samples and noted a significantly higher incidence of MDR1 expression in resistant patients (60%) in comparison to untreated or relapsing patients (27%). Furthermore, 68% of patients positive for MDR1 eventually developed resistance to chemotherapy, in comparison to 23% who did not have MDR1 expression.

In addition, MDR1 has been associated with AML CD34$^+$ blasts. In elderly patients with AML, MDR1 was expressed in 71% of cases, 58% of which demonstrated functional drug efflux (Leith *et al.* 1997). In contrast, younger AML patients who achieved higher remission and longer overall survival rates only expressed MDR1 in 35% of cases (Leith *et al.* 1999). This suggests that the lower frequency of MDR1 expression in the younger AML patients may in part explain the greater response to chemotherapy and in turn suggest that MDR modulators may benefit patients with this disease.

However, although MDR is present in the CD34$^+$ cell population, when the cells were fractionated to determine the role of MDR1 in CD34$^+$38$^-$, the results were surprising. Although MDR1 protein was preferentially expressed in the CD34$^+$38$^-$ population compared to the more mature CD34$^+$38$^+$ BM cells at levels comparable to those observed in normal BM, the MDR1 transport was markedly decreased in the primitive cells (Raaijmakers *et al.* 2006). This would therefore suggest that MDR1 modulation would not circumvent drug extrusion and may explain the relatively poor results in attempting to reverse drug resistance by MDR1 modulation in clinical trials (Lee *et al.* 1999; Chauncey *et al.* 2000; Baer *et al.* 2002; Greenberg *et al.* 2004; van der Holt *et al.* 2005).

However, even in solid tumours such as renal cell cancer and colon cancer, MDR1 modulation therapy does not show significant response despite relatively high MDR1 expression levels, suggesting that there may be other mechanisms contributing to drug resistance. This view, combined with studies indicating that some cell lines with an absent MDR efflux pump still had a resistant phenotype, led to the identification of the second transporter as having a potential role in clinical multidrug resistance.

1.4.2 MRP1 (multidrug resistance-associated protein 1)

MRP1 (also known as ABCC1) was identified by isolating the overexpressed gene in a doxorubicin resistant lung cancer cell line that did not over-express MDR1 (Cole *et al.* 1992). The identified gene was located on chromosome 16 and coded for a 190kD glycoprotein (Krishnamachary and Center 1993; Evers *et al.* 1996). Subsequent analysis has shown that MRP1 is almost ubiquitously expressed in all major tissues and cell types (Burger *et al.* 1994), with high levels in lung, testis, kidney, placenta, skeletal and cardiac muscles. MRP1 is predominately located in the basolateral membrane of epithelial cell layers, suggesting a role as a cellular defence by preventing the accumulation of toxic compounds in the cells (Evers *et al.* 1996).

MRP1 functions mainly as a transporter of amphipathic organic anions. Leukotriene C4 (LTC_4), a potent inflammatory mediator, is the highest affinity substrate for MRP1 protein and *mrp*-/- knockout mice show a reduced response to an inflammatory stimulus (Wijnholds *et al.* 1997). Like MDR1, MRP1 also transports hydrophobic substrates and indeed can confer resistance to many of the same drugs such as vinca alkaloids, anthracyclines and epipodophyllotoxins.

However MRP1 cannot transport these drugs when they are unmodified, but requires conjugation or co-transportation of the substrate with the anionic tripepetide glutathione (Rappa *et al.* 1997a).

As MRP1 is present in virtually all human tissues and most human tumour cell lines and samples, it was assumed that MRP1 contributed to drug resistance. In cell lines, the drugs most affected by the presence of MRP1 are etoposide, vincristine and anthracyclines, yet the evidence in clinical practice is unclear. Patients with relapsed AML have higher *MRP1* expression levels compared to those at diagnosis (Schneider *et al.* 1995; Zhou *et al.* 1995). Furthermore, simultaneous expression of MRP with MDR1 in AML has shown higher daunorubicin and etoposide resistance (Legrand *et al.* 1999). However, there is no correlation between MRP protein expression and clinical response (Filipits *et al.* 1997), suggesting that overcoming resistance may require modulation of both transporters, and possibly others in addition, to achieve a clinical response.

1.4.3 ABCG2

More recently, ABCG2 (also known as BCRP, MXR, ABCP) was identified in the highly doxorubicin-resistant breast cancer subline MCF7/AdrVP (Doyle *et al.* 1998). ABCG2 is a half transporter and requires dimerisation for efficient transmembrane substrate translocation (Allikmets *et al.* 1998; Ross *et al.* 1999). It is located on chromosome 4 and expressed on the plasma membrane of many primitive cell populations, including embryonic stem cells, placenta (Allikmets *et al.* 1998), breast (Doyle *et al.* 1998), liver, muscle (Zhou *et al.* 2001), gastrointestinal tract (Maliepaard *et al.* 2001) and pancreas (Lechner *et al.* 2002). In addition, there has been evidence that ABCG2 is expressed in HSC. HSCs can be

recognised with flow cytometry by their appearance as a SP of cells, based on their ability to exclude Hst. Zhou *et al* (Zhou *et al.* 2001) observed SP cells from mouse and rhesus monkey expressed high levels of *abcg2* mRNA. Moreover, the most primitive mouse HSC (CD34^{-}) highly expressed *abcg2* mRNA, which markedly decreased with stem cell differentiation (CD34^{+}). When *abcg2* expression was enforced in BM, the SP population expanded and caused a reduction in mature cells, suggesting that ABCG2 may be preventing the cellular accumulation of a substrate essential for stem cell differentiation. However, knockout mice showed normal haematological parameters with no developmental or observable organ defects, indicating that ABCG2 is unlikely to mediate a non-redundant role in stem cell regulatory mechanisms (Zhou *et al.* 2003). In addition, although a significant decrease of SP cells was observed in BM compared to the wild type mice, competitive BM transplants resulted in no significant advantage and ABCG2-mediated Hst transport activity can be eliminated without any functional defect in steady state haemopoiesis. This suggests that either ABCG2 functionality is not required for normal stem cell function in mice or that when ABCG2 is knocked out, the activity of this transporter may be substituted by other transporters (Zhou *et al.* 2002).

The only natural substrates of ABCG2 identified so far are porphyrins and porphyrin-like compounds (Jonker *et al.* 2002). Accumulation of porphyrin is detrimental to cells as accumulation ultimately leads to cell damaging reactive oxygen species and deficient mitochondrial function (Antolin *et al.* 1994). In hypoxic conditions, the survival of progenitor cells was markedly reduced in *abcg2* null mice compared to *abcg2*+/+, a condition which was reversed by blocking heme biosynthesis (Krishnamurthy *et al.* 2004). Also, accumulation of dietary pheophorbide, a chlorophyll-breakdown product, was increased in *abcg2* deficient

mice, causing a porphyria-like syndrome of photosensitivity (Jonker *et al.* 2002). Similarly, the dietary carcinogen 2-amino-1-methyl-6-phenylimidazo[4,5-b]pyridine (PhIP) and protoporphyrin XI are natural substrates (Abbott 2003), suggesting that ABCG2 has a physiological role in protecting primitive cells against toxic substances in the hypoxic environment.

As with the other transporters, ABCG2 overexpression has been shown to induce resistance to anticancer drugs, including mitoxantrone, topotecan, doxorubicin, campothecins, flavopiridol and daunorubicin (Doyle *et al.* 1998; Maliepaard *et al.* 1999; Ross *et al.* 1999; Kawabata *et al.* 2001; Komatani *et al.* 2001; Robey *et al.* 2001b). There have also been studies describing elevated levels of ABCG2 in malignancies, especially in AML, although the data have been conflicting. Ross *et al* (Ross *et al.* 2000) showed that 33% of blast cells had a 5 fold increase of *ABCG2* mRNA by RT-PCR with Sargent *et al* (Sargent *et al.* 2001) detecting a similar protein expression. Furthermore, *ABCG2* expression was elevated in patients at time of relapse, in comparison to diagnosis both in adults (van den Heuvel-Eibrink *et al.* 2002) and paediatric AML patients (Steinbach *et al.* 2002). Furthermore, high expression correlated with a poorer outcome despite some patients having favourable cytogenetic abnormalities. In other expression studies, there has been no association of *ABCG2* expression with prognosis, either at diagnosis or at relapse (Sargent *et al.* 2001; van der Kolk *et al.* 2002; van der Pol *et al.* 2003). The discrepancy may partly be attributed to possible contamination from normal HSC. A recent study validated *ABCG2* expression in AML and determined that 85% of newly diagnosed AML patients had higher level of mRNA expression than in BM or PB compared to normal controls, yet the level was below that shown to correlate with drug resistance (Abbott *et al.* 2002). However, flow cytometric analysis detected that the increased level was not due to low

homogenous expression in every leukaemic cell, but to high expression in a small subpopulation which may correlate to the presence of a LSC with a very immature surface immunophenotype. This suggested therefore, that although the overall mRNA expression level detected in the whole population was below that shown to correlate with drug resistance, the relatively high expression in the small subpopulation might be above the threshold level required for drug resistance.

1.4.4 Drug transporters and TKIs

The advent of IM as a targeted therapeutic drug dramatically improved the outcome in patients suffering from CML. Yet molecular resistance leading to persistence of the disease led to the role of drug transporters in mediating this response being the topic of an increasing amount of study (Figure 1-9). Recent reports have shown *hOCT1* to actively mediate the transport of IM into the cells (Thomas *et al.* 2004; White *et al.* 2006). OCT1 (Organic Cation Transporter 1) is a member of the solute carrier transporters encoded by the *SLC22* gene family. It is primarily expressed on the basolateral membrane of kidney, liver, and placenta and has been shown to transport cyclic weak bases and a variety of drugs. Thomas *et al* demonstrated that uptake of IM was an active process by comparing the concentration of radiolabelled IM at $4^{o}C$ and $37^{o}C$ and confirming temperature dependence (Thomas *et al.* 2004). By a process of elimination using a series of inhibitors, the OCT identified to be involved was hOCT1 and not hOCT2 or hOCT3, suggesting that differential expression of this transporter may be a critical determinant of intracellular IM levels. Further expression studies demonstrated that *hOCT1* mRNA in CML patients was not significantly different to normal BM donors. However, patients who remained at least 65% Ph^{+} after 10 months IM treatment had significantly lower *hOCT1* expression prior to IM treatment

compared to those who achieved a CCR within 12 months (Crossman *et al.* 2005a), confirming that *hOCT1* mRNA expression may predict a more favourable molecular response to IM. In contrast, nilotinib was not shown to be a substrate for this transporter, despite being structurally related to IM (White *et al.* 2006).
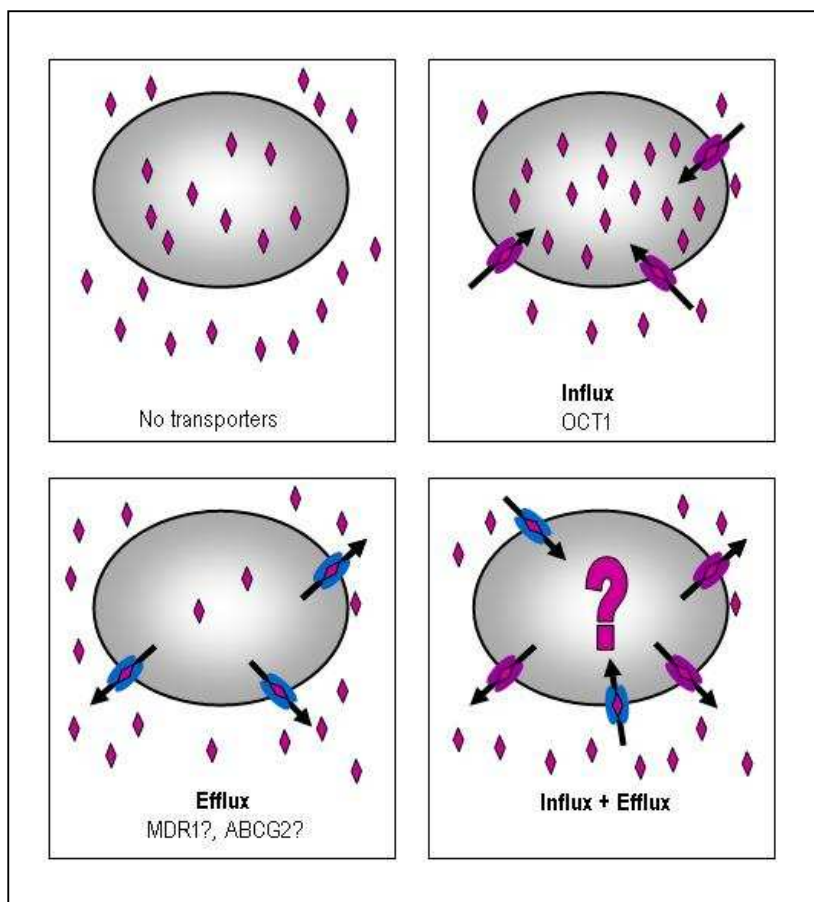
Figure 1-9 Intracellular drug concentration by transporters

In the absence of drug transporters the cellular concentration will be equilibrated with the external medium. Influx transporters such as hOCT1 will actively uptake IM but not nilotinib, against a concentration gradient. However, if the TKIs are also substrates of efflux transporters, overexpression will reduce the accumulation in the cell. It is the balance of the influx and efflux transporters that may mediate resistance to TKI.

In contrast, several reports have identified active efflux by MDR1 as a contributory factor to IM resistance. MDR1 was originally highlighted to interact with IM using a

calcein extrusion assay. Generally the uptake of calcein is slow in cells that have active transporters; however, agents that interact with the proteins inhibit the dye extrusion and accelerate the calcein accumulation. The increased uptake suggested an interaction with IM, although the assay could not delineate between an interaction as a competitive substrate or as a direct inhibitor (Hegedus *et al.* 2002). Other studies demonstrated that a cell line overexpressing *MDR1* was resistant to IM, which was reversed in the presence of MDR1 inhibitors (Mahon *et al.* 2003; Mukai *et al.* 2003), suggesting that IM is a substrate for this transporter. This was further confirmed by a high-performance liquid chromatography-based (HPLC) method demonstrating decreased intracellular IM levels in cell lines overexpressing *MDR1* which was also associated with loss of IM effect on cellular proliferation and apoptosis (Illmer *et al.* 2004). Furthermore, knockdown of *MDR1* in an IM resistant cell line verified sensitivity to IM and reduced CrkL phosphorylation (Rumpold *et al.* 2005).

However, there have also been reports refuting the role of MDR1 in IM resistance. Ferrao *et al* (Ferrao *et al.* 2003) demonstrated no significant growth advantage in the retrovirally transduced *MDR1* cell line, compared to the wild type and concluded that MDR1 was not a substrate of IM, while overexpression of BCL_{XL} conferred partial protection instead. Furthermore, Zong *et al* demonstrated no difference to IM resistance in cell lines overexpressing *MDR1*. The lack of effect was further demonstrated in mice transplanted with *mdr1a/1b* null BM that had been transduced with a *bcr-abl* retroviral vector. Both the wild-type and *mdr1a/ab* null mice displayed similar responses to IM, with no change in incidence of disease (Zong *et al.* 2005). Similarly *MDR1* expression in BM mononuclear cells (MNC) from CML patients did not correlate with response to IM (Carter *et al.*

2001), suggesting that MDR1 does not confer resistance to IM alone and that there may be other transporters contributing to the effect.

Recently, ABCG2 expression has been put forward as a possible mechanism for promoting IM resistance, but with conflicting results. In cell lines, Houghton *et al* (Houghton *et al.* 2004) found IM to be a potent inhibitor of ABCG2 as IM increased topotecan accumulation in *ABCG2* overexpressing cells. They found IM was not a substrate as there was no difference in accumulation of radiolabelled drug in the presence or absence of functional ABCG2. In contrast, Burger *et al* (Burger *et al.* 2004) found IM to be a substrate as the accumulation of radiolabelled IM was significantly lower in the overexpressing *ABCG2* cell lines compared to the wild-type. Both of these investigations, however, used non-haemopoietic cell lines engineered to over-express *ABCG2,* neither of which represented clinical targets for IM. A recent study, however, in ABCG2 knockout mice demonstrated a 2.5 fold greater increase in brain penetration of intravenous IM with a greater increase in wild-type mice with ABCG2 inhibitors, suggesting ABCG2 influences the bioavailability and pharmacokinetics of IM (Breedveld *et al.* 2005).

The role of MRP1 with IM has not been studied extensively, although an interaction has been confirmed (Hegedus *et al.* 2002). Mukai et al (Mukai *et al.* 2003) have determined that IM is not a substrate for MRP1 in the K562 cell line. However, Lange *et al* (Lange *et al.* 2003) demonstrated that low levels of *MRP1* are predictive of IM response in BC CML, thereby suggesting IM may be a substrate of MRP1.

1.4.5 Aims

The role of these transporters in conferring TKI resistance is still in contention. To date, studies demonstrate that the three main active efflux transporters confer resistance to many cytotoxic agents and studies have confirmed expression in AML cells. However, the role of drug transporters in primary cells from CML and, in particular, the immature population that might be responsible for disease resistance and persistence has not been demonstrated. Furthermore, MDR1 and ABCG2 have been shown to interact with current TKIs, although it has not been conclusively confirmed in what capacity. Therefore, this thesis will explore the expression and function of the three main drug transporters associated with malignancy and determine their effect on the efficacy of the current therapeutic TKI agents for CML.

The experiments described in this thesis aim:

1. To determine the expression and function of ABCG2, MDR1 and MRP1 in CP CML CD34$^+$ cells

2. To determine whether IM, nilotinib or dasatinib are substrates or inhibitors of these drug transporters

3. To determine whether inhibition of these drug transporters alters the intracellular concentration of TKIs

4. To determine the effect of drug transporter inhibition on the response of CML cells to IM, nilotinib and dasatinib

5. To determine the expression of drug transporters during TKI therapy *in vitro*

6. To identify other transporters in CP CML CD34$^+$ cells that may have an effect in the resistance to TKI

2 Materials and Methods

2.1 Materials

2.1.1 Tissue culture plastics

Plastics	Supplier
Cryotube	Fisher Scientific, Loughborough, UK
Falcon tubes (FACS)	Fred Baker Scientific, Cheshire, UK
Non-adherent tissue culture dishes (35mm)	Scientific Lab supplies, Coatbridge, UK
Non-adherent tissue culture flasks ($75cm^3$)	Scientific Lab supplies, Coatbridge, UK
Pipette tips	Greiner bio one, Gloucestershire, UK
Plates (24-well)	Greiner bio one, Gloucestershire, UK
Plates (48-well)	Greiner bio one, Gloucestershire, UK
Plates (96-well flat bottomed)	Greiner bio one, Gloucestershire, UK
Tissue culture flasks ($25cm^3$)	Greiner bio one, Gloucestershire, UK
Tissue culture flasks ($75cm^3$)	Greiner bio one, Gloucestershire, UK

Table 2-1 Table of plastics used for tissue culture and suppliers

2.1.2 Tissue culture reagents

Reagent	Supplier
β-mercaptoethanol	Invitrogen, Paisley, UK
Bovine serum albumin (BSA)	Sigma-Aldrich, Dorset, UK
Bovine serum albumin, Insulin/ Transferrin (BIT)	Stem Cell Technologies, British Columbia, Canada
Colcemid	Invitrogen, Paisley, UK
Dimethyl sulphoxide (DMSO)	Sigma-Aldrich, Dorset, UK
Dulbecco's Modified Eagle Medium (DMEM)	Sigma-Aldrich, Dorset, UK
DNase I (Recombinant human DNAse)	Stem Cell Technologies, British Columbia, Canada
Dulbecco's phosphate buffered saline (w/o Ca^{2+} and Mg^{2+}) (PBS)	Invitrogen, Paisley, UK
Ethanol 100% molecular grade	Sigma-Aldrich, Dorset, UK
Filter mats	Perkin Elmer, Buckinghamshire, UK
Foetal Calf serum (FCS)	Invitrogen, Paisley, UK
GM-CSF	RD Systems Inc., California, USA

Human serum albumin 4.5% (HSA 4.5%)	Scottish National Blood Transfusion Service, Edinburgh, UK
Human serum albumin 20% (HSA 20%)	Scottish National Blood Transfusion Service, Edinburgh, UK
Iscove's modified Dulbecco's medium (IMDM)	Sigma-Aldrich, Dorset, UK
L-glutamine 200mM (100x)	Invitrogen, Paisley, UK
Low density lipoprotein (LDL)	Sigma-Aldrich, Dorset, UK
Magnesium Chloride (1.25M)	Sigma-Aldrich, Dorset, UK
Optiphase supermix liquid scintillation cocktail	Perkin Elmer, Buckinghamshire, UK
Penicillin (5000u)/ streptomycin (5mg/ml) solution	Invitrogen, Paisley, UK
Recombinant human erythropoietin (rHu-Epo)	Pharmacy, Glasgow Royal Infirmary, UK
Recombinant human Flt-3 ligand (rHu-Flt-3L)	Stem Cell Technologies, British Columbia, Canada
Recombinant human G-CSF (rHu-G-CSF)	Chugai Pharma, London, UK
Recombinant human IL-3 (rHu-IL-3)	Stem Cell Technologies, British Columbia, Canada
Recombinant human IL-6 (rHu-IL-6)	Stem Cell Technologies, British Columbia, Canada
Recombinant human SCF (rHu-SCF)	Stem Cell Technologies, British Columbia, Canada
Recombinant human thrombopoietin (rHU-Tpo)	RD Systems Inc., California, USA
RPMI 1640 medium (RPMI)	Invitrogen, Paisley, UK
Sodium Azide	Sigma-Aldrich, Dorset, UK
Sterile water (dH$_2$0)	Baxter Healthcare, Northampton, UK
Tri-sodium citrate	Sigma-Aldrich, Dorset, UK
Trypan Blue solution (0.4%)	Sigma-Aldrich, Dorset, UK
Wax scintillant	Perkin Elmer, Buckinghamshire, UK

Table 2-2 Table of reagents used for tissue culture and suppliers

2.1.3 Flow cytometry reagents

FACS reagents	Supplier
Annexin V antibody	Becton Dickinson, Oxford, UK
Annexin V 10x Buffer	Becton Dickinson, Oxford, UK
Anti-mouse IgG2a FITC	Becton Dickinson, Oxford, UK
Anti-rabbit IgG FITC conjugate	Sigma-Aldrich, Dorset, UK
Anti-rabbit IgG horseradish peroxidase-linked secondary antibody	Cell signalling, New England Biolabs, Hitchin, UK
Carboxy-fluorescein diacetate succinimidyl ester (CFSE)	Molecular Probes, Eugene, OR

FACS flow solution	Becton Dickinson, Oxford, UK
FACS clean solution	Becton Dickinson, Oxford, UK
Fix and Perm® A and B	Caltag Laboratories, Silverstone, UK
Mouse anti-human BXP-21 antibody	Alexis Biochemicals, Nottingham, UK
Mouse anti-human C219 antibody	Alexis Biochemicals, Nottingham, UK
Mouse anti-human glycophorin A FITC	Becton Dickinson, Oxford, UK
Mouse anti-human-CD3 PE antibody	Becton Dickinson, Oxford, UK
Mouse anti-human-CD11b FITC antibody	Becton Dickinson, Oxford, UK
Mouse anti-human-CD13 PE antibody	Becton Dickinson, Oxford, UK
Mouse anti-human-CD14 PE antibody	Becton Dickinson, Oxford, UK
Mouse anti-human-CD19 PE antibody	Becton Dickinson, Oxford, UK
Mouse anti-human-CD34 FITC antibody	Becton Dickinson, Oxford, UK
Mouse anti-human-CD34 PE antibody	Becton Dickinson, Oxford, UK
Mouse anti-human-CD45 FITC antibody	Becton Dickinson, Oxford, UK
Mouse anti-human-CD61 FITC antibody	Becton Dickinson, Oxford, UK
Mouse anti-human QCRL-3 antibody	Alexis Biochemicals, Nottingham, UK
Mouse IgG1a FITC	Becton Dickinson, Oxford, UK
Mouse IgG1a PE	Becton Dickinson, Oxford, UK
Propidium Iodide (PI)	Sigma-Aldrich, Dorset, UK
Rabbit anti-human p-CrkL antibody	Cell signalling, New England Biolabs, Hitchin, UK
Viaprobe	Becton Dickinson, Oxford, UK

Table 2-3 Table of FACS reagents used and suppliers

2.1.4 Supply of TKIs

Drugs	Supplier
Dasatinib (BMS-354825, Sprycel®)	Kind gift from Dr F. Lee Bristol-Myers Squibb, Princeton, NJ
^{14}C-dasatinib	Kind gift from Dr F. Lee Bristol-Myers Squibb, Princeton, NJ
Imatinib Mesylate (IM, Gleevec®, Glivec, STI571)	Provided by Dr E. Buchdunger Novartis Pharma, Basel, Switzerland
^{14}C-IM	Provided by Dr E. Buchdunger Novartis Pharma, Basel, Switzerland
Nilotinib (AMN107, Tasigna®)	Provided by Dr E. Buchdunger Novartis Pharma, Basel, Switzerland
^{14}C-nilotinib	Provided by Dr E. Buchdunger Novartis Pharma, Basel, Switzerland

Table 2-4 Table of drugs tested and suppliers

^{14}C-dasatinib (specific activity of 31.9µCi/ml) was stored at $^-$20^{o}C as a stock solution of 20.4mM in DMSO. ^{14}C-IM (specific activity of 84µCi/mg) was stored at 4^{o}C as a stock solution of 100mM in dH$_2$0. ^{14}C-nilotinib (specific activity of 100µCi/mg) was stored at 4°C as a stock solution of 1.34mM in PBS. Dasatinib (MW 489) was stored in multiple aliquots at $^-$20^{o}C at a stock solution of 10mg/ml in DMSO. IM (MW 590) was stored at 4^{o}C at a stock solution of 100mM in dH$_2$0. Nilotinib (MW 529.5) was stored at $^-$20°C as a stock solution of 10mM in DMSO.

2.1.5 Specific substrates and inhibitors of drug transporters

Substrate	Supplier
^{3}H-Mitoxantrone	Moravek Biochemicals, Brae, CA, USA
BODIPY-Prazosin	Molecular probes, Eugene, Oregon, USA
Fluo-3 AM	Axxora, Nottingham, U.K
Rhodamine 123	Invitrogen, Paisley, UK

Table 2-5 Table of substrates tested and suppliers

^{3}H-Mitoxantrone (specific activity 4Ci/mmol), the known ABCG2 substrate, was stored at $^-$20°C at a stock solution of 148.17µg/ml in PBS. BODIPY-Prazosin, the known ABCG2 substrate, was stored at $^-$20°C at a stock solution of 250µM in DMSO and used at a final concentration of 200nM. Fluo-3 AM, the known MRP1 substrate, was stored at $^-$20°C, diluted with DMSO and used at a final concentration of 5µg/ml in DMSO. Rhodamine 123, the known MDR1 substrate, was stored at $^-$20°C at a stock solution of 1mg/ml in 100% ethanol and used at a final concentration of 0.5µg/ml.

Inhibitors	Supplier
Fumitremorgin C (FTC)	Axxora, Nottingham, U.K
PSC 833	Gift from Novartis
MK571	Axxora, Nottingham, U.K

Table 2-6 Table of inhibitors tested and suppliers

FTC, the specific ABCG2 inhibitor, was stored at 4°C at a stock solution of 10mM

in DMSO and used at a final concentration of 10µM. PSC 833, the MDR1 inhibitor,

was stored at $^-$20°C at a stock solution of 10mM in DMSO and used at a final

concentration of 5µM. MK571, the specific MRP1 inhibitor, was stored at $^-$20°C at

a stock solution of 10mM in dH$_2$0 and used at a final concentration of 30µM in

K562 and CML CD34$^+$ cells and 100µM in the transduced MRP cell line (K-MRP).

2.1.6 Cell lines

Cells	Disease	Supplier
AML3 (OCI-AML3)	AML	Donated by Dr B. Sorrentino (St Jude Children's Research Hospital, Memphis, USA)
AML3.3 (OCI-AML3 transfected to over-express *ABCG2*)	AML	Donated by Dr B. Sorrentino (St Jude Children's Research Hospital, Memphis, USA).
AML6.2 (OCI-AML3 transfected to over-express *ABCG2*)	AML	Donated by Dr B. Sorrentino (St Jude Children's Research Hospital, Memphis, USA)
HL60	APML	Donated by Dr J. Mountford (Royal Infirmary, Glasgow, UK) ATCC$^®$ no. CCL-240
HL60-BCRP (HL60 transfected to over-express *ABCG2*)	AML	Donated by Dr J. Mountford (Royal Infirmary, Glasgow, UK)
K562-WT (K-WT)	CML BC	Donated by Dr L. Fairbairn (Paterson Institute for Cancer Research, Christie Hospital NHS Trust, Manchester, UK) ATCC$^®$ no. CCL-243
K562-MDR-GFP (K-MDR: K562-WT	CML BC	Donated by Dr L. Fairbairn (Paterson Institute for Cancer

| transfected to over-express *MDR1* and GFP) | | Research, Christie Hospital NHS Trust, Manchester, UK) and generated as described (Southgate *et al.* 2006). |
| K562-MRP-GFP (K-MRP: K562-WT transfected to over-express *MRP1* and GFP) | CML BC | Donated by Dr L. Fairbairn (Paterson Institute for Cancer Research, Christie Hospital NHS Trust, Manchester, UK) and generated as described (Southgate *et al.* 2006). |

Table 2-7 Table of cell lines used and suppliers

2.1.7 Tissue culture media

2.1.7.1 RPMI/ 10% FCS/ 1% L-glutamine (RPMI medium)

RPMI 1640	500ml
FCS	50ml
L-glutamine (200mM)	5ml

2.1.7.2 Serum-free medium (SFM)

IMDM	77.4ml
BIT	20ml
Penicillin (5000u)/ streptomycin (5mg/ml) solution	1ml
L-glutamine	1ml
ß-mercapto-ethanol (200mM)	200µl (400µM)
LDL (10mg/ml)	400µl (40µg/ml)
Filter sterilised	

2.1.7.3 Serum-free medium supplemented with growth factor cocktail medium (5GF)

	Volume	Final concentration
SFM	10ml	
IL-3 (50µg/ml)	4µl	20ng/ml
IL-6 (50µg/ml)	4µl	20ng/ml
Flt-3L (50µg/ml)	20µl	100ng/ml
G-CSF (20µg/ml)	10µl	20ng/ml

SCF (50µg/ml)	20µl	100ng/ml

2.1.7.4 Differentiation media

	Volume	Final concentration
SFM	10ml	
G-CSF (20µg/ml)	2.5µl	5ng/ml
IL-3 (50µg/ml)	0.2µl	1ng/ml
Epo (1000U/ml)	10µl	1U/ml
rHu-Tpo (5µg/ml)	1µl	5ng/ml
GM-CSF (10µg/ml)	3µl	30ng/ml

2.1.8 Buffers and solutions

2.1.8.1 Annexin buffer

Annexin 10x buffer	1ml
IMDM	9ml

2.1.8.2 Fix perm wash - PBS/ 1% BSA/ 0.1% Azide

BSA	10g
Sodium Azide	1g
PBS	To 1L

2.1.8.3 Freezing solution- for CML samples

HSA 4.5%	8ml
DMSO	2ml

2.1.8.4 Freezing solution- for cell lines

FCS	8ml
DMSO	2ml

2.1.8.5   Lysis buffer -PBS/ 0.2M NaOH/ 1%v/v SDS

NaOH	8g
SDS	10g
PBS	To 1L

2.1.8.6 PBS/ 2% FCS (PBS/2%)

PBS	98ml
FCS	2ml

2.1.8.7 PBS/ 20% FCS (PBS/20%)

PBS	80ml
FCS	20ml

2.1.8.8   PBS buffer- PBS/ 2mM EDTA/ 0.5%v/v HSA

EDTA	2mM
HSA	2.5ml
PBS	To 500ml

2.1.8.9 Thawing solution for cryopreserved CD34^{+} or unmanipulated cell aliquots from liquid nitrogen (DAMP)

	Volume	Final concentration
PBS	418.75ml	
Tri-sodium citrate (0.155M)	53ml	8.2mM
HSA 20%	25ml	1%
DNase I (~2500U/vial (1ml)	2ml	10U/ml
MgCl$_2$ (400x, 1.0M)	1.25ml	2.5mM

2.1.8.10   Wash buffer

DMEM	90ml
FCS	10ml

Table 2-8 Composition of buffers and solutions

2.1.9 Primers and probes for RT-PCR

ABCG2:

forward (ABCG2F): 5'-TGG CTG TCA TGG CTT CAG TA-3'

reverse (ABCG2R): 5'- GCC ACG TGA TTC TTC CAC AA-3'

probe (ABCG2P):   5'-AGC AGG GCA TCG ATC TCT CAC CCT G –3'

Actin:

forward (ACTINF):   5'-CGT GAT GGT GGG CAT GGG TCA G-3'

reverse (ACTINR): 5'-CTT AAT GCT ACG CAC GAT TTC C-3'

2.2 Cell handling and selection

2.2.1 Cell lines

The cell lines were grown in suspension culture in RPMI media. The cells were maintained at 10ml in 25cm^3 tissue culture flasks and passaged every two days by removing ¾ (7.5ml) of the volume and replacing with warm fresh media to maintain a density of between 1×10^5-1×10^6.

2.2.2 Normal CD34$^+$ cells

For qPCR analysis, RNA (1μg aliquots) derived from normal CD34$^+$ cells isolated from mobilized PB (mPB), was purchased from Cambrex Bioscience (Wokingham, United Kingdom) and Stem cell Technologies UK (Vancouver, Canada) and stored

at $^-80^o$C. In addition CD34$^+$ cells were obtained from patients with non-stem cell haematological malignancies (e.g. non-Hodgkin's lymphoma or multiple myeloma) and were classed as 'non-CML' cells and used as comparisons. These cells were isolated and selected as for the CML CD34$^+$ counterparts and stored in liquid nitrogen.

2.2.3 Selection of CD34$^+$ cells from CML samples

All samples were collected with the approval from the Local Research and Ethics Committee and with written informed patient consent from patients at diagnosis of chronic phase CML. Each sample was determined to be Ph$^+$ by FISH and BCR-ABL$^+$ by PCR. Cells were collected by leukapheresis prior to any drug treatment. Enrichment for CD34$^+$ cells was achieved using the sterile CliniMACS system (Miltenyi Biotech, Surrey, UK), which positively selects for CD34$^+$ cells and was performed by the stem cell banking unit within the research group. Briefly, micro magnetic MACS beads coupled with anti-CD34$^+$ monoclonal antibody (Miltenyi Biotec, Germany) were added to the sample, which in turn bound to the sample. The sample was then passed through a magnetic field where the target cells were retained in the column and the unlabelled cells flushed through and discarded. The bound cells were then eluted after removal from the magnetic field, collected and stored in cryotubes within the vapour phase of liquid nitrogen until required.

2.2.4 Freezing cells

Between $2x10^6$-$2x10^7$ CD34$^+$ selected cells and $5x10^6$-$1x10^7$ cell-line cells were resuspended in the appropriate freezing solution and aliquoted into cryotubes. The cryotubes were cooled overnight in a polystyrene box at $^-80^o$C to provide a

controlled temperature reduction and then transferred to the vapour phase of liquid nitrogen for storage.

2.2.5 Recovering frozen cells

CML cells were removed from liquid nitrogen and immediately thawed at $37^{o}C$ in a water bath until most of the ice crystals had melted. The cells were then recovered by slowly adding 10ml of thawing solution (DAMP) drop-wise over a 20 mins period with constant agitation to prevent clumping of the cells. The cells were spun at 1,000rpm for 10 mins, the supernatant was poured away and the pellet loosened by flicking. The pellet was then washed twice in DAMP and centrifuged, then resuspended in 5GF media for counting and cell viability. The CML cells were then plated in 35mm non-adherent tissue culture dishes at $\sim2x10^{6}$/ml.

Cell lines were thawed in a $37^{o}C$ water bath and recovered slowly as above but in PBS/2%. The cells were then washed twice more with PBS/2% and resuspended in 10ml of RPMI media, then plated in $25cm^{3}$ tissue culture flasks.

2.2.6 Cell counting and viability assessment

All cell counts were performed on a Hawksley BS.748 improved Neubauer counting chamber (Weber Scientific International, West Sussex, UK). The cells were counted using trypan blue exclusion. Trypan Blue was diluted at 1:10 with PBS. Ten µl of the diluted solution was then added to 10µl of the cell suspension (1:1 dilution). Approximately 15µl of the mixture was transferred to a haemocytometer. Cells that have damaged membranes are porous and absorb the trypan blue dye, so appear with a distinctive blue colour under the microscope where as the cells with an intact membrane do not absorb the dye. Hence, the

unstained cells were counted and the remaining stained dead cells were deemed non-viable.

2.3 Flow Cytometry

Flow Cytometry is a quantitative technique that permits the visualisation of cells by multiple parameters using fluorescent emissions. In comparison to spectrophotometry, it is capable of measuring fluorescence per cell, hence allowing accurate analysis of single cells. All the flow cytometric analyses were carried out on a Becton Dickinson FACSCalibur.

Following antibody staining (section 2.3.1), the cells were visualised with either a linear or log scale, as appropriate, on a forward scatter (FSC) vs. side scatter (SSC) dot plot. FSC detects cell size whilst SSC determines cytoplasmic granularity. The resulting dot plot view allowed the live cells to be distinguished from the smaller debris and dead cells (Figure 2-1A). When required, the smaller debris and other cell populations were excluded from further analysis by drawing a gate around the key live population using the flow cytometry software palette. The cells within this graphical boundary formed the basis for all further analysis.

The cells were then visualised either in a log scale FL1 (FITC) vs. FL2 (PE) dot plot or a histogram (Figure 2-1B). Isotype controls were used to determine the emission of non-specific binding and these cells were positioned in the first log decade of the parameter(s) by altering the voltage settings. Additionally, positive controls were required to compensate for spectral overlap between the fluorochromes using the compensation settings. This was achieved by subtracting as a percentage, the fluorescence observed in the detector that should not emit

fluorescence. This allocates the cells in the bottom right hand and top left hand corners of the FACS dot plot according to the fluorescent conjugate used (Figure 2-1C). Once the flow cytometer was optimally compensated, the test samples were run and the percentages of the discrete population calculated. At least 10,000 of viable gated cells were collected in all experiments.
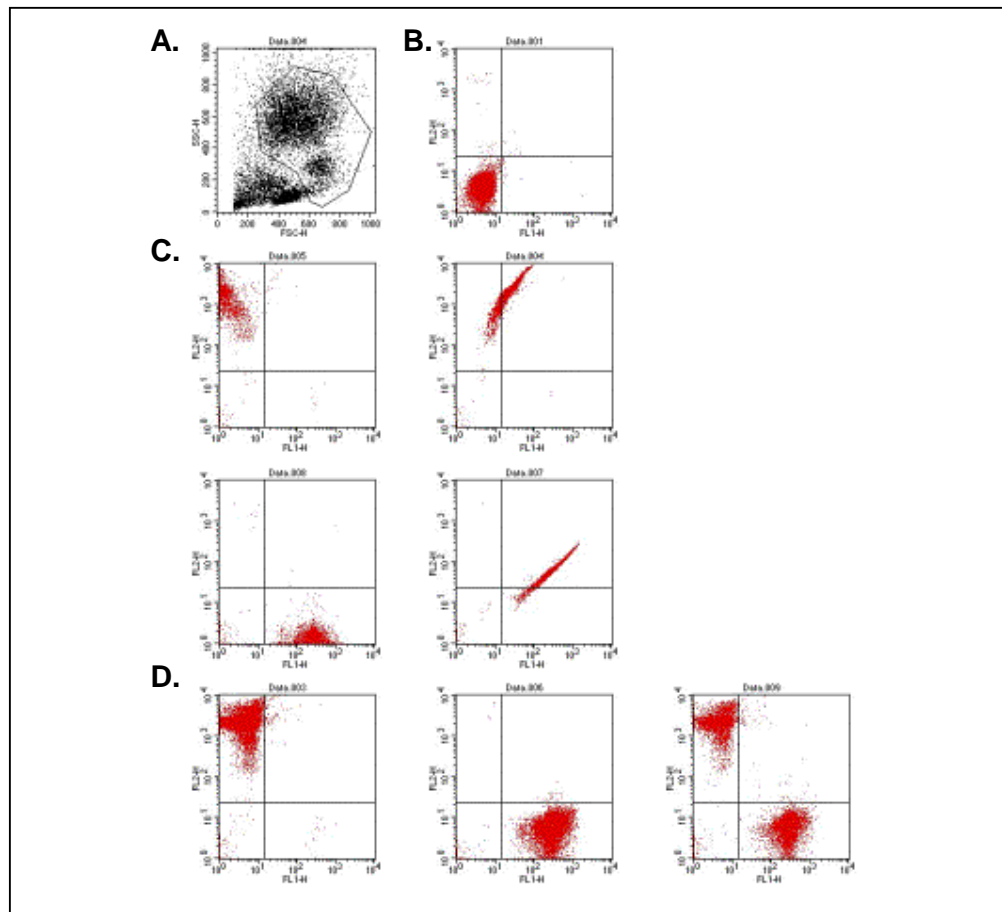
Figure 2-1 Analysis of a flow cytometry plot

A. A FSC vs. SSC dot plot showing the cellular composition of BM. **B.** The gated cells stained with isotype FITC and PE shown on FL1 vs. FL2 dot plot. Using the voltage settings the cells were positioned in the first decade of the parameters. **C.** Uncompensated PE staining (panels 1 and 2) and uncompensated FITC staining (panels 3 and 4). **D**. Compensated PE staining with all the cells positioned in the top left corner, within the first parameter of FL1 (panel 1), compensated FITC staining with all the cells in the bottom right hand corner within the first parameter of FL2 (panel 2), dual staining of FITC and PE (panel 3)

2.3.1 Detection of surface receptors

Prior to any experiments, all samples were confirmed as ≥97% CD34$^+$ and negative for glycophorin A or lymphoid markers (Table 2-9). Briefly, the appropriate antibody conjugated to a fluorochrome was added to 1×10^5 cells at 1:100 dilution for 20 mins at room temperature, then washed twice in PBS/2% and spun at 1000rpm for 10 mins, then resuspended in FACS flow solution.

In addition live populations were gated using PI by staining at 1µg/ml for 5 mins prior to the washing stage of antibody staining to discriminate dead cells. Cells with damaged porous membranes absorb PI, which then binds to DNA by intercalating between the bases. Hence, unstained cells with impermeable membranes were viable and subsequently gated for analysis in the FL3 channel, which detects PI.

Antibody	Target cell(s)	Dilution
CD3	T-lymphocytes	1:100
CD11b	Monocytes, granulocytes	1:100
CD19	B-lymphocytes	1:100
CD13	Monocytes, granulocytes	1:100
CD14	Monocytes	1:100
CD34	Haemopoietic progenitor	1:100
CD45	Leucocytes	1:100
CD61	Megakaryocytes	1:100
Glycophorin A	Erythroid cells	1:100

Table 2-9 Table of surface antibodies used for identification of cell populations

2.3.2 Detection of intracellular receptors

2.3.2.1 Detection of intracellular protein

Using the Fix & Perm® Cell Permeabilisation kit, the cells were permeabilised and stained according to the manufacturer's instructions. Briefly 1×10^5 cells were resuspended in 100µl of fixing reagent (reagent A) from the fix & perm kit and incubated for 15 mins. The cells were then washed in 3ml of fix perm wash, centrifuged at 1200rpm for 3 mins, blotted, and resuspended in 100µl of permeabilising reagent (reagent B) from the kit, with either 1µl (1 in 100 dilution) of the primary monoclonal antibody to MDR1 (C219), or MRP1 (QCRL-3), or 0.875µl (1 in 125 dilution) of the primary monoclonal antibody to ABCG2 (BXP-21), or the equivalent dilution of the isotype control for 1hr. The cells were washed in fix perm wash and spun at 1200rpm for 3 mins twice, then resuspended in 100µl of fix perm wash with the secondary antibody (anti-mouse IgG2a FITC conjugate, i.e. 0.875µl for ABCG2 or 1µl for MDR1 or MRP1) and incubated at room temperature in the dark for 30 mins. The cells were again washed twice with fix perm wash and analysed by flow cytometry.

2.3.2.2 CrkL phophorylation by flow cytometry

There is no specific antibody that is able to detect the activity of BCR-ABL. However, it is known that one of the prominent downstream substrates constitutively phosphorylated by the BCR-ABL oncoprotein is the 39kD adaptor protein CrkL. This protein is the major tyrosyl phoshophoprotein detected in CML neutrophils and it has been shown that CrkL phosphorylation is inhibited in a concentration dependent manner when CML cells are treated with IM, correlating

with BCR-ABL phosphorylation. The specificity of CrkL phosphorylation to BCR-ABL may therefore be used to indirectly assess the status of this oncoprotein.

The rabbit anti-human phospho-CrkL (p-CrkL) antibody used for this assay detected endogenous levels of CrkL only when it was phosphorylated at tyrosine 207, the BCR-ABL phosphorylation site. Measuring the difference in the geometric mean (GM) of p-CrkL peaks determined the effect of the treatments on the inhibition of BCR-ABL.

Samples for analysis of p-CrkL levels were prepared by permeabilisation and staining using the Fix & Perm® Cell permeabilisation kit as above (section 2.3.2.1), but with minor modifications. Following resuspension with 100µl fixing reagent, the cells were resuspended in 25µl of permeabilising reagent with 2.5µl of the p-CrkL antibody for 1hr. The cells were washed twice and resuspended in 100µl fix perm wash with 2µl of the secondary anti-rabbit IgG FITC conjugate and incubated at room temperature in the dark for 30 mins. In addition $1x10^5$ HL60 cells were treated alongside the test population and used as BCR-ABL negative controls.

2.3.3 Assessment of apoptosis and necrosis

For analysis of cell death, cells were incubated with 5µl annexin V-FITC and 10µl Viaprobe in 100µl annexin buffer for 15 mins in the dark. The cells were then topped with 400µl annexin buffer and read by flow cytometry within the hour to identify necrotic (Viaprobe detected in FL-3) and apoptotic (Annexin V detected in FL1) cells.

2.3.4 Substrate displacement assay

The activity of drug transporters may be determined by measuring transport of specific fluorescent compounds against concentration gradients. Using flow cytometry, the GM for each resulting histogram can be used as a measure of fluorescence to calculate the efflux values. Cells with an inactive efflux transporter will retain the fluorescent compound resulting in a higher fluorescent GM compared to cells with an active efflux transporter. Conversely, cells with an active transporter will have decreased dye retention. The addition of a competing substrate or an inhibitor in these cells would then reduce the efflux of the known substrate resulting in an increase in fluorescence and hence confirming active efflux. Similarly, if the addition of a test compound, i.e. drug, also increased the fluorescence, then it can be assumed that the compound is interacting with the protein either as a competitive substrate or inhibitor (Figure 2-2).

To measure the function of transporters, the assay was based on a previously published efflux assay (Robey *et al.* 2001a), but with minor modifications. Approximately $1x10^6$ cells were resuspended in wash buffer ± inhibitor or ± drug and incubated in a water bath at 37°C for 15 mins. This provided the opportunity for the action of the drug and inhibitors on the transporters to take effect. The fluorescent compound was then added and incubated for a further 30 mins at 37°C for ABCG2 or 1hr for MDR1 and MRP1 (a final concentration of 200nM BODIPY-prazosin, 0.5μg/ml Rhodamine or 5μg/ml Fluo-3 AM for ABCG2, MDR1 or MRP1 respectively). This loading step allowed the cells to take up the fluorescent compound and establish uptake and efflux in the cells if present.
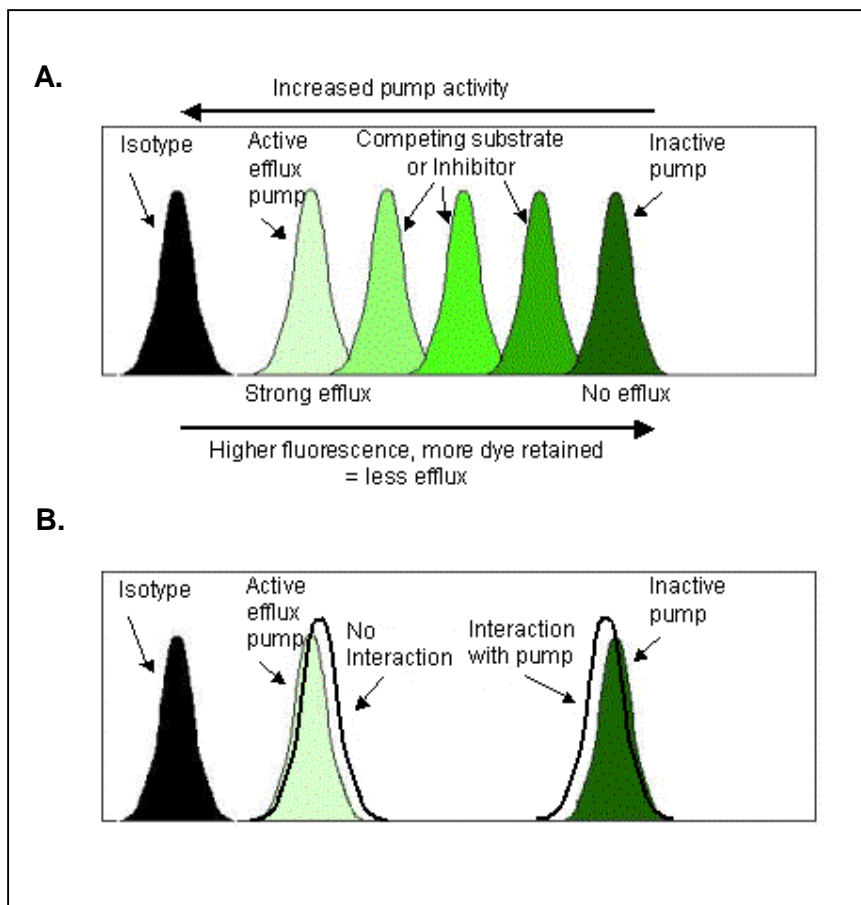
Figure 2-2 Substrate displacement assay

Schematic diagram demonstrating the substrate displacement assay. **A.** Cells with an inactive transporter retain the fluorescent substrate (dark green), cells with an active transporter efflux the substrate and have low fluorescence (light green). The addition of a competing substrate or inhibitor at increasing concentrations reduces the efflux and increasingly retains the dye (progressively darker green). **B.** Replacing the known competitive substrate or inhibitor with the test compound (i.e. TKI) will determine no interaction (i.e. not an inhibitor or a competitive substrate), as shown by plot overlaying the active efflux transporter or an interaction with the transporter (i.e. an inhibitor or a competitive substrate), as shown by the increased fluorescence.

The cells were then washed in ice-cold wash buffer to stop the loading, spun for

10 mins at 1000rpm, resuspended in 1ml wash buffer +/- drug +/- inhibitor and

incubated for 60 mins for ABCG2 or 90 mins for MDR1 and MRP1 at 37°C. This

step allowed the active transporters to efflux the compound and the drug and/or

inhibitors to maintain their action on the transporters. The action of the transporters was then stopped by washing in ice-cold medium and centrifuging at 1000rpm for 10 mins. The cells were then placed on ice in the dark and analysed immediately by flow cytometry. All the dyes can be detected in the FL1 channel. Debris was eliminated by gating around the viable cell population on FSC vs. SSC dot plot and at least 10,000 viable events were collected.

2.4 Cellular techniques

2.4.1 Tracking of CD34$^+$ cells

2.4.1.1 Carboxy-fluorescein diacetate succinimidyl ester (CFSE) staining

CFSE is an intracellular fluorescein-based dye that permits the tracking of stem cell divisions. This is due to the intensity of the fluorescent stain within a cell partitioning equally between the daughter cells with each cell division, thereby allowing the identification of every cell division by tracking the decreasing brightness. Figure 2-3A shows the intensity of CFSE halving with each cell division and Figure 2-3B the subsequent FACS histogram identifying the 'fingers', which each represent a cell division.

Following successful thawing and recovery of cells (section 2.2.5) and resuspension in PBS/2%, a stock solution of 5mM CFSE (in DMSO) was diluted at 1 in 10 dilution with PBS/2% and added to 5ml of cells at a final concentration of 1μM. The cells were then incubated in a water bath at 37°C for exactly 10 mins (as the staining is time dependent). The cells were immediately diluted with 10x volume of ice-cold PBS/20% in order to stop the staining reaction and the cells centrifuged for 10 mins at 1000rpm. The supernatant was discarded and the cells

washed in fresh PBS/2%, then resuspended in 5GF at a concentration of $2x10^6$/ml

and incubated overnight in 35mm non-adherent tissue culture dishes (at 37^oC in

5% CO_2) to allow the excess dye to leach out of the cells.
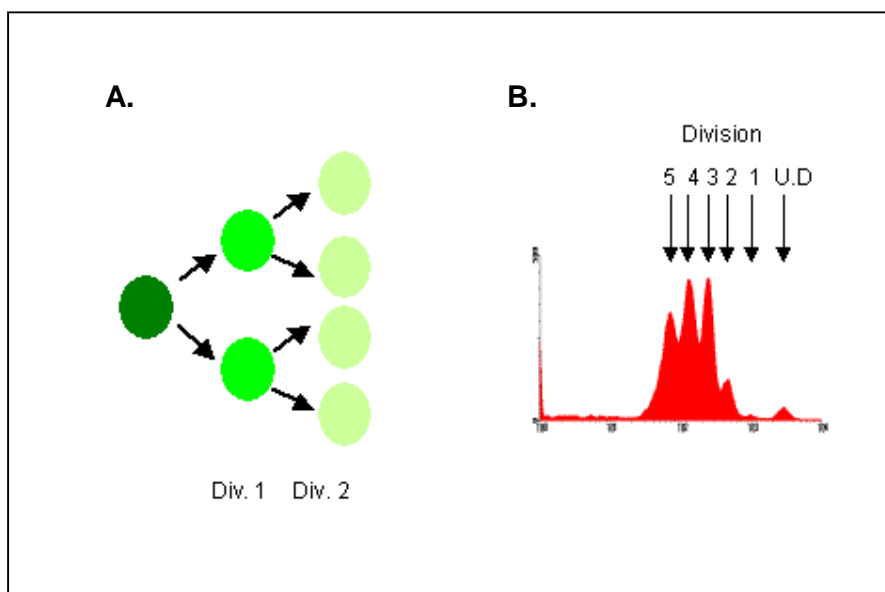
Figure 2-3 Tracking a cell with CFSE stain

A. A schematic diagram of the brightness of the CFSE stain in a cell halving in the daughter cells with each division. **B.** A histogram of a FACS plot showing the classic 'fingers' pattern with the undivided cells showing the highest fluorescence and the intensity halving with each division. A single peak can be gated to determine the percentage of cells in the total population that have undergone the equivalent number of divisions. [U.D=undivided]

2.4.1.2 Cell division tracking with CFSE

After CFSE staining and overnight incubation, 500µl of cells at $2x10^5$/ml were

aliquoted into a 48-well plate ($1x10^5$ per well). The conditions included TKI alone,

TKI +/- drug transporter inhibitors, drug transporter inhibitors alone, an untreated

control, an unstained control (i.e. no CFSE staining) and 100ng/ml colcemid®. The

plate was then incubated for 72hrs (at 37^oC in 5% CO_2).

Following 72 hrs incubation, each well was resuspended in PBS/2%, counted and then stained with the CD34-PE antibody and PI for analysis by flow cytometry. The cells treated with colcemid® were used to identify the position of the undivided population on the FACS plot and the untreated cells to differentiate the position of each division. The region gates were then positioned such that the fluorescence intensity was halved with each cell division. The cells unstained for CFSE were used to alter the voltage settings and optimally compensate for spectral overlap.

2.4.1.3 Calculation of cell recovery

Following 72 hrs treatment, the effect of TKIs on cell survival and proliferation was determined. The viable cell population was initially gated in FSC vs. SSC dot plots and PI staining eliminated any dead cells. By selecting the cell population (R10) (Figure 2-1A) that are also PI negative (R9) (Figure 2-4B) and plotting these on a third dot plot, the upper right quadrant (R1) represents the percentage of viable cells that are CD34$^+$ (Figure 2-4C).

A histogram plotting these viable cells (i.e. those in R1 and R9 and R10) identified the quiescent population and subsequent division peaks. The undivided region was guided by the colcemid® control and the subsequent regions spanning the peaks were positioned by halving the GM according to the halving of the CFSE fluorescence intensity. The percentage of viable cells that were undivided and CD34$^+$ (R2) could then be measured. Similarly, cells that had undergone one division, two divisions etc could also be measured (R3, R4, R5 etc) (Figure 2-4D).
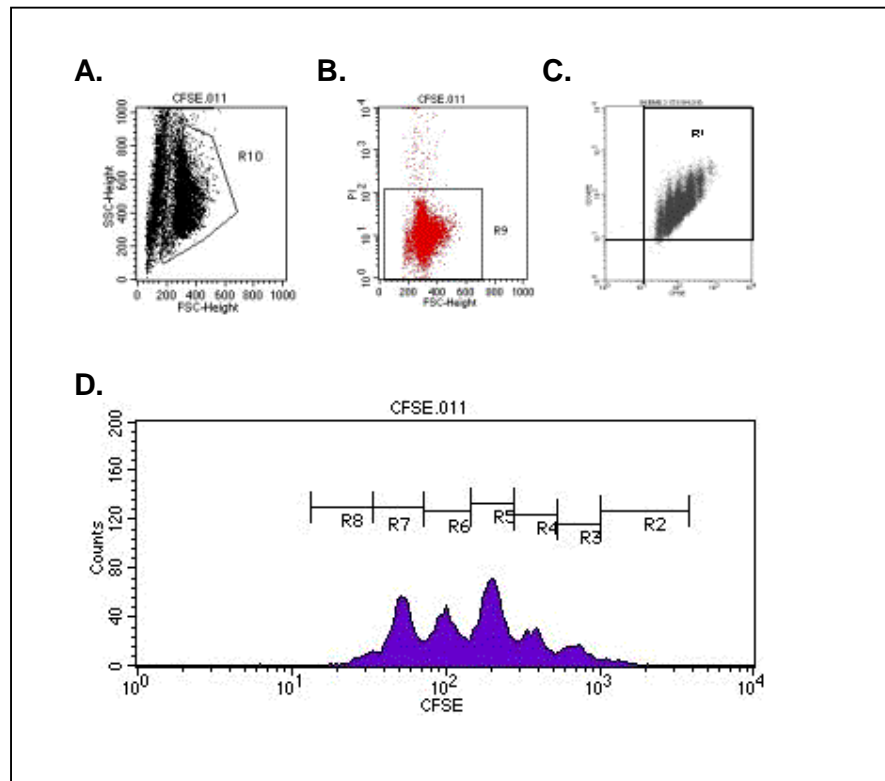
Figure 2-4 Gates and regions used for calculation of cell recovery

A. A FSC vs. SSC FACS dot plot gating on the live population (R10). **B.** A FSC vs. FL3 FACS dot plot presenting only the cells in R10. The gate eliminated any additional apoptotic or necrotic cells that were positive for PI staining (R9). **C.** A FL1 vs. FL2 FACS dot plot presenting only the cells that were in R10 and R9. **D.** A histogram presenting only the cells that were in R10 and R9 and R1. The separate peaks represent cells divisions. Each peak may be separated by a separate region. Region 2 (R2) represents cells that are undivided, R3 represent cells that have undergone 1 division, R4 represent cells that have undergone 2 divisions etc.

The percentages of cells, after 72 hrs treatment, recovered from the starting population in each division, were calculated as below.

$$\left(\frac{\% \text{ in region x total no of viable cells}}{\text{No of input cells}} \right) \times 100$$

The percentage of total viable CD34$^+$ cells recovered in each division was calculated by dividing the absolute number of CD34$^+$ cells in a division region by the total number of starting cells and then multiplying by 100.

In addition, the above calculations were repeated for the total number of viable cells (i.e. CD34$^+$ and CD34$^-$). This was achieved by expanding the gate in Figure 2-4C (R1) to encompass the upper right and lower right quadrant.

2.4.2 Long term cell proliferation

Following successful recovery from frozen and overnight incubation (section 2.2.5) 500µl of 2x10^5/ml cells were plated in a 48 well plate and incubated +/-10µM FTC in 5GF media. On day 4 and day 7, the wells were split by removing half the media from the surface ensuring the cells in the dish that have settled on the well bed were not disturbed and replenished with equal amounts of fresh 5GF media +/- 10µM FTC. The cells were counted and analysed for CD34$^+$ expression by surface staining on days 4, 7 and 10.

2.4.3 Long term cell differentiation

Following successful recovery from frozen and overnight incubation (section 2.2.5) 1ml of 2x10^5/ml cells were added to a 24 well plate and incubated +/-10µM FTC in 5GF media for 3 days. The cells were then harvested with PBS/2% and spun for 10 mins at 1000rpm, then resuspended in 4mls of differentiation media and the resuspended cells were split into 2 wells. On day 7, the wells were again split at 1:1 by removing 1ml media from the surface ensuring the cells that have settled on the well bed were not disturbed and replaced with 1ml fresh differentiation media.

The cells were then analysed by flow cytometry on day 10 with antibodies against surface markers that would be present on differentiated cells.

2.5 Biochemical techniques

2.5.1 Determination of cellular drug levels.

To directly determine the activity of TKIs with regard to drug transporters, specific substrates and TKIs may be labelled with radiolabelled isotypes and the cellular concentration measured by scintillation counting. An accumulation of radiolabelled drugs, in the presence of specific inhibitors, in comparison to the absence of inhibitors, would suggest that the drug might be a substrate of the protein. No difference in the presence or absence of specific inhibitors however would suggest that the drug is not a substrate for the transporter (Figure 2-5A).

Similarly, adding known substrates with radiolabelled isotypes in the presence of TKIs would determine if these drugs are inhibitors of these drug transporters. An increase in the level of specific radiolabelled substrates in the presence of a TKI would suggest it is an inhibitor of the transporter (Figure 2-5B).
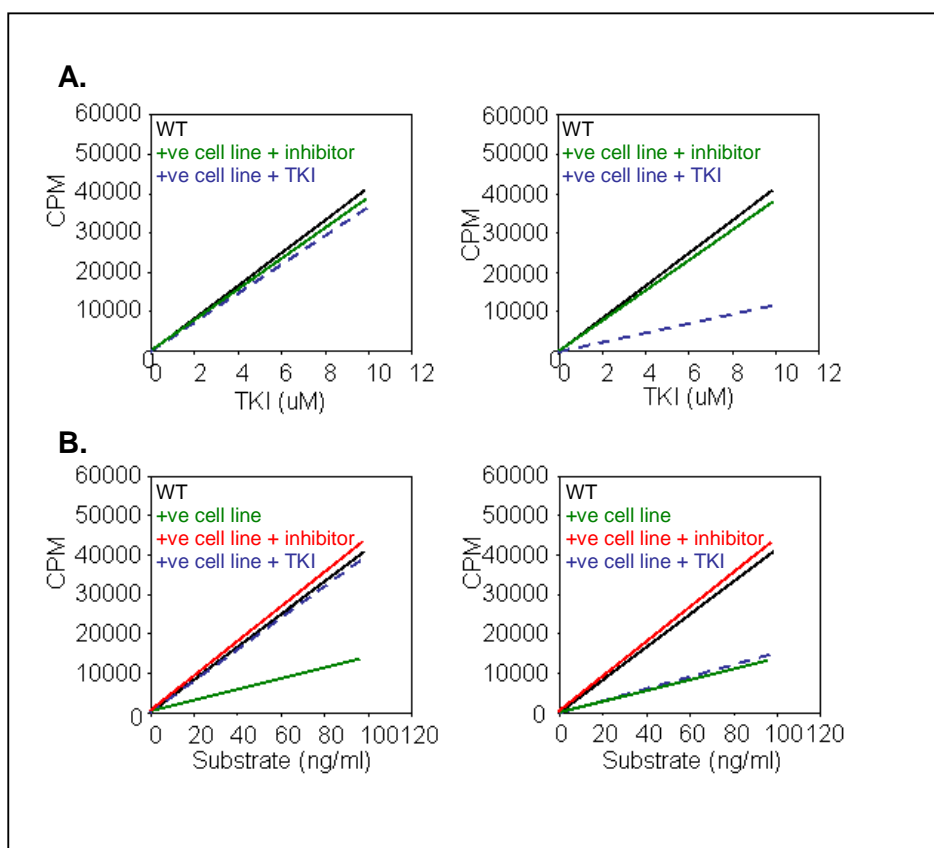
Figure 2-5 Radiolabelled assays to determine interaction of TKI

A. Radiolabelled assay to determine if TKI is a substrate of an efflux transporter using parental (WT) and transduced (+ve cell line) cell lines. The cellular concentration of TKI increases relative to the increasing TKI concentration in the parental cell line (black). Similarly the overexpressing cell line with the specific inhibitor will demonstrate similar CPM (green) with increasing TKI concentration. A similar degree of CPM in the overexpressing cell line in the absence of the specific inhibitor will determine that the TKI is not a substrate (panel 1, dashed blue). In contrast a reduced accumulation of TKI in the overexpressing cell line in the absence of a specific inhibitor will determine that the TKI is a substrate (panel 2, dashed blue). **B.** Radiolabelled assay to determine if TKI is an inhibitor of an efflux transporter using parental (WT) and transduced (+ve cell line) cell lines. The cellular concentration of substrate increases relative to the increasing substrate concentration in the parental cell line (black). The overexpressing cell line will have a much reduced accumulation of the substrate (green), which will be returned to a concentration similar to the parental cell line in the presence of the specific inhibitor (red). A similar degree of CPM in the overexpressing cell line with the specific inhibitor when it is replaced with the TKI will determine that the TKI is an inhibitor (panel 1, dashed blue). In contrast no increase in accumulation in the overexpressing cell line in the presence of TKI will determine that the TKI is not an inhibitor (panel 2, dashed blue).

2.5.1.1 Standard curve of radiolabelled drug

To determine the efficiency of the scintillation counter in detecting the isotopes, a standard curve measuring the counts per minute (CPM) against increasing concentrations of radiolabelled drug were prepared. In the scintillation vials, 500µl of radiolabelled drug were added in increasing concentrations with 3ml of scintillant fluid, mixed well, and counted on a Microbeta TriLux scintillation counter (Perkin Elmer, Wellesley, MA, USA). The results were plotted on Sigma plot software and analysed using GraphPad Prism software to provide a standard curve, which in turn allowed the interpolation of unknown amounts of drug in cell pellets.

2.5.1.2 Radiolabelled inhibitor assay

The cells ($5x10^5$ cell lines or $1x10^5$ CML CD34$^+$) were resuspended in 500µl wash buffer and initially incubated at 37°C for 15 mins +/- inhibitor to allow the action of the inhibitor to take effect. Following incubation, 500µl of ^{14}C-IM, ^{14}C-nilotinib or ^{14}C-dasatinib was added at the desired concentration +/- inhibitor and the cells were incubated for a further 1hr to allow loading and effluxing of drug from the cells. The cells were then washed three times in ice-cold PBS/2% to stop the activity of the protein and spun at 2000rpm for 3 mins. The pellet was then resuspended in 100µl dH$_2$0, vortexed briefly and 200µl lysis buffer was added and incubated for 1hr at 37°C to solubilise the cells and release the drug. The lysed cells were then placed in 4ml scintillation vials with 3ml of scintillant Beta phase Optimix, mixed well, and the CPM measured by the Microbeta TriLux scintillation counter. Each determination was carried out in triplicate within a single experiment.

2.5.1.3 Radiolabelled substrate assay

As above, the cells (5x10^5 cell lines or 1x10^5 CML CD34$^+$) were resuspended in 500µl wash buffer and incubated at 37°C for 15 mins +/- inhibitor +/- drug to allow the action of the inhibitor and drug to take effect. Following incubation 500µl of ^{3}H-mitoxantrone was added at the desired concentration +/-drug +/- inhibitor. The cells were incubated for a further 1hr to allow loading and effluxing of the specific radiolabelled substrate. The cells were then washed three times in ice-cold PBS/2% to stop the activity of the protein and spun at 2000rpm for 3 mins. The pellet was then resuspended in 100µl dH$_2$0, vortexed briefly and 200µl lysis buffer was added and incubated for 1hr to solubilise the cells and release the substrate from the cells. The lysed cells were then placed in 4ml scintillation vials with 3ml of scintillant Beta phase Optimix and the CPM measured by the Microbeta TriLux scintillation counter. Each assay was carried out in triplicate.

2.6 Molecular techniques

2.6.1 Cell pellets for storage

Following successful thawing or after drug treatment, cells that were required for subsequent RNA extraction were washed twice in PBS and spun at 8,000rpm for 2 mins. The pellet was then briefly air-dried and snap-frozen in liquid nitrogen for 20 secs. The resulting pellet was stored at $^-$80°C until further use.

2.6.2 RNA synthesis

Total RNA was isolated from pellets using the RNeasy Mini Kit (Qiagen, Crawley, United Kingdom) according to the manufacturer's instructions. The resulting RNA

was quantitated using a nanodrop spectrophotometer Nd-1000 (Labtech International, East Sussex, UK). An absorbance at 260nm quantified nucleic acid and the ratio of 260/280 determined purity (pure RNA ratio is 2.0).
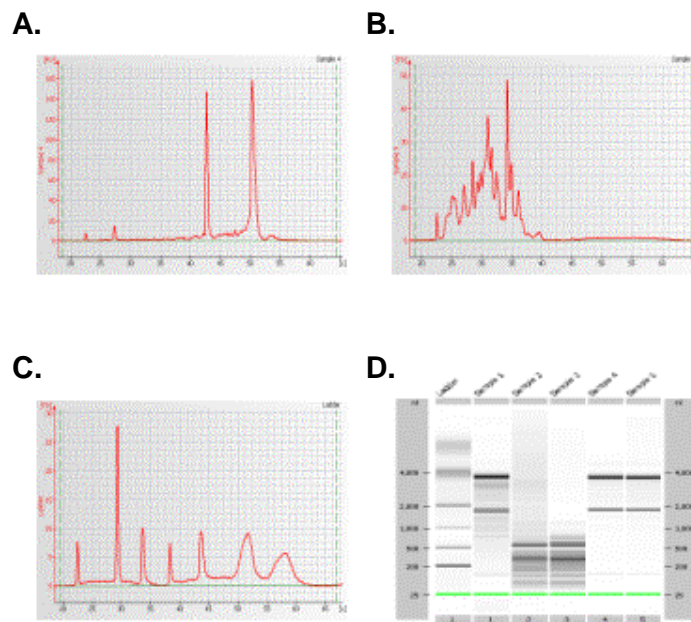
Figure 2-6 Agilent images

An electropherogram plot of a good quality **(A)** or degraded **(B)** RNA and ladder **(C)**. The same data represented as a gel image **(D)**. Lane 1 represents the ladder and lanes 2-6 represent samples. Samples 2 and 3 show degradation, samples 4 and 5 show good quality RNA, sample 1 demonstrates a little degradation.

The integrity of the RNA was observed on a DNA600 LabChip™ kit using the Agilent 2100 Bioanalyser (Agilent Technologies, Wokingham, United Kingdom). This system allowed rapid separation of fragments according to their size by molecular sieving through the microchannels of the well. These fragments were detected by fluorescence at the detection point and the data was displayed either as a gel like image or an electropherogram plot (Figure 2-6) .The chip was prepared for sample loading by spinning a gel dye mix through a spin filter and

injected into the loading well of the chip. One µl of denatured sample was loaded (each chip can analyse 12 samples in each run) along with an upper and lower marker, and a ladder marker. Each run was completed in 30 mins. Two clean bands on the gel indicated good quality RNA. Multiple bands indicated the RNA had degraded.

2.6.3 cDNA synthesis

RNA that was deemed of good quality was synthesised to cDNA either by the Superscript II reverse transcriptase kit and random hexamers (Invitrogen, Paisley, U.K) or by the High Capacity cDNA Archive kit (Applied Biosystems, Warrington, U.K) according to the manufacturer's instructions.

2.6.4 Conventional RT-PCR for analysis of ABCG2 expression

Diane Gilmour, a colleague from Glasgow Royal Infirmary, Glasgow, carried out all the conventional PCR.

PCR primers (Sigma-Genosys, Haverhill, United Kingdom) for the analysis of *ABCG2* expression were as described previously (section 2.1.9). The PCR conditions used were the following: $94°C$ for 3 mins, followed by 40 cycles of $94°C$ for 45 secs, $55°C$ for 30 secs, $72°C$ for 90 secs, final extension of $72°C$ for 10 mins, yielding an amplified product of 202 base pairs (bp).

Correction for loading of RNA and PCR efficiency was achieved by β-actin, an endogenous control gene. The PCR reaction conditions were the following: $94°C$ for 2 mins, followed by 35 cycles of $94°C$ for 1 mins, $58°C$ for 45 sec, $72 °C$ for 1 mins, final extension of $72°C$ for 5 mins to yield an amplified product of 500bp.

2.6.5 Quantitative RT-PCR for analysis of ABCG2 expression

Diane Gilmour carried out the real-time PCR for the analysis of *ABCG2* expression using single primers and probes.

The mRNA levels of *ABCG2* and the endogenous reference gene glyceraldehyde-3-phosphate dehydrogenase (*GAPDH*) were measured using the ABI PRISM 7900HT sequence detector (Applied Biosystems (ABI), Warrington, U.K). The *ABCG2* PCR products were detected using a probe containing a FAM reporter and TAMRA quencher. For the GAPDH reaction VIC replaced FAM. The *GAPDH* mRNA levels were measured using the pre-developed Taqman Assay reagents for human GAPDH (Applied Biosystems, Warrington, U.K).

Two μl of the first strand reaction was used as template and added to 300nM of forward and reverse ABCG2 primers and 200nM of probe, made to a total volume of 50μl with qPCR Mastermix Plus (Eurogentec, Southampton, UK). Each reaction was carried out in triplicate. Samples were run on the ABI PRISM 7900 with the following reaction conditions: 50°C for 2 mins, 95°C for 10 mins followed by 40 cycles of 95°C for 15 sec and 60°C for 1 mins. The relative expression levels of ABCG2 were calculated using the validated $2^{-\Delta\Delta CT}$ method to calculate the relative expression.

2.6.6 Quantitative RT-PCR by Taqman Low Density Array technology

The expressions of transporter genes were measured using Taqman® Low Density Array (TLDA) cards (Applied Biosystems, Warrington, U.K) (Figure 2-7). TLDA

cards are micro fluidic cards that allow 384 reactions to run simultaneously. Each well contains custom-made lyophilised primers and probes and are all supplied by 8 ports in total, with each port delivering mastermix and cDNA to 48 wells in a total reaction volume of 2µl. The plate may be designed to detect from a minimum of 12 genes in quadruplicate, to 384 genes (including 3 endogenous controls) singly.
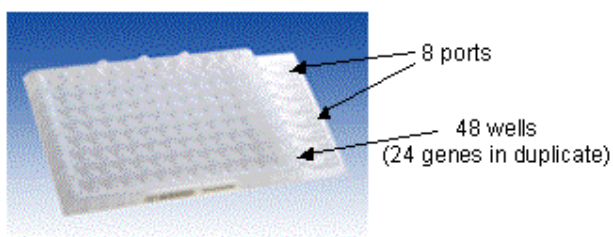
Figure 2-7 TLDA card

The cDNA required for the Taqman was synthesised from 100ng of RNA and prepared to a total volume of 50µl. This was then added in equal volume to the Taqman universal master mix (Applied Biosystems, Warrington, U.K) and 100µl pipetted into each loading port. The plate was then spun twice at 1200rpm for 1min, sealed and placed into the ABI PRISM 7900HT real-time PCR system.

The genes of interest for this project were chosen, ordered and preloaded from a database of ~47,000 optimised human, mouse and rat assays (http://www.appliedbiosystems.com). The customised TLDA card ordered had 24 genes in duplicate and included all the available drug transporters, genes for stem cells and an array of endogenous controls. The list is in table 2-1.

Gene	Alternative name(s)	Assay ID	NCBI gene ref.
18S		18S	N/A
ABL1		Hs00245443_m1	NM_005157
ABCB1	MDR1, P-gp	Hs00184491_m1	NM_000927
ACTB	β-actin	Hs99999903_m1	NM_001101
ABCC1	ABCC, MRP1	Hs00219905_m1	NM_004996
ABCC4	MOAT-B, MRP4	Hs00195260_m1	NM_005845
ABCG2	ABCP, BCRP, MXR	Hs00184979_m1	NM_004827
AKT1	PKB, RAC-α	Hs00178289_m1	NM_001014431
BCR		Hs00244731_m1	NM_004327
CASP3		Hs00234385_m1	NM_004346
CD34		Hs00156373_m1	NM_001025109
CD38		Hs00233552_m1	NM_001775
GAPDH		Hs99999905_m1	NM_002046
HIF1A	HIF-1α	Hs00153153_m1	NM_181054
PROM1	CD133	Hs00195682_m1	NM_006017
SLC22A1	OCT1	Hs00427554_m1	NM_003057
SLC22A2	OCT2	Hs00161893_m1	X98333
SLC22A3	OCT3	Hs00222691_m1	NM_021977
SLC22A4	OCTN1	Hs00268200_m1	NM_003059
SLC22A5	OCTN2	Hs00161895_m1	NM_003060
SLC22A6	OAT1	Hs00191220_m1	NM_153276
SLC22A7	OAT2	Hs00198527_m1	NM_153320
SLC22A8	OAT3	Hs00188599_m1	NM_004254
SLC22A9	OAT4	Hs00375768_m1	NM_080866

Table 2-10 A table of genes included on the TLDA card with their alternative names, assay ID and NCBI gene reference

2.7 Statistics

The results are shown as the mean +/- standard error (s.e) values unless otherwise stated. Differences between treatments in samples were assessed using paired student's t-test while differences between groups that were not linked were assessed using normal student's t-test. A level of $p \leq 0.05$ was deemed significant.

3 Results 1- ABCG2 in CML CD34$^+$ cells

There is a population of persisting stem cells in CML that is likely to be responsible for the MRD detected in the majority of IM treated patients (Bhatia *et al.* 2003) and it has been shown that increasing the IM concentration against CML CD34$^+$ cells does not eliminate the primitive quiescent cells *in vitro* (Graham *et al.* 2002). It has been hypothesised that this may be due to sub optimal intracellular drug concentrations, because of the activity of drug resistance proteins, including ABC proteins (Hegedus *et al.* 2002).

ABCG2 mRNA expression has been observed in normal HSCs and in particular in cells in the G_0/G_1 phase of cell cycle. As described in section 1.1, HSCs can be recognised using flow cytometry by their appearance as a small side population (SP) of cells, evident by their ability to exclude Hst. This was found to be attributable to ABCG2 activity (Zhou *et al.* 2001), thus identifying ABCG2 as an important molecular marker for the SP phenotype and the most primitive stem cell associated transporter.

ABCG2 expression has also been shown in AML, although evidence relating to the level and correlation with disease relapse has been conflicting. Elevated levels of ABCG2 have been shown to be attributable to a small subpopulation rather than the homogeneous expression of the whole population, suggesting *ABCG2* expression is predominantly restricted to LSCs (Abbott *et al.* 2002).

However, although *ABCG2* is expressed in AML and normal HSCs, it has not been previously shown if *ABCG2* is expressed on primitive CML CD34$^+$ cells. To date there has only been an indication of an unidentified transporter other than MDR1

or MRP1 mediating resistance in CML MNCs (Carter *et al.* 2001). Hence, the following studies were designed to:

1.   determine the expression of *ABCG2* in CML CD34$^+$ cells

2.   confirm the function of ABCG2 in CML CD34$^+$ cells

3.   identify whether the current TKIs are substrates or inhibitors of ABCG2

4.   ascertain the effect of ABCG2 in the treatment of CML HSCs with TKIs

3.1 Expression of *ABCG2* mRNA

The expression of *ABCG2* was first investigated in CML CD34$^+$ cells using semi-quantitative RT-PCR. Distinct bands in all the CML samples tested (n=8) were shown in Figure 3-1A panel 1, with bands of the same size as that seen in the positive controls AML3.3 and AML6.2 (two transduced AML cells expressing *ABCG2* at low and high levels respectively) and placenta, a naturally high expressing tissue. In panel 2, the signals from CML CD34$^+$ cells were shown to be stronger compared to normal mPB CD34$^+$ cells, suggesting that CML CD34$^+$ may have higher levels of *ABCG2*. To confirm, the experiment was replicated using sensitive Taqman$^®$ technology, with single probes and primers, designed specifically to isolate and amplify the *ABCG2* gene. Human placenta was again used as a positive control and *GAPDH* as the endogenous reference gene. As shown in Figure 3-1B, a signal was detected at an earlier cycle in the CML samples in comparison to normal PB indicating a higher level of mRNA expression.

A.

B.

C.
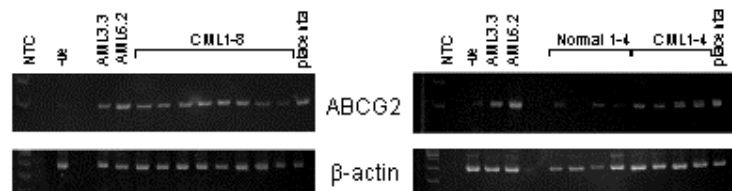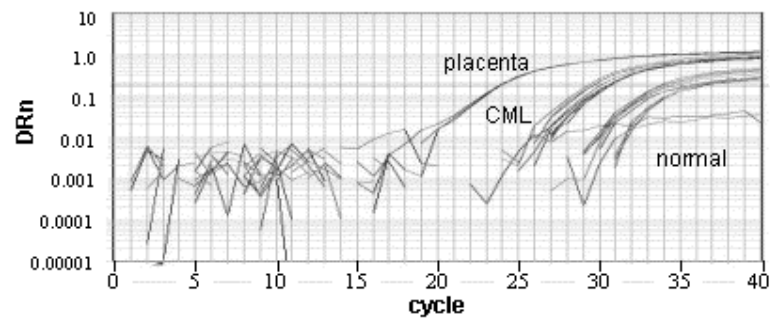
ΔCT Normal	ΔCT CML
14.51	11.25
13.47	12.94
16.95	12.50
16.04	13.11
	11.22
	14.60
	11.71

Figure 3-1 Expression of *ABCG2* mRNA in CML CD34+ cells

Expression of *ABCG2* mRNA in normal and CML CD34+ cells. **A.** Semi-quantitative PCR assay of cDNA synthesised from mRNA from two transduced cell lines, AML3.3 and AML6.2; CD34+ cells from 4 normal controls and from 8 CML CD34+ cells. NTC- no template control. All samples were positive for β-actin control. Samples 1-4 in left panel were included in the set of 1-8 in right panel. **B.** Taqman amplification plot of placenta (n=2 in duplicate), CML and normal samples (n=4 in duplicate). **C.** Mean ΔCT of all CML and normal samples tested by taqman technology. All samples were tested in duplicate.

The advantage of the qPCR over the semi-quantitative PCR is the ability to relatively quantify the gene in one sample and compare it to another sample. This is independent of the initial amount of starting material as the amount of gene in the sample is quantified relative to the amount of endogenous gene present. This provides a relative value that may then be used to compare samples and accurately determine differing expression. This comparative crossing threshold method is achieved by subtracting the endogenous control Ct (cycle number at which the curve intersects the threshold) from the target gene Ct (in this case *ABCG2*) to give a ΔCt (Figure 3-1C). To obtain a comparison between samples, the ΔCt of the calibrator sample (in this case a normal mPB CD34$^+$ sample) is calculated and then subtracted from the ΔCt value of the target sample (CML CD34$^+$) to give ΔΔCt. The resulting number is then used as the power figure in the equation $2^{-\Delta\Delta Ct}$ to give expression levels of normalised *ABCG2* in CML CD34$^+$ in comparison to the normal samples (Figure 3-2).

ΔCt =   Ct [gene] - Ct [endogenous control]
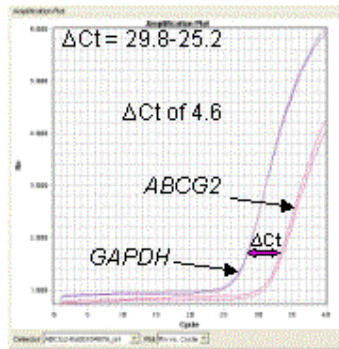
ΔΔCT=   ΔCt [target sample] - ΔCt [calibrator sample]
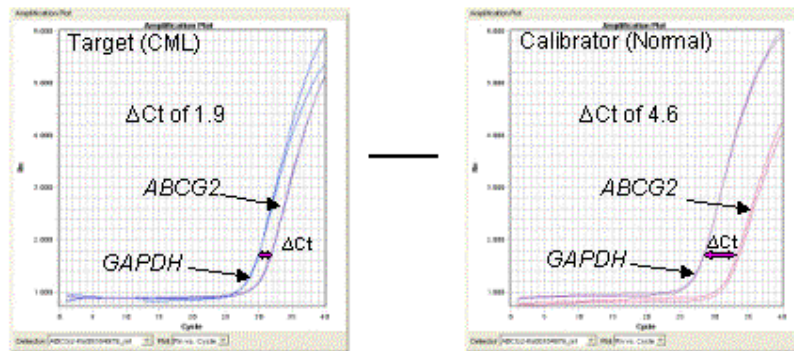
$2^{-\Delta\Delta Ct}$ =   Expression level of target sample in relation to calibrator

sample

$RQ^{-(2.7)}$ =   6.5 fold greater in target (CML) compared to calibrator (normal)

Figure 3-2 A representative example of the calculation for relative quantification

Using the equation above, data from 7 CML and 4 normal samples resulted in mean ΔCt values of 15.2±0.8 and 12.5±0.5 respectively (p<0.01) and a ΔΔCt of 2.76. Using the equation $2^{-\Delta\Delta Ct}$ this assay determined that CML CD34^{+} cells expressed 6.8 fold more *ABCG2* than their normal counterparts (Figure 3-3).
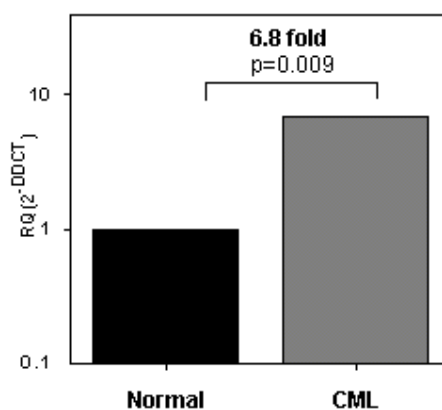
Figure 3-3 Expression of *ABCG2* mRNA expression in CML CD34^{+} cells relative to normal CD34^{+} cells

Relative quantification ($2^{-\Delta\Delta CT}$) of *ABCG2* expression in CML CD34^{+} cells (dark grey fill; n=8 in dupicate) compared to normal CD34^{+} cells (black fill; n=4 in duplicate).

3.2 Expression of ABCG2 protein

CML samples were also tested for protein expression using the specific antibody BXP-21. This antibody has been generated against an N-terminal intracellular epitope (Maliepaard *et al.* 2001) and hence requires permeabilisation of the cell membrane in order to access the epitope. The BXP-21 antibody was initially optimised by comparing the staining in the HL60 cell line transduced with ABCG2 (HL60-BCRP), a cell line in which approximately 60% of the cells express ABCG2, against a wild type control (HL60-WT) that does not express ABCG2. Serial dilutions of the antibody established that a 1:125 dilution of the antibody followed by the same dilution of the secondary antibody produced the most distinct peaks (Figure 3-4).
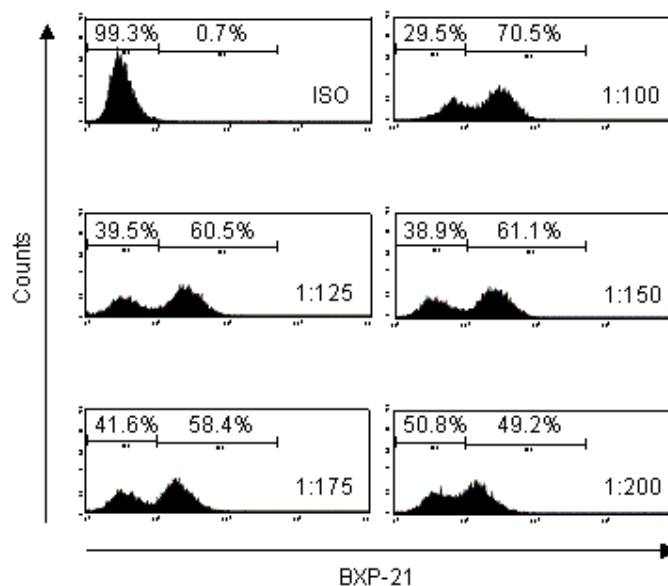
Figure 3-4 Optimisation and validation of the ABCG2 antibody BXP-21

Increasing dilutions of the ABCG2 antibody BXP-21 in HL60 cell line transduced to over-express ABCG2 in 60% of the cells (HL60-BCRP). Panel 1 represents cells stained with the FITC isotype. Panels 2-6 illustrate increasing dilutions of the BXP-21 antibody and resulting percentages. A dilution of 1:125 produced the optimal segregation in the two populations.

Following optimisation, the assay was carried out in parental AML3 (ABCG2-ve) (Figure 3-5A) and transduced AML6.2 (ABCG2+ve) (Figure 3-5B) cells. A significant increase in fluorescence was shown in the transduced cells (AML6.2-isotype geometric mean (GM)=4.3 vs. AML6.2-BXP21 GM=12.7) demonstrating protein expression.

A.

B.

C.
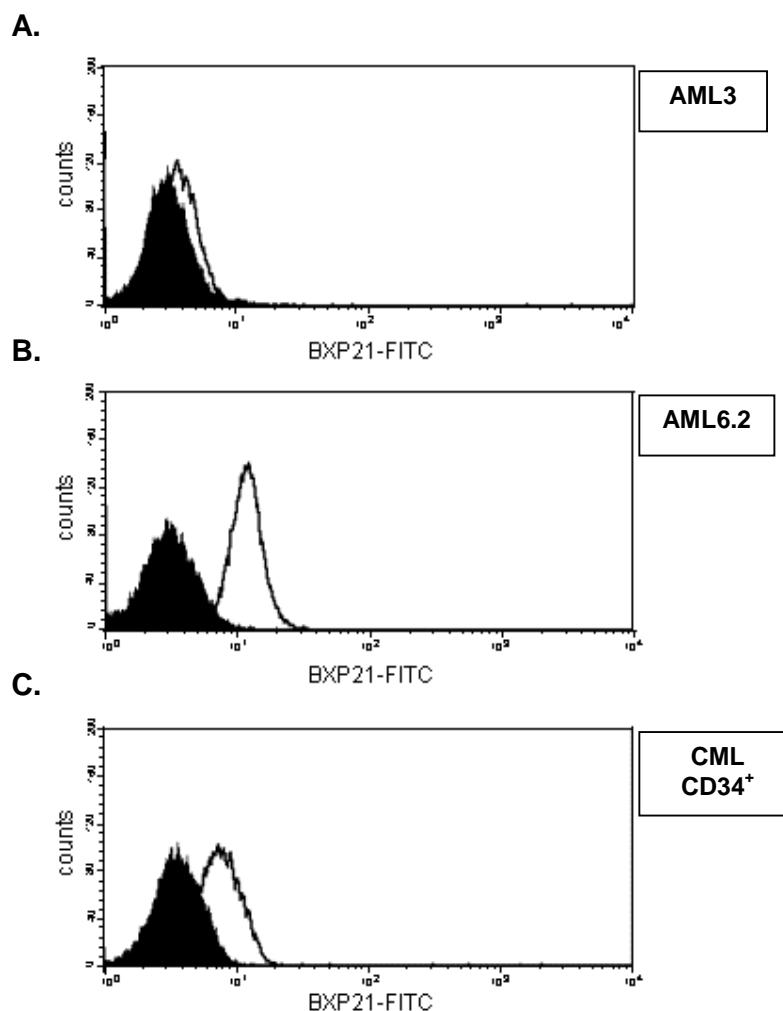
Figure 3-5 Expression of ABCG2 protein in cell lines and CML CD34$^+$ cells

A representative example of ABCG2 protein expression in AML3 **(A)**, AML6.2 **(B)** and CML CD34$^+$ cells **(C)** with the isotype (black fill) and the ABCG2 test antibody BXP21 (white fill). n=4 for cell lines, n=7 for CML CD34$^+$ cells. Each sample was run in duplicate and all replicates were consistent.

The protein expression of ABCG2 was then measured in 7 CML samples (Figure 3-5C). The staining was positive in all the samples and staining resulted in significantly higher mean fluorescence than the isotype control counterpart (isotype GM=3.8±0.2, BXP 21 GM=7.8±0.8, p<0.002). Furthermore, in 5 of the 7 samples $\geq$25% of the cells (range 25.3-79.0%) were positive for ABCG2 staining

indicating that the increase in fluorescence and subsequent higher GM was not due to a small subpopulation of cells but to an expression of the ABCG2 protein by more than a quarter of the cells.

3.3 Function of ABCG2 protein

It has been previously described that in some cases the level of *ABCG2* mRNA and/or protein expression may not always correlate with function (Suvannasankha *et al.* 2004). Hence the CML CD34^{+} cells were tested in a substrate displacement assay to confirm that the ABCG2 protein was also functional by tracking a fluorescent ABCG2 substrate in the presence or absence of a known inhibitor.

BODIPY-Prazosin is a fluorescent conjugate of the specific ABCG2 substrate, Prazosin (Robey *et al.* 2001a) that can be detected by flow cytometry and FTC is a specific chemosensitising agent isolated from *Aspergillus fumigatus* (J. Antibiotics **49:**527 (1996), that is a specific inhibitor of ABCG2. The combination of specific substrate and inhibitor was used to demonstrate inhibition of functional efflux. This assay was first optimised and validated in cell lines before being conducted in primary CML samples.

The substrate displacement assay was optimised in the parental and transduced cell lines. It was initially established that an incubation period of 15 mins with FTC prior to the addition of BODIPY-Prazosin was required, to allow effective protein inhibition. To determine the optimal concentration of BODIPY-Prazosin, serial dilutions were then added in the transduced AML6.2 cell line. A concentration of 200nM BODIPY-Prazosin resulted in maximal efflux, which in turn was maximally inhibited by 10µM FTC to a similar degree to that of AML3 (Figure 3-6). The significant increase in fluorescence confirmed that ABCG2 was functional in these

cell lines and that this assay could be used to examine the function of ABCG2 in
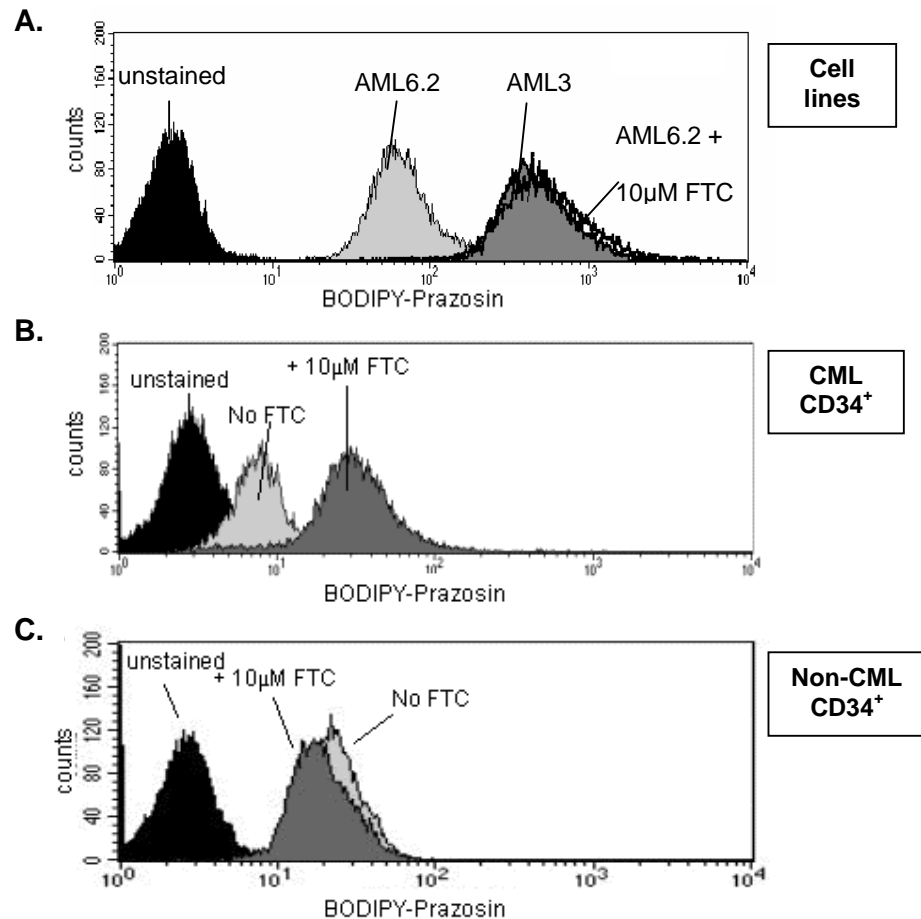
CML CD34$^+$ cells.

Figure 3-6 Function of ABCG2 protein in cell lines and CD34$^+$ cells

ABCG2 function by efflux of a known substrate in a cell line model **(A)**, CML CD34$^+$ cell **(B)** and non-CML CD34$^+$ cells **(C)**. **A.** Unstained cells (black fill), AML6.2 and BODIPY/Prazosin (light grey fill), AML3 and BODIPY/Prazosin (dark grey fill) and AML6.2 and BODIPY/Prazosin with 10µM FTC (black line). **B.** and **C.** Unstained cells (black fill), with BODIPY/Prazosin (light grey fill), with BODIPY/Prazosin and 10µM FTC (dark grey fill).

Six CML patients were tested for function of ABCG2 (Figure 3-6B demonstrates a representative example). In order to reduce inter-experimental variation, cells with 10µM FTC were considered to be maximally loaded with BODIPY-Prazosin and classed as the control condition. The mean data from the 6 CML samples indicated a significant efflux from the cells in the absence of FTC (54.4±19.3% retention in comparison to the control, p=0.04), indicating functional ABCG2 protein. In contrast, no difference in fluorescence was detected in the non-CML samples (n=3), demonstrating no functional ABCG2 in these cells (Figure 3-6C).

3.4 Interaction of IM with ABCG2 protein

The substrate displacement assay was repeated as above but this time the inhibitor FTC was replaced by the TKI IM. This drug was added at increasing concentrations in the parental and transduced cell lines AML3 and AML6.2 to test its effect on the ABCG2 protein. The addition of IM resulted in a dose dependent decrease in efflux of BODIPY-Prazosin. Furthermore, at >0.5µM IM, a similar decrease in reduction was seen to that with 10µM FTC, suggesting that ABCG2 mediated efflux was inhibited by IM at a clinically achievable dose (Figure 3-7A).

The substrate displacement assay was then repeated in CML CD34^{+} cells. The efflux of BODIPY-Prazosin in CD34^{+} cells was inhibited by the addition of therapeutic IM concentrations (Figure 3-7C) with 5µM IM resulting in retention values of 223.5±66.4%, p=0.03, in comparison to the CD34^{+} cells with the substrate alone (54.4±19.3%, Figure 3-7D). Although appearing to result in more retention, the effect observed with IM was statistically similar to that shown with FTC and no significant additive effect resulted from the combination of both drugs.

In contrast, the addition of IM to non-CML CD34$^+$ cells showed no significant retention (Figure 3-7B).
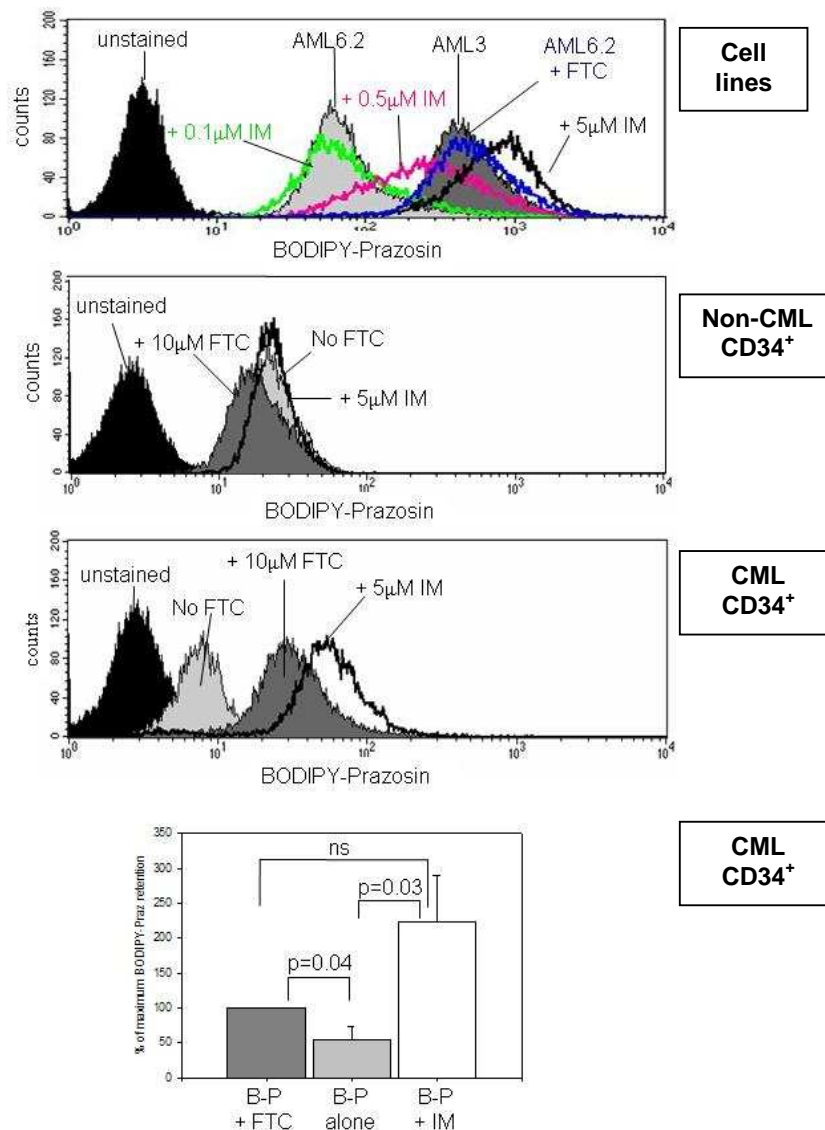
Figure 3-7 Efflux inhibition of an ABCG2 substrate by IM

Interaction of IM with the protein ABCG2 in cell line AML 6.2 **(A)**, non-CML cell **(B)** and CML cells **(C)**. Unstained cells (black fill), with BODIPY-Prazosin (light grey fill), with BODIPY-Prazosin and 10µM FTC (dark grey fill), with BODIPY-Prazosin and 0.1µM (green line), 0.5µM (pink line) or 5µM IM (black line), AML6.2 and 10µM FTC (blue line) **D.** Percentage of efflux by ABCG2. Cells with BODIPY-Prazosin and 10µM FTC (dark grey-fill) were considered to have maximal retention, BODIPY-Prazosin alone (light grey-fill) and BODIPY-Prazosin with 5µM IM (white fill); n=6 in duplicate, ns=not significant.

The interaction of IM with ABCG2 in CML cells suggested that IM may be either acting as an inhibitor by blocking the transporter and hence retaining the substrate within the cell or, alternatively, behaving as a competitive substrate and being preferentially effluxed out of the cell by ABCG2.

3.5 Assessment of IM as a substrate of ABCG2

The substrate displacement assay above demonstrated an interaction of IM with ABCG2, however, it cannot delineate between reduction of efflux by inhibitory activity or as a competitive substrate. Other groups have also investigated the effect of IM, but with conflicting results. Houghton *et al* (Houghton *et al.* 2004) have shown IM to be a potent inhibitor, but not a substrate of ABCG2, where as Burger *et al* (Burger *et al.* 2004) have observed IM to be a substrate for this transporter. The investigations however, were performed in cell lines engineered to over-express ABCG2 that were Ph$^-$ and therefore not responsive to IM.

In order to determine the mechanism of IM binding to ABCG2, the cellular concentration of radiolabelled IM was determined in AML3 (ABCG2-ve) and AML6.2 (ABCG2+ve). A reduction of IM accumulation in the cell line with functional ABCG2 protein would suggest that IM is a substrate, while no difference would determine that IM is not a substrate. There was no significant reduction of ^{14}C-IM in AML6.2 in comparison to AML3 indicating that the presence of ABCG2 in the transduced cell line did not reduce the drug concentration and suggests that IM was not a substrate of ABCG2. The IM in the cell was not altered even with the addition of the specific ABCG2 inhibitor FTC; further confirming that IM was not effluxed by ABCG2 (Figure 3-8A).
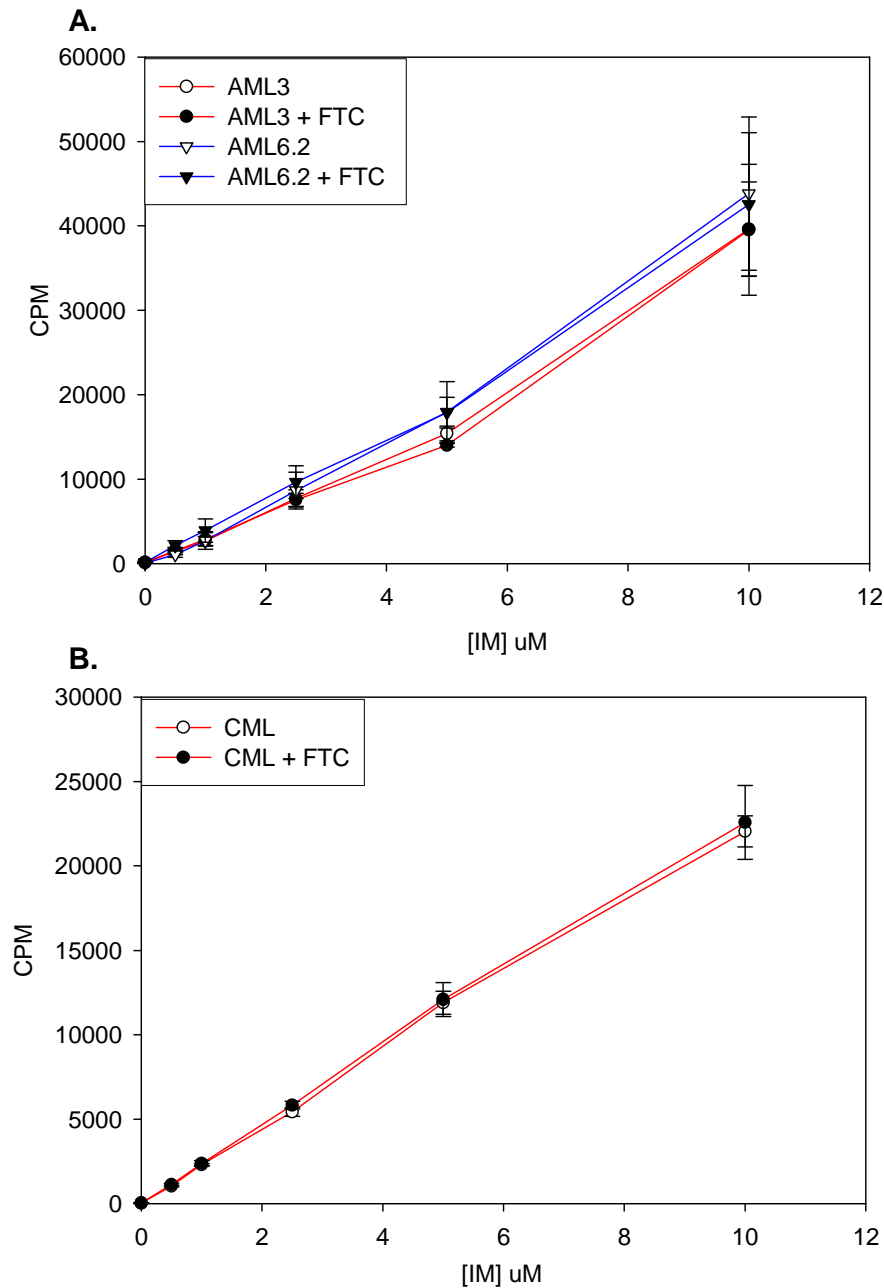
Figure 3-8 Radiolabelled IM in cell lines and CML CD34⁺ cells

Cellular concentration of ^{14}C-IM in cell lines **(A)** and CML CD34⁺ **(B)** cells in the presence and absence of FTC. **A.** ABCG2-ve cell line AML3 (red lines, circles) and ABCG2+ve cell line AML6.2 (blue lines, triangles) in the presence (black symbols) or absence (white symbols) of FTC. **B.** CML CD34⁺ cells in the presence (black symbols) and absence (white symbols) of FTC. All data are mean of duplicate analyses of n=3.

The protocol was then repeated in 3 CML CD34^{+} cells with 5µM ^{14}C-IM and again demonstrated that ABCG2 inhibition by 10µM FTC had no effect on the cellular concentration of IM in these cells (Figure 3-8B), confirming that IM was not a substrate of ABCG2.

3.6 Assessment of IM as an inhibitor of ABCG2

In order to establish whether ABCG2 was an inhibitor of ABCG2, a radiolabelled assay was designed using a specific ABCG2 substrate. Radiolabelled ^{3}H-mitoxantrone was added to the two cell lines AML3 (ABCG2-ve) and AML6.2 (ABCG2+ve) and the level of ^{3}H-mitoxantrone was assessed in the presence and absence of the specific ABCG2 inhibitor, FTC. In AML3 cells, ^{3}H-mitoxantrone accumulated in the cell in a dose dependent manner and as expected the cellular concentration was significantly reduced in the ABCG2+ve cell line (AML3 vs. AML6.2 $p<0.001$ at 50ng/ml and 100ng/ml). As expected, the addition of 10µM FTC, in the ABCG2+ve cell line, restored the concentration of the radiolabelled substrate within the cell to that of the ABCG2-ve cells (AML3 vs. AML6.2 + FTC $p=n/s$, AML6.2 vs. AML6.2 + FTC $p<0.001$ at 50ng/ml and 100ng/ml). When the assay was repeated with 5µM IM instead of the specific inhibitor FTC there was a similar degree of ABCG2 inhibition, with a similar accumulation of ^{3}H-mitoxantrone (AML3 vs. AML6.2 + IM $p=n/s$, AML6.2 vs. AML6.2 + IM $p<0.01$ at 50ng/ml, $p<0.001$ at 100ng/ml) (Figure 3-9A) suggesting that IM was an inhibitor of ABCG2.

Assessment of CML CD34^{+} cells in this protocol produced a similar pattern. The addition of 10µM FTC significantly increased the concentration of mitoxantrone at 100ng/ml (CML vs. CML + FTC $p=0.003$). Replacing the inhibitor with 5µM IM demonstrated similar retention of the mitoxantrone (CML vs. CML + IM $p=0.004$ at

50ng/ml, p=0.01 at 100ng/ml). This increased accumulation of mitoxantrone by the

addition of IM confirmed that IM was an inhibitor of ABCG2 (Figure 3-9B).
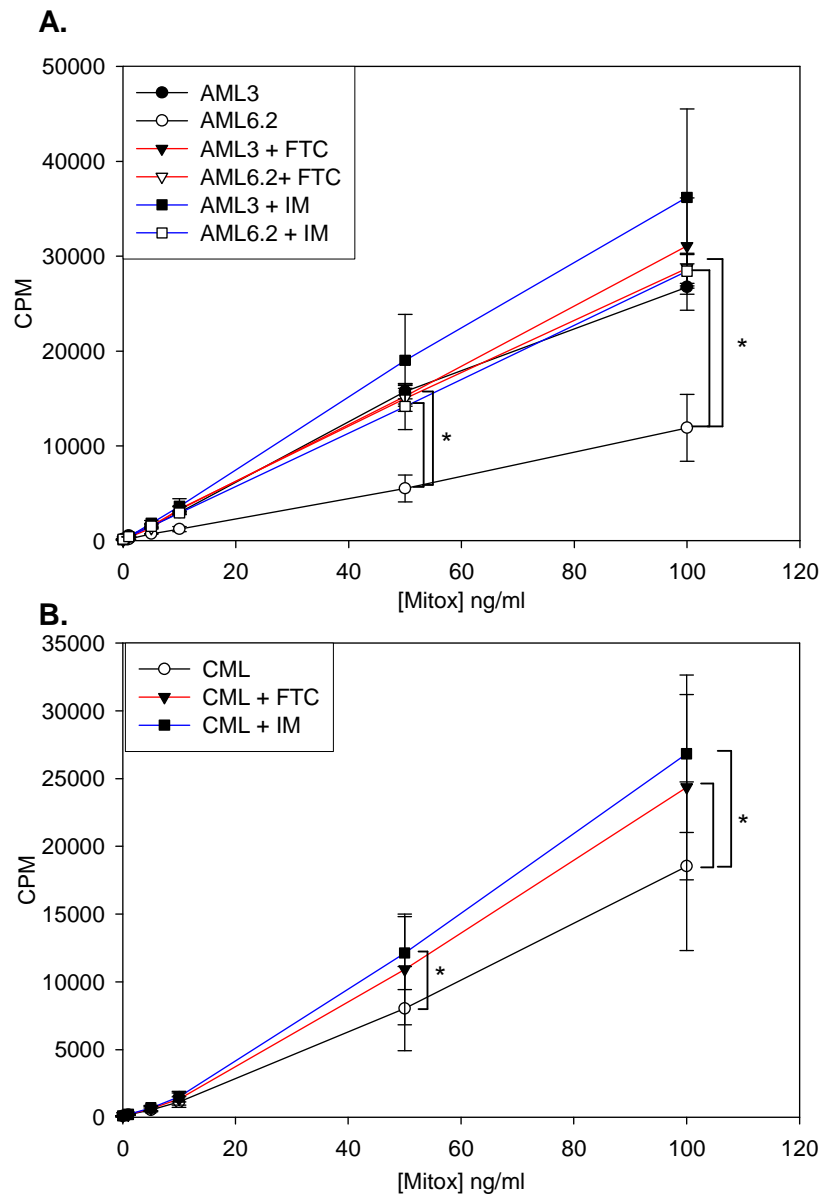
Figure 3-9 Radiolabelled mitoxantrone in cell lines and CML CD34^{+} cells

Cellular concentration of ^{3}H-mitoxantrone in cell lines **(A)** and CD34^{+} **(B)** cells in the presence and absence of FTC or IM. **A**. ABCG2-ve cell line AML3 (black symbols) and ABCG2+ve cell line AML6.2 (white symbols) in the presence of 10µM FTC (red lines), 5µM IM (blue lines) or alone (black lines). **B**. CML CD34^{+} cells with mitoxantrone alone (black line), + 10µM FTC (red line), + 5µM IM (blue line). All data are mean of duplicate analyses of n$\geq$3. *=p$\leq$0.05

3.7 Cellular concentration of IM

By plotting increasing concentrations of radiolabelled IM in scintillant against their corresponding CPM, a standard curve can be generated. The curve can then be extrapolated to predict the cellular IM concentration by generating the equation:

ng= -44.21+0.01629*CPM (as calculated by graphpad prism software)

In CML CD34$^+$ cells, 11899 counts were observed in 5×10^5 cells with 5μM ^{14}C-IM. This equated to a cellular concentration of IM equivalent to 150ng per 5×10^5 cells and represented an uptake of 5.1% of the available ^{14}C-IM in the incubation medium.
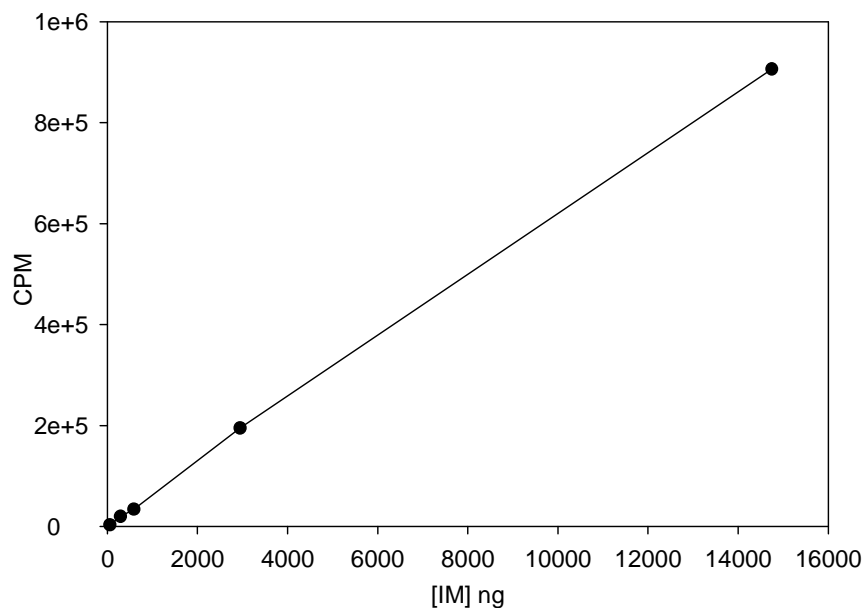
Figure 3-10 Standard curve of radiolabelled IM

Increasing concentrations of ^{14}C-IM in scintillant plotted against counts per minute (CPM)

3.8 Assessment of nilotinib interaction with ABCG2

In addition to the conflicting data in the literature regarding the interaction of IM with ABCG2, there had been no studies to date determining the interaction of the new generation drugs nilotinib or dasatinib with ABCG2. Therefore, the assay using radiolabelled drug was repeated with ^{14}C-nilotinib. As with ^{14}C-IM, no significant difference in the cellular level was demonstrated between the two cell lines, AML3 and AML6.2. Furthermore, the addition of the specific inhibitor FTC did not alter the cellular concentration (Figure 3-11A). This showed that the presence of ABCG2 protein did not reduce the drug concentration, suggesting that nilotinib was not a substrate of ABCG2.

Replacing the cell lines with primary CML cells replicated the cell line results with no difference in cellular nilotinib concentration, confirming that, like IM, nilotinib was not a substrate of ABCG2 (Figure 3-11B).
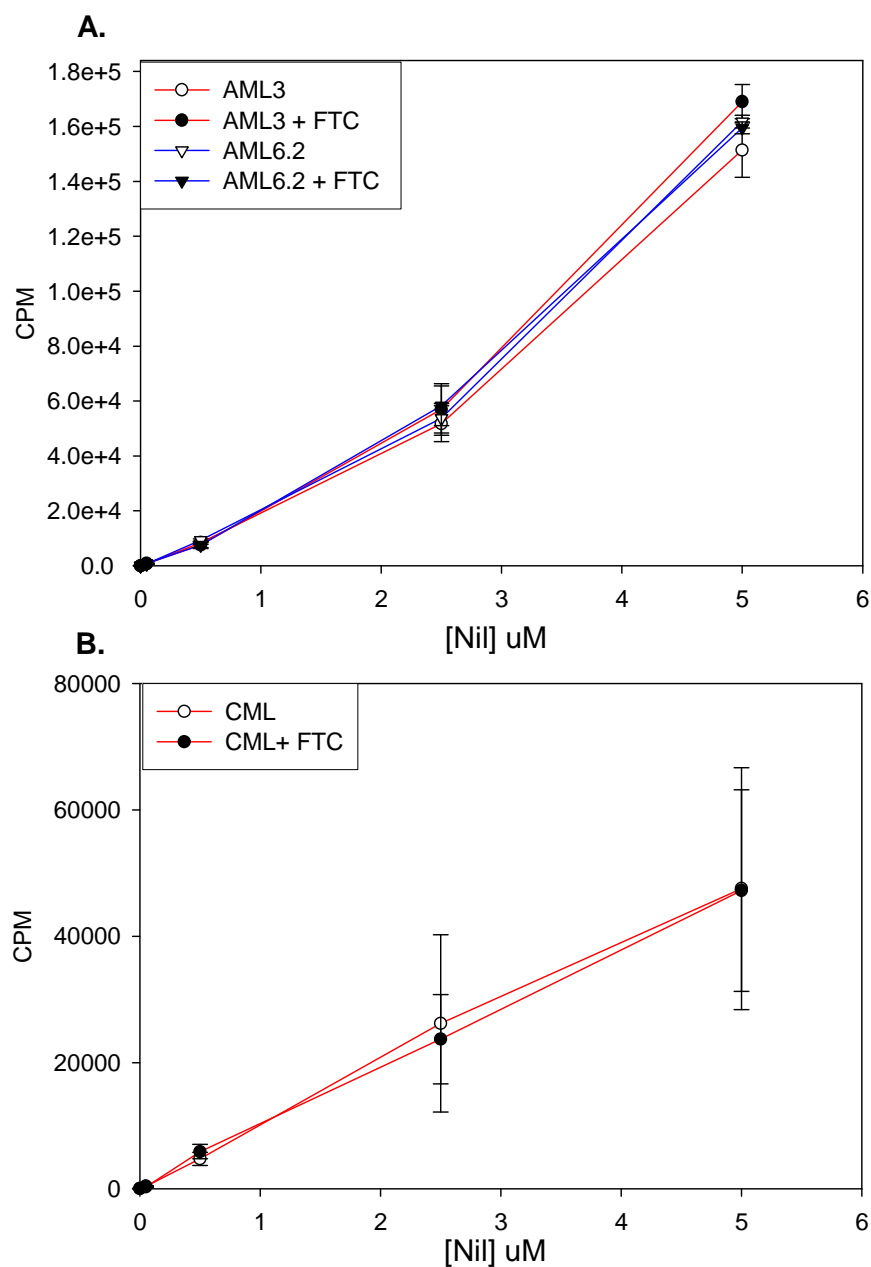
Figure 3-11 Radiolabelled nilotinib in cell lines and CML CD34+ cells

Cellular concentration of ^{14}C-nilotinib in cell lines **(A)** and CML CD34+ **(B)** cells in the presence and absence of FTC. **A.** ABCG2-ve cell line AML3 (red lines, circles) and ABCG2+ve cell line AML6.2 (blue lines, triangles) in the presence (black symbols) and absence (white symbols) of FTC. **B.** CML CD34+ cells in the presence (black symbols) and absence (white symbols) of FTC. All data are mean of duplicate analyses of n=3.

To test whether nilotinib is an inhibitor of ABCG2 the assay with ^{3}H-mitoxantrone was performed. As previously demonstrated, the cellular concentration in the ABCG2+ve cell line was significantly reduced (AML3 vs. AML6.2 $p<0.05$ at 50ng/ml and 100ng/ml). Furthermore, the addition of 10µM FTC not only restored the cellular accumulation but also significantly increased the retention of mitoxantrone in relation to the ABCG2-ve cell line (AML6.2 vs. AML6.2 + FTC $p<0.001$ at 50ng/ml and 100ng/ml), although this was not significantly different to AML3 (AML3 vs. AML6.2 + FTC p=ns). Replacing FTC with 5µM nilotinib also resulted in a significant mitoxantrone accumulation (AML6.2 vs. AML6.2 + nilotinib $p<0.05$ at 50ng/ml, $p<0.001$ at 100ng/ml) suggesting that nilotinib was acting as an inhibitor (Figure 3-12A).

Replacing the cell lines with primary CML cells replicated the pattern generated by the cell lines with significant accumulation by the addition of nilotinib compared to CML alone (p=0.04 at 100ng/ml). This confirmed, that, like IM, nilotinib was not a substrate of, but an inhibitor for ABCG2 (Figure 3-12B).

A.

B.
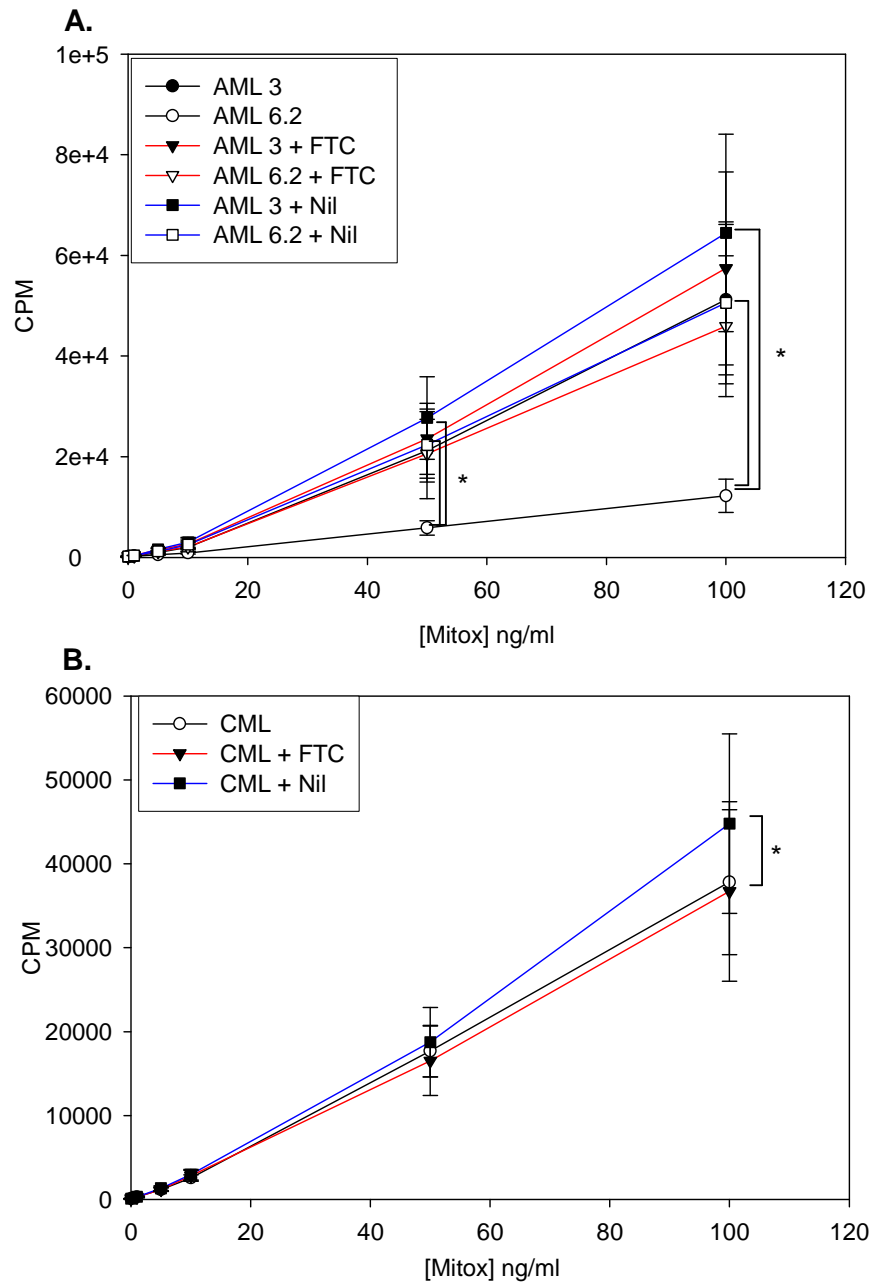
Figure 3-12 Radiolabelled mitoxantrone in cell lines and CML CD34$^+$ cells

Cellular concentration of ^{3}H-mitoxantrone in cell lines **(A)** and CD34$^+$ **(B)** cells in the presence and absence of FTC or nilotinib. **A**. ABCG2-ve cell line AML3 (black symbols) and ABCG2+ve cell line AML6.2 (white symbols) in the presence of 10µM FTC (red lines), 5µM nilotinib (blue lines) or alone (black lines). **B**. CML CD34$^+$ cells with mitoxantrone alone (black line), + 10µM FTC (red line), + 5µM nilotinib (blue line). All data are mean of duplicate analyses of n=3. *=p$\leq$0.05

3.9 Cellular concentration of nilotinib

Increasing concentrations of radiolabelled nilotinib were plotted against their corresponding CPM, to generate a standard curve. The curve was then extrapolated to predict the cellular nilotinib by the equation:

 ng= 15.56+0.005711*CPM (as calculated by graphpad prism software)

In CML CD34$^+$ cells, 5629 counts were observed in 5x10^5 cells with 5μM ^{14}C-nilotinib, equating to a cellular concentration of 48ng per 5x10^5 cells, representing an uptake of 1.8% of the available ^{14}C-nilotinib in the incubation medium.
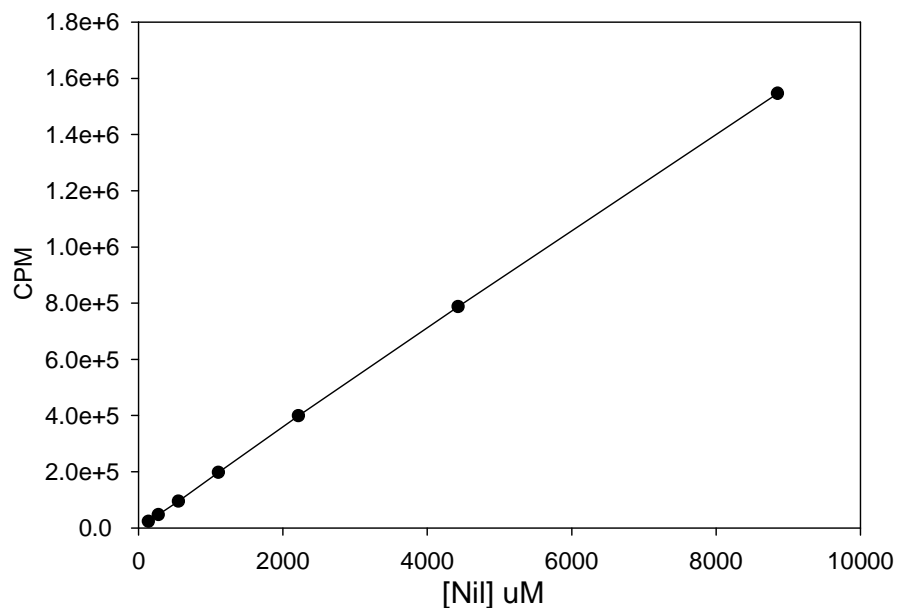
Figure 3-13 Standard curve of radiolabelled nilotinib

Increasing concentrations of ^{14}C-nilotinib in scintillant alone plotted against counts per minute (CPM)

3.10 Assessment of dasatinib interaction with ABCG2

The assay using radiolabelled drug was repeated with ^{14}C-dasatinib. However, unlike nilotinib and IM, when the ABCG2+ve cell line was incubated with ^{14}C-dasatinib, the level accumulated in the cells was significantly lower ($p < 0.001$ at 150nM, 300nM and 600nM) in comparison to the ABCG2-ve cell line. Furthermore, the addition of 10µM FTC to the ABCG2+ve cell line restored the level of radiolabelled drug in the cell to a similar level to the ABCG2-ve cell line (AML6.2 vs. AML6.2+ FTC $p < 0.001$ at 150nM, 300nM and 600nM, AML6.2 + FTC vs. AML3 p=ns) (Figure 3-14). This suggested that dasatinib was effluxed from the cell via ABCG2, suggesting that it was a substrate, and the blocking of this transporter by the specific inhibitor restored the cellular drug level to that of the cell line with no ABCG2 (AML3-ve).

The experiment was also attempted in CML CD34^{+}. However, the specific activity of the radiolabelled drug was too low to produce statistically significant CPM values in this assay. In addition, combination of the small number of cells available at each concentration for this assay (only 1×10^5 per data point for CD34^{+} CML cells in comparison to 5×10^5 per vial for cell lines) and the low concentration of drug required (nM for dasatinib in comparison to µM for IM and nilotinib) meant that the CPM accrued were not enough to distinguish from the background level and determine efflux activity.

The above assay in cell lines suggested that dasatinib was a substrate of ABCG2. However, to confirm this speculation the assay was repeated with ^{3}H-mitoxantrone in the presence and absence of 150nM dasatinib to determine whether it is an inhibitor.
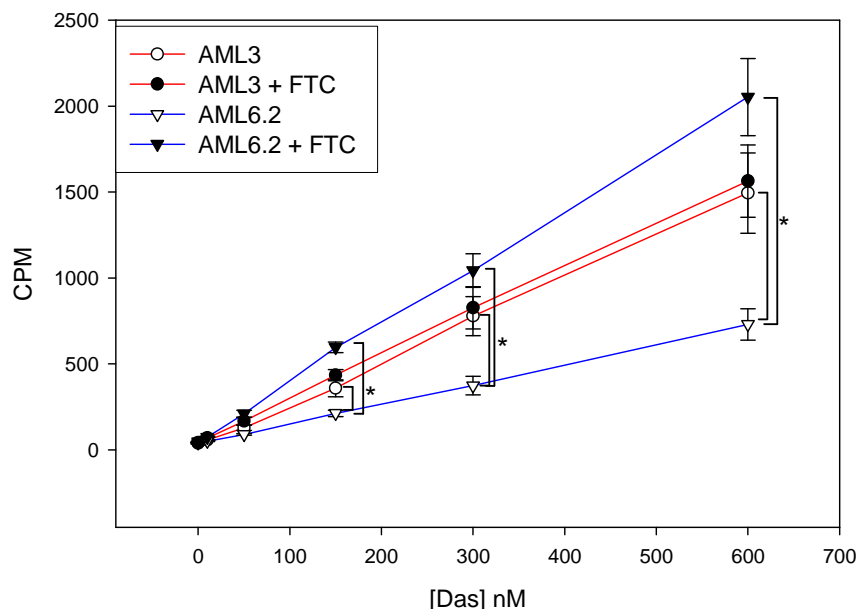
Figure 3-14 Radiolabelled dasatinib in cell lines

Cellular concentration of ^{14}C-dasatinib in cell lines in the presence and absence of FTC. ABCG2-ve cell line AML3 (red lines, circles) and ABCG2+ve cell line AML6.2 (blue lines, triangles) in the presence (black symbols) and absence (white symbols) of FTC. All data are mean of duplicate analyses of n=3. *p$\leq$0.05

As expected, the concentration of ^{3}H-mitoxantrone was significantly reduced in the ABCG2+ve cells and only restored to the level similar to ABCG2-ve cells when the transporter was inhibited by the addition of 10μM FTC. Replacing the specific inhibitor with 150nM dasatinib did not however, have the same effect and indeed ^{3}H-mitoxantrone in the ABCG2+ve cell line remained significantly reduced and at a similar level to the cell line alone (Figure 3-15). This was significantly different to the addition of 5μM nilotinib or 5μM IM and suggested that dasatinib does not act as an inhibitor of ABCG2.

A.

B.
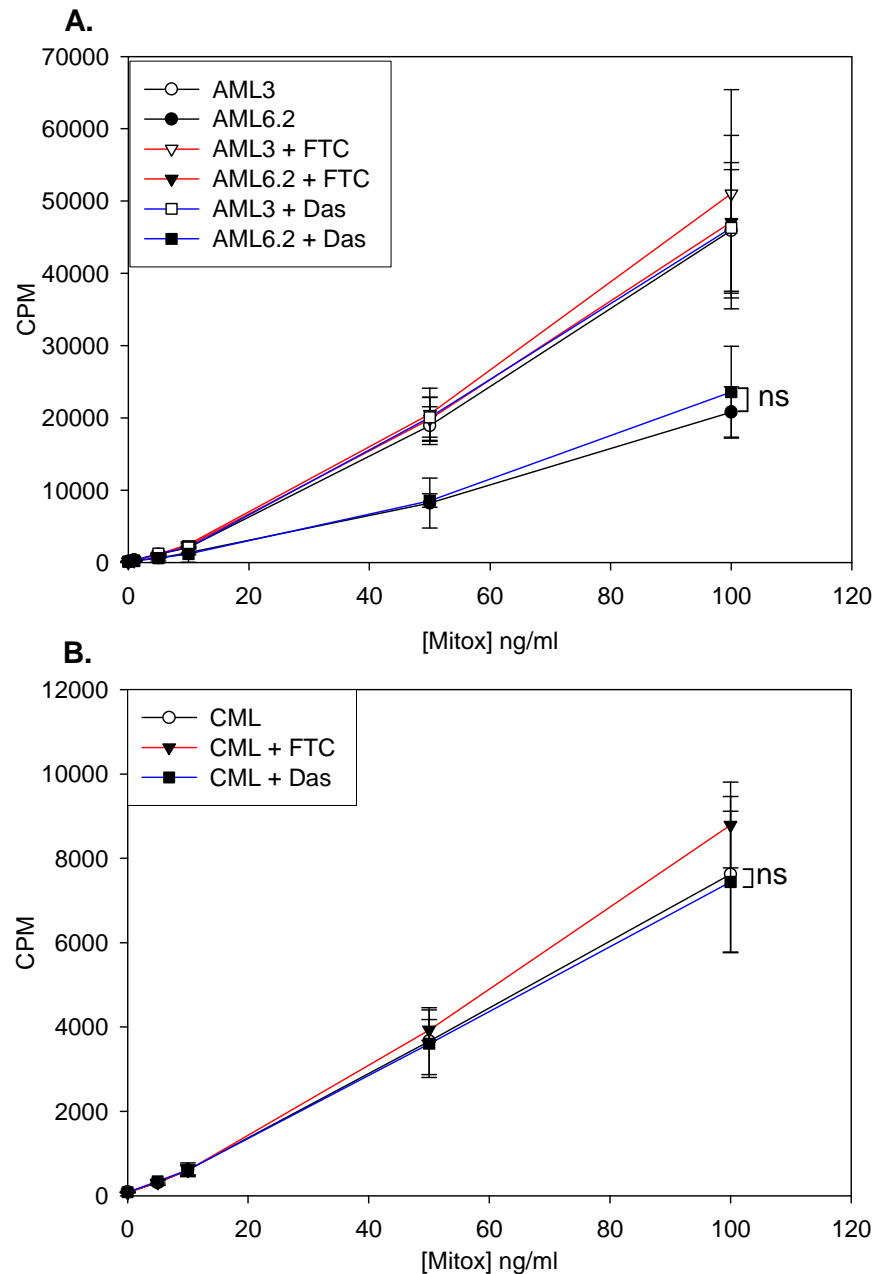
Figure 3-15 Radiolabelled Mitoxantrone in cell lines and CML CD34$^+$ cells

Cellular concentration of ^{3}H-mitoxantrone in cell lines **(A)** and CD34$^+$ **(B)** cells in the presence and absence of FTC or dasatinib. **A**. ABCG2-ve cell line AML3 (black symbols) and ABCG2+ve cell line AML6.2 (white symbols) in the presence of 10µM FTC (red line), 150nM dasatinib (blue line) or alone (black line). **B**. CML CD34$^+$ cells with mitoxantrone alone (black line), + 10µMFTC (red line), + 150nM dasatinib (blue line). All data are mean of duplicate analyses of n=3, ns=not significant

When the experiment was repeated in 3 CML CD34$^+$ cells, there was again no significant accumulation of ^{3}H-mitoxantrone in the presence of dasatinib, confirming that in CML CD34$^+$ cells, dasatinib was not an inhibitor at therapeutic concentrations.

3.11 Effect of ABCG2 inhibition on CML CD34$^+$ cells following 72hrs culture

To ascertain the effect of the aberrant ABCG2 expression in CML, CD34$^+$ cells were cultured with TKIs, in the presence and absence of the specific inhibitor FTC, to determine if the inhibition of the transporter further enhanced the overall kill with dasatinib specifically (apparent substrate for ABCG2), but also with IM and nilotinib (not expected if both drugs act as pure inhibitors of ABCG2).

Consistent with previous reports (Graham *et al.* 2002; Jorgensen *et al.* 2005a), treatment of CD34$^+$ cells with 5µM IM for 72hrs resulted in a reduction in the total number of cells in comparison to the 5GF alone (14.0±3.7 x10^5 in 5GF alone, 4.7±1.3 x10^5 with IM, p=0.04) (Figure 3-16A). Blocking the ABCG2 transporter by the addition of 10µM FTC had no effect on the total number of viable cells compared to the 5GF alone (13.6±3.3 x10^5 with FTC, p=ns), indicating that FTC alone was not toxic to the cells. This was of importance to confirm since any additional differences in the presence of IM would be due to a synergistic or additive effect rather than a toxic effect.

When the cells were cultured in the combination of IM and FTC, an enhanced reduction was observed in the total number of cells in comparison to the 5GF alone. However, this did not reach statistical significance when compared to IM

alone ($3.9\pm1.1 \times10^5$ with IM + FTC, p=ns) (Figure 3-16A). This suggested that the inhibition of ABCG2 in the absence of IM did not have an effect on CML cells and did not significantly enhance the reduction of total cells in combination with IM.

Similarly, treatment of CD34$^+$ cells with nilotinib for 72hrs resulted in a reduction of total number of cells ($16.4\pm2.8\times10^5$ in 5GF alone, $5.6\pm0.7\times10^5$ with nilotinib, p=0.03). The combination of nilotinib and FTC demonstrated no further reduction in the total number of cells in comparison to the nilotinib alone ($6\pm0.6\times10^5$ with nilotinib and FTC, p=ns), suggesting that, as expected, the co-treatment of IM or nilotinib with the ABCG2 inhibitor did not significantly enhance the reduction of total cells (Figure 3-16B).

The treatment of CD34$^+$ cells with dasatinib for 72hrs resulted in a reduction of total number of cells ($16.4\pm2.8\times10^5$ in 5GF alone, $7.3\pm1.6\times10^5$ with dasatinib, p=0.006). Unexpectedly, the combination of dasatinib with FTC did not significantly reduce the number of total cells in comparison to dasatinib alone ($5.2\pm0.9\times10^5$ with dasatinib and FTC, p=ns), indicating that blocking the transporter with FTC does not significantly enhance the reduction of total cells by dasatinib, despite this TKI being a substrate for this transporter (Figure 3-16C).
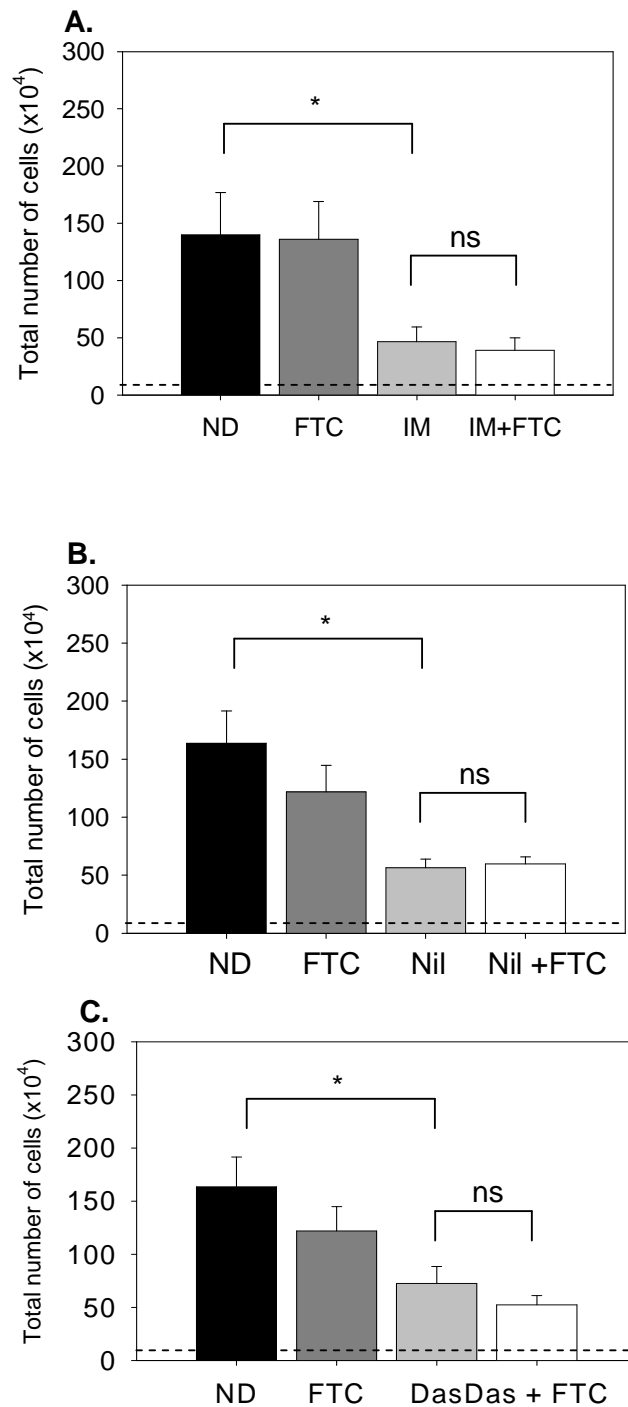
Figure 3-16 Inhibition of ABCG2 in total viable cells

Total number of cells remaining following 3 days in culture in the presence of FTC and IM n=6 **(A)**, nilotinib n=4 **(B)**, or dasatinib n=4 **(C)**; CD34^{+} cells treated with 5GF alone (ND-black fill), +10μM FTC (dark grey fill), +TKI (light grey fill) or combination of 10μM FTC and TKI (white fill). CD34^{+} cells were seeded at 1x10^{5} cells at d0 (dotted line) All data are mean of duplicate analysis, *=p≤0.05, ns=not significant.

3.12 Assessment of q34$^+$ cells following 72hrs culture

Following 72hrs of culture, the population of cells remaining quiescent was assessed for enhanced reduction in the presence of FTC and in combination with TKIs. These experiments were performed using CFSE to track cell division, with the quiescent population identified on a FACS plot by their maximal bright fluorescence that was comparable to the cells treated with colcemid (see section 2.4.1). The recovered q34$^+$ cells were then calculated as a percentage of the starting cell number. The different conditions were plotted relative to the no drug control to identify the effect of treatment on the quiescent population.

There was no significant reduction in the presence of FTC alone (Figure 3-17). Similarly the addition of IM, nilotinib or dasatinib did not significantly reduce the q34$^+$ population, but accumulated the cells arrested in the G_0/G_1 phase, although this was not significant. These findings correlate with published reports that have also reported accumulation of q34$^+$ in the presence of TKIs (Graham *et al.* 2002; Copland *et al.* 2006; Jorgensen *et al.* 2007b). The combination of the ABCG2 inhibitor with any of the TKIs also showed no significant reductions. These results therefore suggest that blocking the ABCG2 protein did not enhance the ability of the TKIs to target the most primitive quiescent CML stem cells.
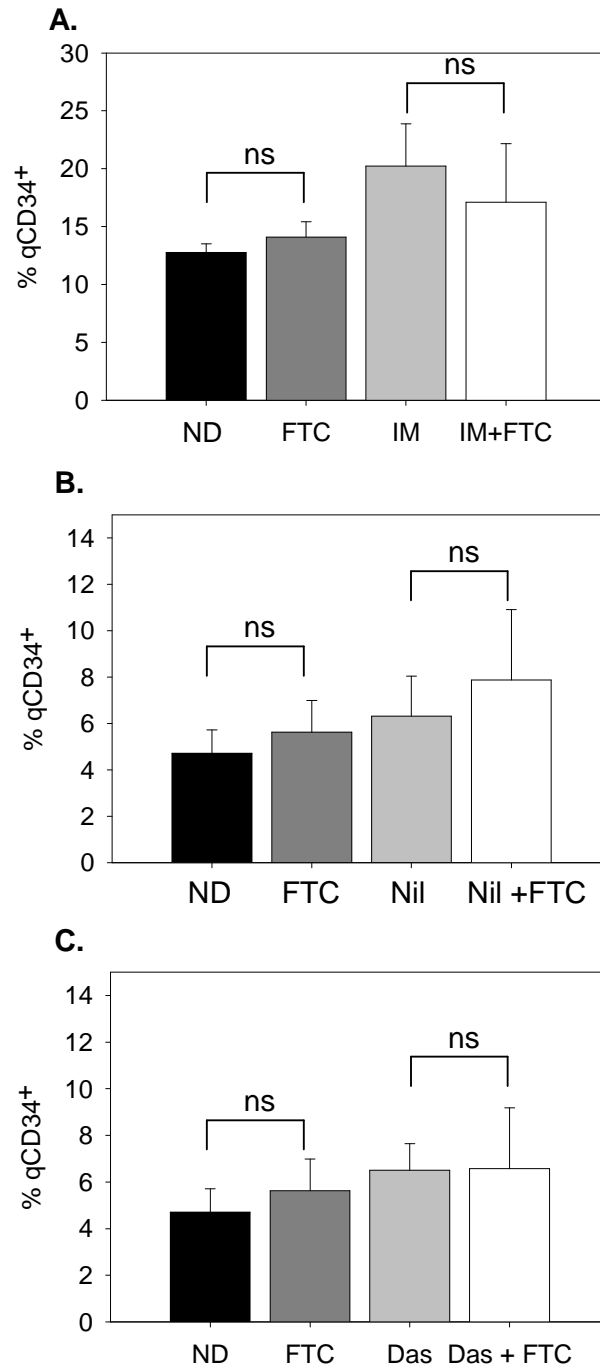
Figure 3-17 Inhibition of ABCG2 on quiescent CD34$^+$ CML cells

Percentage of q34$^+$ following 72hrs of culture as a percentage of input cells with IM; n=6 **(A)**, nilotinib; n=4 **(B)** or dasatinib, n=4 **(C)**. No drug control (ND, black fill), + FTC (dark grey fill), + TKI alone (light grey fill), + TKI + FTC (white bar). All data are mean of duplicate analysis, ns=not significant.

3.13 Assessment of CrkL phosphorylation

To further define the effects of ABCG2 inhibition on the efficiency of TKI to inhibit BCR-ABL activity, the phosphorylation of the downstream BCR-ABL substrate CrkL was examined at 16 and 72hrs. As previously reported (Hamilton *et al.* 2006), at 16hrs, the addition of the TKIs significantly reduced the percentage of p-CrkL compared to the untreated control (IM- 52.5±11.3%, nilotinib- 46±5.2%, dasatinib- 45.4±5.5%, untreated control 100%, $p < 0.05$, Figure 3-18A). At 72hrs (Figure 3-18B), the p-CrkL remained significantly reduced with nilotinib (62.2±12.2%, $p = 0.03$) and dasatinib (65.1±9.2%, $p = 0.01$), but was not inhibited with IM at this time point. These data confirm that these TKIs inhibit the activity of BCR-ABL. This was in contrast to FTC, which, as expected, did not significantly reduce p-CrkL at either 16hrs (87.8±6.4%, $p = ns$) or 72hrs (98.3±13.4%, $p = ns$), demonstrating that FTC alone does not inhibit BCR-ABL activity.

When co-treating CML CD34^{+} cells with TKIs in combination with FTC, there was no further reduction in p-CrkL compared to TKIs alone, at 16hrs (IM 52.5±11.3%, vs. IM+ FTC 66±22.7%, nilotinib 46±5.2% vs. nilotinib + FTC 67±23.4%, dasatinib 45.4±5.5% vs. dasatinib + FTC 48.8±4.7%, $p = ns$ for all combinations) or at 72 hrs ($p = ns$ for all combinations), confirming that blocking ABCG2 does not enhance the potency of the TKIs (Figure 3-18).

A.

B.
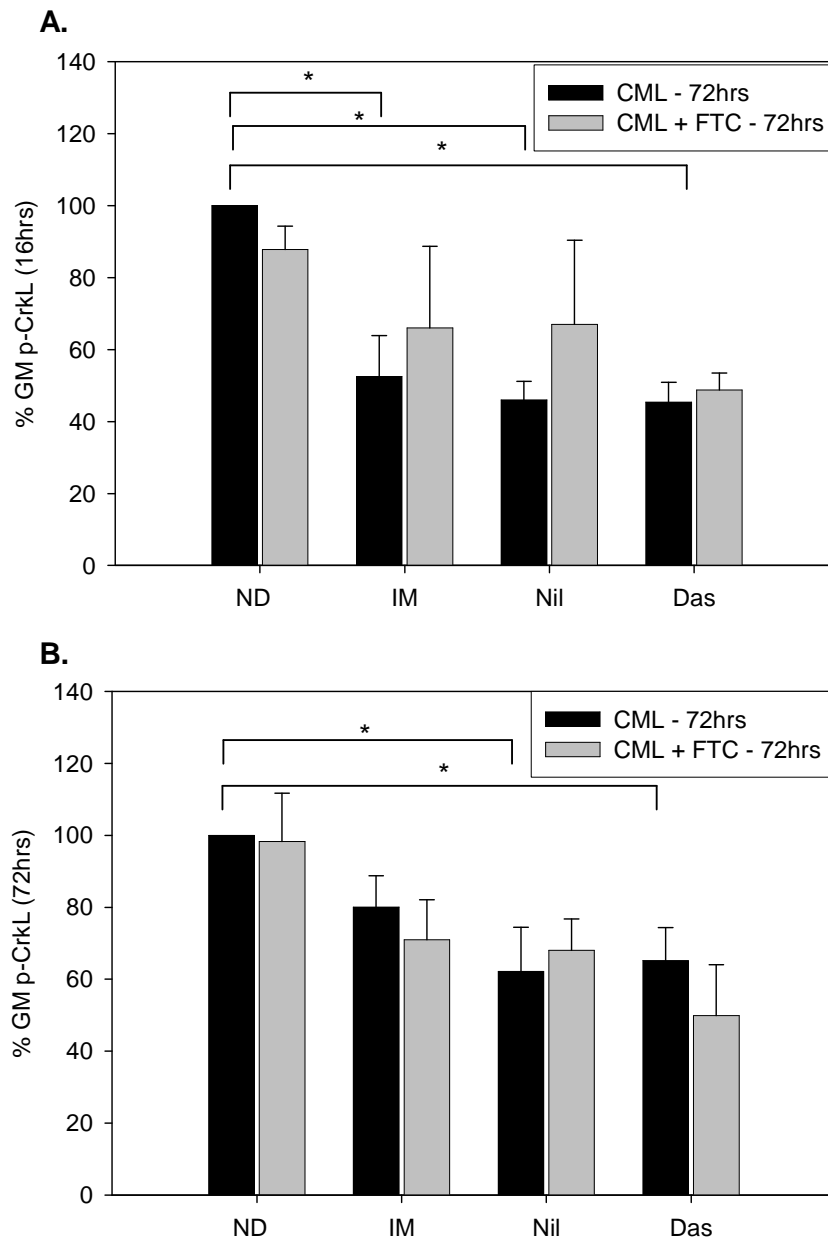
Figure 3-18 BCR-ABL inhibition as a measure of percentage p-CrkL in CML CD34$^+$ cells

Percentage of GM p-CrkL remaining relative to no drug control (ND) and in the presence (grey fill) or absence (black fill) of FTC at 16hrs **(A)** or 72hrs **(B)** n=5 for IM, n=6 for nilotinib and dasatinib, *p$\leq$0.05

3.14 Assessment of apoptosis

In order to determine the effect of blocking ABCG2 transporter by FTC, CML CD34^{+} cells were stained with annexin and viaprobe to determine early and late apoptosis respectively. A significant increase in apoptosis was observed in the presence of nilotinib compared to the untreated control (37.7±3% vs. 19.0±4.6%, p=0.01). In contrast, the treatment with FTC alone did not significantly increase apoptosis (23.3±4.4%), demonstrating that FTC was not toxic to the cells.
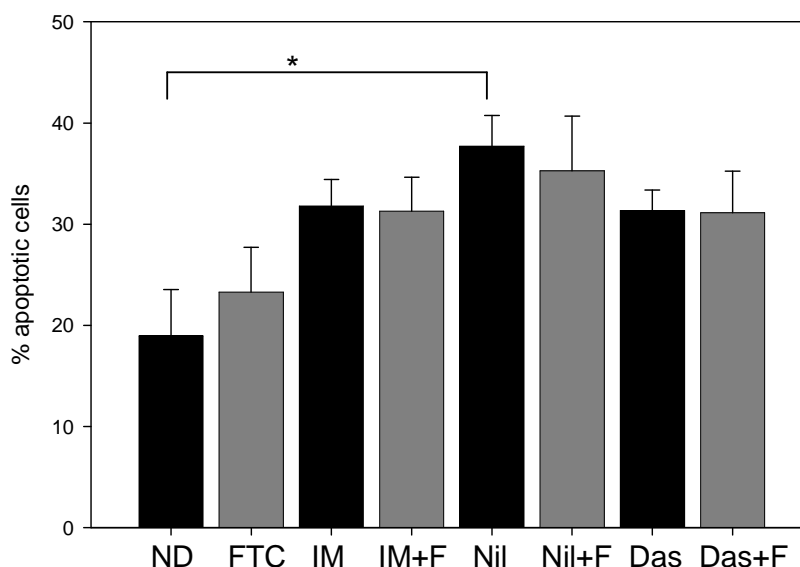
Figure 3-19 Apoptosis in the presence and absence of FTC

Percentage of cells undergoing apoptosis following treatment with TKIs in the presence (dark grey fill) or absence (black fill) of FTC; *p≤0.05; n=3, ND-no drug, F-FTC.

The co-treatment of TKIs with FTC did not result in any further increase in apoptosis demonstrating that inhibition of ABCG2 does not further enhance the apoptotic effect of TKIs.

3.15 Effect of ABCG2 inhibition on CD34$^+$ CML cells

A closer inspection as to the effect of FTC on the cells following a 72hr culture period revealed differences in the phenotype of the cells. Whilst FTC alone did not reduce the absolute number of cells compared to the 5GF control, nor alter the number of qCD34$^+$ cells, treatment resulted in a significant decrease in the proportion of CD34$^+$ cells remaining compared to 5GF alone (4.45±0.8x10^5 in 5GF alone, 2.5±0.5 x10^5 with FTC, p=0.01) and this reduction was of a similar degree to that seen with IM alone (1.7±0.3 x10^5 with IM, FTC vs. IM, p=ns, Figure 3-20).
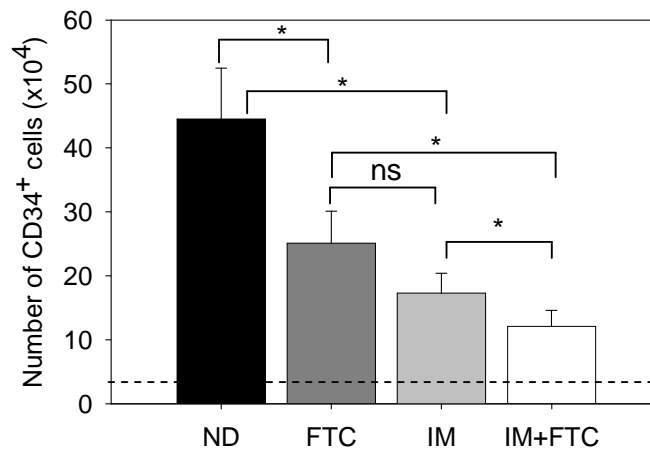
Figure 3-20 Inhibition of ABCG2 in viable CD34$^+$ cells

Total number of viable CD34$^+$ cells remaining following 72hrs in culture in 5GF alone (black fill), + 10µM FTC (dark grey fill), + 5µM IM (light grey fill) or 5µM IM + 10µM FTC (white fill). CD34$^+$ cells were seeded at 1x10^5 cells at d0 (dotted line) n=6 in duplicate; *=p$\leq$0.05; ns=not significant, [ND-no drug]

The combination of IM and FTC further reduced the CD34$^+$ cells compared to treatment with either IM or FTC alone (1.2±0.3 x10^5, p=0.04 either drug alone). Furthermore, the combination was the only treatment under which the CD34$^+$ cells did not significantly increase from the initial cells seeded at d0 of 1x10^5. Therefore,

combining the inhibition of ABCG2 with IM treatment may enhance the ability of IM to reduce the CML CD34$^+$ cells.

3.16 Effect of ABCG2 inhibition on proliferation and differentiation of CD34$^+$ cells

The reduction of CD34$^+$ cells by inhibition of ABCG2 suggested that functional ABCG2 might have an effect on survival or differentiation. To validate this, a number of experiments were carried out to identify how FTC may target the CD34$^+$ cells. CML CD34$^+$ cells (n=4) were cultured in a combination of growth factors designed to support differentiation rather than proliferation over a long time period and assayed for a range of surface markers to determine if ABCG2 inhibition led to altered differentiation. The presence of FTC did not alter the total cell number after 10 days (Figure 3-21).
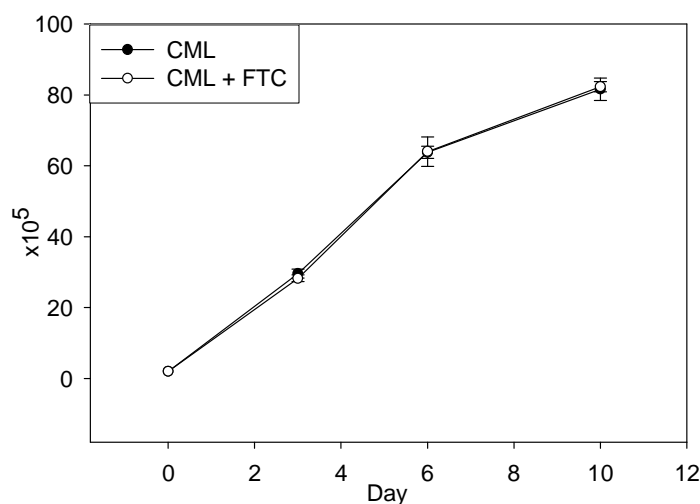
Figure 3-21 Effect of ABCG2 inhibition on long-term proliferation

Total cell counts following long-term culture in differentiation media in the presence (white symbols) or absence (black symbols) of FTC; n=4 in duplicate.

Furthermore, there was no significant difference by paired t-test analysis in a range of surface markers that are characteristic of differentiating cells in the presence or absence of FTC (Figure 3-22), suggesting that the reduction of CD34$^+$ cells by the inhibition of ABCG2 was not due to alteration of the number of maturing cells in the CML cultures.
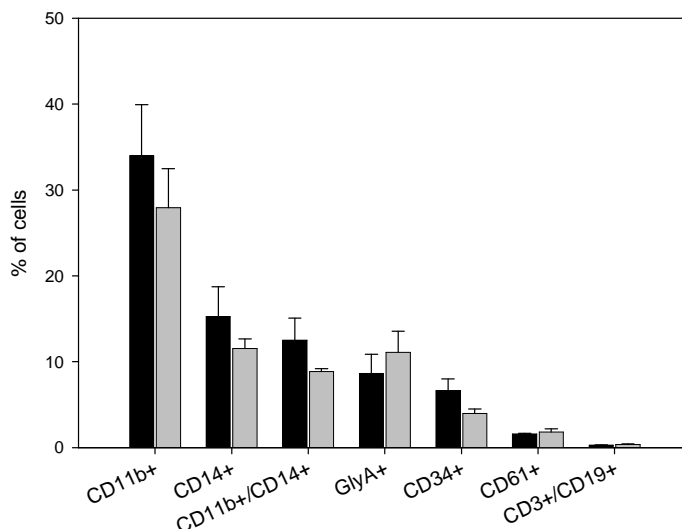
Figure 3-22 Effect of ABCG2 inhibition on the maturation of CML cells

The percentage of cells expressing mature surface markers following culture in differentiation media including G-CSF, GM-CSF, rHu-Epo, rHu-Tpo, low IL-3 for 7 days, in the presence (grey fill) or absence (black fill) of 10µM FTC; n=4 in duplicate.

3.17 Effect of ABCG2 inhibition on CD34$^+$ cells by apoptosis

In section 2-14 (see Figure 3-19), the apoptotic effect of FTC was observed at 72hrs with no significant difference compared to 5GF alone. The experiment was repeated but with additional time points to determine whether apoptosis occurred

at an earlier stage compared to the control arm, which may explain the difference in CD34$^+$ count.

CD34$^+$ CML cells (n=3) were cultured in control 5GF media ± FTC and assayed with annexin V and viaprobe and analysed periodically. Analysis revealed there was no significant difference between the 5GF alone and cells treated with the inhibitor FTC throughout the 72hr period (Figure 3-23), suggesting that early induction of apoptosis did not account for the reduction of CD34$^+$ cells.
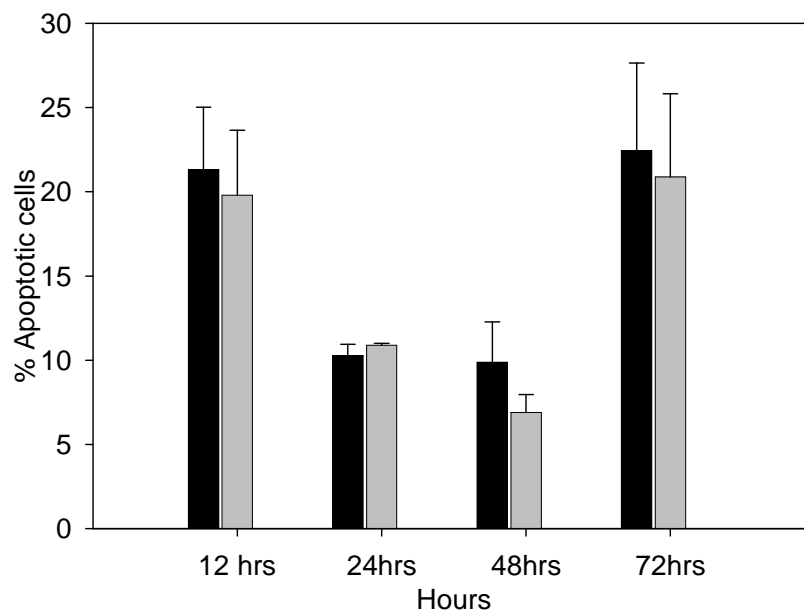
Figure 3-23 Assessment of early apoptosis by ABCG2 inhibition

The percentage of cells undergoing apoptosis in the presence (grey) or absence (black) of FTC. All data are mean of n=3 in duplicate.

3.18 Effect of ABCG2 inhibition on proliferating CD34$^+$ cells

The effect of FTC in CD34$^+$ cells was examined further in the 72hr cultures using the stain CFSE. This allows the cells to be tracked at each division as the CFSE intensity within a cell is halved during each division, hence identifying the proliferating and non-proliferating cells.

For this analysis the cells were grouped into 2 categories, 'non-proliferating' and 'proliferating'. The non-proliferating category included the cells that had not divided at all (CFSEmax) and those that had undergone one cycle of replication. The rationale for adding the cells that had completed one cycle of replication was based on the view that when the drug was added and experiment initiated, the cells may all be in different stages of cycle. Some cells may therefore complete the division despite the addition of the drug at this stage. Hence, the first opportunity for a dividing cell to "see" the drug and arrest would be after division 1.

As demonstrated in Figure 3-24A, there was no effect of FTC on the total cells remaining after culture in either the proliferating or the non-proliferating compartment. The data was then reanalysed to include only the cells that had CD34$^+$ expression and plotted at each division. The percentage of non-proliferating CD34$^+$ cells (the undivided cells and those that had undergone 1 division) were not significantly different in the presence of FTC compared to 5GF alone (Figure 3-24B), which matched the cell data shown in Figure 3-24A. However, the expansion of CD34$^+$ cells within the proliferating set of cells was significantly reduced in the presence of FTC in comparison to growth factor alone

(5GF alone vs. FTC, p=0.03), suggesting a reduction in the expression of CD34 by

cells that are proliferating.

A.

B.
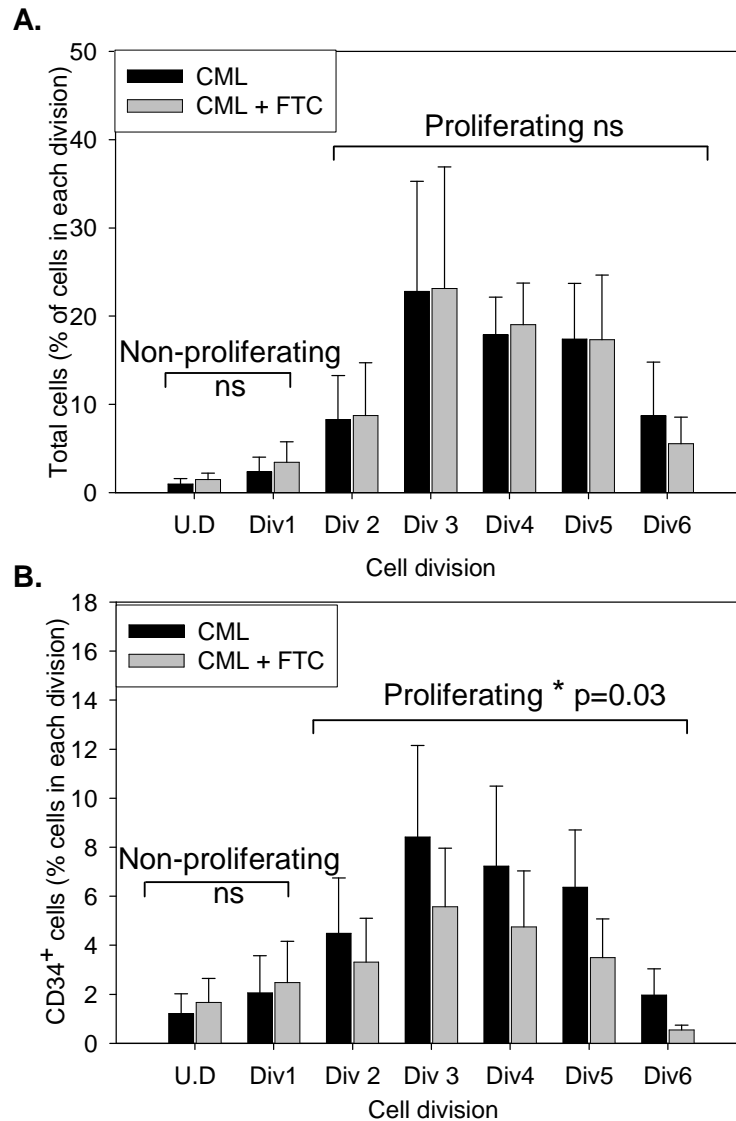
Figure 3-24 Effect of ABCG2 inhibition on cell division in CML cells following 72hrs culture

Cells were labelled with CFSE to allow tracking of their proliferative history. The number of total cells **(A)** or CD34$^+$ cells **(B)** that remain undivided (U.D), have divided once (Div 1), twice (Div 2) etc. were calculated using the % of cells detected in each division, the cell number and % CD34$^+$ cells within each division (see calculation in 2.4.1.3). Cells treated with 5GF alone (black fill) compared with cells treated with 10μM FTC alone (grey fill). The divisions are grouped as 'non-proliferating' (CFSE max and 1 division) and 'proliferating' (2 or more divisions). All data are mean of duplicate analyses of n=4 samples; * p≤0.05, ns=not significant.

3.19 Summary

These experiments demonstrate that ABCG2 was not only present in CML CD34$^+$ cells, but also that *ABCG2* expression was 6.8 fold higher in the leukaemic cells in comparison to normal HSCs. In addition, the protein was expressed showing that mRNA was translated. Furthermore, the ABCG2 protein was functional in CML CD34$^+$ cells as evidenced by the retention of the fluorescent substrate in the presence of FTC.

Replacing FTC with increasing concentrations of IM also reduced the efflux of the substrate, with a similar reduction to FTC observed at 5µM IM, indicating an interaction with ABCG2. Further analysis with radiolabelled IM and mitoxantrone demonstrated that IM was an inhibitor and not a substrate of ABCG2, suggesting that the intracellular concentration will not be affected by the aberrant expression of ABCG2. The experiments were repeated for the new generation drugs nilotinib and dasatinib. Similarly to IM, nilotinib was also shown to be an inhibitor and not a substrate of ABCG2. Interestingly, the accumulation of nilotinib in the CML CD34$^+$ cells were lower than that observed with IM and this may be explained by the lack of OCT1 effect for uptake of nilotinib. Hence in a short tem assay, IM will accumulate to higher levels than nilotinib.

In contrast, inhibiting ABCG2 with FTC increased the intracellular concentration of dasatinib. Furthermore, efflux of radiolabelled mitoxantrone was not affected in the presence of dasatinib, confirming that dasatinib is a substrate and not an inhibitor of ABCG2. These data suggested that inhibition of the ABCG2 transporter may increase the intracellular concentration of dasatinib and might enhance the effect of dasatinib in reducing the total cells.

Following 72hrs culture of CML CD34$^+$ with TKIs and FTC, there was no further reduction of total cells in comparison to TKIs alone. This was supported by analysis of CrkL phosphorylation, which showed no significant difference in the presence or absence of FTC, either at 16 or 72hrs, indicating no additional BCR-ABL inhibition. Apoptosis analysis confirmed no difference when inhibiting the ABCG2 transporter. These results were expected for both IM and nilotinib as they were demonstrated to interact as inhibitors of ABCG2. The inhibition by FTC therefore, would not increase the cellular concentration and hence not further enhance the effect of IM and nilotinib on the leukaemic cells. However, dasatinib was observed to be a substrate for ABCG2. Hence it could be postulated that the inhibition of ABCG2 by FTC would increase the accumulation of dasatinib within the CML CD34$^+$ cells (as occurred in the cell line), predicting an enhanced dasatinib effect. Unexpectedly, no difference was observed suggesting two possible scenarios. It may be that the drug has reached its maximal effect, such that increasing the intracellular concentration will not further inhibit BCR-ABL or enhance cell kill. Alternatively, it may also suggest that the maximal intracellular concentration required for full inhibition is prevented by active efflux of dasatinib by other transporters that are functional on CML CD34$^+$ cells.

In conclusion, these data suggest that although ABCG2 is over-expressed and functional in CML CD34$^+$ cells, inhibition of this protein does not reduce the total number of cells with any of the tested TKIs, does not increase apoptosis and does further inhibit BCR-ABL, inferring that the aberrant ABCG2 expression does not mediate resistance in CML CD34$^+$ cells.

In addition, although ABCG2 did not mediate CML stem cell resistance to TKIs, inhibition by FTC apparently reduced the number of CD34$^+$ cells remaining

following 72hrs of culture. Further analysis showed this reduction was not due to increased differentiation or apoptosis or reduced proliferation overall, but due to a reduction in proliferating cells that expressed the CD34$^+$ phenotype. This suggests that inhibition of ABCG2 may have a role in the behaviour of CML CD34$^+$ cells by down-regulating the expression of CD34$^+$.

4 Results 2- MDR1 in CML CD34$^+$ cells

The data described in chapter 3 demonstrated that although ABCG2 is over-expressed and functional in CML CD34$^+$ cells, inhibition of this transporter does not reduce the total number of cells in combination with any of the three TKIs tested, or increase apoptosis or further inhibit BCR-ABL activity, demonstrating that the aberrant ABCG2 expression does not mediate resistance in CML CD34$^+$ cells. However, it is well known that ABC transporters are promiscuous and share many substrates. Furthermore, recent literature has demonstrated MDR1 to be of importance with elevated expression in many tumours and active extrusion of chemotherapeutic agents (van der Zee *et al.* 1995; Trock *et al.* 1997).

Several reports have identified active efflux of IM by MDR1 as a contributory factor to multidrug resistance. Increased resistance, combined with reduced IM accumulation in cell lines (Mahon *et al.* 2000) and CML cells overexpressing *MDR1* (Thomas *et al.* 2004) suggests that IM is a substrate for this transporter. In contrast, other studies report no increased sensitivity to IM in mice transplanted with *mdr1* null BM retrovirally transduced with *bcr-abl* (Zong *et al.* 2005).

At the beginning of the project, only MNC from CML patients had been tested for *MDR1* expression and no correlation between MDR1 expression and response was observed with therapeutic doses of IM (Carter *et al.* 2001). However CML is a stem cell disease, hence to determine the role of MDR1, it was necessary to analyse the CD34$^+$ population. The following studies were designed to examine the expression of MDR1 in CML HSCs and to identify any interaction of the current TKIs with MDR1.

4.1 Expression of *MDR1* mRNA

In order to optimise experiments that would determine expression, function and the role of MDR1 in the presence of TKIs in CML CD34$^+$, a valid cell line model was required. The K562 WT cell line was chosen as a model for transduction as it has no MDR1 expression. This cell line, generated and donated by Dr L.Fairbairn, was transduced to express the *MDR1* gene, producing the K-MDR cell line (MDR1+ve).

The expression of *MDR1* in cell lines and CML CD34$^+$ cells was investigated using real time qPCR. The Taqman Low Density Array (TLDA) cards consisted of a range of targets including the 3 clinically relevant efflux transporters (ABCG2, MDR1, MRP1), the clinically relevant influx transporter (SLC22a1/OCT1), an additional 8 OCT transporters (SLC22a2-9), and a range of endogenous controls (18S, GAPDH, β-actin). The two cell lines K-WT and K-MDR were analysed on the TLDA card. As seen in Figure 4-1A, K-WT had no expression of MDR1, whilst the K-562 cell line transduced with MDR1 (K-MDR) had a Ct value of 19.9±0.98, confirming effective transduction.

The expression of *MDR1* was also investigated in CML CD34$^+$ and normal counterparts. Figure 4-1B shows the CML samples consistently expressed *MDR*1 mRNA, although the signal was detected at a later cycle than normal samples indicating a lower level of mRNA expression. Using *GAPDH* as the endogenous control, 7 CML CD34$^+$ and 11 normal CD34$^+$ samples gave ΔCt values of 8.33±0.47 and 5.44±0.24 respectively (p=0.0003) and a ΔΔCt of 2.89. Using the equation $2^{-\Delta\Delta CT}$ to determine relative quantification, this assay determined that

CML CD34$^+$ cells expressed 7.41 fold less *MDR1* than their normal counterparts

(Figure 4-1C).

A.

B.

C.
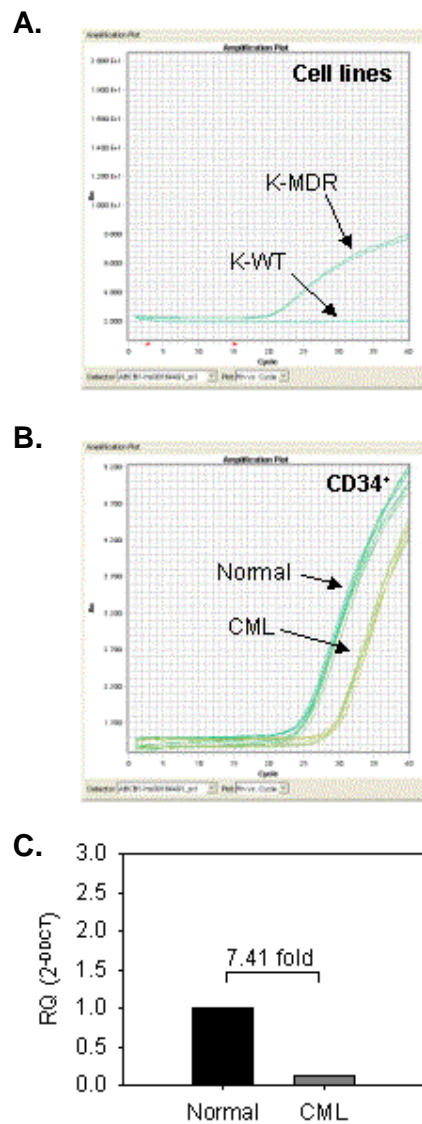
Figure 4-1 Expression of *MDR1* mRNA in cell lines and CML CD34$^+$ cells

Expression of *MDR1* mRNA. **A**. Taqman amplification plot of the cell line K-WT and the transduced cell line K-MDR. **B**. Taqman amplification plot of CML and normal CD34$^+$ cells (n=2 in duplicate). **C**. Relative quantification ($2^{-\Delta\Delta CT}$) of *MDR1* expression in CML CD34$^+$ cells (dark grey fill; n=11 in duplicate) compared to normal CD34$^+$ cells (black fill; n=7 in duplicate).

4.2 Expression of MDR1 protein

The MDR1 protein was detected using the specific antibody C219. This antibody recognises an internal, highly conserved amino acid sequence found on MDR1 and MDR3 isoforms (Georges *et al.* 1990). Serial dilutions of the antibody in the two cell lines established that a 100x dilution of the antibody followed by the same dilution of the secondary antibody produced the most distinct peaks. The assay demonstrated protein expression in the transduced cells (K-MDR isotype GM=3.27 vs. K-MDR-C219 GM=4.89).
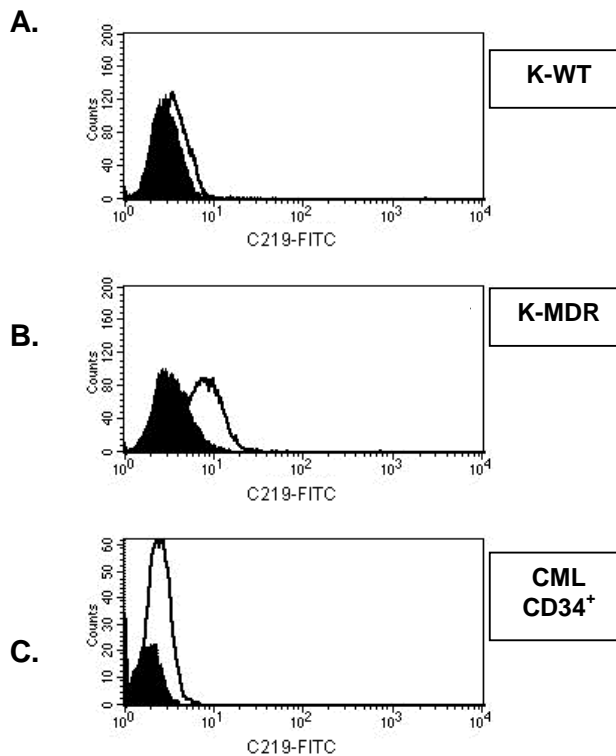
Figure 4-2 Expression of MDR1 protein in cell lines and CML CD34^{+} cells

A representative example of MDR1 protein expression in K-WT **(A)**, K-MDR **(B)** and CML CD34^{+} cells **(C)** with the isotype (black fill) and the MDR1 test antibody C219 (white fill); n=3 in duplicate, all replicates were consistent.

The protein expression was then measured in 3 CML samples. However, the staining was undetectable in all 3 samples with no difference to controls (isotype GM, 2.96±0.7, C219 GM 2.98±0.4, p=ns).

4.3 Function of MDR1 protein

The protein assay suggested that CML CD34$^+$ cells had no detectable MDR1 protein. However, the apparent absence of expression may be attributable to the sensitivity of the assay. Intracellular staining is often less sensitive than assays such as Western blotting for protein detection, hence the level in CML CD34$^+$ cells may be below the threshold of detection. Indeed, even though the transduced cell line K-MDR had high mRNA expression, there was only a small increase in the GM in the transduced cell line, suggesting that the assay may be less sensitive. For complete analysis of MDR1 in CML, the CD34$^+$ samples were tested for MDR1 function, which by association will also confirm protein expression.

The substrate displacement assay was carried out with the fluorescent substrate rhodamine 123 and the specific inhibitor PSC 833, a cyclosporin A analog. Initially, the assay was validated in the parental and transduced cell lines. In the K-WT cell line the addition of rhodamine 123 resulted in maximal retention, which was not further increased in the presence of PSC 833 (Figure 4-3A).

The cell line K-MDR was then tested (Figure 4-3B). The background fluorescence observed in the K-MDR cell line isotype control (black fill) was due to the green fluorescent protein (GFP) present in the vector, which had been added to confirm effective transduction. Two peaks were identified in the isotype control, a large peak on the right and a smaller peak within the first decade. The smaller peak

accounting for ~20% of the population represent the cells that were not effectively transduced with MDR1, as they do not possess the background GFP.

It was established that the cell line K-MDR effluxed 50ng/ml of rhodamine 123 resulting in two distinct peaks. The larger peak with the lower fluorescence (left peak of light grey fill) represented the cells expressing MDR1. The smaller peak with the higher fluorescence, accounting for ~20% of the population, represented the cells that do not express MDR1, and were assumed to be the same small population as those demonstrated in the isotype control. The efflux of rhodamine 123 in MDR1 expressing cells was maximally inhibited by 5µM PSC 833, confirming that MDR1 was functional in the cell line K-MDR.

This assay was then repeated in 3 CML patients (Figure 4-3C). As with the analysis of ABCG2, cells with the transporter inhibitor 5µM PSC 833 were considered to be maximally loaded with rhodamine 123 and classed as the control condition. The mean data from 3 CML samples indicated some efflux from the cells in the absence of PSC 833, suggesting a low level of functional MDR1 protein, although the difference observed was not significantly different (Figure 4-3D).

A.

B.

C.

D.
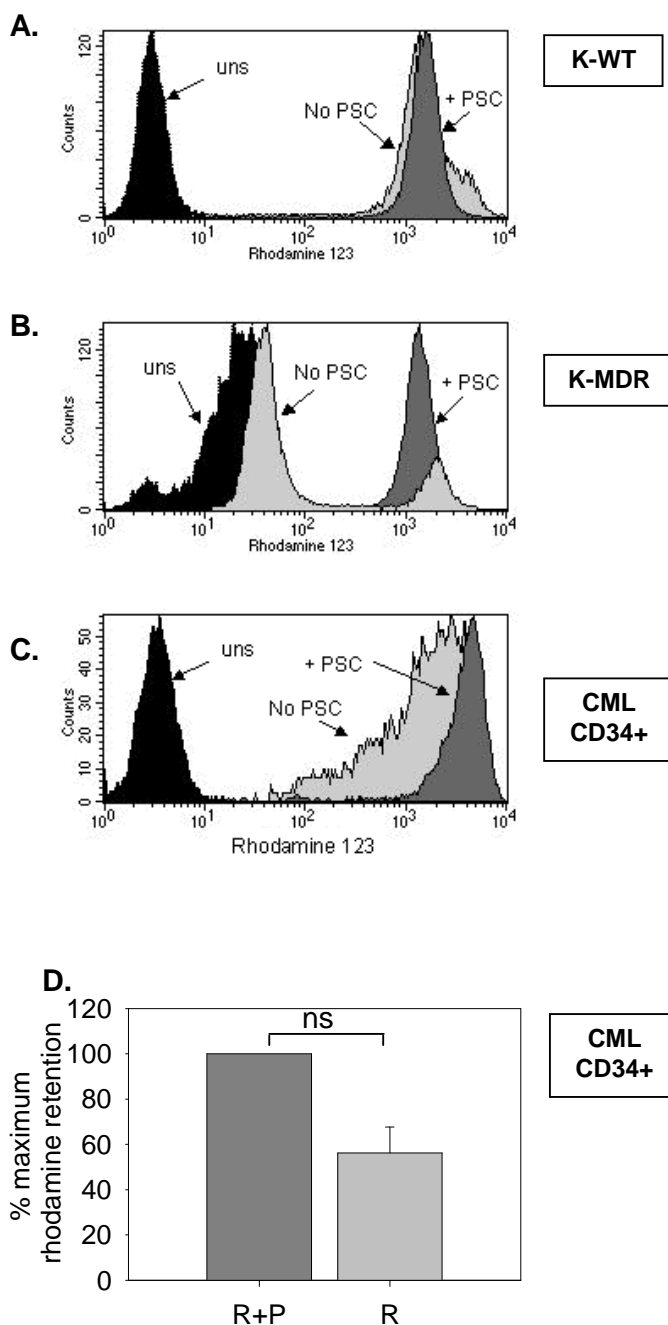
Figure 4-3 Function of MDR1 protein in cell lines and CD34+ cells

MDR1 function by efflux of a known substrate in K-WT **(A)**, K-MDR **(B)** and CML CD34+ cells **(C)**. Unstained cells (black fill), cells with rhodamine 123 (light grey fill), cells with rhodamine 123 and 5µM PSC 833 (dark grey fill). **D**. Percentage of efflux by MDR1 in CML CD34+ cells. Rhodamine 123 and 5µM PSC 833 (dark grey-fill) was considered to have maximal retention, rhodamine 123 alone (light grey-fill). R-rhodamine, P-PSC 833, ns=not significant.

4.4 Interaction of IM with MDR1 by a substrate displacement assay

The substrate displacement assay was repeated by replacing the specific inhibitor with IM. This drug was added at increasing concentrations in the two cell lines to test its effect on the MDR1 transporter. The addition of IM resulted in a small dose dependent decrease in efflux of rhodamine 123 in K-MDR (Figure 4-4A). This interaction suggested that IM was acting as a possible weak inhibitor or competitive substrate for this transporter.

A.

B.
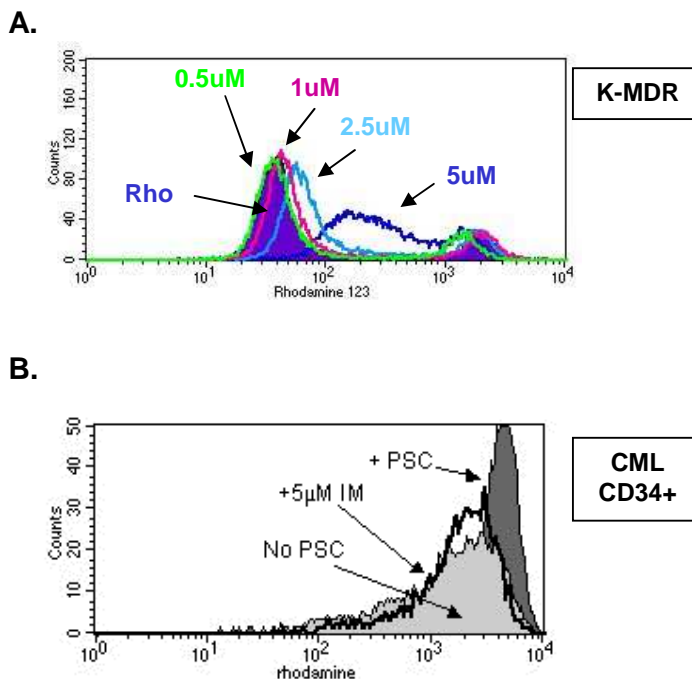
Figure 4-4 Efflux inhibition of a MDR1 substrate by IM

Interaction of IM with the protein MDR1. **A-** Cell line K-MDR with rhodamine 123 (blue fill), with rhodamine and 0.5µM (green line), 1µM (pink line), 2.5µM (light blue line) or 5µM IM (dark blue line); n=3 in duplicate. **B-** CML CD34^{+} cells with rhodamine 123 (light grey fill), with rhodamine and 5µM PSC 833 (dark grey fill), with rhodamine and 5µM IM (black line); n=3 in duplicate.

However, when this assay was repeated in CML samples, only 1 of 3 tested demonstrated an increase in fluorescence in the presence of IM, suggesting that IM was a very weak inhibitor/substrate that did not significantly affect the transporter (Figure 4-4B).

4.5 Assessment of IM as a substrate of MDR1

The substrate displacement assay above demonstrated some reduction of efflux by IM with MDR1 in cell lines and a small reduction in 1 of 3 CML samples. The reduction of efflux in the cell lines may be by inhibitory activity or as a competitive substrate. In order to test whether IM is a substrate for MDR1, increasing concentrations of radiolabelled IM were used to track the cellular retention in K-WT (MDR1-ve) and K-MDR (MDR1+ve). There was no significant accumulation of ^{14}C-IM in K-WT in comparison to K-MDR, indicating that the presence of MDR1 did not reduce the drug concentration within the cell and that IM was not a substrate of MDR1. Furthermore, ^{14}C-IM did not accumulate in K-MDR cells in the presence of the known inhibitor PSC 833, further confirming that IM was not effluxed by MDR1 (Figure 4-5A).

The experiment was also repeated in 3 CML samples. Similarly, there was no significant increase in IM accumulation in the presence of PSC 833. These results suggest, either that IM was not a substrate for this transporter or that the MDR1 was insufficiently expressed in these cells for the effect to be apparent (Figure 4-5B).
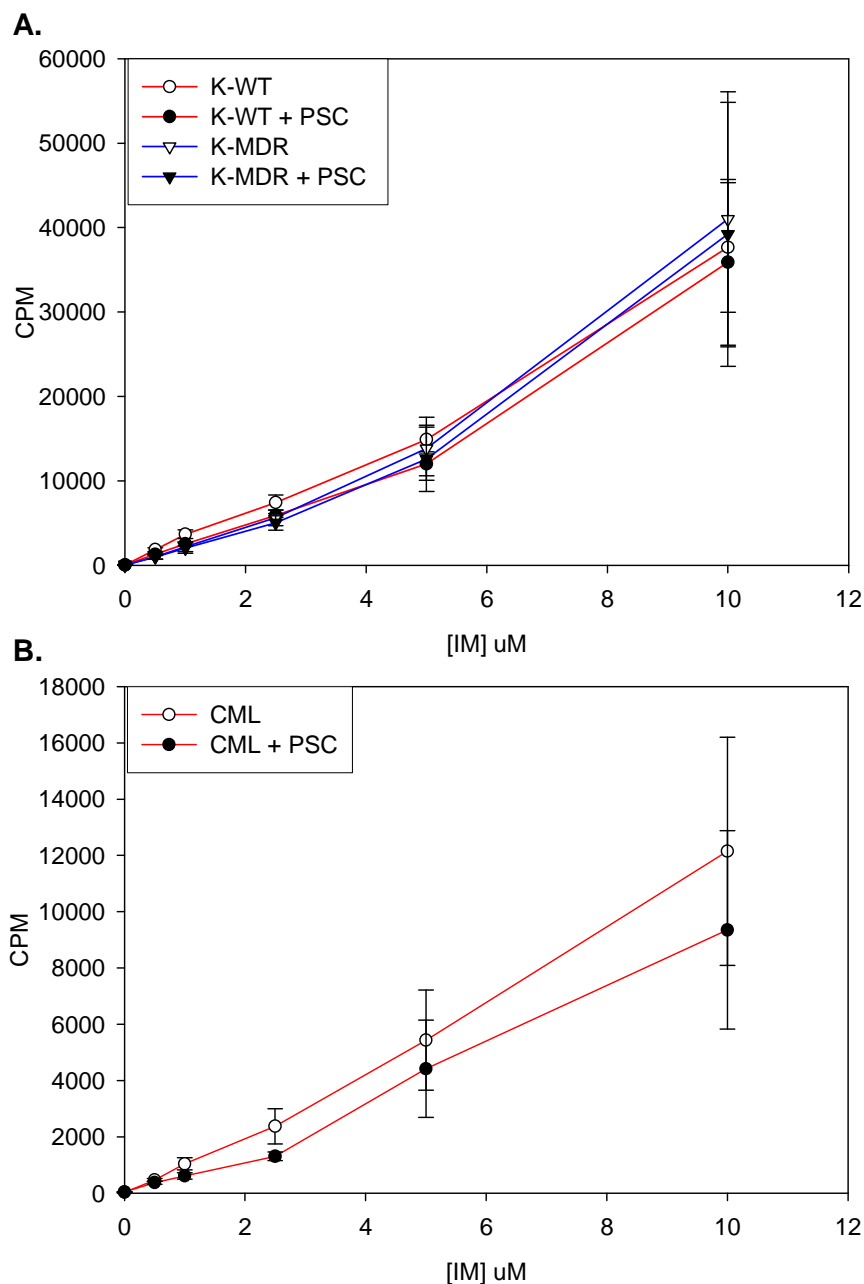
Figure 4-5 Radiolabelled IM in cell lines and CML CD34$^+$ cells

Cellular concentration of ^{14}C-IM in cell lines **(A)** and CML CD34$^+$ **(B)** cells in the presence and absence of PSC 833. **A.** K-WT (MDR1-ve) (red lines, circles) and K-MDR (MDR1+ve) cell line (blue lines, triangles) in the presence (black symbols) and absence (white symbols) of PSC 833. **B.** CML CD34$^+$ cells in the presence (black symbols) and absence (white symbols) of PSC 833. All data are mean of duplicate analyses of n=3.

4.6 Interaction of nilotinib with MDR1 by a substrate displacement assay

The substrate displacement assay with rhodamine 123 was repeated, this time with nilotinib as a potential inhibitor. This drug was again added at increasing concentrations in the two cell lines to test its effect on the MDR1 protein. As with IM, the addition of nilotinib resulted in a dose dependent decrease in efflux of rhodamine 123. However, the decrease in efflux was to a higher degree with nilotinib, with 5µM resulting in a reduction of efflux similar to that seen with 5µM PSC 833, suggesting that MDR1 mediated efflux was inhibited by nilotinib at a clinically achievable dose (Figure 4-6A). This interaction suggested that nilotinib was acting as an inhibitor or as a strong competitive substrate for this transporter.

The assay was repeated using CML CD34^{+} cells (Figure 4-6B). The low level of rhodamine 123 efflux was inhibited by therapeutic nilotinib concentrations, with 5µM nilotinib resulting in retention values of 70.6±9.8%, in comparison to the CD34^{+} cells with the substrate alone (56.2±11.5%), however this did not reach statistical significance (Figure 4-6C). This may be due to the low protein expression observed in CML CD34^{+} cells, resulting in insufficient efflux to reproducibly see the inhibition.

A.

B.

C.
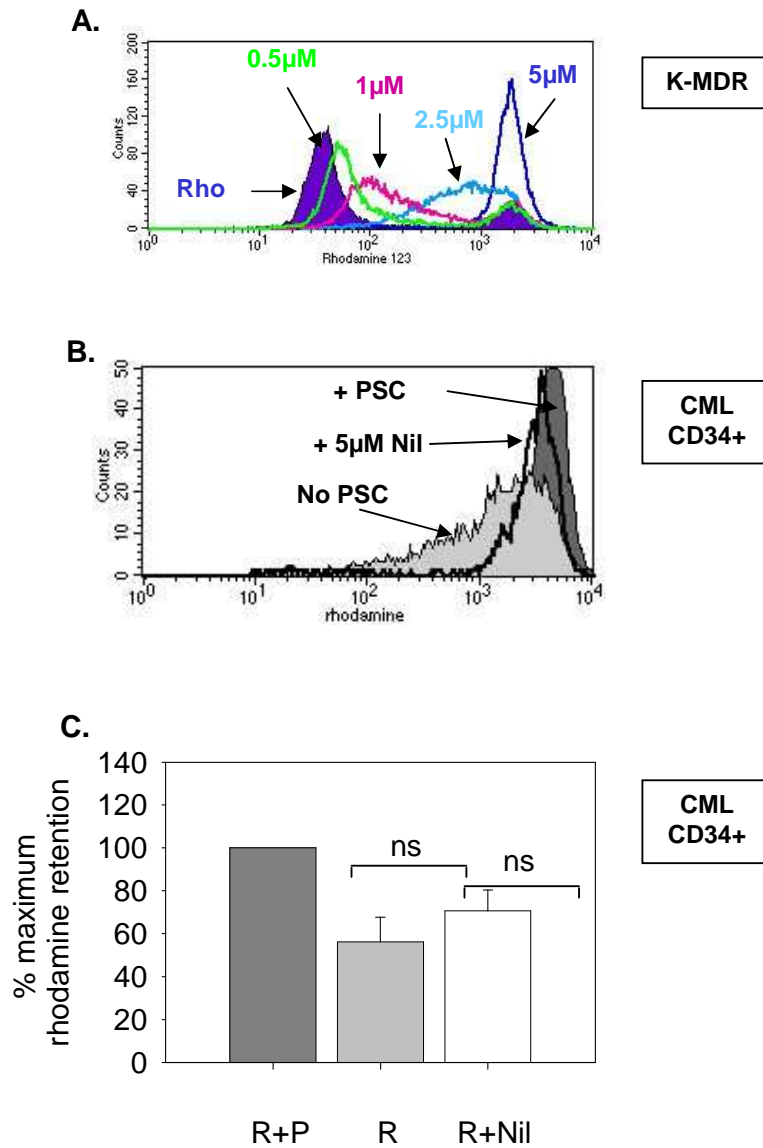
Figure 4-6 Efflux inhibition of a MDR1 substrate by nilotinib

Interaction of nilotinib with the protein MDR1. **A.** Cell line K-MDR with rhodamine 123 (blue fill), with rhodamine and 0.5µM (green line), 1µM (pink line), 2.5µM (light blue line) or 5µM nilotinib (dark blue line); n=3. **B.** CML CD34^{+} cells with rhodamine 123 (light grey fill), with rhodamine and 5µM PSC 833 (dark grey fill), with rhodamine and 5µM nilotinib (black line); n=3. **C.** Percentage of efflux by rhodamine 123. Rhodamine 123 and 5µM PSC 833 (dark grey-fill) was considered to have maximal retention, rhodamine 123 alone (light grey-fill) and rhodamine 123 with 5µM nilotinib (white fill); n=3 in duplicate. R-rhodamine, P-PSC 833, ns=not significant.

4.7 Assessment of nilotinib as a substrate of MDR1

The substrate displacement assay above again cannot delineate between reduction of efflux by inhibitory activity or competitive substrate. In order to establish the interaction of nilotinib with MDR1, increasing concentrations of radiolabelled nilotinib were used to track the cellular concentration in K-WT (MDR1-ve) and K-MDR (MDR1+ve). There was no significant accumulation of ^{14}C-IM in K-WT in comparison to K-MDR, indicating that the presence of MDR1 did not reduce the drug concentration within the cell and hence suggesting that ^{14}C-nilotinib was not a substrate of MDR1. Similarly, the addition of PSC 833 did not alter the cellular accumulation; further confirming that nilotinib was not effluxed by MDR1 (Figure 4-7A).

The intracellular accumulation was also observed in 3 CML CD34^{+} samples (Figure 4-7B). There was no significant accumulation of ^{14}C-nilotinib in the presence of the inhibitor PSC 833. The results of this experiment combined with the substrate displacement assay suggested that nilotinib was a potent inhibitor, and not a substrate of, MDR1.
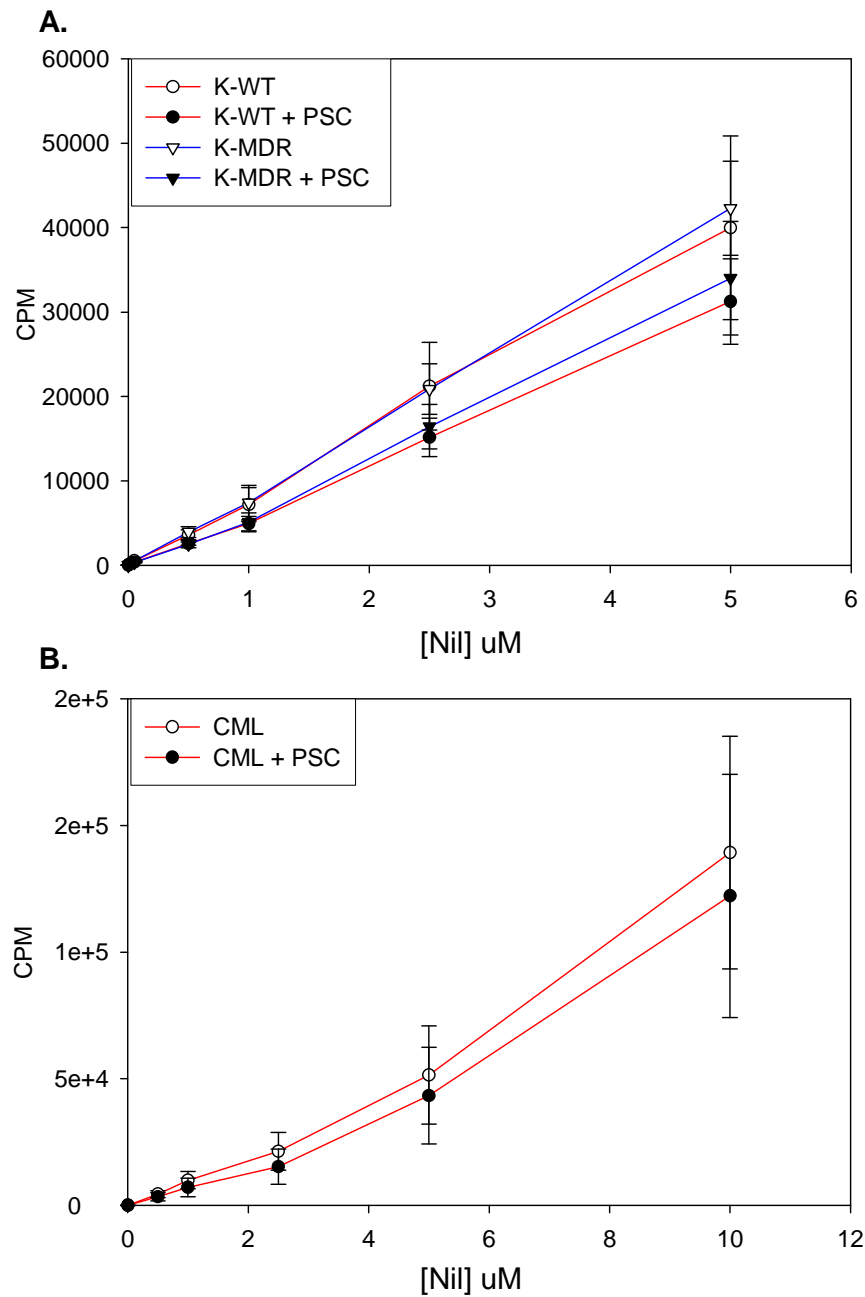
Figure 4-7 Assessment of radiolabelled nilotinib accumulation in the presence of MDR1 protein

Cellular concentration of ^{14}C-nilotinib in cell lines **(A)** and CML CD34$^+$ **(B)** cells in the presence and absence of PSC 833. **A.** K-WT (MDR1-ve) (red lines, circles) and K-MDR (MDR1+ve) cell lines (blue lines, triangles) in the presence (black symbols) and absence (white symbols) of PSC 833. **B.** CML CD34$^+$ cells in the presence (black symbols) and absence (white symbols) of PSC 833. All data are mean of duplicate analyses of n=3.

4.8 Interaction of dasatinib with K-MDR

Finally, the substrate displacement assay was repeated in the presence of dasatinib. As before, this drug was added at increasing concentrations in the two cell lines to test its effect on the MDR1 protein. The addition of dasatinib however, resulted in no significant difference between the two cell lines, even at therapeutic concentrations, suggesting that dasatinib is not an inhibitor for this transporter (Figure 4-8A).

Similarly, no significant difference was observed in 3 CML CD34^{+} samples, confirming that dasatinib was not an inhibitor of MDR1 in primary cells (Figure 4-8B).
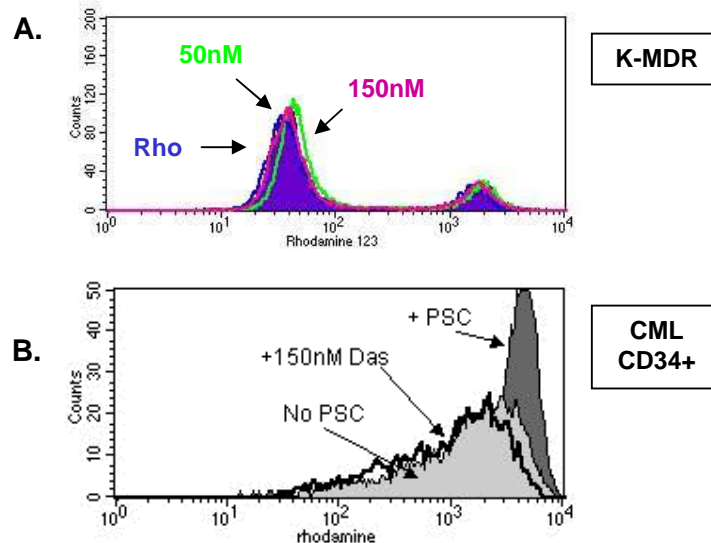
**Figure 4-8 Efflux inhibition of a MDR1 substrate by dasatinib**

Interaction of dasatinib with the protein MDR1. **A.** Cell line K-MDR with rhodamine 123 (blue fill), with rhodamine and 50nM (green line) and 150nM (pink line) dasatinib; n=3. **B.** CML CD34^{+} cells with rhodamine 123 (light grey fill), with rhodamine and 5µM PSC 833 (dark grey fill), with rhodamine and 150nM dasatiniib (black line no fill); n=3.

4.9 Assessment of dasatinib as a substrate of MDR1

The substrate displacement assay above demonstrated no interaction of dasatinib with MDR1, demonstrating that dasatinib is not an inhibitor. However, to conclusively determine whether dasatinib was a substrate, increasing concentrations of radiolabelled dasatinib were added to measure the cellular retention in K-WT (MDR1-ve) and K-MDR (MDR1+ve), in the presence and absence of PSC 833. Although not significant, there was less accumulation of ^{14}C-dasatinib in the K-MDR transduced cell line compared to the wild type (Figure 4-9). However, the concentration of ^{14}C-dasatinib was not restored by the addition of the specific MDR1 inhibitor, nor was the accumulation significantly increased. This suggested therefore that dasatinib was not a substrate of MDR1.

However, the significant difference in the two cell lines suggested that there might be another transporter that is capable of effluxing this TKI from these cells. Indeed, the results from chapter 3 have confirmed that dasatinib was a substrate for ABCG2 and hence the reduced accumulation in K-MDR might be due to the action of this transporter. Furthermore, expression analysis of these cell lines (detailed in chapter 5) demonstrated that although only transfected with MDR1, K-MDR cells had significantly elevated levels of ABCG2 (16.4 fold) compared to K-WT. Hence, it can be postulated that ABCG2 attributed to the difference in the dasatinib accumulation in the two cell lines.

As previously, this assay could not be performed using CML samples due to the low specific activity of dasatinib and the low cell numbers available for each assay (as detailed in 3.10).
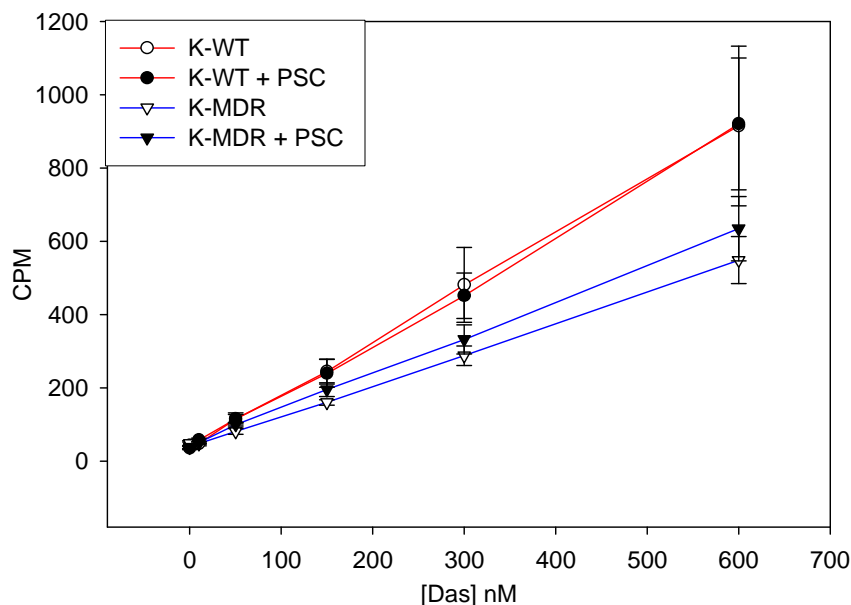
Figure 4-9 Radiolabelled dasatinib in cell lines

Cellular concentration of ^{14}C-dasatinib in cell lines cells in the presence and absence of PSC 833. K-WT (MDR1-ve) (red lines, circles) and K-MDR (MDR1+ve) cell line (blue lines, triangles) in the presence (black symbols) and absence (white symbols) of PSC 833, n=3 in duplicate

4.10 Effect of MDR1 inhibition on CML CD34$^+$ cells following 72hrs culture

The previous experiments determined that IM was a weak and nilotinib a strong inhibitor of the MDR1 transporter, while dasatinib was neither a substrate nor an inhibitor for this protein. As with the ABCG2 transporter, the three TKIs were tested in combination with the inhibitor PSC 833 to determine and confirm any effect of transporter inhibition on CML CD34$^+$ cells in culture.

As shown in chapter 3, treatment of CD34$^+$ cells with 5μM IM, 5μM nilotinib, or 150nM dasatinib for 72hrs resulted in a reduction in the total number of cells in

comparison to the 5GF alone (p<0.05)

(
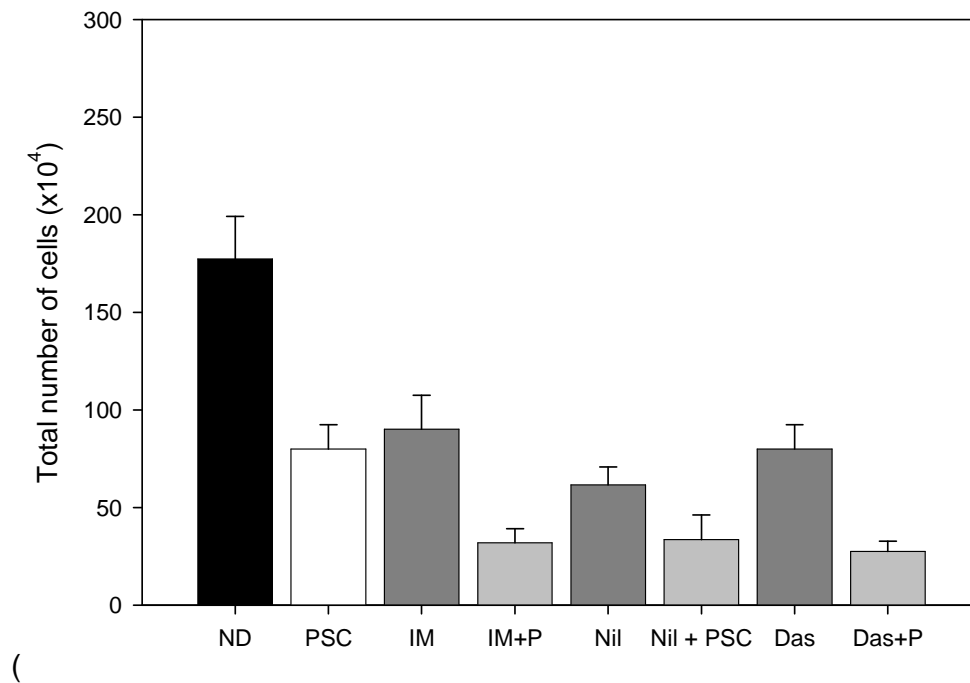
Figure 4-10). Blocking the MDR1 transporter by the addition of 5µM PSC 833 also resulted in a reduction in the total number of cells in comparison to 5GF alone ($17.7\pm2.19\times10^5$ in 5GF alone, $8\pm1.2\times10^5$ with PSC 833, p=0.002), indicating that PSC 833 alone had an effect on the cells.
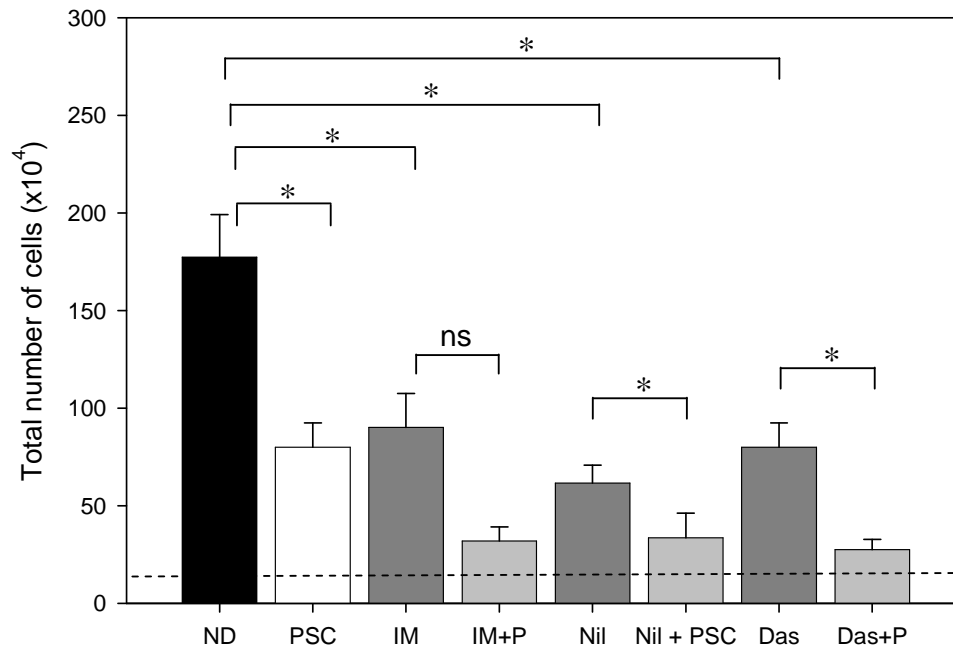
Figure 4-10 Inhibition of MDR1 in total viable cells

Total number of cells following 3 days in culture, in the presence of TKIs alone (dark-grey fill) or combined with PSC 833 (light grey fill). In addition, total number of cells in 5GF alone (black fill), or PSC 833 alone (white fill) are plotted. CD34$^+$ cells were seeded at $1x10^5$ cells at d0 (dotted line); n=4 for IM, n=6 for nilotinib, n=7 for dasatinib. All data are mean of duplicate analysis, $^*=p{\leq}0.05$, ns=not significant, [ND-no drug]

The combination of nilotinib or dasatinib and PSC 833 further reduced the total number of cells in comparison to the drug alone ($6.17{\pm}0.9x10^5$ with nilotinib, $3.37{\pm}1.3x10^5$ with nilotinib and PSC 833, p=0.01, $8{\pm}1.3x10^5$ with dasatinib, $2.77{\pm}0.5x10^5$ with dasatinib and PSC 833, p=0.001). Although these data would appear to imply that there is an additive effect with the combination, the reduction of cells in the presence of PSC 833 alone suggests that it this may not be due to an increase in TKI effect, but based upon a separate PSC 833 action that is unconnected to the action of TKI.

4.11 Assessment of q34$^+$ cells following 72hrs culture

Following 72hrs culture, the population of cells remaining quiescent was assessed for further reduction in the presence of PSC 833 ± TKI. There was no significant reduction in the presence of PSC 833 alone. Similarly the combination with TKIs also did not further reduce the q34$^+$ population (IM 11.7±8.3 vs. IM + PSC 3.6±0.9, nilotinib 8±4.4 vs. nilotinib + PSC 6.5±2, dasatinib 5.2±1.7 vs. dasatinib + PSC 5.1±1.5, p=ns for all combinations). These results therefore demonstrated that blocking the MDR1 transporter did not enhance the reduction of q34 cells in the presence of TKIs.
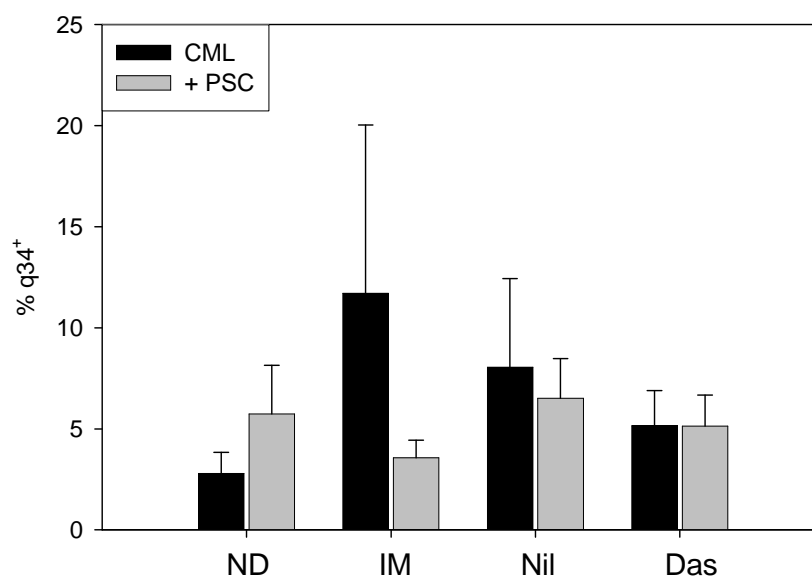
Figure 4-11 Inhibition of MDR1 on quiescent CD34$^+$ CML cells

Percentage of q34 following 72hrs of culture as a percentage of input in the presence of TKIs or 5GF alone (black bars) or combined with PSC 833 (grey bars), n=4 for IM, n=6 for nilotinib, n=7 for dasatinib, [ND-no drug]

4.12 Effect of PSC 833 on cell division in CML cells following 72hrs culture

To dissect the effect of PSC 833 alone on cells following 72hrs culture, the stain CFSE was used to track cell division. The data was then analysed either as the whole population (top right and bottom right quadrant as detailed in section 2.4.1.3, Figure 4-12B) or as the population that are still CD34^{+} (Figure 4-12C).

As demonstrated in Figure 4-12B, although there was no significant difference between the non-proliferating and proliferating populations, there was a trend towards a higher number of cells in the early divisions compared to the later divisions, just reaching statistical significance at division 4 ($p=0.05$). This would suggest that PSC 833 was acting as an anti-proliferative agent, and hence accounting for the significant reduction in total cells (Figure 4-12A).

Additionally, the total number of CD34^{+} cells at each division was also analysed (Figure 4-12C). There was no significant difference at any division, nor when comparing the non-proliferating with the proliferating population. However, there again was a trend towards higher number of cells in the early divisions compared to the later divisions, supporting the observation of PSC 833 acts as an anti-proliferative agent.
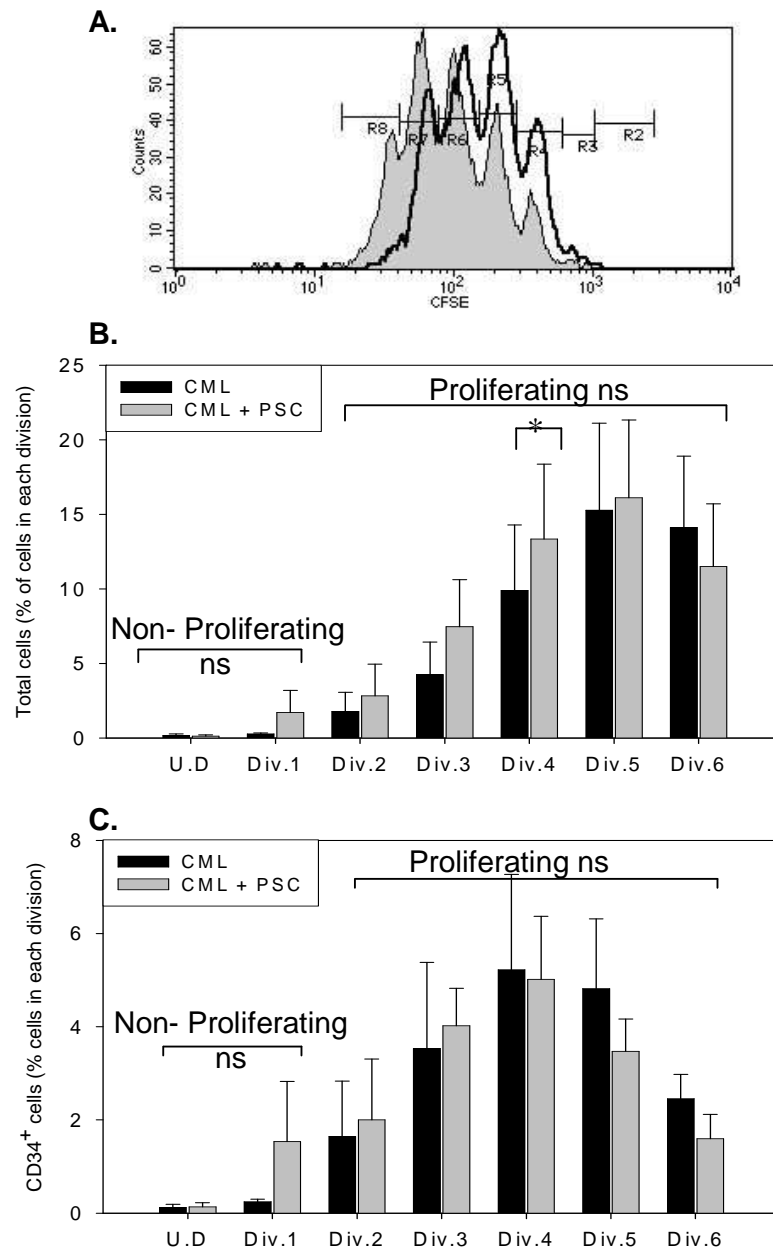
Figure 4-12 Effect of PSC 833 on cell division in CML cells following 72hrs culture

Cells were labelled with CFSE to allow tracking of their proliferative history. **A**. A representative FACS histogram plot demonstrating the anti-proliferative effect of PSC 833 (black line) compared to untreated control (grey fill). **B** and **C.** The percentage of total cells and CD34$^+$ cells in each division following 72hrs culture respectively. The cell numbers are expressed as a percentage of the starting cell number. Cells treated with 5GF alone (black fill) compared with cells treated with 5μM PSC 833 alone (grey fill). The divisions are grouped as 'non-proliferating' (CFSE max and 1 division) and 'proliferating' (2 or more divisions). All data are mean of duplicate analyses of n=4 samples, * p=0.05, ns=not significant. U.D-undivided, Div 1- division 1, etc.

4.13 Assessment of CrkL phosphorylation

To define the effects of MDR1 inhibition in the presence of TKIs, the downstream substrate CrkL was examined at 16 and 72hrs for BCR-ABL activity. As demonstrated in the previous chapters, the addition of the TKIs significantly reduced p-CrkL at 16 hrs ($p \leq 0.05$), with significant reduction retained with nilotinib and dasatinib at 72hrs ($p \leq 0.05$). The treatment with PSC 833 alone also demonstrated significant CrkL phosphorylation compared to the untreated control at 16hrs (PSC 833- 50.6±6.4% vs. ND- 100%; p=0.01), which was restored to control levels at 72hrs.

However, the co-treatment of PSC 833 with either TKI did not further reduce p-CrkL at 16rs or 72hrs (p=ns for all combinations), suggesting that blocking MDR1 does not further enhance the potency of the TKIs. It can therefore be suggested that the inhibition of MDR1 does not further increase the ability of TKIs to reduce p-CrkL and does not increase their potency.

A.

B.
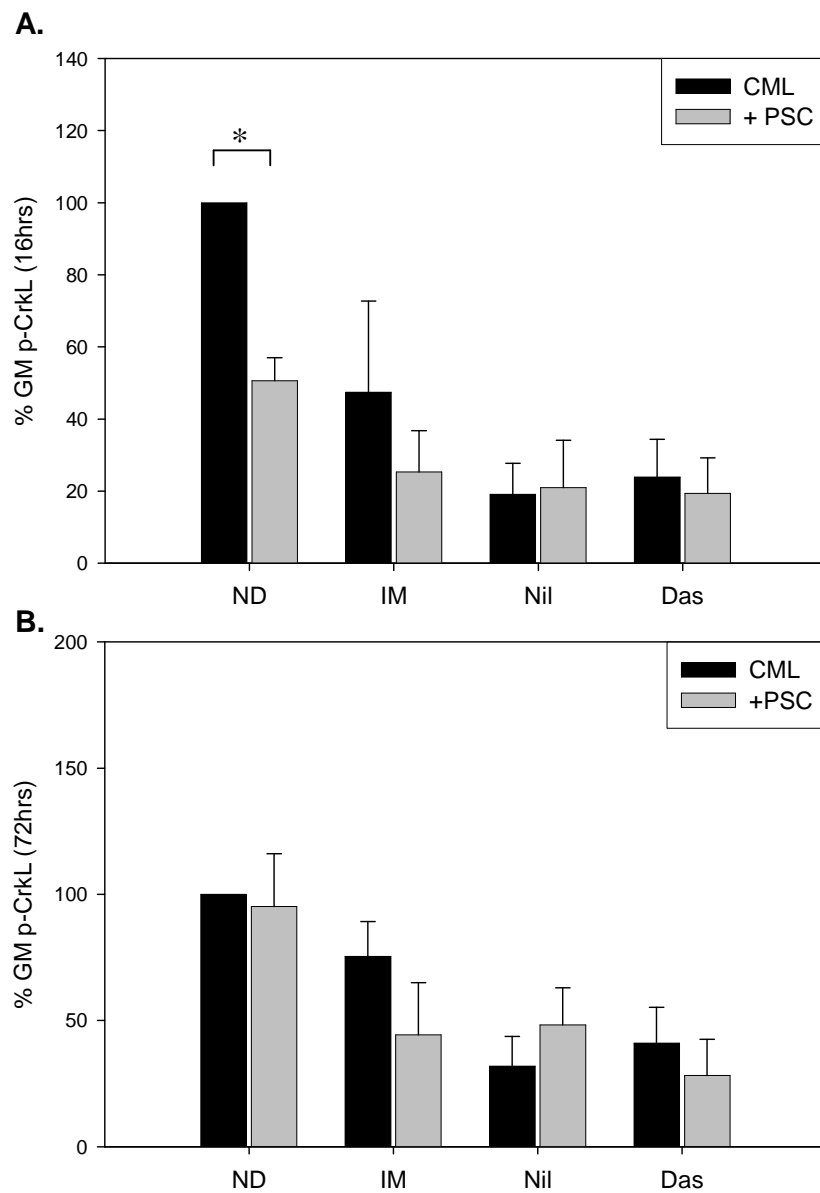
Figure 4-13 BCR-ABL inhibition as a measure of percentage p-CrkL in CML CD34$^+$ cells

Percentage of GM p-CrkL remaining relative to no drug control (ND) in the presence (grey fill) or absence (black fill) of PSC 833 at 16hrs **(A)** or 72hrs **(B)** n=5, *=p<0.05.

4.14 Assessment of apoptosis

In order to determine the effect of blocking the MDR1 transporter by PSC 833, CML CD34+ cells were stained with annexin and viaprobe to determine early and late apoptosis. As shown in chapter 3, apoptosis was increased in the presence of nilotinib (p=0.01). However, this was not enhanced when co-treated with PSC 833 (TKI vs. TKI + PSC 833, n/s for all combinations), suggesting that inhibition of MDR1 does not further induce the apoptotic effect of the TKIs.

In addition, increased apoptosis was also observed in the presence of PSC 833 alone compared to growth factor alone (ND-18.95±4.6% vs. PSC 833 30.37±5.1%, p=0.03). These data suggest that MDR1 inhibition does not further enhance the apoptotic effect of the TKIs, but that PSC 833 alone increased apoptosis in a manner unrelated to TKIs.
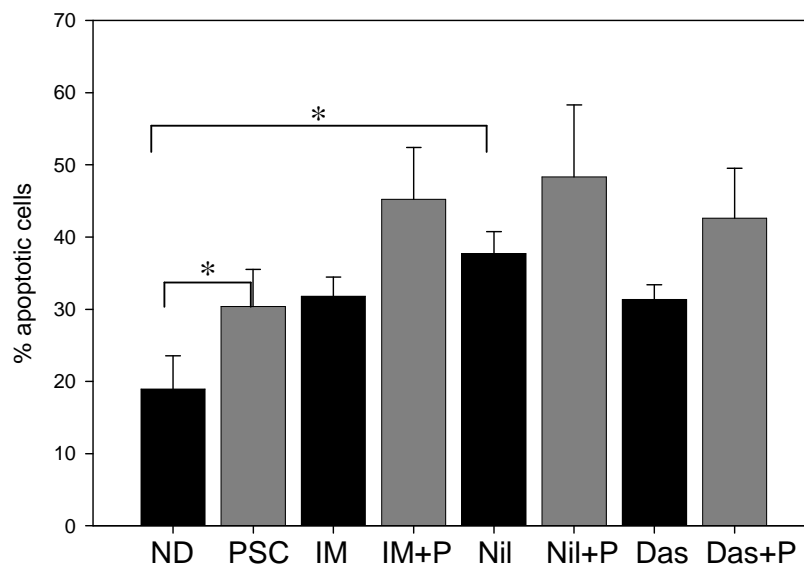
Figure 4-14 Apoptosis in the presence and absence of PSC 833

Percentage of apoptosis in the presence (dark grey) or absence (black) of PSC 833; * p$\leq$0.05; n=3, ND-no drug, P-PSC 833

4.15 Summary

The previous experiments demonstrated that although *MDR1* was expressed in CML CD34$^+$ cells, it was significantly lower (7.41 fold) than the expression in normal counterparts. Although there was some protein function, it was weak, and the protein was immeasurable by intracellular staining. Intracellular staining as an assay has reduced sensitivity compared to other protein detection assays such as Western blotting and the low expression might have been due to the level being below the threshold range of the assay. Confirmation of protein expression might have been demonstrated with the more sensitive Western blot assay. However, the substrate displacement assay was able to confirm both protein expression and protein function at low levels, demonstrating that this assay was more sensitive.

Replacing the specific MDR1 inhibitor with TKIs demonstrated interactions with this transporter. The effect was more obvious in the cell line model as high MDR1 expression allowed the interaction with increasing concentrations to be easily assessed. Increasing concentrations of IM in the MDR1 overexpressing cell line demonstrated a small reduction of efflux, suggesting that it might be acting either as a substrate or weak inhibitor. However, the effect was only seen in 1 of the 3 CML patient samples tested, suggesting that the level of MDR1 present in CML CD34$^+$ was either insufficient to see any effect of IM or that the IM interaction was so weak that it did not affect efflux via MDR1. In contrast, nilotinib showed a stronger interaction with MDR1 in the MDR1 cell line model. At therapeutic concentrations (>1µM), nilotinib increased rhodamine 123 retention to a similar degree as PSC 833 in cell lines. However, as above, the degree of efflux seen in the CML samples was small and was not significantly altered by nilotinib.

Although the MDR1 protein was minimal in CML CD34$^+$ cells, the significant increase in fluorescence in cell lines demonstrated that these TKIs have an interaction with MDR1. Assays with radiolabelled IM and nilotinib in cell lines demonstrated no significant difference in the presence of the inhibitor PSC 833, suggesting that IM and nilotinib were not substrates of this transporter. Therefore the interaction observed in the substrate displacement assay suggested that these drugs were inhibitors of MDR1. Repeating the assay in CML CD34$^+$ cells further confirmed that IM or nilotinib were not substrates for this transporter.

In contrast, the addition of dasatinib did not increase rhodamine 123 fluorescence in the cell lines or CML, even at the maximal therapeutic concentration, suggesting that dasatinib was not an inhibitor for this transporter. Further assessment with radiolabelled dasatinib also demonstrated no reduction in retention in the MDR1 positive cells, demonstrating that dasatinib was not a substrate for this transporter either. Interestingly, the intracellular concentration of dasatinib in the transduced cell line was lower than the wild-type, suggesting that there might be increased expression of another transporter in this cell line. Drug transporters are promiscuous in that they actively efflux many shared compounds and are often co-expressed and co-regulated. Further analysis of the expression of the wild type (K-WT) and the transduced cell line (K-MDR) (and detailed in chapter 6) showed elevated expression of ABCG2 in K-MDR. The data presented in chapter 3 demonstrated that dasatinib was a substrate for ABCG2, hence the reduced cellular concentration in the transduced cell line might be attributable to the increased endogenous expression of ABCG2. However, the cell line model in this assay was only used to test the difference in cellular concentration of dasatinib in the presence or absence of PSC 833. As there was no difference in retention

when MDR1 was blocked in the two cell lines, then it was conclusively determined that dasatinib was not a substrate for MDR1.

As with ABCG2, for completion, the effect of blocking this transporter in the presence of TKIs was tested. The treatment with PSC 833 significantly reduced the total number of cells remaining after culture. However, this was not selective for the CD34$^+$ population nor targeted the quiescent population. Instead PSC 833 alone reduced the number of cells remaining both by exerting an anti-proliferative effect and by inducing apoptosis, as demonstrated by the trend of increased number of cells at the earlier divisions both in the total and CD34$^+$ population. The co-treatment with TKI and PSC 833 did result in significantly lower total cell numbers compared to TKIs alone, however this can be attributed to the additional anti-proliferative and apoptotic effects seen with PSC 833 alone. Furthermore, there was no further reduction in p-CrkL and more importantly, there was no reduction in the q34$^+$ population.

Interestingly, there was a significant reduction in p-CrkL with PSC 833 alone at 16hrs compared to the untreated control. This reduction by PSC 833 might either be a consequence of the increased concentration of an endogenous substrate caused by blocking MDR1, or the direct inhibition of p-CrkL by PSC 833. The underlying mechanism for this surprising result though, has not been resolved.

Furthermore, there was no further increase in apoptosis with the combination of PSC 833 and TKIs compared to TKIs alone, although PSC 833 alone significantly increased both apoptosis. Therefore, it can be concluded that the additive reduction of cell number and reduced p-CrkL was not due to potentiation of TKI activity or concentration.

5 Results 3- MRP1 in CML CD34$^+$ cells

The previous two chapters have concentrated on the clinically relevant ABC transporters ABCG2 and MDR1. For completion, the third transporter implicated in MDR in other forms of leukaemia was also studied. There have been fewer reports describing the role of MRP1 in mediating drug resistance, however it has been demonstrated that it can transport many of the same chemotherapeutic agents as MDR1 (Rappa *et al.* 1997b). MRP1 is also expressed in virtually all human tissues and most tumour cell lines, suggesting that MRP1 may contribute to drug resistance (Burger *et al.* 1994). Indeed, AML cells from patients who have relapsed compared to those with responsive disease have higher expression levels of MRP1 (Zhou *et al.* 1995) and increased resistance to chemotherapeutic agents correlates with simultaneous MDR1 and MRP1 expression (Legrand *et al.* 1999).

The analyses of ABCG2 and MDR1 have shown different interaction profiles for the current TKIs. Dasatinib is a substrate for ABCG2, but does not interact with MDR1. In contrast, IM and nilotinib are both inhibitors for ABCG2 and MDR1. The following experiments were therefore designed to identify any interaction of the current TKIs in relation to MRP1 and to examine the expression and function of MRP1 in CML CD34$^+$ cells.

5.1 Expression of *MRP1* mRNA

As for the other transporters, the expression of *MRP1* was investigated in CML CD34$^+$ cells and compared to normal counterparts using real time PCR. As shown in Figure 5-1, CML samples expressed *MRP1* mRNA at similar amplitude in

comparison to normal PB CD34$^+$ cells. Using *GAPDH* as the endogenous control, 11 CML CD34$^+$ and 7 normal CD34$^+$ samples gave ΔCt values of 4.8±0.4 and 4.7±0.4 respectively and a ΔΔCt of 0.11. Using the equation $2^{-\Delta\Delta CT}$ this assay determined that CML CD34$^+$ cells expressed equal amounts of *MRP1* to normal PB CD34$^+$ cells (1.08 fold) (Figure 5-1C).

A.

B.

C.
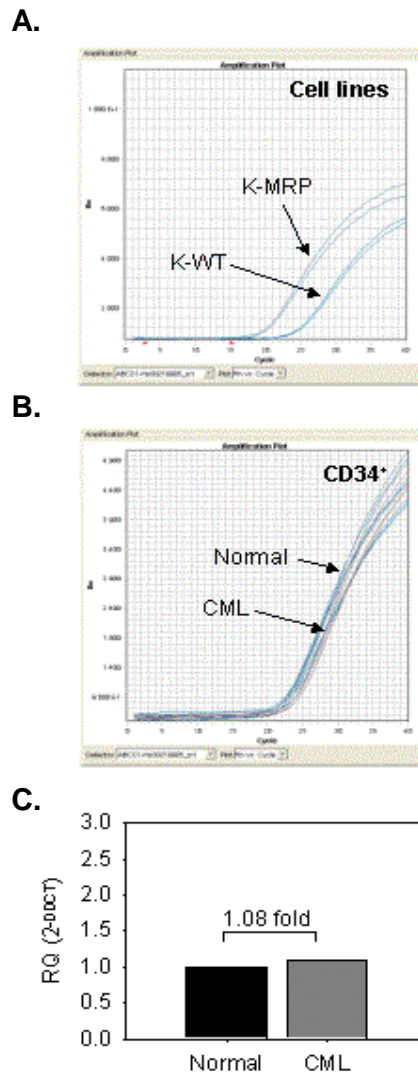
Figure 5-1 Expression of *MRP1* mRNA in cell lines and CML CD34$^+$ cells

Expression of *MRP1* mRNA. **A**. Taqman amplification plot of the cell line K-WT and the transduced cell line K-MRP. **B**. Taqman amplification plot of CML and normal CD34$^+$ samples. **C**. Relative quantification ($2^{-\Delta\Delta CT}$) of *MRP1* expression in CML CD34$^+$ cells (dark grey fill; n=11) compared to normal CD34$^+$ cells (black fill; n=7).

In order to optimise experiments that would determine expression, function and the interaction of MRP1 with TKIs in CML CD34$^+$, a valid cell line model that expressed *MRP1* was required. The K562 WT cell line, generated and donated by Dr L.Fairbairn, was transduced to express the *MRP1* gene, producing the K-MRP cell line. These two cell lines were then analysed on the TLDA card. However, as seen in Figure 5-1A, there was endogenous expression of *MRP1* in the wild-type control cell line, with a similar expression to the expression level in CML samples (K-WT ΔCt 4.7±0.2 n=3; CML ΔCt 4.8±0.4 n=11), although this expression was greatly increased in the transduced K-MRP cell line (K-MRP ΔCt -0.03, n=2).

5.2 Expression of MRP1 protein

The MRP1 protein was detected using the specific antibody QCRL3. This antibody detects an intracellular epitope of the 190kD transmembrane phosphoglycoprotein and does not cross react with human MDR1 (Hipfner *et al.* 1994). As for the antibody staining for MDR1, serial dilutions of the antibody established that a 100x dilution of the antibody, followed by the same dilution of the secondary antibody, produced the most distinct peaks. Following optimisation, the assay was carried out in parental K-WT (MRP1+ve, Figure 5-2A) and transduced K-MRP cells (MRP1++ve, Figure 5-2B). K-WT cells demonstrated an increase in fluorescence compared to the isotype (K-WT isotype GM=3.2±0.3 vs. test GM=5.3±0.6, p=0.01), while the transduced cells demonstrated an even higher increase in fluorescence (K-MRP isotype GM=3.7±0.6 vs. K-MRP1 GM=12.1±1.1 p=0.02), demonstrating protein expression in both cells lines.

The antibody staining for MRP1 was repeated in 3 CML samples (Figure 5-2C). The assay demonstrated positive staining in all the samples, resulting in

significantly higher mean fluorescence than the isotype control (isotype GM, 3.0±0.7, QCRL3 GM 5.0±1.0, p=0.02).
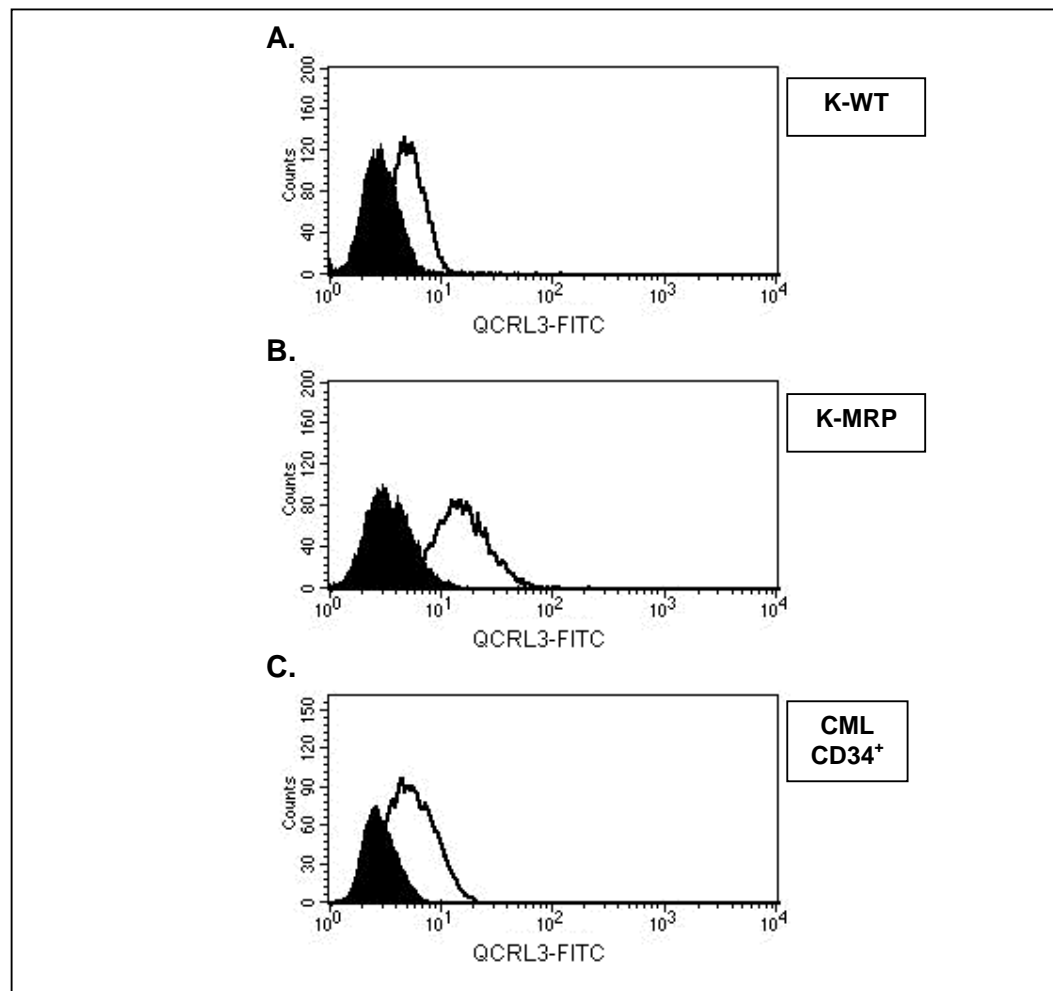
Figure 5-2 Expression of MRP1 protein in cell lines and CML CD34^{+} cells

A representative example of MRP1 protein expression in K-WT **(A)**, K-MRP **(B)** and CML CD34^{+} cells **(C)** with the isotype (black fill) and the MRP1 test antibody QCRL3 (white fill); n=3 in duplicate, all replicates were consistent.

Comparing the change in GM (ΔGM) in the K-WT cell line to the ΔGM in the CML sample demonstrated that the two samples had similar protein levels (K-WT

ΔGM=2.1, CML ΔGM=2). This correlated with similar mRNA expression levels demonstrated by the TLDA card in section 5.2.

5.3 Function of MRP1 protein

To confirm the function of MRP in the transduced cell line, the substrate displacement assay was repeated with the fluorescent MRP1 substrate Fluo-3 AM, in a similar manner to the use of BODIPY-Prazosin for the function of ABCG2 and rhodamine 123 for the function of MDR1. The specific inhibitor of MRP1 used for these experiments was the competitive antagonist of the leukotriene D4 (LTD4) receptor, MK571 (Gekeler *et al.* 1995).

Using the K-WT cell line, it was established that the cell line actively effluxed Fluo-3 AM, and that this efflux was inhibited by the addition of 30µM MK571 (Figure 5-3A). The use of K-MRP cells in this assay was complicated by the presence of GFP as a marker, as both GFP and fluo-3 AM are detected in the FL1 channel (Figure 5-3C). The presence of GFP meant that when fluo-3 AM was added to the K-MRP cells, no further increase in fluorescence was observed. This may be either because there was maximal efflux or the fluorescence emitted by GFP was so bright it masked the signal.
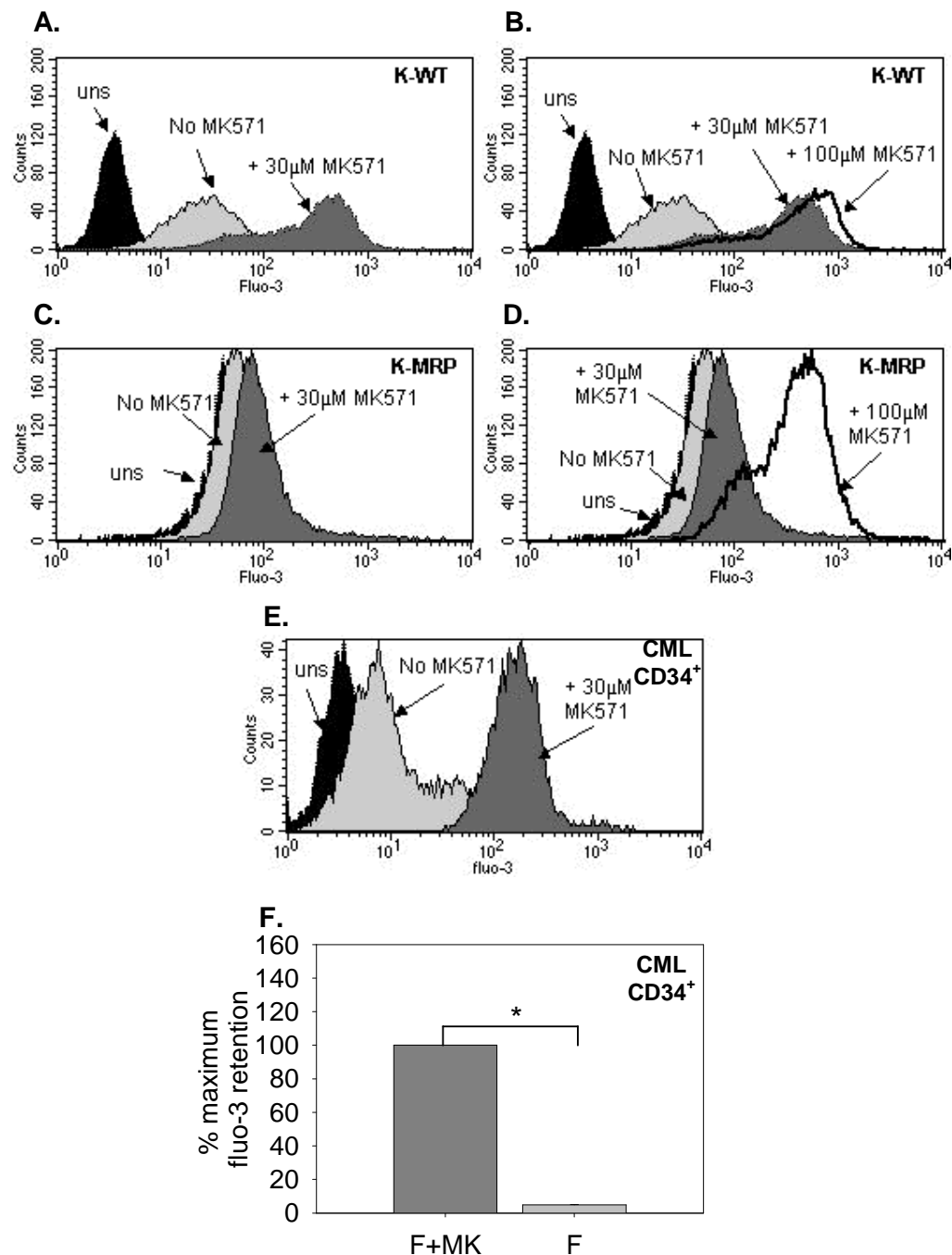
Figure 5-3 Function of MRP1 protein in cell lines and CD34$^+$ cells

MRP1 function by efflux of a known substrate in K-WT (**A** and **B**), K-MDR (**C** and **D**) and CML CD34$^+$ cells **(E)**. Unstained cells (black fill), cells with fluo-3 AM (light grey fill), cells with fluo-3 AM and 30µM MK571 (dark grey fill), cells with fluo-3 AM and 100µM MK571 (black line). **F**. Percentage of efflux by MRP1 in CML CD34$^+$ cells. Fluo-3 AM and 30µM MK571 (dark grey fill), was considered to have maximal retention, fluo-3 AM alone (light grey-fill) *=p<0.001. F-Fluo3-AM

To test this, the function of MRP1 in the transduced cell line was measured in the presence of fluo-3 AM and the inhibitor. At 30µM MK571, a small inhibition in efflux was observed, however, increasing the concentration of the inhibitor to 100µM caused a high degree of inhibition confirming that these cells have functional MRP1 (Figure 5-3D). The requirement for increased doses of MK571 reflected the high level of MRP1 in this cell line. In contrast, the WT cell line showed no further inhibition in the presence of the higher MK571 concentration (Figure 5-3B). As CML samples had similar expression levels of MRP1 to K-WT, 30µM MK571 was used for inhibition of CML CD34$^+$ cells.

The assay was then repeated in 2 CML samples (Figure 5-3E). The fluorescence observed in cells with 30µM MK571 was considered to be maximally loaded and classed as the control condition. In the absence of MK571, there was a significant decrease in fluorescence demonstrating almost complete efflux by functional MRP1 protein (4.89±0.2% retention in comparison to the control, p=0.01 (Figure 5-3F).

5.4 Interaction of IM with MRP1 by a substrate displacement assay

Due to the GFP potentially concealing the functional efflux of fluo-3 AM in the transduced cells and the need for increased inhibitor concentration to inhibit the protein, it was decided that all further substrate displacement assays assessing the interaction of TKIs would be carried out in the wild-type cell line. Unfortunately, there was no cell line available as a negative control due to high MRP1 expression observed in every cell line tested in the laboratory and no MRP1-ve cell line

identified in the current literature. Therefore, the parental cell line K-WT and 30µM were used as a control for all substrate displacement assays.

To determine whether IM interacts with MRP1, increasing concentrations were added to the substrate displacement assay using the K-WT cell line (Figure 5-4A). The addition of IM resulted in no inhibition of efflux, even at 5µM IM, suggesting that IM did not interact with this drug transporter as either a competitive substrate or inhibitor.

Similarly, when this assay was repeated with CML CD34$^+$ cells, IM did not reduce the level of fluo-3 AM efflux, confirming that IM does not interact with MRP1 in primary cells either (Figure 5-4B).
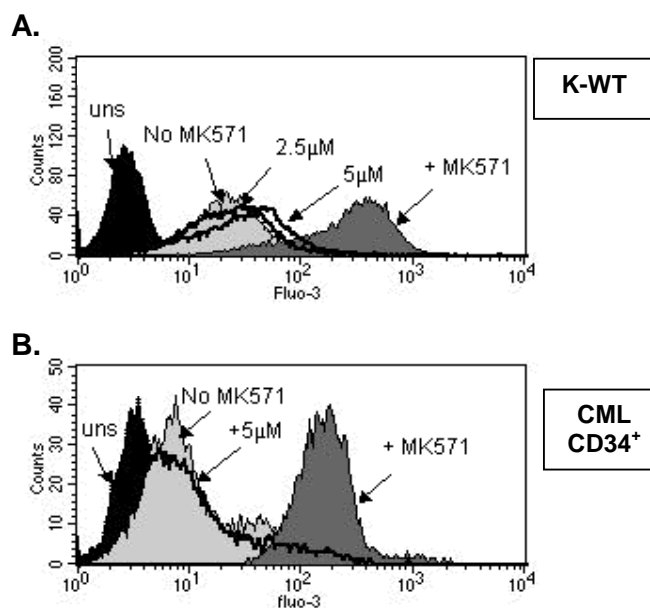
Figure 5-4 Efflux inhibition of a MRP1 substrate by IM

Interaction of IM with the protein MRP1 in the cell line K-WT; n=3 in duplicate **(A)** and CML CD34$^+$ cells; n=2 in duplicate **(B)**. Unstained cells (black fill), with fluo-3 AM (light grey fill), with fluo-3 AM and 30µM MK571 (dark grey fill), with fluo-3 AM and [IM] (black line no fill)

5.5 Assessment of IM as a substrate of MRP1

The substrate displacement assay above demonstrated no interaction of IM with MRP1, suggesting that it was not an inhibitor or a strongly competitive substrate. However, in order to determine whether IM was a substrate of MRP1, increasing concentrations of ^{14}C-IM were added to assess the cellular concentration in K-WT (MRP1+ve) and K-MRP (MRP1++ve) cells. There was no significant accumulation of ^{14}C-IM in either cell line in the presence of the inhibitor MK571, compared to the cell line in the absence of the specific inhibitor, suggesting that IM was therefore not a substrate of MRP1 (Figure 5-4A).

The assay was also repeated using CD34$^+$ cells from 5 CML patients. There was no difference in the cellular accumulation of IM in the presence or absence of the inhibitor, again supporting the conclusion that IM was not a substrate for this transporter in cell lines or primary CD34$^+$ cells (Figure 5-4B).

A.

B.
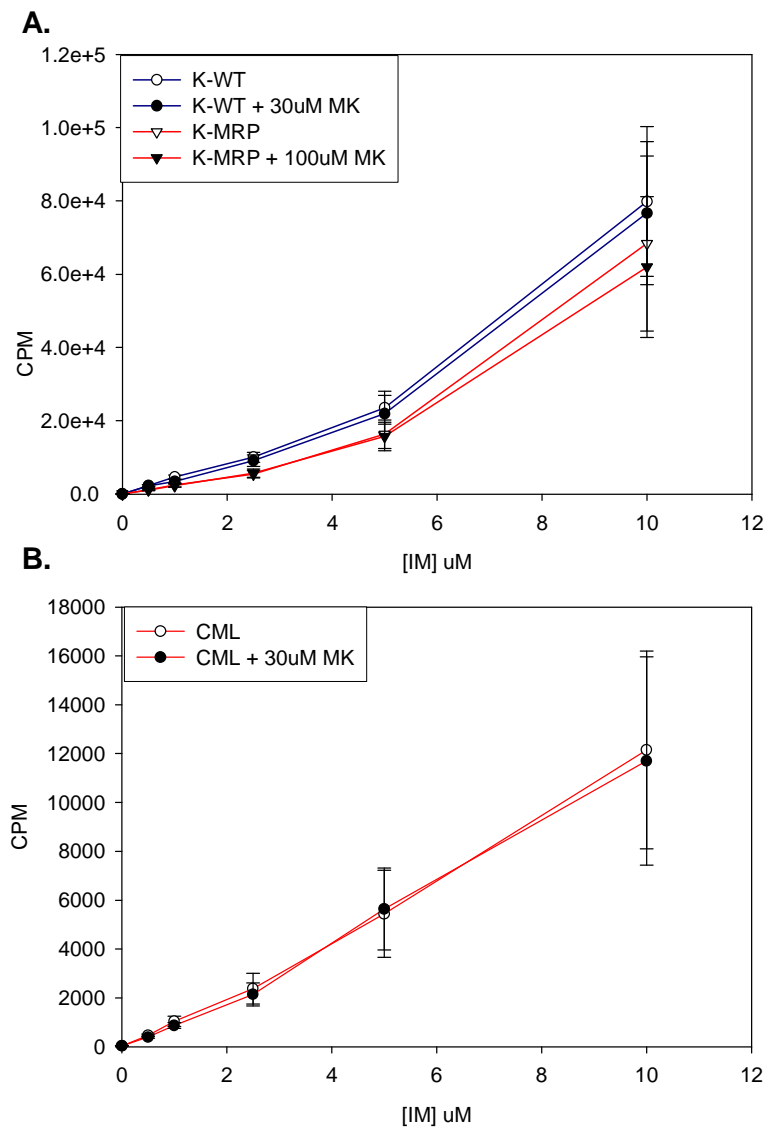
Figure 5-5 Radiolabelled IM in cell lines and CML CD34$^+$ cells

Cellular concentration of ^{14}C-IM in cell lines **(A)** and CML CD34$^+$ **(B)** cells in the presence and absence of 30μM MK571. **A.** K-WT (MRP1+ve) (blue lines, circles) and K-MRP (MRP1++ve) cell line (red lines, triangles) in the presence (black symbols) or absence (white symbols) of MK571, n=3 in duplicate. **B.** CML CD34$^+$ cells in the presence (black symbols) or absence (white symbols) of MK571; n=5 in duplicate.

5.6 Interaction of nilotinib with MRP1 by a substrate displacement assay

To test whether other TKIs interact with MRP1, the substrate displacement assay was repeated, this time with the tyrosine kinase inhibitor nilotinib. This drug was again added at increasing concentrations in K-WT loaded with fluo-3 AM, to determine the effect on the MRP1 protein. The addition of nilotinib resulted in a dose dependent decrease in efflux of fluo-3 AM, although complete reduction of the protein comparable to 30µM MK571 was not reached with 5µM nilotinib (Figure 5-6A).

The assay was again repeated in CML CD34^{+} cells. The efflux of fluo-3 AM was inhibited with increasing nilotinib concentrations (Figure 5-6B), however the retention values observed with 5µM nilotinib (15.31±6%) although slightly higher, were not significantly different to the substrate alone (4.89±0.2%, p=ns) and were significantly lower than 30µM MK571 (100% control, p=0.03) (Figure 5-6C). This incomplete reduction in fluo-3 AM efflux suggests that nilotinib might be either a weak inhibitor or a competitive substrate in CML CD34^{+} cells.
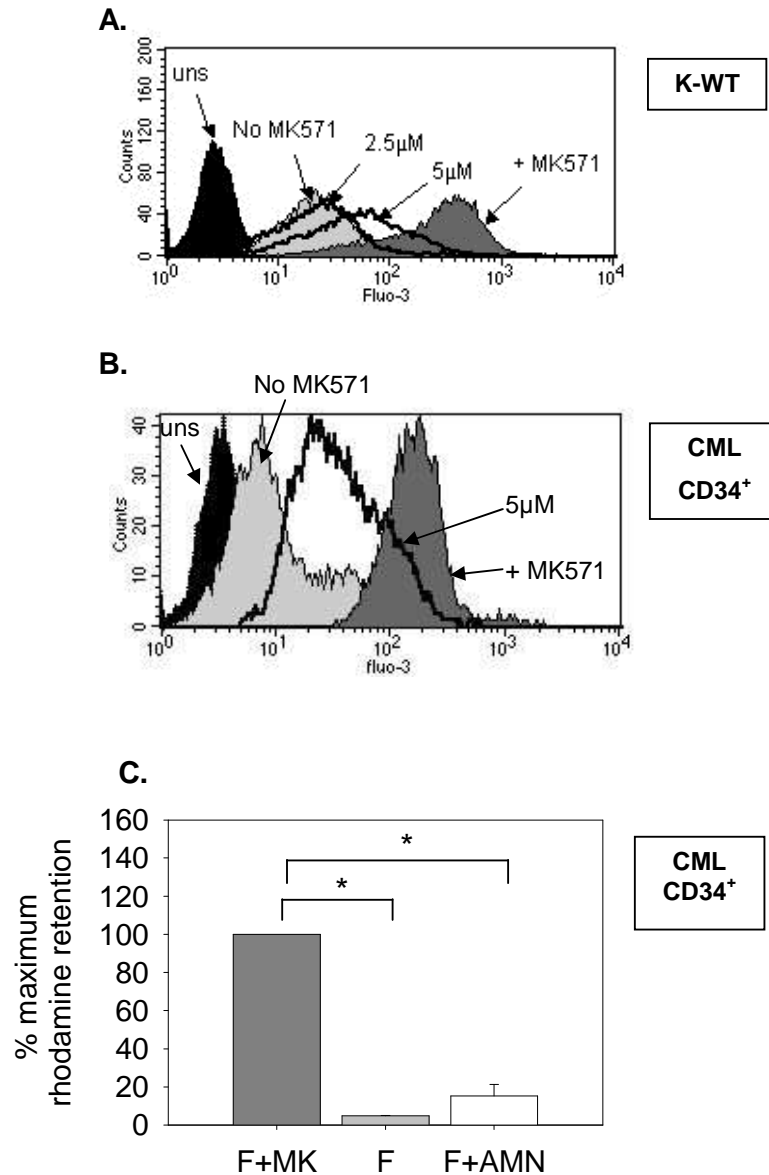
Figure 5-6 Efflux inhibition of a MRP1 substrate by nilotinib

Interaction of Nilotinib with the protein MRP1 in cell line K-WT **(A)** and CML CD34^{+} cells **(B)**. Unstained cells (black fill), with fluo-3 AM (light grey fill), with fluo-3 AM and 30μM MK571 (dark grey fill), with fluo-3 AM and nilotinib (black line no fill); n=3. **C.** Percentage of efflux by fluo-3 AM. Fluo-3 AM and 30μM MK571 (dark grey-fill) was considered to have maximal retention, fluo-3 AM alone (light grey-fill) and fluo-3 AM with 5μM nilotinib (white fill); n=3 *=p≤0.05. F-Fluo3-AM

5.7 Assessment of nilotinib as a substrate of MRP1

The substrate displacement assay demonstrated an interaction of nilotinib with MRP1, however, it cannot delineate between a competitive substrate and an inhibitor. To clarify the interaction, increasing concentrations of radiolabelled nilotinib were added and the cellular CPM measured in the presence and absence of MK571.

There was no reduced accumulation of ^{14}C-nilotinib in the cell line transduced to over-express MRP1 (K-MRP) compared to the wild type that had some MRP1 protein (K-WT). Similarly, there was no significantly increased accumulation of radiolabelled nilotinib in K-WT or K-MRP in the presence of MK571 compared to the cell lines alone, demonstrating nilotinib was not a substrate for MRP1.

The assay was repeated in 3 CML CD34$^+$ samples. As with the cell lines, there was no significant difference of ^{14}C-nilotinib in the presence or absence of MK571, suggesting the interaction observed in the substrate displacement assay was most likely due to nilotinib acting as a weak inhibitor but certainly not a competitive substrate.
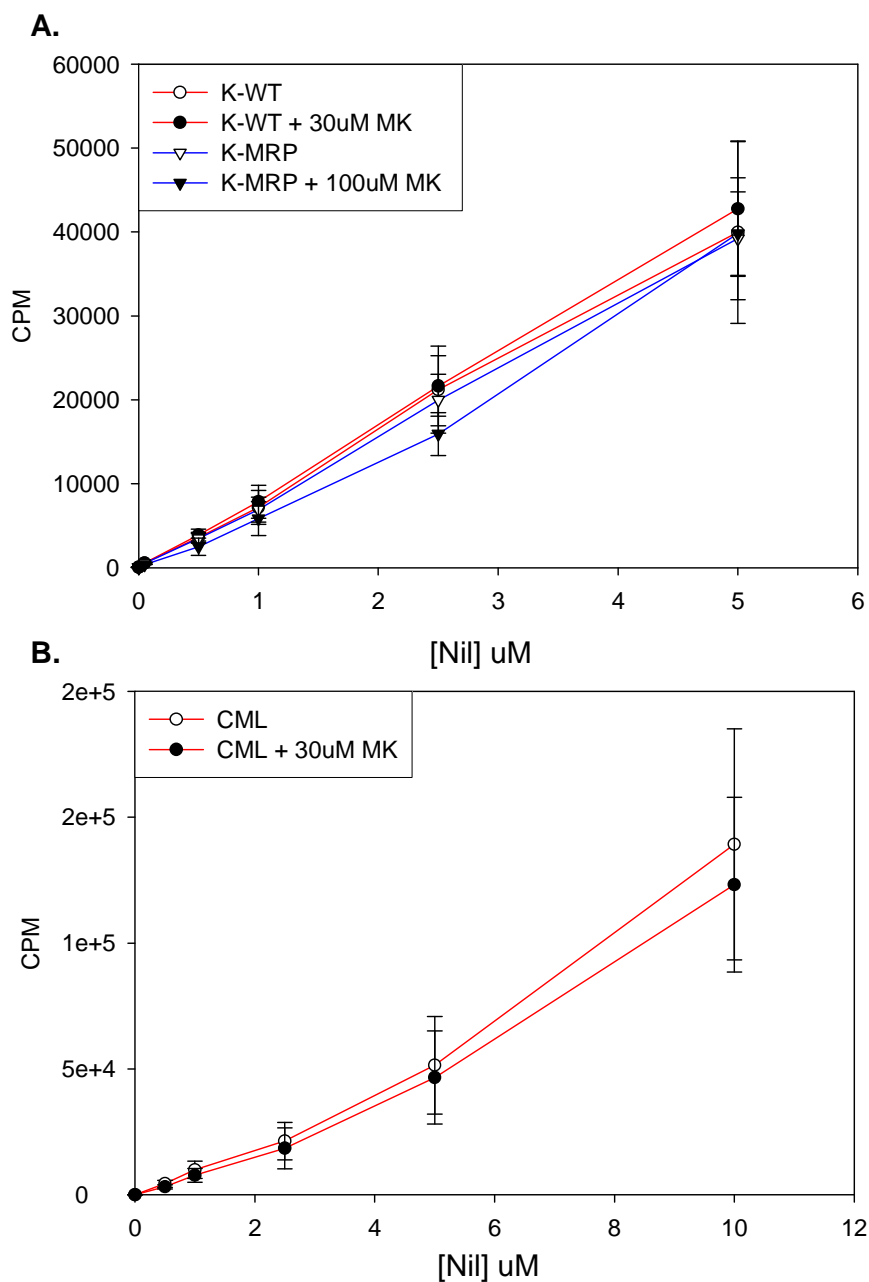
Figure 5-7 Assessment of radiolabelled nilotinib accumulation in the presence of MRP1 protein

Cellular concentration of ^{14}C-nilotinib in cell lines **(A)** and CML CD34$^+$ **(B)** cells in the presence and absence of MK571. **A.** K-WT (MRP1+ve) (red lines with circles) and K-MRP (MRP1++ve) cell line (blue lines with triangles) in the presence (black symbols) and absence (white symbols) of MK571. **B.** CML CD34$^+$ cells in the presence (black symbols) and absence (white symbols) of MK571. All data are mean of duplicate analyses of n=3.

5.8 Interaction of dasatinib with MRP1 protein by a substrate displacement assay

The substrate displacement assay was repeated by replacing the specific inhibitor with the tyrosine kinase inhibitor dasatinib. As demonstrated earlier, there is significant reduction of efflux in the presence of MK571 demonstrating active protein. However, replacing the inhibitor with dasatinib did not result in an increase in fluo-3 AM retention in the K-WT cell line, suggesting that dasatinib was not an inhibitor for this drug transporter (Figure 5-8A).
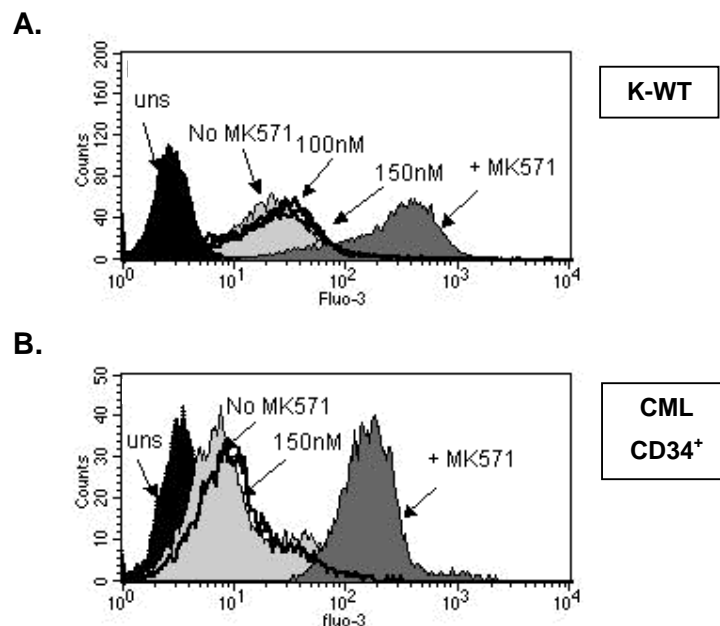
Figure 5-8 Efflux inhibition of a MDR1 substrate by dasatinib

To investigate the interaction with MRP1, IM was added into this assay in place of the known inhibitor, MK571 in K-WT cells **(A)** and CML CD34+ cells **(B)**. **A.** K-WT cells unstained (black fill), with fluo-3 AM (light grey fill), with fluo-3 AM and 30μM MK571 (dark grey fill), with fluo-3 AM and dasatinib (black line no fill). **B.** CML CD34+ cells unstained (black fill), with fluo-3 AM (light grey fill), with fluo-3 AM and 30μM MK571 (dark grey fill), with fluo-3 AM and 150nM dasatinib (black line no fill). All data are mean of n=3 in duplicate.

The assay was repeated in 3 CML samples. There was no significant retention of fluo-3 AM in the presence of dasatinib, even at the maximum clinical dose of 150nM, demonstrating that dasatinib was not an inhibitor of MRP1 (Figure 5-8A).

5.9 Assessment of dasatinib as a substrate of MRP1

The substrate displacement assay described above demonstrated no interaction of dasatinib with MRP1, and showed that dasatinib was not an inhibitor of this transporter. To determine whether dasatinib was a substrate of MRP1, ^{14}C-dasatinib was added to the cells in increasing concentrations. The addition of 30µM MK571 did not significantly increase the accumulation of dasatinib in the K-MRP cell line (p=ns). However, there was a significant increase in ^{14}C-dasatinib accumulation in the K-WT cell line with 30µM MK571 compared to the cell line alone at 150nM (p=0.05), 300nM (p=0.01) and 600nM (p=0.01).

Increasing the concentration of MK571 to 100µM in the K-WT cell line also demonstrated a significant accumulation at 10nM (p=0.01) and 50nM (p=0.02), as well as at 150 and 300nM (p<0.02). Increasing the concentration of MK571 to 100µM in the transduced cell line K-MRP demonstrated significant accumulation at 50nM (p=0.001).

These results demonstrated that although 30µM MK571 resulted in significant accumulation in the wild-type cell line, it was insufficient to inhibit the MRP1 in the transduced cell line. This correlates to the increased concentration of MK571 required in the substrate displacement assay (figure 4-3) whereby the elevated MRP1 expression was maximally inhibited by 100µM MK571. These results demonstrated that dasatinib was a substrate for MRP1.
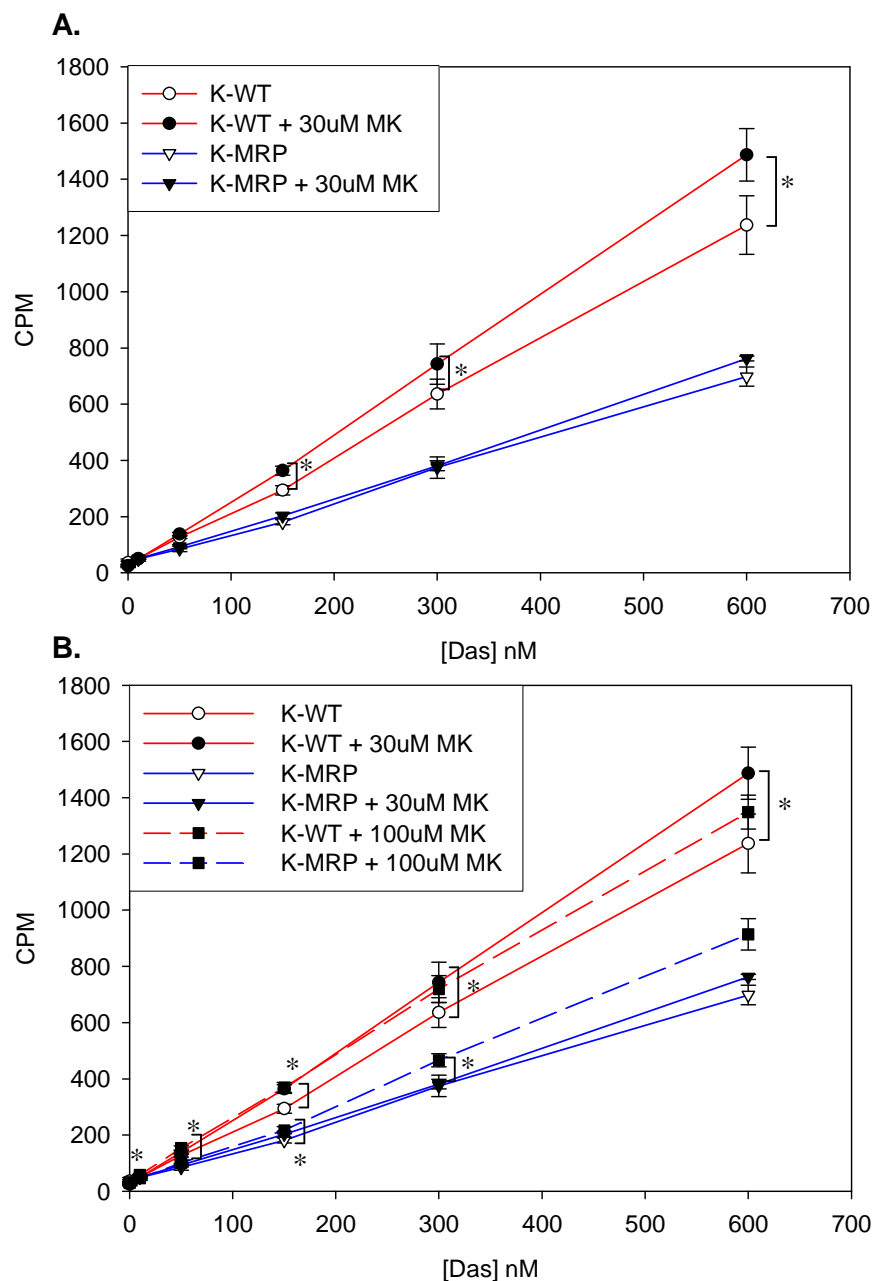
Figure 5-9 Assessment of radiolabelled dasatinib accumulation in the presence of MRP1 protein

Cellular concentration of ^{14}C-dasatinib in the presence and absence of 30µM MK571 **(A)** or 100µM Mk571 **(B)**. K-WT (MRP1+ve) (red lines) and K-MRP (MRP1++ve) cell line (blue lines) in the presence (black symbols) and absence (white symbols) of 30µM (solid lines) or 100µM (dashed lines, squares) MK571. All data are mean of duplicate analyses of n=3; *=p$\leq$0.05.

Despite the addition of 100µM MK571 in the transduced cell line, the accumulation in this cell line remained significantly lower than the wild-type cell line (p<0.05 for 50-600nM). This may suggest that there is another transporter on the transduced cell line contributing to the reduced accumulation.

The low specific activity of ^{14}C-dasatinib prevented this assay from being repeated in CML CD34$^+$ cells as the reduced radiolabelled ^{14}C counts accumulated in the low cell numbers available for each determination would not be above the threshold of detection.

5.10 Effect of MRP1 inhibition on CML CD34$^+$ cells following 72hrs culture

The combination of substrate displacement assays and cellular concentration measurements demonstrated that nilotinib was an inhibitor, dasatinib was a substrate and IM had no effect on MRP1. To determine the effect of MRP1 inhibition on the capacity of these TKIs to kill CML cells, CD34$^+$ cells were incubated for 72hrs in the presence of TKIs alone or TKI and MK571 to inhibit transport via MRP1.

As in the previous chapters (chapters 3 and 4), treatment with the TKIs alone resulted in a reduction in the total number of cells in comparison to cells in 5GF alone. Blocking the MRP1 transporter by the addition of 30µM MK571 resulted in no reduction of the total number of viable cells compared to 5GF alone (20.1±1.6x10^5 with MRP1, 17.7±2.2 alone; p=ns), indicating that MK571 alone does not reduce proliferation.

When the cells were co-treated with IM, nilotinib or dasatinib and MK571, there was no difference in the total number of cells remaining in comparison to TKIs alone (IM 90.3±17.4% vs. IM + MK571 88.5±22.9%, nilotinib 61.7±9.2% vs. nilotinib + MK571 59.5±12%, dasatinib 80±12.5% vs. dasatinib + MK571 81.3±21.4%, p=ns for all combinations). This suggested that blocking the MRP1 protein does not further enhance the effect of TKI in reducing total cells.
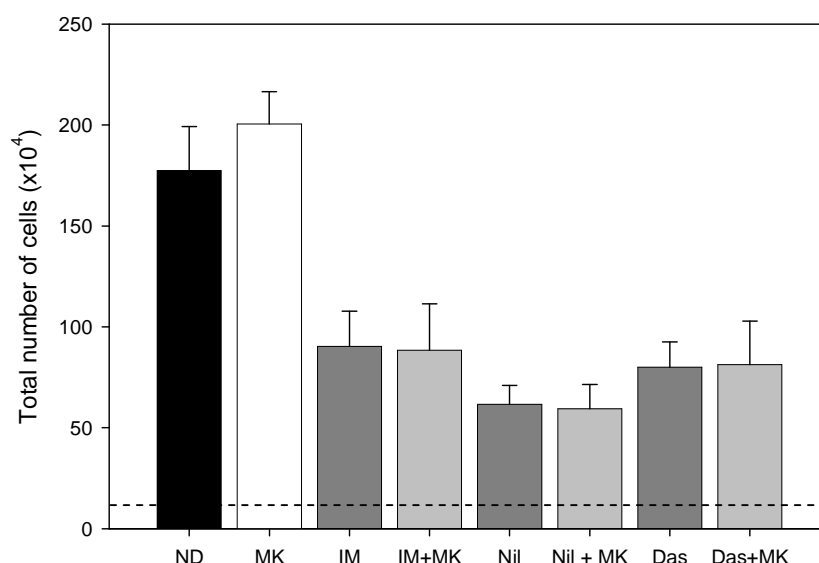
Figure 5-10 Inhibition of MRP1 in total viable cells

Total number of cells following 3 days in culture, in the presence of TKIs alone (dark-grey fill) or combined with MK571 (light grey fill). In addition, total number of cells in 5GF alone (ND, black fill), or MK571 alone (white fill) are plotted. CD34$^+$ cells were seeded at 1×10^5 cells at d0 (dotted line); n=4 for IM, n=4 for nilotinib, n=3 for dasatinib. All data are mean of duplicate analysis, *=p$\leq$0.01

5.11 Assessment of q34$^+$ cells following 72hrs culture

The quiescent population remaining following 72hrs of culture was examined for further reduction in 2 CML patients. There was no reduction in the presence of

MK571 alone (ND 4.6±1% vs. MK571 4.6±3.2%) suggesting blocking the
transporter alone does not reduce the quiescent population. The co-treatment of
MK571 with IM, nilotinib or dasatinib did not further reduce the accumulation of
q34$^+$ cells (IM 11.7±8.3% vs. IM + MK571 12.2±8.5%, nilotinib 8±4.4% vs. nilotinib
+ MK571 15±10.5%, dasatinib   5.2±1.7%   vs.   5.6±2.9%,   p=ns   for   all
combinations), suggesting that blocking MRP1 does not enhance the reduction of
the quiescent population.
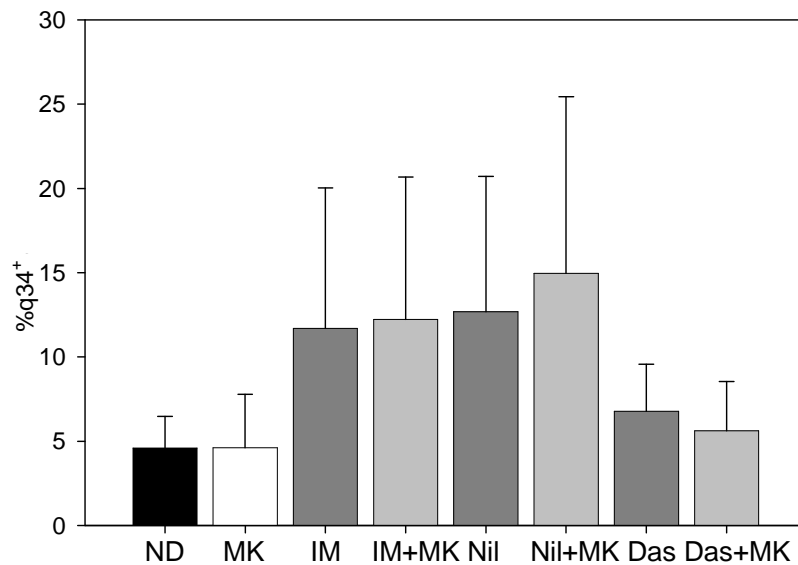
Figure 5-11 Inhibition of MRP1 on quiescent CD34$^+$ CML cells

Percentage of q34 following 72hrs of culture as a percentage of input in
5GF alone (ND, black fill), with MK571 (white fill), in the presence of TKIs
alone (dark grey fill) or combined with PSC 833 (light grey fill). n=4 for IM,
n=6 for nilotinib, n=7 for dasatinib

5.12 Effect of MK571 on cell division in CML cells following 72hrs culture

The effect of MK571 in CD34$^+$ cells following 72hrs culture was examined further using the stain CFSE to track cell division. The data was analysed as previously, measuring the population remaining following treatment (Figure 5-12A) and the cells that are still CD34$^+$ (Figure 5-12B). There was no significant difference either in the absolute number of cells or CD34$^+$ cells remaining compared to 5GF alone either in the proliferating or non-proliferating cells (p=ns for all combinations). In addition there was no further difference at each division, suggesting that MK571 alone is not toxic to the cells and does not alter the divisional kinetics of the cells.

A.

B.
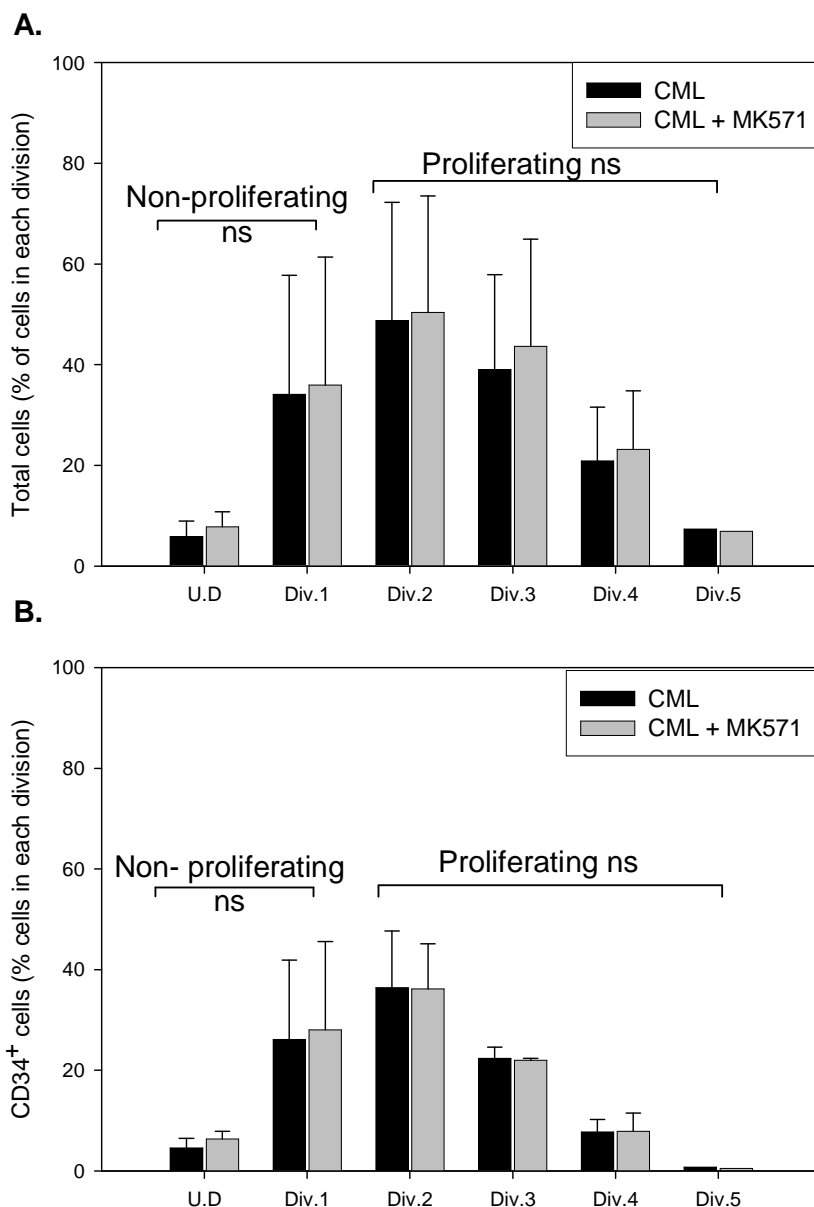
Figure 5-12 Effect of MK571 on cell division in CML cells following 72hrs culture

Cells were labelled with CFSE to allow tracking of their proliferative history. The number of **(A)** total cells or **(B)** CD34$^+$ cells that remain undivided (U.D), have divided once (Div 1), twice (Div 2) etc. were calculated using the % of cells detected in each division, the cell number and % CD34$^+$ cells within each division. Cells treated with 5GF alone (black fill) compared with cells treated with 30μM MK571 alone (grey fill), n=3

5.13 Assessment of CrkL phosphorylation

To further define the effects of MRP1 inhibition on the efficacy of TKI to inhibit BCR-ABL activity, the phosphorylation of the downstream substrate CrkL was examined at 16 and 72hrs. As demonstrated earlier, p-CrkL was significantly reduced at 16hrs with the addition of TKIs, with p-CrkL reduction maintained at 72hrs with nilotinib and dasatinib (see section 3.13). Combining IM or nilotinib with MK571 did not further reduce p-CrkL, demonstrating that MRP1 inhibition does not enhance the effect of TKIs at 16hrs (IM 52.5±11.3% vs. IM + MK571 59.4±6.9%, nilotinib 46±5.2% vs. nilotinib + MK571 43.5±6.6%, p=ns) or 72hrs (p=ns for all combinations). Surprisingly however, the combination of dasatinib with TKI also did not further reduce p-CrkL either at 16hrs (dasatinib 45.4±5.5% vs. dasatinib + MK571 38.5±3.7%, p=ns) or 72hrs (p=ns), despite being shown to be a substrate for this transporter. The inhibition of MRP1 with MK571 alone also demonstrated no difference in the activity of CrkL at 16 or 72hrs (n=3, p=ns at both timepoints), suggesting that inhibition of MRP1 does not further reduce BCR-ABL activity.

A.

B.
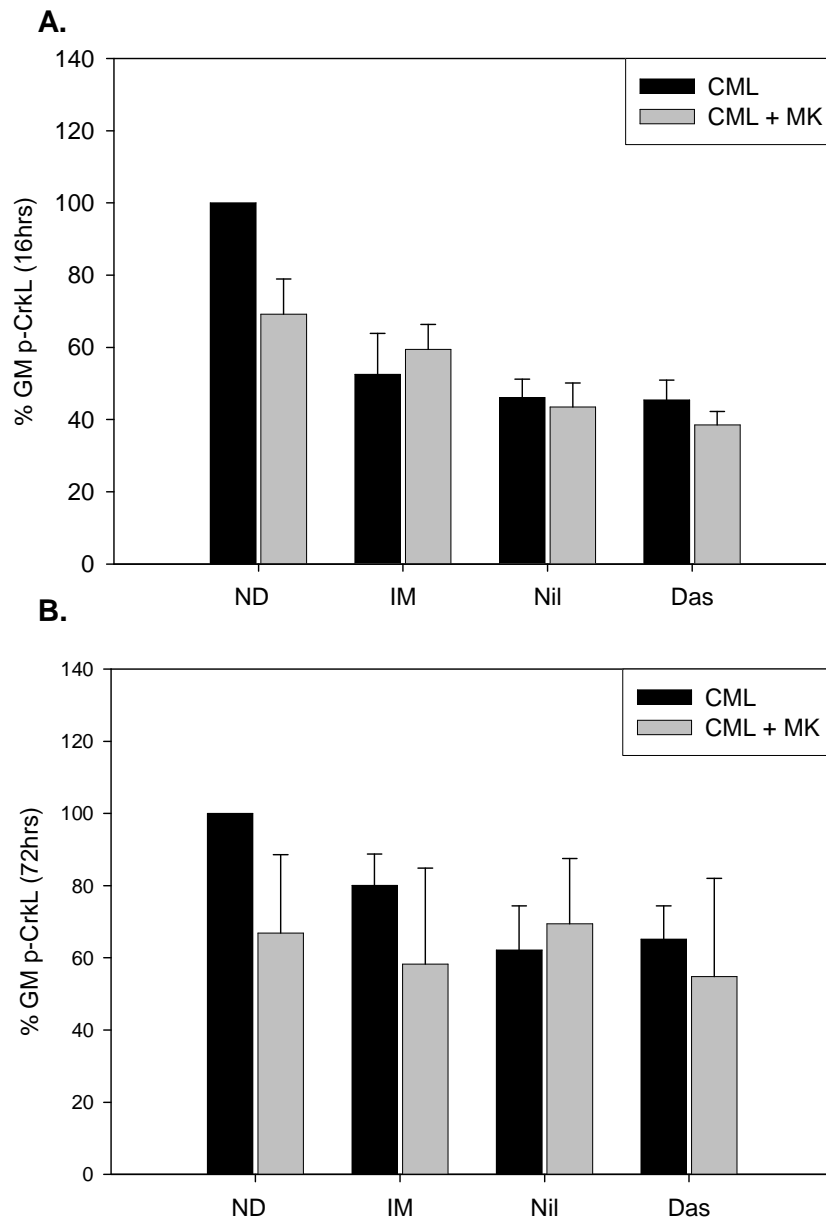
Figure 5-13 BCR-ABL inhibition as a measure of percentage of p-CrkL in CML CD34$^+$ cells

Percentage p=CrkL remaining relative to no drug control (ND) at 16hrs (black bars) or 72hrs (grey bars) n=3

5.14 Assessment of apoptosis

In order to fully investigate the effect of blocking the MRP1 transporter, CML CD34$^+$ cells were stained with annexin and viaprobe to determine apoptosis. Increased apoptosis was observed in the presence of nilotinib as demonstrated earlier (see section 3-14). In contrast to FTC though, there was also a small but significant increase in apoptosis in the presence of MK571 compared to growth factor alone (23.9±4.4% vs. 19±4.69%, p=0.004), demonstrating slight toxicity to the cells. The co-treatment with TKI however did not further increase apoptosis (IM 31.8±2.6% vs. IM + MK571 33.2±3.3%, nilotinib 37.7±3% vs. nilotinib + MK571 36.1±4%, dasatinib 31.3±2% vs. 32.8±3.7%, p=ns for all combinations), suggesting that the effect of TKI was not further enhanced by inhibition of MRP1.
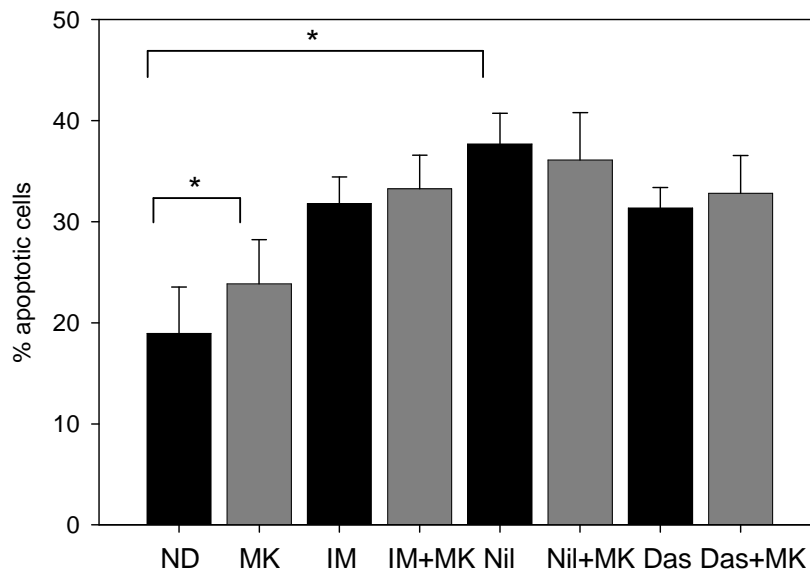
Figure 5-14 Apoptosis in the presence and absence of MK571

Percentage of apoptosis in the presence (dark grey) or absence (black) of MK571 and TKIs; n=3. ND-no drug, MK-MK571

5.15 Summary

The above experiments conclusively demonstrate that *MRP1* was expressed in both CML CD34$^+$ and normal CD34$^+$ at similar levels. In addition, the protein was functional demonstrating effective translation.

Replacing the known inhibitor, MK571, with TKIs demonstrated an interaction with nilotinib, although this did not reach statistical significance. Further analysis with radiolabelled nilotinib demonstrated no additional accumulation in the presence of the known MRP1 inhibitor, suggesting that nilotinib is at best a weak inhibitor of MRP1.

In contrast, replacing the known inhibitor, MK571, with either IM or dasatinib had no effect, suggesting that these agents were not inhibitors of MRP1. Further analysis with radiolabelled IM demonstrated no additional accumulation in the presence of MK571, concluding that IM is neither a substrate nor an inhibitor for this protein. However, blocking the transporter with MK571 in the cell lines significantly increased the accumulation of dasatinib, suggesting that dasatinib is indeed a substrate for, and not an inhibitor of, MRP1.

The effect of blocking the transporter either in the presence or absence of TKIs was then studied. The treatment with MK571 alone did not affect the overall number of cells remaining and the proportion of cells in each division was not altered, indicating that MK571 does not have an anti-proliferative effect like PSC833. However, there was a small increase in apoptosis observed at 72hrs, demonstrating that MK571 alone was slightly toxic to the cells.

However, the co-treatment of MK571 with IM, nilotinib or dasatinib did not further reduce the cells in comparison to TKIs alone, despite dasatinib being a substrate for this transporter. Furthermore, the inhibition of MRP1 did not enhance the reduction of total cells and more importantly did not reduce the quiescent population. In addition, the co-treatment of MK571 and TKIs did not further reduce p-CrkL or increase apoptosis compared to TKIs alone. These results therefore suggest that although MRP1 is functional and dasatinib is a substrate, the expression does not mediate resistance in CML CD34$^+$ cells. It may therefore suggest that, as detailed in chapter 3 (section 3.19) the maximal concentration required for full inhibition is limited by active efflux of dasatinib by ABCG2 and possibly other transporters as yet unidentified. Indeed, the co-treatment of FTC and MK571 with dasatinib may further enhance the overall cell kill of the progenitor and quiescent population and further limit BCR-ABL activity. Alternatively, these data may again suggest that dasatinib may be inhibiting BCR-ABL to its maximum, such that increasing the cellular concentration will not further reduce p-CrkL.

6 Results 4- Drug transporters in cell lines and

CML CD34⁺ cells

The results presented in the previous chapters have investigated the three main clinically relevant drug transporters in CML CD34⁺ cells and compared their expression to normal counterparts. Following confirmation of protein function, their interaction with the TKIs was determined. Nilotinib was identified as an inhibitor for every drug transporter examined, while IM was an inhibitor for ABCG2 and MDR1. In contrast dasatinib was found to be a substrate for ABCG2 and MRP1, which were the two transporters that were highly expressed in CML CD34⁺ cells. Yet despite this, co-treatment of TKIs in the presence of drug transporter inhibitors did not further reduce the total number of cells or further reduce p-CrkL. This suggests that either dasatinib is inhibiting BCR-ABL activity to its maximum efficiency such that increasing the concentration will not further reduce p-CrkL, or that the dasatinib concentration is still being limited by the active efflux of other transporters. Indeed, the previous three chapters have only investigated the effect of inhibiting each transporter in isolation and have only looked at the 3 clinically relevant transporters. The transporter family have many members and they are inherently promiscuous, sharing many substrates. It is therefore likely that other transporters, perhaps not yet identified, may also mediate resistance by actively effluxing the TKIs. In addition, treatment of cells with TKIs may induce expression of transporters that are inactive at initial diagnosis, or may stimulate overexpression of the currently active transporters. This chapter therefore looked at a wider selection of transporters, including the solute carrier family SLC22a, which might be expressed on CML CD34⁺ cells, either at diagnosis or post treatment with TKIs and which may have a role in drug resistance. The first three

members of this family (SLC22a1-3) are organic cation transporters and are also known as OCT1-3, the following 2 members (SLC22a4 and SLC22a5) are organic cation/carnitine transporters and are also known as OCTN1 and OCTN2 and the next 4 members are organic anion transporters (OAT1-4). For clarity and elimination of confusion due to their similarity in nomenclature, in figures the first 3 members will be referred to as OCT1-3 and the remaining will be referred to by their family gene names SLC22a4-9.

6.1 Experimental variation of TLDA cards

The expression of drug transporters was investigated by designing a custom-made TLDA card with a range of drug transporter genes. The advantage of analysis by this method is the small amount of material required. Each card possesses 384 wells of which 48 are supplied by 1 port (i.e. 8 ports in total) and each port requires only 100ng of RNA converted to cDNA for optimum experimentation, which therefore amounts to only ~2ng per well.

Prior to any sample testing, the technique was validated in our hands. Firstly, the layout of the TLDA card was such that each gene for every sample was tested in duplicate. Table 6-1 represents an example from one of the cell lines showing the change in crossing thresholds (ΔCt) between the endogenous control (*GAPDH*) and gene, and the corresponding standard deviation (S.D.), generated by the Taqman software "RQ Manager 1.2". A ΔCT value that is lower in one gene compared to another represents a higher relative expression and *vice versa*. Similarly, when comparing genes from two samples, the sample with the lower value will have higher gene expression. Negative values, as demonstrated with *18S* and *β-ACTIN*, represent genes that had a signal detected earlier than *GAPDH*

and hence have higher expression than this endogenous control. Genes that have

no signal after 40 cycles were termed "nd" demonstrating an expression level

below the threshold of detection.

Detector	Plate 1	
	Avg ΔCt	ΔCt S.D.
18S	-13.16	0.03
MDR1	nd	nd
MRP1	6.38	0.13
MRP4	6.46	0.09
ABCG2	0.84	0.03
ABL1	5.19	0.06
B-actin	-0.91	0.09
AKT1	3.09	0.19
BCR	6.91	0.24
CASP3	6.82	0.06
CD34	nd	nd
CD38	2.61	0.31
GAPDH	Endogenous control	
HIF1A	4.43	0.03
PROM1	nd	nd
SLC22a1 (OCT1)	nd	nd
SLC22a2 (OCT2)	nd	nd
SLC22a3 (OCT3)	nd	nd
SLC22a4 (OCTN1)	8.35	0.35
SLC22a5 (OCTN2)	8.19	0.09
SLC22a6 (OAT1)	nd	nd
SLC22a7 (OAT2)	nd	nd
SLC22a8 (OAT3)	nd	nd
SLC22a9 (OAT4)	nd	nd

Table 6-1 A representative example of one sample tested in duplicate with the corresponding S.D.

GAPDH was used as the endogenous control, nd=not detected

Secondly, in excess of 3 samples were tested on different days in different port

positions to determine inter-experimental variation. Table 6-2 details the CT and

ΔCt of K-WT tested on TLDA cards on different days with the corresponding S.D.

The analysis from the combined data in the two tables confirmed that the data

obtained from the TLDA cards was optimised and valid for comparative analysis.

Detector	Plates 1-3			
	Mean Ct	Ct S.D.	Mean ΔCt	ΔCt S.D.
18S	6.56	0.12	-14.07	0.13
MDR1	21.08	0.05	0.60	0.11
MRP1	24.49	0.05	3.87	0.28
MRP4	25.84	0.02	5.22	0.23
ABCG2	25.22	0.26	4.59	0.48
ABL1	27.40	0.14	6.78	0.39
β-actin	19.56	0.09	-1.07	0.30
AKT1	24.99	0.38	4.37	0.49
BCR	26.37	0.31	5.74	0.08
CASP3	27.25	0.20	6.62	0.18
CD34	>40.00	N/A	Nd	nd
CD38	>40.00	N/A	Nd	nd
GAPDH	20.62	0.25	Endogenous control	
HIF1A	24.94	0.14	4.32	0.34
CD133	>40.00	N/A	19.38	0.25
SLC22a1 (OCT1)	33.47	1.89	12.85	1.85
SLC22a2 (OCT2)	>40.00	N/A	Nd	nd
SLC22a3 (OCT3)	>40.00	N/A	Nd	nd
SLC22a4 (OCTN1)	27.88	0.18	7.26	0.22
SLC22a5 (OCTN2)	27.59	0.09	6.96	0.33
SLC22a6 (OAT1)	>40.00	N/A	nd	nd
SLC22a7 (OAT2)	>40.00	N/A	nd	nd
SLC22a8 (OAT3)	>40.00	N/A	nd	nd
SLC22a9 (OAT4)	>40.00	N/A	nd	nd

Table 6-2 An example of one sample tested in duplicate on different plates representing the S.D. both at Ct and ΔCT

The experiment was completed in 40 cycles. A value of greater than 40 cycles suggested either expression was below the level of detection or there was no expression. GAPDH was used as the endogenous control; n=3, nd=not detected, n/a= not applicable

6.2 Expression of drug transporters in cell lines

Following validation, the cell lines used as models for optimisation of experiments in the previous chapters were analysed. Table 6-3 details the ΔCt of the drug transporters in the cell lines.

Detector	K-WT ΔCt Mean	K-WT ΔCt S.E	K-MDR ΔCt Mean	K-MDR ΔCt S.E	K-MRP ΔCt Mean	K-MRP ΔCt S.E	AML3 ΔCt Mean	AML3 ΔCt S.E	AML6.2 ΔCt Mean	AML6.2 ΔCt S.E
MDR1	nd	nd	0.51	0.56	15.91	0.56	nd	nd	nd	nd
MRP1	4.71	0.21	3.93	0.09	-0.03	0.09	6.42	0.02	6.54	0.16
MRP4	4.76	0.20	5.22	5.28	4.30	0.20	7.09	0.12	6.47	0.02
ABCG2	8.77	0.28	4.73	0.26	6.13	0.26	nd	nd	0.81	0.03
GAPDH	Endogenous control									
SLC22a1 (OCT1)	2 of 5		12.85	1.07	1 of 2		1 of 3		5.46	6.98
SLC22a2 (OCT2)	nd	nd	nd	nd	nd	nd	nd	nd	nd	nd
SLC22a3 (OCT3)	nd	nd	nd	nd	nd	nd	nd	nd	nd	nd
SLC22a4 (OCTN1)	8.20	0.15	7.27	0.02	7.08	0.02	9.98	0.23	8.62	0.27
SLC22a5 (OCTN2)	6.11	0.34	7.05	0.09	6.60	0.09	8.98	0.05	8.17	0.01
SLC22a6 (OAT1)	nd	nd	nd	nd	nd	nd	nd	nd	nd	nd
SLC22a7 (OAT2)	nd	nd	nd	nd	nd	nd	nd	nd	nd	nd
SLC22a8 (OAT3)	nd	nd	nd	nd	nd	nd	nd	nd	nd	nd
SLC22a9 (OAT4)	nd	nd	nd	nd	nd	nd	nd	nd	nd	nd

Table 6-3 Expression of drug transporters in parental and transfected cell lines

n=5 for K-WT, n=3 for K-MDR, n=2 for K-MRP, n=3 for AML3, n=3 for AML6.2. All samples were carried out in duplicate, nd=not detected

The genes analysed demonstrate effective *MDR1* and *MRP1* transduction of the parental cell line (K-WT) to produce the cell line K-MDR and K-MRP respectively

(*MDR1* in K-WT ΔCT=nd vs. K-MDR ΔCt=0.51; *MRP1* in K-WT ΔCt=4.71 vs. K-MRP ΔCt=⁻0.03, p=0.02). Similarly, effective *ABCG2* transduction of the parental AML3 cell line was observed to produce AML6.2 (AML3 ΔCT=nd vs. AML6.2 ΔCt=0.81).

However, in addition to the elevated expression of the transduced genes, other drug transporters also demonstrated significant differences of expression in these cell lines compared to the parental cell line. In K-MDR cell line, there was a significant increase in the ΔCT of *MRP1* (p=0.02), *ABCG2* (p=0.001) and *SLC22a4* (p=0.02), compared to K-WT cell line. The ΔCT for *ABCG2* and *SLC22a4* were also increased in the K-MRP cell line, compared to K-WT (p=0.003 and p=0.008 respectively) and *MDR1* was expressed in the transduced K-MRP cell line (K-MRP ΔCt=15.91), compared to K-WT, where expression was below the threshold of detection or not expressed (K-WT ΔCT=nd). Similarly, the ΔCt of *MRP4*, *SLC22a4* and *SLC22a5* were also elevated in the AML6.2 cell line, compared to the AML3 parental line (p=0.03, p=0.03, p=0.001 respectively). These findings suggest that manipulation of one transporter resulted in the modulation of the endogenous levels of other transporters. This therefore emphasises the necessity to fully characterise cell lines before interpreting results.

The ΔCt values were analysed with the RQ equation (see section 3-1), thereby translating the ΔCT values into relative differences, which allows the comparison of the target sample (i.e. transduced cell line) against the calibrator sample (i.e. parental cell line, Figure 6-1). Although the *MDR1* cell line had statistically elevated ΔCt values for *MRP1*, *ABCG2* and *SLC22a4*, only the gene *ABCG2* demonstrated greater than 3 fold increase in K-MDR compared to K-WT (1.72 fold for *MRP1*, 16.39 fold for *ABCG2* and 1.9 fold for *SLC22a4*).

The RQ equation was also used to compare the ΔCt values of drug transporters in the K-MRP cell line with K-WT. The transduction of *MRP1* resulted in a 26.7 fold overexpression of the gene in the transduced cell line. In addition, *ABCG2* was 6.2 fold higher in K-MRP compared to K-WT. However, although there was a significant difference in ΔCT values with *SLC22a4*, the relative difference resulted in only 2.2 fold increase in K-MRP compared to K-WT.
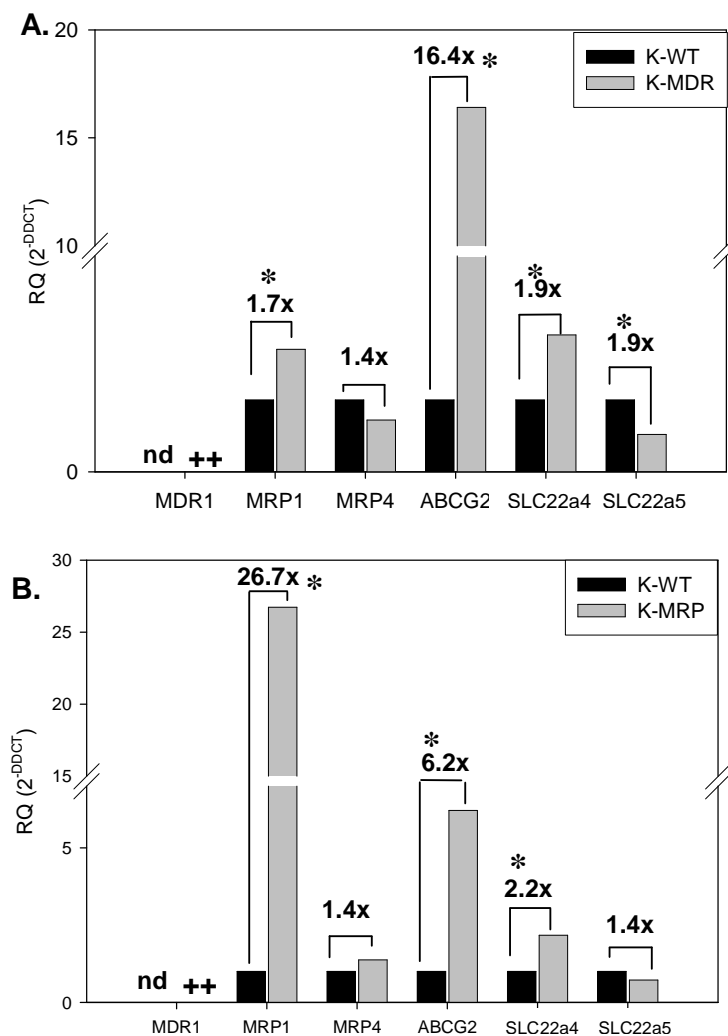
Figure 6-1 Relative expression of drug transporters in the transduced cell lines K-MDR and K-MRP relative to the parental cell line K-WT

Relative expression of K-MDR (**A**) and K-MRP (**B**) relative to the parental cell line K-WT; nd=not detected, ++= signal, *ΔCT=$p \leq 0.05$, n=3

Similarly, the transduction of *ABCG2* in the parental AML3 cell line resulted in differences in the ΔCt values of *MRP4*, *SLC22a4* and *SLC22a5*; although none demonstrated greater than 3 fold relative difference (1.5 fold, 2.6 fold and 1.8 fold greater expression in AML6.2 compared to AML3, Figure 6-2).
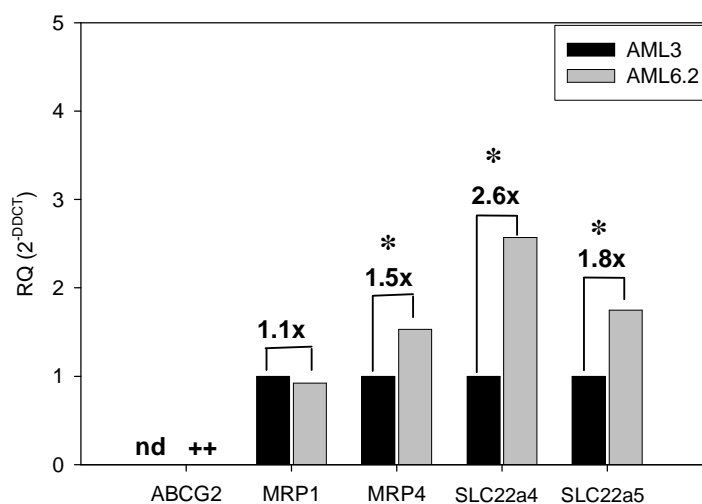
Figure 6-2 Relative expression of drug transporters in the transduced cell line AML6.2 relative to the parental cell line AML3

nd=not detected, ++= signal, *ΔCT=p$\leq$0.05, n=3

6.3 Expression of drug transporter genes in a CML cell line (K562) following drug treatment with TKIs

The parental cell line was then treated with TKIs to determine whether the exposure to these drugs modulated the expression of drug transporters (Figure 6-3).
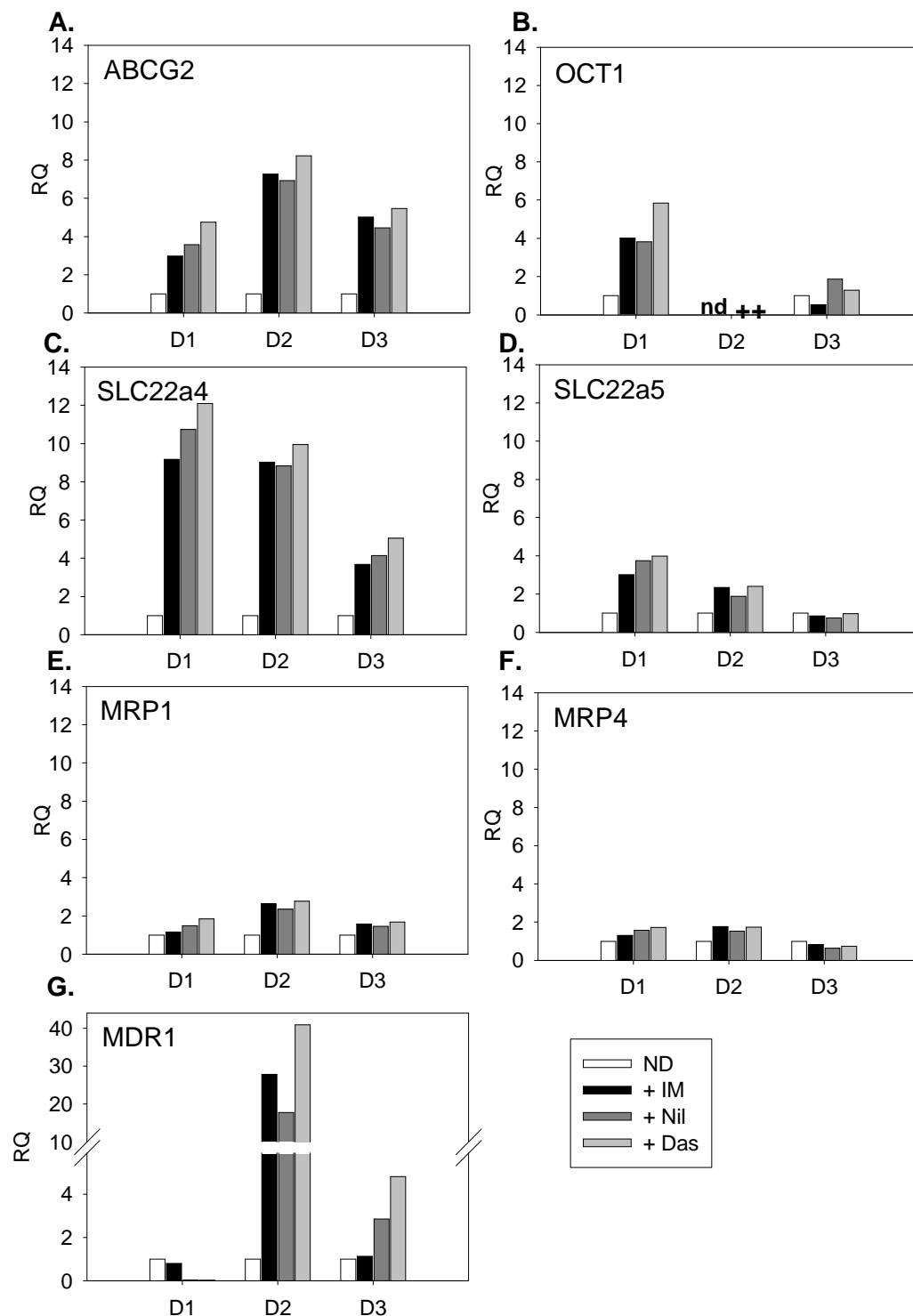
Figure 6-3 Relative expression of drug transporters in a K-WT cell line during treatment with TKIs.

The relative expression of *ABCG2* **(A)**, *OCT1* **(B)**, *SLC22a4* **(C)**, *SLC22a5* **(D)**, *MRP1* **(E)**, *MRP4* **(F)** and *MDR1* **(G)** in K-WT cell line treated with 5μM

IM (black fill), 5µM nilotinib (dark grey fill), or 150nM dasatinib (light grey fill), compared to no drug control (ND, white fill) at days 1, 2 and 3; n=1 in duplicate, nd=not detected, ++= signal. Figure **G** has a larger RQ scale compared to the other figures

The relative expression of *ABCG2* (Figure 6-3A) was increased in the presence of TKIs at day 1, 2 and day 3, with the maximal increase observed on day 2 compared to the control. Similarly, this trend was also observed with *MRP1* (Figure 6-3E), although the fold change in *MRP1* did not reach above 3 fold. In addition, there was maximal expression of *MDR1* at day 2 (Figure 6-3G), although, in contrast to the trend for *ABCG2* and *MRP1*, there was much lower relative expression of the treated arms compared to the untreated control at day 1.

The expression of *OCT1* (Figure 6-3B) was elevated at day 1 with active expression observed at day 2 with all three TKIs. However, at day 2 there was no expression of *OCT1* detected in the control group after 40 cycles, suggesting that either there was no expression or the expression was below the threshold of detection. Therefore, although *OCT1* was detected on day 2 in the presence of TKIs, the expression could not be quantified due to the absence in the untreated control. At day 3 the expression of *OCT1* was reduced compared to the control with IM and reduced to less than 2 fold higher with nilotinib and dasatinib. This suggested that the TKIs maintain increased *OCT1* expression in cells that may have very little or no expression otherwise.

This suggested that TKIs induced the expression of these drug transporters to varying degrees, with the maximal effect shown on day 2. It might be that this trend was related to cell death caused by the TKIs, which may affect the expression of these transporters. Also by cells dying that did not express the transporters you would get an apparent increase in expression in the remaining cells.

In contrast the greatest expression of *SLC22a4* (Figure 6-3C) and *SLC22a5* (Figure 6-3D) were shown on day 1, which was increasingly reduced at days 2 and 3. Indeed the expression of *SLC22a5* was similar to the control group by day 3. This suggested that the TKIs exert their maximal effect on these transporters earlier compared to transporters *ABCG2* and *MDR1* where the maximal effect was demonstrated on day 2. These transporters are present on the same chromosome and hence are co-regulated, which would support the similar trend.

In contrast to these transporters the expression of *MRP4* (Figure 6-3F) was elevated slightly on day 1 and 2, but did not reach greater than 2 fold, suggesting there was minimal effect by TKIs on this transporter.

The greatest elevation at each day was shown in the cells treated with dasatinib and indeed this trend was shown for every transporter with the exception of *OCT1*, suggesting that dasatinib had the most effect in modulating the regulation or expression of drug transporters.

6.4 Expression of drug transporters on CML and normal CD34$^+$ cells

In total, 11 CML CD34$^+$ samples were analysed and compared to 7 normal counterparts. In table 6-1, the values presented are of the crossing thresholds normalised to *GAPDH*.

Detector	Normal ΔCt		CML ΔCt		
	Mean	S.E.	Mean	S.E.	ΔΔCT
ABCG2	9.09	0.33	7.55	0.22	-1.54
MDR1	5.44	0.24	8.33	0.47	2.89
MRP1	4.70	0.39	4.81	0.35	0.11
MRP4	6.55	0.22	4.31	0.20	-2.24
SLC22a1 (OCT1)	nd	nd	nd	nd	nd
SLC22a2 (OCT2)	nd	nd	nd	nd	nd
SLC22a3 (OCT3	nd	nd	nd	nd	nd
SLC22a4 (OCTN1)	10.28	0.22	8.68	0.26	-1.60
SLC22a5 (OCTN2)	7.53	0.40	7.36	0.43	-0.17
SLC22a6 (OAT1)	nd	nd	nd	nd	nd
SLC22a7 (OAT2)	nd	nd	nd	nd	nd
SLC22a8 (OAT3)	nd	nd	nd	nd	nd
SLC22a9 (OAT4)	nd	nd	nd	nd	nd

Table 6-4 ΔCT values of drug transporters in CML and normal CD34^{+} with their corresponding ΔΔCT values

n=11 for CML, n=7 for normal, nd=not detected

In comparison to normal ΔCT values, CML samples demonstrated significantly higher levels of *ABCG2* (p<0.001), *MRP4* (p<0.0001) and *SLC22A4* (p<0.001) and significantly lower expression of *MDR1* (p=0.0028).

Using the RQ equation comparing the target CML sample against the calibrator sample (normal mPB), the difference in the drug transporters was calculated (Figure 6-4). The mRNA levels of A*BCG2*, *MRP4* and *SLC22A4* were 2.91 fold, 4.72 fold and 3.03 fold higher respectively in CML CD34^{+}. In contrast CML CD34^{+} cells had 7.42 fold less *MDR1* expression than the normal counterparts. There was no difference with either *MRP1* or *SLC22a5*.
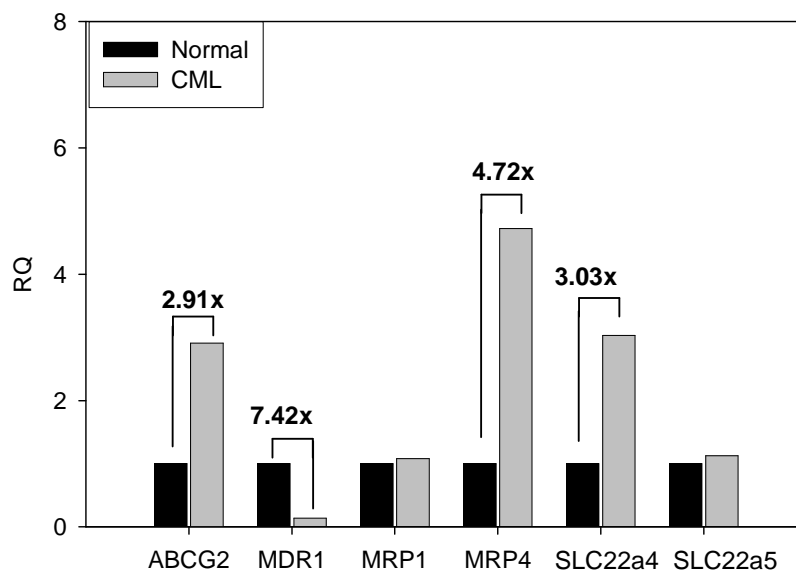
Figure 6-4 Relative expression of drug transporters in CML CD34$^+$

The relative expression of the drug transporters in CML CD34$^+$ (light grey) relative to normal (black) counterparts, n=11 for CML, n=7 for normal

In addition, 4 CML samples and 4 normal counterparts were also analysed on a separate TLDA card specific for another project. GAPDH was again used as the endogenous control (Table 6-5).

	Normal ΔCt		CML ΔCt		
Detector	**Mean**	**S.E.**	**Mean**	**S.E.**	**ΔΔCT**
ABCA1	7.97	0.32	11.33	0.66	3.36
ABCG1	6.1	0.13	9.67	0.48	3.57

Table 6-5 ΔCT values of drug transporters in CML and normal CD34$^+$ with their corresponding ΔΔCT value (second set)

n=4 for CML, n=4 for normal, nd=not detected

In comparison to normal ΔCT values, CML samples demonstrated significant lower levels of *ABCA1* and *ABCG1* (p<0.001), two additional transporters from the ABC family that mainly efflux cholesterol. Using the RQ equation comparing the target CML sample against the collaborator sample, the mRNA of *ABCA1* and *ABCG1* were 10.27 and 11.88 fold lower in CML cells.
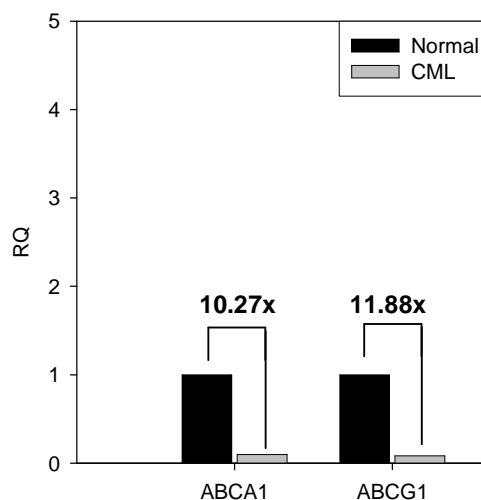
Table 6-6 Relative expression of drug transporters in CML CD34$^+$, (second set)

The relative expression of the drug transporters in CML CD34$^+$ (light grey) relative to normal (black) counterparts, n=4 for CML, n=4 for normal

6.5 Expression of drug transporters following treatment with TKI

Following expression analysis of drug transporters, CML CD34$^+$ cells were treated with 5µM IM for 72hrs in an attempt to identify the drug transporters that are modulated.

Significant differences of CT were observed with every drug transporter, however, significant differences of CT were also observed with the endogenous controls, which were not consistent, raising the possibility of technical issues. Further investigation of the quality of the RNA demonstrated significant degrading by 72hrs (Figure 6-5). Indeed, degradation was observed as early as 24hrs post culture even in the absence of TKI treatment, preventing comparative analysis. This may be due to the high levels of proteases and endonucleases in CML cells which will decrease the possibility of isolating good quality RNA from these cells.
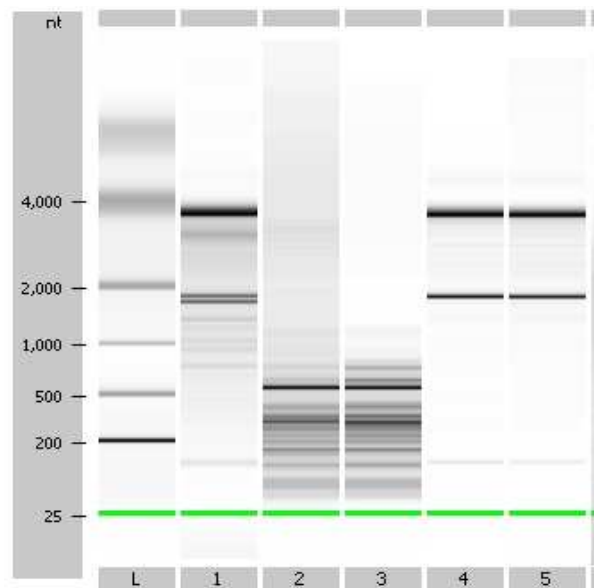
Figure 6-5 Agilent gel of RNA extracted from CML CD34^{+} cells ± IM treatment

L-Ladder, **1-** untreated CML CD34^{+} at day 0, **2-** untreated CML CD34^{+} at day 3, **3-** CML CD34^{+} cell treated with 5µM IM, **4-** K-WT, **5-** AML3.

6.6 Summary

This chapter demonstrated the expression of drug transporters in cell lines, CML CD34$^+$ and normal counterparts and attempted to investigate the expression following treatment with TKIs. Prior to any investigations however, the TLDA card was validated in our lab.

The cell lines used as models for optimisation in the previous chapters were then analysed. Surprisingly, when individual transporters were overexpressed, we observed modulation of not only the transduced gene but also other related transporters. Indeed the ΔCT of *ABCG2* was significantly lower (demonstrating higher expression) when either *MDR1* or *MRP1* were transduced, demonstrating >6 fold increased expression by the relative quantification calculation. Similarly, the overexpression of *MRP1* induced the endogenous expression of *MDR1*, which was either absent or below the level of detection in the wild-type cell line. This observation may be due to two possibilities. It may suggest that the induced expression of drug transporters in cell lines modulate the expression of other drug transporters, demonstrating a linkage between *ABCG2*, *MDR1* and *MRP1*, which are the clinically relevant efflux transporters in CML. Alternatively, the induced expression may be due to the presence of GFP, either directly acting as a substrate and hence inducing transporter activity, or indirectly inducing transporter expression via an unknown mechanism. In order to confirm whether GFP alone can induce the expression of transporters, the same K-WT cell line used to transduce the specific transporters should also be transduced with an empty vector containing only GFP to be tested as a control. Unfortunately, such a control was not available during this project and hence the cause of the modulation was not confirmed. These modulations however, do highlight the possible limitations of

relying on experiments directly comparing engineered cell lines to wild-type, and re-affirm the importance of using specific inhibitors that target only the gene in question.

The treatment of the wild-type K562 with IM, nilotinib or dasatinib demonstrated an effect on the drug transporters tested. Indeed, modulation was shown in all the drug transporters with at least a 3 fold increase compared to the no drug control group in all transporters except for *MRP4* during a 72hr period. Treatment with TKIs showed greatest modulation of *MDR1*, reaching >17 fold higher expression at 48hrs. These data suggest that the presence of the TKIs induce the cell to increase the expression of the drug transporters. This may be as a cellular defence mechanism as the role of transporters is to actively extrude foreign toxic compounds. However, these results are only based on one experiment and require several repeats for confirmation of these trends.

The expression of drug transporters in CML CD34^{+} cells was compared to normal counterparts. As detailed in the earlier chapters, there was a significant reduction of *MDR1* mRNA in the CML cells compared to the normal counterparts and similar expression of *MRP1* in both cohorts. In this population, the *ABCG2* expression was significantly elevated in CML cells (2.91 fold) compared to the normal counterparts. However the fold change was much lower than that detailed in chapter 3. The CD34^{+} cells in this cohort were handled in the same manner yet it includes a different set of patients, which may explain the variation.

The comparison of drug transporter expression in CML CD34^{+} cells following treatment with TKIs was not possible due to the problems faced in obtaining RNA of good quality. Even after 24hrs, the RNA extracted had significantly degraded.

The isolation of RNA was attempted with several kits, including Qiagen (Qiagen, Crawley, United Kingdom) and PARIS RNA isolation (Ambion, Austin, USA), but the problem persisted. This outcome was also faced by colleagues in a collaborative laboratory who also were unable to extract good quality RNA following IM treatment (personal communication), and other laboratories, suggesting that this may not be achievable.

7 Discussion

Although CML was probably first described as early as the nineteenth century, until recently there was little progress in understanding the biology of the disease, and hence the treatment options available were limited to either allogeneic transplantation, for a minority of patients, or a combination of IFNα and Ara-C; both of which were associated with risks and problems. However, the discovery of the Ph[+] chromosome in the 1960's (Rowley 1973) and realisation that the resulting *BCR-ABL* fusion gene was the molecular cause of disease in >95% of patients (Druker *et al.* 2001), presented the opportunity for molecularly targeted therapy. The first targeted small molecule drug IM was the result of this insight and dramatically altered the course of CML treatment. Following the success of Ph[+] tumour eradication in murine models, IM has been part of an ongoing multicentre phase III clinical trial (IRIS) designed to compare this agent to the previous best treatment of conventional IFNα and Ara-C. Within the first 18 months of the clinical trial, patients treated with IM demonstrated excellent cytogenetic responses and fewer patients progressed to more aggressive disease compared to conventional treatment (O'Brien *et al.* 2003). This resulted in the widespread use of IM for the initial treatment of CP CML and currently it is the first choice in patients, even for those who are eligible for transplantation. However, it is now becoming evident that only a few patients treated with IM achieve CMR, and another set of patients lose their initial cytogenetic and haematological response (Hochhaus *et al.* 2002; Hughes *et al.* 2003). The underlying reasons for this have not been resolved and are the topic of much debate (Figure 7-1).
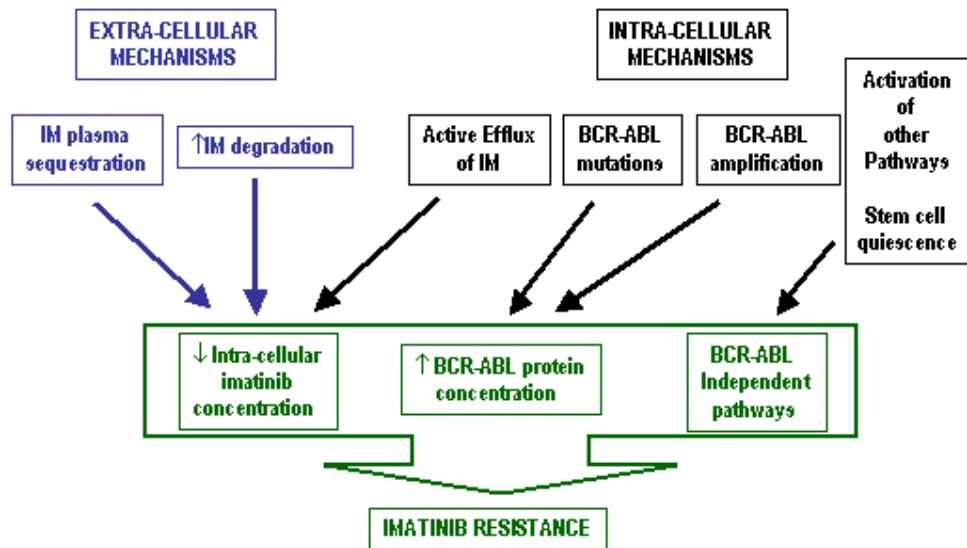
Figure 7-1 Mechanisms of resistance

One of the most described mechanisms of resistance observed in relapsed leukaemia patients is the development of point mutations within the kinase domain (Gorre *et al.* 2001). To date, there are approximately 50 different aa substitutions (Azam *et al.* 2003) described in IM resistant clinical samples and the emergence of these mutations generally confers a poor prognosis (Branford *et al.* 2003). Although these mutations have been shown to exist prior to IM therapy (Roche-Lestienne *et al.* 2002), it has been suggested that they offer no survival advantage until the cells are exposed to IM. In order to overcome such resistance, there has been the development of new generation agents that have successfully inhibited most of the kinase domain mutations and can bind to both the active and inactive conformations of BCR-ABL. However, the incidence of mutations as the underlying mechanism for resistance is uncertain. Some studies have detected a low level of BCR-ABL kinase mutations in CD34^{+} cells from patients both pre (Jiang *et al.*

2007a) and post IM treatment (Chu *et al.* 2005) however other studies have demonstrated no mutants in the resistant population *in vitro* (Copland *et al.* 2006).

BCR-ABL amplification has also been described as a resistance mechanism, as it may lead to increased mRNA and protein concentration. Amplified transcripts have been shown in Ph[+] BC cell lines and patients with advanced disease (Gorre *et al.* 2001). Furthermore, prolonged IM exposure has been shown to increase gene amplification (le Coutre *et al.* 2000). However, gene amplification has not previously been reported in early CP. Indeed, it has been reported that primitive CD34^{+} cells have higher transcript levels despite only having one copy of *BCR-ABL* (Copland *et al.* 2006; Jiang *et al.* 2007b). Therefore, it is possible that high protein level is still important, but not as a result of gene amplification.

Although many groups have described these mechanisms, resistance cannot be wholly attributed to gene mutations or amplifications, as IM does not eradicate all the leukaemic cells even in the best responders. Recently a small subpopulation of cells that remains resistant to IM has been detected; these qSC are resistant even at IM concentrations 10 fold higher than those achievable *in vivo* ((Holyoake *et al.* 1999; Graham *et al.* 2002). It has therefore been hypothesised that it is these primitive cells that are responsible for MRD and may form a pool of cells that can reactivate and cause disease relapse. Indeed, patients who stopped IM after achieving CMR relapsed rapidly (Cortes *et al.* 2004), demonstrating the existence of this population. Furthermore, *in vitro* studies have shown that these cells still persist with nilotinib treatment (Jorgensen *et al.* 2007a) and, although a little more responsive, persist in the presence of dasatinib (Copland *et al.* 2006).

In light of these qSC there have been 2 mathematical models proposed that discuss the potential ability of IM to eradicate CML cells, including this qSC population, which may then also be applied to the activity of other TKIs. Michor *et al* (Michor *et al.* 2005) suggest that although IM can reduce the proliferating and differentiating cells, it will not reduce the qSC population. This assumption is based on the initial biphasic decline in the *BCR-ABL* transcripts, whereby the initial rapid decline represents the death of the differentiated cells followed by the much slower decrease of the more primitive CML progenitors. Indeed the *BCR-ABL* transcripts rapidly increased in patients who discontinued IM therapy following CMR (Cortes *et al.* 2004; Mauro *et al.* 2004). Therefore, this model suggests that IM is unlikely to eradicate CML.

In contrast, the second hypothesis is based on the key assumption that stem cells will be recruited into cell cycle periodically (Roeder *et al.* 2006). When this occurs these cells will begin cycling and become sensitive to IM. Hence, over time, the qSC pool will be depleted, supporting the observation that levels of MRD continue to fall over prolonged periods of IM treatment (Branford *et al.* 2004). Thus, assuming no IM resistant clone arises, this model predicts that IM may eventually completely eradicate the leukaemic cells, although it is estimated it will take in excess of 20 years to achieve. They further propose however, that the IM effect may be accelerated using agents that induce cycling activity, producing a more efficient tumour load reduction.

Based upon the latter proposal, Jorgensen *et al* (Jorgensen *et al.* 2006) have investigated the effect of treating CML CD34^{+} cells with IM in combination with the growth factor G-CSF. A significant reduction of primitive CD434^{+} cells was observed following intermittent exposure to G-CSF compared to continuous

treatment of IM alone, which was further enhanced when the cells were treated with a combination of IM and intermittent G-CSF, supporting the above mathematical model. Indeed, the enhanced reduction of cells *in vitro* led to a multicentre clinical trial that further investigated the potential clinical use of growth factors in combination with IM to improve long-term outcomes in CP CML. However, no significant difference was observed in patients treated with the combination of G-CSF and IM compared to continuous IM alone, indicating no further benefit compared to standard IM treatment (Heaney 2007).

In addition, combinations of IM with other agents have been attempted to optimise established therapies, but with limited success. However, lonafarnib, a farnesyl transferase inhibitor (FTI), showed effects on the quiescent CD34$^+$ population in combination with IM (Jorgensen *et al.* 2005a) and as a single agent, lonafarnib improved treatment in a limited number of patients who failed IM (Borthakur *et al.* 2006).

However, for these models to succeed, optimal TKI plasma and intracellular concentrations are necessary. It has been suggested that suboptimal intracellular TKI concentration may contribute to drug resistance. Gambacorti *et al* suggested that excessive IM binding to plasma proteins might significantly alter the availability of active drug. Alpha-1 acid glycoprotein (AGP) is a hepatic acute phase protein that was shown to bind and inhibit IM (Gambacorti-Passerini *et al.* 2000), although another study did not support this finding and demonstrated that CML-derived AGP does not contribute to the leukaemic resistance (Jorgensen *et al.* 2002).

Alternatively, active efflux transporters may prevent optimal TKI concentrations being achieved in the cell. It is well established that ABC transporters are present on normal stem cells and their role is to extrude toxic substances. Furthermore, these transporters have been shown to efflux chemotherapeutic substrates and small molecule drugs, therefore it can be postulated that intracellular TKI concentrations are limited by active transport by this family of transporters. Indeed, until recently, an option for patients failing IM was to increase the dose. Although some found that this improved or reinstated the previous response, (Kantarjian *et al.* 2003; Zonder *et al.* 2003) this was not universal (Marin *et al.* 2003). This thesis has concentrated on the role of ABC proteins in mediating drug resistance, with the aim of further enhancing the TKI effect in the CML CD34$^+$ cell population and the IM resistant qSC.

7.1 Expression and function of drug transporters

In this study, we compared the expression of the most clinically relevant of these transporters and demonstrated that, at the mRNA level, *ABCG2* was significantly elevated in CML samples compared to normal counterparts, while *MDR1* was significantly reduced. This is in partial agreement with *Jiang et al* (Jiang *et al.* 2007b) who have reported elevated expression of both genes in leukaemic CD34$^+$ cells. However, the disparity in the results may be due to a number of factors that would render valid comparison of these two studies impossible. First and foremost, the choice of samples may influence the expression levels. Jiang *et al* examined only the specimens in which long-term culture initiating cells (LTC-ICs) were predominately Ph$^+$/BCR-ABL$^+$ and may therefore be preferentially selecting the samples with more aggressive CML. Secondly, it seems that all of the *Jiang et al* samples were subject to cell sorting into different populations by Hst and Py prior

to experimental analysis. Both stains are actively effluxed by the ABCG2 and MDR proteins (Goodell *et al.* 1996) thus this selection protocol may preferentially select the CD34+ cells with the more active transporters or induce their expression. Indeed, as demonstrated in chapter 6, the expression of drug transporters are often linked, hence the induced efflux by the use of substrate dyes of one transporter may also alter or induce the expression of another. In contrast, in our study we randomly selected a number of CML samples from the cell bank for investigation, which were then thawed and the RNA was immediately extracted for analysis. Hence, the cohort analysed in this project was selected in a different manner, without manipulation or subfractionation, other than CD34+ enriching by positive immunomagnetic selection. We consider that our data will therefore better reflect the baseline expression in standard CML CP CD34+ cells, as increased *MDR1* may be a sign of aggressive disease or sample manipulation. We would also suggest that caution should be employed in using substrate dyes for selection of samples to be used in transporter assays.

In addition we determined that the mRNA level of *MRP1* in CML CD34+ cells was similar to that in normal mPB CD34+ cells. The transcript levels of *MRP1* in CML CD34+ cells has not previously been reported by other groups, although Carter *et al* (Carter *et al.* 2001) have demonstrated equal mRNA transcripts in MNCs from healthy donors and CML patients. However, these populations had less than 3% CD34+ content so, again, a direct comparison cannot be made.

Further analysis confirmed that these drug transporters were also functional in these cells, suggesting that it is reasonable to propose that active efflux of TKIs from cells may take place and may have a role in drug resistance. Interestingly, the expression pattern of ABCG2 on these CML cells contrasted to that previously

observed in AML patient samples. In this study we observed that a greater proportion of the cell population had active ABCG2 expression rather than higher expression on a small subpopulation, suggesting that ABCG2 expression is not only restricted to the primitive CD34$^+$38$^-$ population as in normal cells (Figure 7-2).
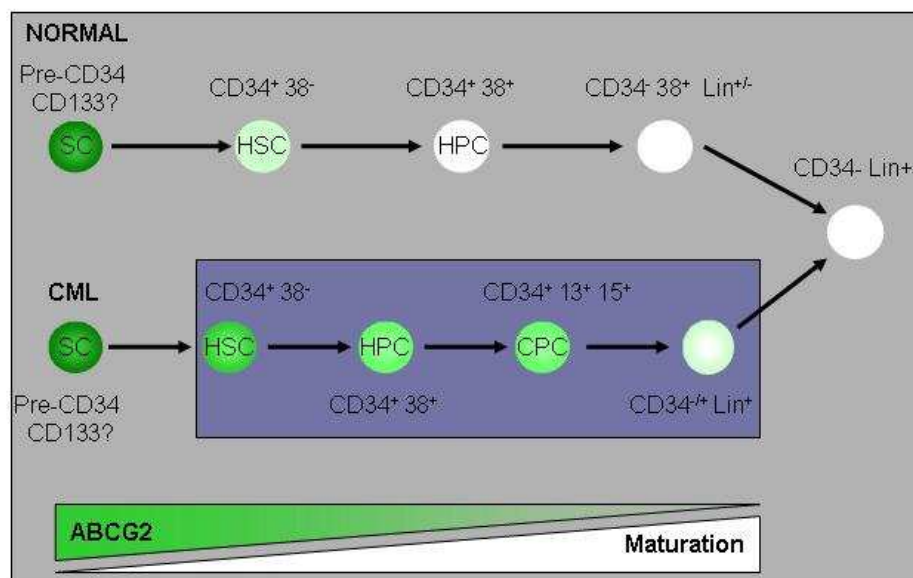
Figure 7-2 ABCG2 expression in normal and CML haemopoietic cells

ABCG2 is normally highly expressed in CD34$^+$38$^-$ HSC and switched off in the more maturing cell lineages. In CML we propose that the expression of ABCG2 may be found on the majority of the CD34$^+$ cells, suggesting a greater proportion have the active transport rather than a high expression level restricted to a small subpopulation; SC-multipotent stem cell/haemangioblast, HSC- haemopoietic stem cell, HPC-haemopoietic progenitor, CPC- CML progenitor. Green shading indicates ABCG2 expression levels.

Our observation that ABCG2 expression was also detected in the more mature CD34$^+$ cells suggests that the activity is regulated by BCR-ABL in the CML cells. Indeed, it has been shown that BCR-ABL phosphorylates the tyrosine kinase AKT (Mayerhofer et al. 2002) and that AKT also increases the translocation of ABCG2

(Mogi et al. 2003; Takada et al. 2005), supporting this hypothesis. In addition, the

activation of AKT induces HIF1α (Mayerhofer et al. 2002), which has also been

shown to up-regulate the expression of *ABCG2* mRNA (Mogi et al. 2003;

Krishnamurthy et al. 2004), suggesting that BCR-ABL driven AKT activity would

both upregulate *ABCG2* mRNA and increase translocation to the surface. More

recently, Nakanishi et al (Nakanishi et al. 2006) have confirmed this connection

and demonstrated that BCR-ABL enhances the expression of ABCG2 via

activation of the AKT pathway; although this work was carried out in cell lines, it

complements our data that ABCG2 is up-regulated in CML CD34^{+} cells (Figure

7-3).
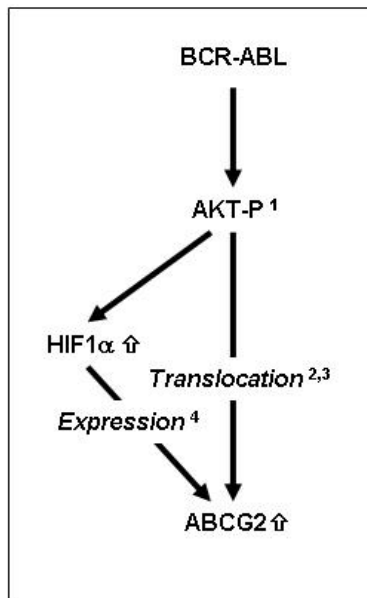
Figure 7-3 ABCG2 regulation by BCR-ABL activity

BCR-ABL phosphorylates the tyrosine kinase AKT, which in turn may increase the translocation of ABCG2. In addition, phosphorylated AKT may induce HIF1α, which in turn regulates *ABCG2* mRNA. 1. (Mayerhofer *et al.* 2002). 2. (Mogi *et al.* 2003). 3. (Takada *et al.* 2005), 4. (Krishnamurthy *et al.* 2004)

Furthermore, we can postulate that ABCG2 may be regulating the expression of the CD34 protein itself as inhibition of this transporter resulted in a reduction of proliferating CD34$^+$ cells by a mechanism other than apoptosis or maturation/differentiation. Indeed, over-expression of ABCG2 in HSC has been shown to result in an accumulation of CD34$^+$ cells (Krishnamurthy *et al.* 2004; Takada *et al.* 2005) and over-expression in human BM cells has resulted in an increase in proliferation of progenitor cells and myeloid engraftment in NOD/SCID mice (Ahmed 2005). If ABCG2 therefore does regulate CD34$^+$ expression, then it may further question whether all the CML cells that are ABCG2$^+$ and CD34$^+$ are immature or whether the expression of both these "stem cell" markers are aberrantly regulated by BCR-ABL. Indeed, some CML CD34$^+$ cells have been shown to have aberrant expression of other surface proteins such as CD56 (Lanza *et al.* 1993) and CD7 (Yong *et al.* 2006), so it may therefore not be unrealistic to postulate that BCR-ABL has an effect on the expression of such surface proteins. These suggestions could be confirmed using murine transplantation assays to investigate the reconstituting capacity and tumourgenicity of CML CD34$^+$ cells treated with FTC, an inhibitor of ABCG2, in comparison to control CML and normal cells.

7.2 Interaction of TKIs with drug transporters

7.2.1 Influx transporters

Having confirmed that the transporters are expressed and functional in these cells we aimed to further establish their role with regard to TKIs. There has been much debate as to the role of both influx and efflux transporters in limiting the intracellular concentration of IM and other TKIs. Several recent studies have

identified that the active transport of IM is dependent upon OCT1 (Thomas *et al.* 2004; White *et al.* 2006). Indeed, low activity of OCT1 has been identified as a cause of suboptimal clinical response to IM in CML patients (White *et al.* 2007), which may be overcome by increasing the IM dose. Surprisingly, nilotinib is not transported by OCT1, despite being highly structurally related to IM (White *et al.* 2006), therefore suggesting that there may be other transporters not yet identified that also play a role in TKI transport. Alternatively, the increased lipophilic nature of nilotinib compared to IM may also suggest that uptake may be a passive process (unpublished data).

However, there is controversy as to whether the baseline expression of *OCT1* prior to therapy correlates with disease progression. Wang *et al* (Wang *et al.* 2007) showed high baseline *OCT1* mRNA and demonstrated that expression of this transporter was a powerful indicator of CCR within 6 months. However, most of these patients had prior treatment or were in the late stages of CP. Similarly, Crossman *et al* (Crossman *et al.* 2005a) also demonstrated *OCT1* expression although their cohort also comprised of patients who had undergone prior therapy. In contrast, White *et al* (White *et al.* 2007) demonstrated that despite a correlation with *OCT1* mRNA and activity, the expression of *OCT1* alone is not itself a strong indicator of molecular response. The limiting factor of all these expression studies however, was that they were all examined in MNCs of PB or BM and Jiang *et al* (Jiang *et al.* 2007b) have previously shown that the expression differs in the cell populations, with the highest *OCT1* mRNA expression in the lin^+CD34^- subset. Therefore, the varying level of expression in the different lineages may conceal the correlation of *OCT1* expression and activity in the primitive progenitor population. We examined the expression of *OCT1* in $CD34^+$ cells from newly diagnosed CP patients prior to commencement of IM treatment, but demonstrated the level to be

below the threshold of detection. We have not monitored these patients during their treatment, but can say that due to the lack of expression of *OCT1* levels prior to onset of therapy in CP patients, this is unlikely to be a useful indicator of molecular response at onset of treatment. It is probable that the expression may develop with disease progression and/or it may be induced by therapy. Indeed, although only demonstrated once, we have shown that treatment with TKIs in K-WT cell lines induced the expression of *OCT1*. If this is confirmed with further testing, then induction of *OCT1* may prove to be a valuable prognostic tool in late CP patients and for disease monitoring rather than as a predictive tool prior to treatment commencement.

In addition to *OCT1*, there are many other influx transporters that may also mediate TKI transport. To date, the studies reported on influx transporters have been limited to *OCT1-3*. In our study, we also included other members of the *SLC22* family. Our data showed that the cation and carnitine transporters *SLC22A4* and *SLC22A5* (*OCTN1* and *OCTN2*) were also expressed on the primary CML CD34$^+$ cells, with 3 fold higher expression of SLC22a4 compared to expression levels on their normal counterparts. This suggests that they may have a role in TKI transport. Future studies of TKI uptake should be extended to include these transporters in addition to OCT1-3.

7.2.2 Efflux transporters

There have also been many reports investigating the interaction of efflux transporters with the current TKIs, but with strongly contrasting results. The interaction of IM with ABCG2 was first examined by Houghton *et al* (Houghton *et al.* 2004), who reported that IM is not a substrate but rather a potent inhibitor for

this transporter. However, shortly after, Burger *et al* (Burger *et al.* 2004) demonstrated that ABCG2 over-expressing cell lines were resistant to IM, concluding IM to be a substrate for ABCG2. This was supported by another report describing the active transport of IM across transepithelial layers of MDCKII cells that have been transfected with ABCG2 (Breedveld *et al.* 2005). However, there has been a recent study that has suggested the interaction between ABCG2 and IM is more complex and concentration dependent so IM may be both acting as an inhibitor and a substrate due to its high affinity for ABCG2 (Hegedus *et al.* 2002; Nakanishi *et al.* 2006; Shukla *et al.* 2007). At very low concentrations, IM behaves like a substrate, but becomes an inhibitor at high concentrations. Shukla *et al* (Shukla *et al.* 2007) have demonstrated that IM does not interact at the ATP binding site of ABCG2, but that it stimulates ATP hydrolysis, which is coupled with efflux function. However, IM can effectively inhibit the binding of a known ABCG2 substrate with an IC_{50} value of 0.47µM (Shukla *et al.* 2007) and another group has further reported that 0.8µM IM can effectively inhibit ABCG2-mediated Hst transport (Brendel *et al.* 2007). Therefore, the high affinity of IM for ABCG2, suggests that there is a narrow concentration range in which ABCG2 can transport IM, and that it can inhibit the protein at a higher concentration (Shukla *et al.* 2007). This may therefore explain why Burger *et al* observed active IM efflux when they used 200nM ^{14}C IM in their transport studies, where as Houghton *et al* confirmed inhibition with a higher IM concentration of 1µM.

Nevertheless, the observation that IM is a substrate at <0.8µM is not relevant in a clinical scenario as a standard 400mg once-daily administration of IM produces plasma cellular concentration ranging between 1.2µg/ml (2µM) at trough to 2.6µg/ml (4.8µM) at peak levels (Peng *et al.* 2005). Therefore, *in vivo*, the concentration of IM will be 2-3 fold higher than that required for ABCG2 inhibition,

even at trough levels. Also, it has been shown that the IM concentration is similar in plasma and BM (unpublished data), therefore, in compliant patients, IM will never be at a level at which active efflux will occur, but instead IM will inhibit this transporter.

Although these reports hint at the interaction of IM with ABCG2, the limitation of all these transport studies is that they have not been carried out in primary tumour cells, hence do not resemble *in vivo* conditions. Indeed, they have not even been performed in the correct cell lines that represent the clinical targets for IM - that is CML or gastro-intestinal stromal tumour (GIST) lines, but instead in cell lines engineered to over-express ABCG2. Furthermore, the interaction of IM with ABCG2 should be tested at a clinically relevant therapeutic concentration. In our studies, we investigated the interaction of IM with ABCG2 and initially established the assays in CML cell lines that had not previously been selected for drug resistance, which is closer to the situation found in clinical settings, and then confirmed all the findings in primitive CD34^{+} CML cells, harvested from newly diagnosed patients prior to therapy. We observed that, at 5µM, IM is an inhibitor of ABCG2, which is in agreement with the current view of the IM/ABCG2 interaction. In addition, we have performed HPLC analysis of IM levels in our laboratory on CML CD34^{+} cells and have observed no difference in cellular accumulation in the presence or absence of the specific ABCG2 inhibitor, FTC, confirming these findings (unpublished data).

However, with hindsight, the experimental procedure chosen to determine the interaction of TKIs with drug transporters could be criticised and might be improved by a different approach. We compared the cellular concentration of radiolabelled IM, in the presence and absence of the specific ABCG2 inhibitor

FTC, to determine whether IM is a substrate of ABCG2. The washed cells were then lysed and counted. With this experiment therefore, any residual radiolabelled drug that may have attached to the external surface of the cell membrane that may not have been washed off was also counted. It may therefore be suggested that any differences in the two treatments in terms of genuine intracellular levels may have been masked by excessive amounts of cell-bound IM, hence the similar cellular IM concentrations in the presence or absence of FTC. A more accurate analysis would require a HPLC measurement of the IM concentration in the cytoplasm derived from a membrane-free preparation of the cells. However, not only is this difficult, if not impossible to achieve with current laboratory techniques, but there is also every chance that the agents such as IM will be lost with the membrane.

However, our conclusion that IM is an inhibitor of ABCG2 at therapeutic concentration corresponds with the recent reports. Furthermore, we also tested the effect of drug transporter inhibition in the presence of IM and further confirmed no increase in apoptosis or in BCR-ABL inhibition. The activity of BCR-ABL cannot be directly measured, but may be assessed by detection of CrkL phosphorylation (Hamilton *et al.* 2006), either by flow cytometry or by Western blotting. Due to the low cell numbers available however, we were restricted to measuring by flow cytometry and although this has the advantage of separating and observing different subpopulations, recent comparative experiments carried out in our lab demonstrate that Western blotting is more sensitive. Therefore, small differences in BCR-ABL inhibition may have been present, but were not detected with the less sensitive flow technique. In addition, CrkL has also been suggested to be a substrate for SRC kinases (Qiao *et al.* 2006), therefore IM, which does not inhibit SRC kinase activity, will not achieve complete p-CrkL inhibition in cells in which

SRC kinase signalling is active. It may therefore be that a different indirect target for measuring BCR-ABL activity, or a few alternative methods to allow confirmation, may be preferable, such as inhibition of STAT5 phosphorylation.

Regardless of these potential weaknesses in our approach, our investigations demonstrated no further IM effect in the presence of FTC, using a range of methods and hence, in our opinion conclusively demonstrate that IM is an inhibitor of ABCG2 in primary CML CD34^{+} cells when used at therapeutic levels. Therefore, inhibiting ABCG2-mediated substrate efflux will not further enhance the cellular concentration of IM; hence, the increased expression of ABCG2 on CML cells compared to their normal counterparts is not relevant in the context of this drug.

A similar debate has been ongoing regarding the interaction of IM with MDR1. The over-expression of MDR1 in K562 cell lines resulted in increased IM resistance (Mahon *et al.* 2003) and a reduced intracellular drug concentration (Widmer *et al.* 2003). Indeed, RNAi mediated knockdown of MDR1 in IM-resistant CML cell lines has been shown to restore IM sensitivity (Rumpold *et al.* 2005). These data are consistent with other reports suggesting that IM is a substrate for MDR1 (Mukai *et al.* 2003; Illmer *et al.* 2004). However, in contrast, other groups have shown that over-expression of MDR1 in K562 cells does not confer resistance to IM (Ferrao *et al.* 2003). The recent study by Shukla *et al* (Shukla *et al.* 2007) though suggests that, like ABCG2, IM may interact with MDR1 as a substrate at low concentrations, but as an inhibitor at higher concentrations. Yet again, as with the reports with ABCG2, these studies were limited, as they have been performed in cell lines engineered to over-express MDR1, achieved by *in vitro* passaging of cells in progressively increasing doses of chemotherapeutic agents. In addition, the increased sensitivity of cells, in the presence of specific MDR1 inhibitors, may also

not be wholly attributed to enhanced intracellular concentrations of IM. Indeed, clinical trials that have administered PSC 833 (valspodar) as a MDR1 modulator have had to terminate early due to increased morbidity and mortality in the patients (Baer *et al.* 2002). We investigated the effect of PSC 833 in CML CD34^{+} cells alone *in vitro* and demonstrated that PSC 833 alone was profoundly anti-proliferative and caused significant apoptosis. Therefore, we can postulate that previous reports demonstrating increased overall kill by MDR1 inhibition with PSC 833 in combination with IM may not be due to increased IM effect, but either due to the inhibition of MDR1 leading to anti-proliferative effects or to off target toxicity. Surprisingly, PSC 833 as a single agent also demonstrated significant reduction in p-CrkL at 16hrs. This may reflect either the increased concentration of an endogenous substrate that has p-CrkL inhibitory activity, caused by blocking MDR1, or the direct inhibition of p-CrkL by PSC 833. However, as PSC 833 is a cyclosporin, we do not anticipate that it is the latter, although the underlying mechanism has not been resolved and will need further investigation.

In our studies we also investigated the interaction of IM with MDR1. In our studies, we demonstrated that IM was an inhibitor of MDR1 and although the combination with PSC 833 reduced total cell numbers, this did not appear to be due to an enhanced IM effect. Therefore, like ABCG2, the expression of MDR1 does not appear to mediate IM resistance in CML cells. This is in agreement with *in vitro* studies by Ferrao *et al* (Ferrao *et al.* 2003) and *in vivo* studies by Zong *et al*, who demonstrated that IM response in a CML murine model was not improved by inhibiting MDR1 (Zong *et al.* 2005). Indeed, they suggested one of the reasons leukaemia initiating cells were not sensitised to IM by loss of MDR1 might be due to the inhibitory effect of IM on this drug transporter. Furthermore, a previous clinical study reported no significant difference in MDR1 expression in BM cells

from patients who responded to IM compared to those that had not (Crossman *et al.* 2005b), and showed that low levels of *MDR1* gene expression in CML blast cells was not a predictor of response to IM (Lange *et al.* 2003).

For completeness, the interaction of IM with MRP1 was also investigated. Previously, Mukai *et al* had demonstrated that IM was not a substrate for MRP1 in cell lines (Mukai *et al.* 2003). We confirmed this finding and additionally demonstrated that IM is not an inhibitor of MRP1, nor does MRP1 modulation increase the IM effect i*n vitro*. The difference in interaction between the drug transporters and IM may be due to the mechanism of action of MRP1. In contrast to ABCG2 and MDR1, MRP1 cannot transport or interact with unmodified substrates, but requires them to be conjugated to glutathionine. It may therefore be that IM is not conjugated to glutathionine in these cells and hence is neither transported by, nor interacts with, MRP1.

The interaction of nilotinib with the drug transporters has previously been investigated, although to a much lesser extent than IM. A recent publication has demonstrated that, like IM, nilotinib was as effective as the known specific inhibitor FTC in preventing Hst transport by ABCG2 (Brendel *et al.* 2007). Indeed, nilotinib was more potent than IM and only 100nM was required for complete inhibition in mouse SP cells. This is in agreement with our results, which confirmed that at therapeutic concentrations, nilotinib is a potent inhibitor of ABCG2. In addition, Brendel *et al* observed that at very low molecular concentrations, nilotinib interacts at the substrate binding site of ABCG2 in K562 cell lines. This suggests that like IM, nilotinib may be a substrate at very low doses. However, as discussed with IM, these concentrations are considerably lower than those in compliant CML patients, with peak-trough levels of 3.6-1.7µM when treated with a standard twice-daily

dose of 400 mg (Kantarjian *et al.* 2007), therefore nilotinib concentrations will always be in the range that cause inhibition. We have also demonstrated that nilotinib is an inhibitor for MDR1 and MRP1 at therapeutic concentrations. This finding is in agreement with White *et al* (White *et al.* 2006), who also demonstrate that inhibition of MDR1 in MNCs from CP CML patients did not increase the intracellular nilotinib concentration.

Surprisingly, the addition of PSC 833 resulted in a reduction in the accumulation of ^{14}C-nilotinib. In support of this White and colleagues also reported unexpected results when treating CML cells with PSC 833 (White *et al.* 2006), with significant reduction in nilotinib uptake. It may suggest that PSC 833 is directly competing with nilotinib uptake, or down-regulating the nilotinib uptake mechanism. Alternatively, PSC 833 might be forming a complex with nilotinib, which in turn reduces the active transport into the cells.

As with IM, the effect of drug transporter inhibition in combination with nilotinib was investigated and resulted in no further cell kill or BCR-ABL inhibition. We can therefore conclude that the ABC transporters do not mediate resistance to IM or nilotinib in these primary CML CD34^{+} cells. Hence, in a clinical setting, the effect of IM or nilotinib cannot be further enhanced by the inhibition of these drug transporters.

In contrast to the Novartis agents above, there have been fewer studies of the Bristol-Myers Squibb agent dasatinib. Kamath *et al* (Kamath *et al.* 2007) have demonstrated that the absorption of dasatinib in MDR1 knock-out mice was no different compared to the wildtype, and that dasatinib did not alter the absorption or disposition of known MDR1 substrates, suggesting that dasatinib is neither a

substrate nor an inhibitor of MDR1. This is in agreement with our studies, which have also demonstrated that dasatinib is neither a substrate nor an inhibitor of this drug transporter.

However, Kamath *et al* (Kamath *et al.* 2007) did observe that dasatinib was actively effluxed from Caco-2 cells, suggesting that it may be a substrate for another efflux transporter. We investigated dasatinib further and observed that, in contrast to IM and nilotinib, dasatinib was a substrate for both ABCG2 and MRP1. These results are of great interest, as they would suggest that in clinical practice, the cellular concentration of dasatinib might be increased and the potency of this drug may be enhanced by blockade of these transporters. This is an attractive possibility and one that could efficiently be put into practice with specific inhibitors. There are now clinically safe drug transporter inhibitors such as Ko 143 for ABCG2, or alternatively a second TKI that inhibits the transporter, such as nilotinib or IM, could also be used. The use of the latter would then also provide a dual hit against BCR-ABL, although caution is also advisable in using these agents as transporter inhibitors in patients, as nilotinib has been associated with detrimental side effects, including QT prolongation, which may result in an increased risk of developing ventricular arrhythmias. Furthermore, the combination of two TKIs may lead to an increased antiproliferative effect (Copland *et al.* 2006; Jorgensen *et al.* 2007b), therefore, secondary usages may not be permitted.

However, before clinical application becomes feasible there are a number of questions that need to be addressed. Although dasatinib has been identified as a substrate for ABCG2 and MRP1, there is no confirmation that drug transporter blockade will increase BCR-ABL inhibition and cell kill. In this study, we tested the effect of drug transporter inhibition in the presence of dasatinib and surprisingly did

not observe any enhanced kill with either ABCG2 or MRP1 inhibition, and, more importantly, no further BCR-ABL inhibition or reduction in q34$^+$ cells.

The studies that were carried out only examined one transporter at a time though, and therefore it may be that a combination of inhibitors may alter the outcome. If the combination of inhibitors with dasatinib produced further BCR-ABL inhibition and reduced q34$^+$ cells, then it may provide a basis for increased effect.

However, caution must still be employed, as targeting these transporters will also have an effect on normal primitive progenitor cells. Indeed, the role of these drug transporters is to actively extrude toxic substances from essential sites such as the blood brain barrier and the kidney. If this role is inhibited in normal cells, and especially stem cells, then the effect may have disadvantageous consequences. It is reasonable to assume that there may be no short term problems with the inhibition of ABCG2, as *abcg2* null mice show normal haematological response with no developmental or observable organ defects (Zhou *et al.* 2002). However, it is not confirmed that ABCG2 functionality is not required for normal human stem cell function or whether the activity of this transporter is substituted by other transporters; a point that requires further investigation.

Furthermore, this hypothesis is reliant upon there being the only two transporters involved in dasatinib efflux. It is not improbable that as both ABCG2 and MRP1 actively efflux dasatinib, then there may be other, as yet, unidentified transporters that may also actively efflux the TKI, which would therefore still maintain a suboptimal intracellular concentration. Our expression studies identified *MRP4* mRNA to be significantly elevated in CML CD34$^+$ cells compared to their normal counterparts, and it is extremely likely there are other transporters present. Thus,

the concentration of dasatinib within the cell may still be suboptimal even with the combination of ABCG2 and MRP1 inhibitors. Our pilot data in chapter 6 may also indicate that dasatinib and other TKIs induce the expression of other transporters; hence we can speculate that the cell may still find a way to extrude these drugs. This is in agreement with Burger *et al* (Burger and Nooter 2004), who also observed induced mRNA and protein expression of *ABCG2* and *MDR1* in Caco2 cells when exposed to IM.

However, it may be revealed that, even if all the transporters that efflux dasatinib are identified and inhibited, and the intracellular concentration is further increased, the activity of BCR-ABL and cell kill may still not be reduced. It may be that, even with active efflux, the current cellular concentration of dasatinib is such that maximal inhibition of BCR-ABL is already achieved. Indeed, significant inhibition of CrkL phosphorylation is already achieved in primitive progenitor CD34^{+}38^{-} cells at the IC$_{50}$ dose of 10nM (Copland *et al.* 2006). Furthermore, we have recently treated 2 CML CD34^{+} samples with >1000nM dasatinib compared to 10nM dasatinib for 72 hrs and shown no measurable difference in p-CrkL inhibition, suggesting that even extreme doses still do not fully inhibit this pathway (unpublished data). Thus, the very low effective dose range of this agent suggests that a low cellular concentration will still have a strong inhibitory effect on BCR-ABL, with no further demonstrable effect at much higher doses. Therefore, as supported by our inhibition data from ABCG2/MRP1, further increasing the cellular concentration of dasatinib may not further enhance BCR-ABL inhibition after all.

An alternative explanation for the persistence of CML stem cells may be that TKI such as dasatinib do maximally inhibit BCR-ABL activity, but that the cells are no longer reliant upon BCR-ABL for survival. Indeed, the residual p-CrkL observed

may not be due to suboptimal inhibition, but may be residual normal p-CrkL levels which are not dependent on either BCR-ABL or SRC activity. In addition, it may be that the cells have acquired secondary genetic abnormalities that provide alternative pathways for proliferation. If this is the case even complete inhibition of BCR-ABL by TKI will never eradicate these cells. Indeed, despite the ability of dasatinib to target BCR-ABL cells deeper in to the stem cell compartment, the quiescent CML cells still appear to be intrinsically resistant to dasatinib (Copland *et al.* 2006). It may be suggested therefore that BCR-ABL has a minimal effect on the qSC population. Evidence for BCR-ABL independence has been demonstrated in a murine model, whereby inactivation of p190$^{BCR-ABL}$ did not rescue the malignant phenotype, suggesting that p190$^{BCR-ABL}$ is not required for disease maintenance (Perez-Caro *et al.* 2007) once initiated. It was hypothesised that other epigenetic changes or mutations in the LSCs may have rendered them insensitive to inactivation of p190$^{BCR-ABL}$. In contrast however, there have been other studies clearly demonstrating the requirement of BCR-ABL for disease maintenance and a recent study has demonstrated that dasatinib treatment achieved complete remission of Ph^{+} B-ALL in a murine model (Hu *et al.* 2006). Therefore to confirm whether CML SCs are oncogene dependent, studies are currently been undertaken to combine siRNA knockdown of BCR-ABL with dasatinib to completely inhibit the oncogenic protein.

7.3 Summary and future directions

Overall, based on these findings, there are avenues to continue this study to identify new drug transporters involved in active TKI transport. There is evidence that there will be other influx transporters in addition to OCT1 that mediate the intake of TKIs. However, it is unlikely that a suitable technique will be devised to

exploit this effect *in vivo,* as methods of increasing the expression and function of these transporters are not yet established. However, identifying which influx transporters are involved in the uptake of the TKIs may be utilised as prognostic tools to direct treatment by allowing the clinician to select the most suitable TKI and also monitoring for treatment response. In contrast, there is more scope to actively manipulate efflux transporters using specific inhibitors. The data presented here indicate that with the current drug transporters, the effect of the Novartis agents cannot be enhanced. However the cellular concentration of dasatinib can be increased and may, with a suitable combination of inhibitors, further inhibit BCR-ABL activity and increase overall cell kill. Hence a more comprehensive analysis of all the transporters in primitive CML cells would be of interest, which may then lead to combination studies with specific inhibitors and TKIs to maximise the cellular TKI concentration and determine whether resistance can be overcome. However, it is my opinion that even after identifying all the transporters that actively efflux TKIs and maximal BCR-ABL inhibition by these agents is achieved, the TKI effect will not be enhanced, nor will it prove to be a cure for CML. The evidence suggests to me that the resistance of progenitor and primitive cells is not the result of limiting intracellular concentration of dasatinib. This is certainly not the case for IM and nilotinib and yet disease still persists. I believe the primary direction for future therapy lies in conclusively confirming whether the cells are addicted to BCR-ABL as this will impact on the development of agents or protocols to combat this disease. If the qSC population are not oncogene dependent, then there will be a need to identify and develop agents that target other essential aspects of SC maintenance for effective eradication and cure.

One such novel agent that has shown promising results in CML is the farnesyl transferase inhibitor (FTI) BMS-214662. This agent has demonstrated favourable

activity in patients with acute leukaemias (Cortes *et al.* 2005) and preferentially targets the non-proliferating cells in tumour models (Rose *et al.* 2001). Copland *et al* (Copland *et al.* 2005) have demonstrated induction of apoptosis in both CD34$^+$38$^+$ progenitors and the more primitive CD34$^+$38$^-$ CP CML cells, including the quiescent population, with synergism when combined with TKIs. LTC-IC data has also demonstrated almost total ablation of CML SC and preferential cytotoxicity for these cells compared to their normal counterparts, demonstrating novel and potent activity in eliminating quiescent CML stem cells. Furthermore, BMS-214662 was equally cytotoxic in cell lines harbouring the mutant BCR-ABL with T315I kinase domain mutation (Copland *et al.* 2007), demonstrating superior activity to IM and nilotinib. However the mode of action of this novel agent is to date unknown. Elucidation of this mechanism is essential, as it will prove a useful tool for developing novel therapeutic strategies for targeting cancer stem cells.

An alternative novel approach to efficiently target the leukaemic SC may be by working in partnership with BCR-ABL. Instead of attempting to eradicate SC by actively inhibiting this oncogene itself, its presence in SC may be used as a marker to deliver an apoptotic agent that is only activated in a BCR-ABL cell. For example, this apoptotic agent may be delivered in two inactive halves that are completely harmless to normal cells. However, upon binding to BCR-ABL, the two separate halves may be brought in close proximity such that they may bind, causing activation and subsequent apoptosis only in the cell with the oncogene. This will therefore specifically target the tumour population, while avoiding the normal SC. Furthermore, this form of targeting will be effective regardless of whether the SC is found to be dependent or independent upon BCR-ABL activity, as this technique only requires the oncogene to be present. Indeed, such a mechanism for delivering an agent that can specifically target an oncogenic

marker will also prove to be useful in other cancers with a SC origin. Such technology is currently being developed in mitochondrial RNA (Ozawa *et al.* 2007; Valencia-Burton *et al.* 2007), but will prove extremely useful if it can be manipulated to target specific oncogenes such as BCR-ABL.

Overall, this thesis provides a comprehensive study of the current TKIs and their interaction with transporters. Although there have already been numerous studies on this interaction, the reports have been conflicting and the experiments carried out have been in unsuitable cell lines that have been engineered to over-express the transporter. This thesis has significantly improved upon the existing literature as the interaction of TKIs and transporters has been investigated in drug naïve primary CML CD34^{+} cells and tested at clinically relevant doses. Therefore, the results more closely reflect the true interaction of TKIs with these transporters and their effect on these cells. Furthermore, this thesis presents a promising lead for drug transporter modulation in combination with dasatinib for overcoming TKI resistance, although further testing is required. Finally, we can summarise with conviction that although ABC transporters are present and functional in CML CD34^{+} cells, blockade of these proteins by specific inhibitors do not increase IM and nilotinib accumulation or enhance their effect, providing evidence that resistance to these agents is not mediated by active drug efflux. More importantly, neither inhibitor was able to target the quiescent population, highlighting the importance of finding agents that specifically target the cancer stem cells. It is likely therefore, that future directions will most likely focus on understanding the biology of the CSC to identify other characteristics specific for the leukaemic cell and to develop agents with a different mechanism of action, or to develop novel approaches of delivering agents that specifically target the known oncogenic markers.

8 References

Abbott, B. L. (2003). "ABCG2 (BCRP) expression in normal and malignant hematopoietic cells." Hematol Oncol **21**(3): 115-30.

Abbott, B. L., A. M. Colapietro*, et al.* (2002). "Low levels of ABCG2 expression in adult AML blast samples." Blood **100**(13): 4594-601.

Abolhoda, A., A. E. Wilson*, et al.* (1999). "Rapid activation of MDR1 gene expression in human metastatic sarcoma after in vivo exposure to doxorubicin." Clin Cancer Res **5**(11): 3352-6.

Ahmed, F., Arseni, Natalia, Hiddemann, Wolfgang, Buske, Christian, Feuring-Buske, Michaela (2005). Constitutive Expression of the ABCG2 (BCRP), the Molecular Determinant of the Side Population, Increases the Proliferative Potential of Human Clonogenic Progenitors and Supports Human Myeloid Engraftment in the NOD/SCID Mouse Model. ASH Annual Meeting Abstracts.

Al-Hajj, M., M. S. Wicha*, et al.* (2003). "Prospective identification of tumorigenic breast cancer cells." Proc Natl Acad Sci U S A **100**(7): 3983-8.

Allikmets, R., L. M. Schriml*, et al.* (1998). "A human placenta-specific ATP-binding cassette gene (ABCP) on chromosome 4q22 that is involved in multidrug resistance." Cancer Res **58**(23): 5337-9.

Anderson, S. M. and J. Mladenovic (1996). "The BCR-ABL oncogene requires both kinase activity and src-homology 2 domain to induce cytokine secretion." Blood **87**(1): 238-44.

Antolin, I., H. Uria*, et al.* (1994). "Porphyrin accumulation in the harderian glands of female Syrian hamster results in mitochondrial damage and cell death." Anat Rec **239**(4): 349-59.

Atallah, E., M. Talpaz*, et al.* (2002). "Chronic myelogenous leukemia in T cell lymphoid blastic phase achieving durable complete cytogenetic and molecular remission with imatinib mesylate (STI571; Gleevec) therapy." Cancer **94**(11): 2996-9.

Azam, M., T. Raz*, et al.* (2003). "A screen to identify drug resistant variants to target-directed anti-cancer agents." Biol Proced Online **5**: 204-210.

Baer, M. R., S. L. George*, et al.* (2002). "Phase 3 study of the multidrug resistance modulator PSC-833 in previously untreated patients 60 years of age and older with acute myeloid leukemia: Cancer and Leukemia Group B Study 9720." Blood **100**(4): 1224-32.

Bates, S. E., R. Robey*, et al.* (2001). "The role of half-transporters in multidrug resistance." J Bioenerg Biomembr **33**(6): 503-11.

Bedi, A., B. A. Zehnbauer*, et al.* (1994). "Inhibition of apoptosis by BCR-ABL in chronic myeloid leukemia." Blood **83**(8): 2038-44.

Berenson, R. J., R. G. Andrews*, et al.* (1988). "Antigen CD34+ marrow cells engraft lethally irradiated baboons." J Clin Invest **81**(3): 951-5.

Bhatia, R., M. Holtz*, et al.* (2003). "Persistence of malignant hematopoietic progenitors in chronic myelogenous leukemia patients in complete cytogenetic remission following imatinib mesylate treatment." Blood **101**(12): 4701-7.

Biernaux, C., M. Loos*, et al.* (1995). "Detection of major bcr-abl gene expression at a very low level in blood cells of some healthy individuals." Blood **86**(8): 3118-22.

Bonnet, D. and J. E. Dick (1997). "Human acute myeloid leukemia is organized as a hierarchy that originates from a primitive hematopoietic cell." Nat Med **3**(7): 730-7.

Borthakur, G., H. Kantarjian, *et al.* (2006). "Pilot study of lonafarnib, a farnesyl transferase inhibitor, in patients with chronic myeloid leukemia in the chronic or accelerated phase that is resistant or refractory to imatinib therapy." Cancer **106**(2): 346-52.

Bose, S., M. Deininger, *et al.* (1998). "The presence of typical and atypical BCR-ABL fusion genes in leukocytes of normal individuals: biologic significance and implications for the assessment of minimal residual disease." Blood **92**(9): 3362-7.

Branford, S., Z. Rudzki, *et al.* (2004). "Real-time quantitative PCR analysis can be used as a primary screen to identify patients with CML treated with imatinib who have BCR-ABL kinase domain mutations." Blood **104**(9): 2926-32.

Branford, S., Z. Rudzki, *et al.* (2002). "High frequency of point mutations clustered within the adenosine triphosphate-binding region of BCR/ABL in patients with chronic myeloid leukemia or Ph-positive acute lymphoblastic leukemia who develop imatinib (STI571) resistance." Blood **99**(9): 3472-5.

Branford, S., Z. Rudzki, *et al.* (2003). "Detection of BCR-ABL mutations in patients with CML treated with imatinib is virtually always accompanied by clinical resistance, and mutations in the ATP phosphate-binding loop (P-loop) are associated with a poor prognosis." Blood **102**(1): 276-83.

Breedveld, P., D. Pluim, *et al.* (2005). "The effect of Bcrp1 (Abcg2) on the in vivo pharmacokinetics and brain penetration of imatinib mesylate (Gleevec): implications for the use of breast cancer resistance protein and P-glycoprotein inhibitors to enable the brain penetration of imatinib in patients." Cancer Res **65**(7): 2577-82.

Brendel, C., C. Scharenberg, *et al.* (2007). "Imatinib mesylate and nilotinib (AMN107) exhibit high-affinity interaction with ABCG2 on primitive hematopoietic stem cells." Leukemia **21**(6): 1267-75.

Burger, H. and K. Nooter (2004). "Pharmacokinetic Resistance to Imatinib Mesylate: Role of the ABC Drug Pumps ABCG2 (BCRP) and ABCB1 (MDR1) in the Oral Bioavailability of Imatinib." Cell Cycle **3**(12): 1502-5.

Burger, H., K. Nooter, *et al.* (1994). "Expression of the multidrug resistance-associated protein (MRP) in acute and chronic leukemias." Leukemia **8**(6): 990-7.

Burger, H., H. Van Tol, *et al.* (2004). "Imatinib mesylate (STI571) is a substrate for the breast cancer resistance protein (BCRP) / ABCG2 drug pump." Blood.

Carter, A., E. J. Dann, *et al.* (2001). "Cells from chronic myelogenous leukaemia patients at presentation exhibit multidrug resistance not mediated by either MDR1 or MRP1." Br J Haematol **114**(3): 581-90.

Chaudhary, P. M. and I. B. Roninson (1991). "Expression and activity of P-glycoprotein, a multidrug efflux pump, in human hematopoietic stem cells." Cell **66**(1): 85-94.

Chauncey, T. R., C. Rankin, *et al.* (2000). "A phase I study of induction chemotherapy for older patients with newly diagnosed acute myeloid leukemia (AML) using mitoxantrone, etoposide, and the MDR modulator PSC 833: a southwest oncology group study 9617." Leuk Res **24**(7): 567-74.

Choudhuri, S. and C. D. Klaassen (2006). "Structure, function, expression, genomic organization, and single nucleotide polymorphisms of human

ABCB1 (MDR1), ABCC (MRP), and ABCG2 (BCRP) efflux transporters." <u>Int J Toxicol</u> **25**(4): 231-59.

Chu, S., H. Xu*, et al.* (2005). "Detection of BCR-ABL kinase mutations in CD34+ cells from chronic myelogenous leukemia patients in complete cytogenetic remission on imatinib mesylate treatment." <u>Blood</u> **105**(5): 2093-8.

Clift, R. A. and C. Anasetti (1997). "Allografting for chronic myeloid leukaemia." <u>Baillieres Clin Haematol</u> **10**(2): 319-36.

Cole, S. P., G. Bhardwaj*, et al.* (1992). "Overexpression of a transporter gene in a multidrug-resistant human lung cancer cell line." <u>Science</u> **258**(5088): 1650-4.

Copland, M., A. Hamilton*, et al.* (2005). "BMS-214662 targets quiescent chronic myeloid leukaemia stem cells and enhances the activity of both imatinib and dasatinib (BMS-354825)." <u>Blood</u> **106**(11): 693.

Copland, M., A. Hamilton*, et al.* (2006). "Dasatinib (BMS-354825) targets an earlier progenitor population than imatinib in primary CML but does not eliminate the quiescent fraction." <u>Blood</u> **107**(11): 4532-9.

Copland, M., F. Pellicano*, et al.* (2007). "BMS-214662 potently induces apoptosis of chronic myeloid leukemia stem and progenitor cells and synergises with tyrosine kinase inhibitors." <u>Blood</u>.

Cortes, J., S. Faderl*, et al.* (2005). "Phase I study of BMS-214662, a farnesyl transferase inhibitor in patients with acute leukemias and high-risk myelodysplastic syndromes." <u>J Clin Oncol</u> **23**(12): 2805-12.

Cortes, J., S. O'Brien*, et al.* (2004). "Discontinuation of imatinib therapy after achieving a molecular response." <u>Blood</u> **104**(7): 2204-5.

Cozzio, A., E. Passegue*, et al.* (2003). "Similar MLL-associated leukemias arising from self-renewing stem cells and short-lived myeloid progenitors." <u>Genes Dev</u> **17**(24): 3029-35.

Crossman, L. C., B. J. Druker*, et al.* (2005a). "hOCT 1 and resistance to imatinib." <u>Blood</u> **106**(3): 1133-4; author reply 1134.

Crossman, L. C., M. Mori*, et al.* (2005b). "In chronic myeloid leukemia white cells from cytogenetic responders and non-responders to imatinib have very similar gene expression signatures." <u>Haematologica</u> **90**(4): 459-64.

Daley, G. Q., R. A. Van Etten*, et al.* (1990). "Induction of chronic myelogenous leukemia in mice by the P210bcr/abl gene of the Philadelphia chromosome." <u>Science</u> **247**(4944): 824-30.

Diekmann, D., S. Brill*, et al.* (1991). "Bcr encodes a GTPase-activating protein for p21rac." <u>Nature</u> **351**(6325): 400-2.

Donato, N. J., J. Y. Wu*, et al.* (2003). "BCR-ABL independence and LYN kinase overexpression in chronic myelogenous leukemia cells selected for resistance to STI571." <u>Blood</u> **101**(2): 690-8.

Donato, N. J., J. Y. Wu*, et al.* (2004). "Imatinib mesylate resistance through BCR-ABL independence in chronic myelogenous leukemia." <u>Cancer Res</u> **64**(2): 672-7.

Doyle, L. A., W. Yang*, et al.* (1998). "A multidrug resistance transporter from human MCF-7 breast cancer cells." <u>Proc Natl Acad Sci U S A</u> **95**(26): 15665-70.

Druker, B. (2001). "Signal transduction inhibition: results from phase I clinical trials in chronic myeloid leukemia." <u>Semin Hematol</u> **38**(3 Suppl 8): 9-14.

Druker, B. J., M. Talpaz*, et al.* (2001). "Efficacy and safety of a specific inhibitor of the BCR-ABL tyrosine kinase in chronic myeloid leukemia." <u>N Engl J Med</u> **344**(14): 1031-7.

Druker, B. J., S. Tamura*, et al.* (1996). "Effects of a selective inhibitor of the Abl tyrosine kinase on the growth of Bcr-Abl positive cells." <u>Nat Med</u> **2**(5): 561-6.

Evers, R., G. J. Zaman*, et al.* (1996). "Basolateral localization and export activity of the human multidrug resistance-associated protein in polarized pig kidney cells." <u>J Clin Invest</u> **97**(5): 1211-8.

Faderl, S., M. Talpaz*, et al.* (1999). "The biology of chronic myeloid leukemia." <u>N Engl J Med</u> **341**(3): 164-72.

Ferrao, P. T., M. J. Frost*, et al.* (2003). "Overexpression of P-glycoprotein in K562 cells does not confer resistance to the growth inhibitory effects of imatinib (STI571) in vitro." <u>Blood</u> **102**(13): 4499-503.

Filipits, M., R. W. Suchomel*, et al.* (1997). "Multidrug resistance-associated protein in acute myeloid leukemia: No impact on treatment outcome." <u>Clin Cancer Res</u> **3**(8): 1419-25.

Fu, J., Z. Chen*, et al.* (2000). "Expression of the human multidrug resistance gene mdr1 in leukemic cells and its application in studying P-glycoprotein antagonists." <u>Chin Med J (Engl)</u> **113**(3): 228-31.

Gambacorti-Passerini, C., R. Barni*, et al.* (2000). "Role of alpha1 acid glycoprotein in the in vivo resistance of human BCR-ABL(+) leukemic cells to the abl inhibitor STI571." <u>J Natl Cancer Inst</u> **92**(20): 1641-50.

Gambacorti-Passerini, C., P. le Coutre*, et al.* (1997). "Inhibition of the ABL kinase activity blocks the proliferation of BCR/ABL+ leukemic cells and induces apoptosis." <u>Blood Cells Mol Dis</u> **23**(3): 380-94.

Gekeler, V., W. Ise*, et al.* (1995). "The leukotriene LTD4 receptor antagonist MK571 specifically modulates MRP associated multidrug resistance." <u>Biochem Biophys Res Commun</u> **208**(1): 345-52.

Georges, E., G. Bradley*, et al.* (1990). "Detection of P-glycoprotein isoforms by gene-specific monoclonal antibodies." <u>Proc Natl Acad Sci U S A</u> **87**(1): 152-6.

Goga, A., J. McLaughlin*, et al.* (1995). "Alternative signals to RAS for hematopoietic transformation by the BCR-ABL oncogene." <u>Cell</u> **82**(6): 981-8.

Goodell, M. A., K. Brose*, et al.* (1996). "Isolation and functional properties of murine hematopoietic stem cells that are replicating in vivo." <u>J Exp Med</u> **183**(4): 1797-806.

Goodell, M. A., M. Rosenzweig*, et al.* (1997). "Dye efflux studies suggest that hematopoietic stem cells expressing low or undetectable levels of CD34 antigen exist in multiple species." <u>Nat Med</u> **3**(12): 1337-45.

Gorre, M. E., M. Mohammed*, et al.* (2001). "Clinical resistance to STI-571 cancer therapy caused by BCR-ABL gene mutation or amplification." <u>Science</u> **293**(5531): 876-80.

Gottesman, M. M. and S. V. Ambudkar (2001). "Overview: ABC transporters and human disease." <u>J Bioenerg Biomembr</u> **33**(6): 453-8.

Graham, S. M., H. G. Jorgensen*, et al.* (2002). "Primitive, quiescent, Philadelphia-positive stem cells from patients with chronic myeloid leukemia are insensitive to STI571 in vitro." <u>Blood</u> **99**(1): 319-25.

Gratwohl, A., J. Hermans*, et al.* (1998). "Risk assessment for patients with chronic myeloid leukaemia before allogeneic blood or marrow transplantation. Chronic Leukemia Working Party of the European Group for Blood and Marrow Transplantation." <u>Lancet</u> **352**(9134): 1087-92.

Greenberg, P. L., S. J. Lee*, et al.* (2004). "Mitoxantrone, etoposide, and cytarabine with or without valspodar in patients with relapsed or refractory acute

myeloid leukemia and high-risk myelodysplastic syndrome: a phase III trial (E2995)." J Clin Oncol **22**(6): 1078-86.

Guilhot, F., J. Apperley*, et al.* (2007). "Dasatinib induces significant hematologic and cytogenetic responses in patients with imatinib-resistant or -intolerant chronic myeloid leukemia in accelerated phase." Blood **109**(10): 4143-50.

Guilhot, F., C. Chastang*, et al.* (1997). "Interferon alfa-2b combined with cytarabine versus interferon alone in chronic myelogenous leukemia. French Chronic Myeloid Leukemia Study Group." N Engl J Med **337**(4): 223-9.

Hamilton, A., L. Elrick*, et al.* (2006). "BCR-ABL activity and its response to drugs can be determined in CD34+ CML stem cells by CrkL phosphorylation status using flow cytometry." Leukemia **20**(6): 1035-9.

Heaney, N., Drummond, Mark, Kaeda, Jaspal, Nicolini, Franck, Clark, Richard, Wilson, George, Shepherd, Pat, Tighe, Jane, McLintock, Lorna, Hughes, Timothy, Holyoake, Tessa L. (2007). A Phase 3 Pilot Study of Continuous Imatinib Versus Pulsed Imatinib with or without G-CSF in Patients with Chronic Phase CML Who Have Achieved a Complete Cytogenetic Response to Imatinib. ASH Annual Meeting.

Heaney, N. B. and T. L. Holyoake (2007). "Therapeutic targets in chronic myeloid leukaemia." Hematol Oncol **25**(2): 66-75.

Hegedus, T., L. Orfi*, et al.* (2002). "Interaction of tyrosine kinase inhibitors with the human multidrug transporter proteins, MDR1 and MRP1." Biochim Biophys Acta **1587**(2-3): 318-25.

Heinrich, M. C., D. J. Griffith*, et al.* (2000). "Inhibition of c-kit receptor tyrosine kinase activity by STI 571, a selective tyrosine kinase inhibitor." Blood **96**(3): 925-32.

Higgins, C. F. (1992). "ABC transporters: from microorganisms to man." Annu Rev Cell Biol **8**: 67-113.

Higgins, C. F. (1995). "The ABC of channel regulation." Cell **82**(5): 693-6.

Hipfner, D. R., S. D. Gauldie*, et al.* (1994). "Detection of the M(r) 190,000 multidrug resistance protein, MRP, with monoclonal antibodies." Cancer Res **54**(22): 5788-92.

Hochhaus, A., B. Druker*, et al.* (2007). "Favorable long-term follow-up results over six years for response, survival and safety with imatinib mesylate therapy in chronic phase chronic myeloid leukemia post failure of interferon-alpha treatment." Blood.

Hochhaus, A., S. Kreil*, et al.* (2002). "Molecular and chromosomal mechanisms of resistance to imatinib (STI571) therapy." Leukemia **16**(11): 2190-6.

Holyoake, T., X. Jiang*, et al.* (1999). "Isolation of a highly quiescent subpopulation of primitive leukemic cells in chronic myeloid leukemia." Blood **94**(6): 2056-64.

Horita, M., E. J. Andreu*, et al.* (2000). "Blockade of the Bcr-Abl kinase activity induces apoptosis of chronic myelogenous leukemia cells by suppressing signal transducer and activator of transcription 5-dependent expression of Bcl-xL." J Exp Med **191**(6): 977-84.

Houghton, P. J., G. S. Germain*, et al.* (2004). "Imatinib mesylate is a potent inhibitor of the ABCG2 (BCRP) transporter and reverses resistance to topotecan and SN-38 in vitro." Cancer Res **64**(7): 2333-7.

Hu, Y., S. Swerdlow*, et al.* (2006). "Targeting multiple kinase pathways in leukemic progenitors and stem cells is essential for improved treatment of Ph+ leukemia in mice." Proc Natl Acad Sci U S A **103**(45): 16870-5.

Hughes, T. and S. Branford (2003). "Molecular monitoring of chronic myeloid leukemia." Semin Hematol **40**(2 Suppl 2): 62-8.

Hughes, T. P., J. Kaeda, *et al.* (2003). "Frequency of major molecular responses to imatinib or interferon alfa plus cytarabine in newly diagnosed chronic myeloid leukemia." N Engl J Med **349**(15): 1423-32.

Huntly, B. J., H. Shigematsu, *et al.* (2004). "MOZ-TIF2, but not BCR-ABL, confers properties of leukemic stem cells to committed murine hematopoietic progenitors." Cancer Cell **6**(6): 587-96.

Illmer, T., M. Schaich, *et al.* (2004). "P-glycoprotein-mediated drug efflux is a resistance mechanism of chronic myelogenous leukemia cells to treatment with imatinib mesylate." Leukemia **18**(3): 401-8.

Jiang, X., A. Lopez, *et al.* (1999). "Autocrine production and action of IL-3 and granulocyte colony-stimulating factor in chronic myeloid leukemia." Proc Natl Acad Sci U S A **96**(22): 12804-9.

Jiang, X., E. Ng, *et al.* (2002). "Primitive interleukin 3 null hematopoietic cells transduced with BCR-ABL show accelerated loss after culture of factor-independence in vitro and leukemogenic activity in vivo." Blood **100**(10): 3731-40.

Jiang, X., K. M. Saw, *et al.* (2007a). "Instability of BCR-ABL gene in primary and cultured chronic myeloid leukemia stem cells." J Natl Cancer Inst **99**(9): 680-93.

Jiang, X., Y. Zhao, *et al.* (2007b). "Chronic myeloid leukemia stem cells possess multiple unique features of resistance to BCR-ABL targeted therapies." Leukemia.

Jonker, J. W., M. Buitelaar, *et al.* (2002). "The breast cancer resistance protein protects against a major chlorophyll-derived dietary phototoxin and protoporphyria." Proc Natl Acad Sci U S A **99**(24): 15649-54.

Jorgensen, H. G., E. K. Allan, *et al.* (2005a). "Lonafarnib reduces the resistance of primitive quiescent CML cells to imatinib mesylate in vitro." Leukemia.

Jorgensen, H. G., E. K. Allan, *et al.* (2007a). "Nilotinib exerts equipotent anti-proliferative effects to imatinib and does not induce apoptosis in CD34+ CML cells

10.1182/blood-2006-11-057521." Blood: blood-2006-11-057521.

Jorgensen, H. G., E. K. Allan, *et al.* (2007b). "Nilotinib exerts equipotent antiproliferative effects to imatinib and does not induce apoptosis in CD34+ CML cells." Blood **109**(9): 4016-9.

Jorgensen, H. G., E. K. Allan, *et al.* (2005b). "Enhanced CML stem cell elimination in vitro by bryostatin priming with imatinib mesylate." Exp Hematol **33**(10): 1140-6.

Jorgensen, H. G., M. Copland, *et al.* (2006). "Intermittent exposure of primitive quiescent chronic myeloid leukemia cells to granulocyte-colony stimulating factor in vitro promotes their elimination by imatinib mesylate." Clin Cancer Res **12**(2): 626-33.

Jorgensen, H. G., M. A. Elliott, *et al.* (2002). "Alpha1-acid glycoprotein expressed in the plasma of chronic myeloid leukemia patients does not mediate significant in vitro resistance to STI571." Blood **99**(2): 713-5.

Juliano, R. L. and V. Ling (1976). "A surface glycoprotein modulating drug permeability in Chinese hamster ovary cell mutants." Biochim Biophys Acta **455**(1): 152-62.

Kamath, A. V., J. Wang, *et al.* (2007). "Preclinical pharmacokinetics and in vitro metabolism of dasatinib (BMS-354825): a potent oral multi-targeted kinase inhibitor against SRC and BCR-ABL." Cancer Chemother Pharmacol.

Kantarjian, H., F. Giles*, et al.* (2006). "Nilotinib in imatinib-resistant CML and Philadelphia chromosome-positive ALL." N Engl J Med **354**(24): 2542-51.

Kantarjian, H. M., F. Giles*, et al.* (2007). "Nilotinib (formerly AMN107), a highly selective BCR-ABL tyrosine kinase inhibitor, is effective in patients with Philadelphia chromosome positive chronic myelogenous leukemia in chronic phase following imatinib resistance and intolerance." Blood **110**(10): 3540-6.

Kantarjian, H. M., M. Talpaz*, et al.* (2003). "Dose escalation of imatinib mesylate can overcome resistance to standard-dose therapy in patients with chronic myelogenous leukemia." Blood **101**(2): 473-5.

Kawabata, S., M. Oka*, et al.* (2001). "Breast cancer resistance protein directly confers SN-38 resistance of lung cancer cells." Biochem Biophys Res Commun **280**(5): 1216-23.

Kitazono, M., T. Sumizawa*, et al.* (1999). "Multidrug resistance and the lung resistance-related protein in human colon carcinoma SW-620 cells." J Natl Cancer Inst **91**(19): 1647-53.

Klejman, A., S. J. Schreiner*, et al.* (2002). "The Src family kinase Hck couples BCR/ABL to STAT5 activation in myeloid leukemia cells." Embo J **21**(21): 5766-74.

Komatani, H., H. Kotani*, et al.* (2001). "Identification of breast cancer resistant protein/mitoxantrone resistance/placenta-specific, ATP-binding cassette transporter as a transporter of NB-506 and J-107088, topoisomerase I inhibitors with an indolocarbazole structure." Cancer Res **61**(7): 2827-32.

Krishnamachary, N. and M. S. Center (1993). "The MRP gene associated with a non-P-glycoprotein multidrug resistance encodes a 190-kDa membrane bound glycoprotein." Cancer Res **53**(16): 3658-61.

Krishnamurthy, P., D. D. Ross*, et al.* (2004). "The stem cell marker Bcrp/ABCG2 enhances hypoxic cell survival through interactions with heme." J Biol Chem **279**(23): 24218-25.

Laneuville, P. (1995). "Abl tyrosine protein kinase." Semin Immunol **7**(4): 255-66.

Lange, T., C. Gunther*, et al.* (2003). "High levels of BAX, low levels of MRP-1, and high platelets are independent predictors of response to imatinib in myeloid blast crisis of CML." Blood **101**(6): 2152-5.

Lanza, F., S. Bi*, et al.* (1993). "Abnormal expression of N-CAM (CD56) adhesion molecule on myeloid and progenitor cells from chronic myeloid leukemia." Leukemia **7**(10): 1570-5.

le Coutre, P., L. Mologni*, et al.* (1999). "In vivo eradication of human BCR/ABL-positive leukemia cells with an ABL kinase inhibitor." J Natl Cancer Inst **91**(2): 163-8.

le Coutre, P., E. Tassi*, et al.* (2000). "Induction of resistance to the Abelson inhibitor STI571 in human leukemic cells through gene amplification." Blood **95**(5): 1758-66.

Lechner, A., C. A. Leech*, et al.* (2002). "Nestin-positive progenitor cells derived from adult human pancreatic islets of Langerhans contain side population (SP) cells defined by expression of the ABCG2 (BCRP1) ATP-binding cassette transporter." Biochem Biophys Res Commun **293**(2): 670-4.

Lee, E. J., S. L. George*, et al.* (1999). "Parallel phase I studies of daunorubicin given with cytarabine and etoposide with or without the multidrug resistance modulator PSC-833 in previously untreated patients 60 years of age or older with acute myeloid leukemia: results of cancer and leukemia group B study 9420." J Clin Oncol **17**(9): 2831-9.

Legrand, O., G. Simonin, *et al.* (1999). "Simultaneous activity of MRP1 and Pgp is correlated with in vitro resistance to daunorubicin and with in vivo resistance in adult acute myeloid leukemia." Blood **94**(3): 1046-56.

Leith, C. P., K. J. Kopecky, *et al.* (1999). "Frequency and clinical significance of the expression of the multidrug resistance proteins MDR1/P-glycoprotein, MRP1, and LRP in acute myeloid leukemia: a Southwest Oncology Group Study." Blood **94**(3): 1086-99.

Leith, C. P., K. J. Kopecky, *et al.* (1997). "Acute myeloid leukemia in the elderly: assessment of multidrug resistance (MDR1) and cytogenetics distinguishes biologic subgroups with remarkably distinct responses to standard chemotherapy. A Southwest Oncology Group study." Blood **89**(9): 3323-9.

Lion, T., A. Gaiger, *et al.* (1995). "Use of quantitative polymerase chain reaction to monitor residual disease in chronic myelogenous leukemia during treatment with interferon." Leukemia **9**(8): 1353-60.

Lombardo, L. J., F. Y. Lee, *et al.* (2004). "Discovery of N-(2-chloro-6-methyl-phenyl)-2-(6-(4-(2-hydroxyethyl)-   piperazin-1-yl)-2-methylpyrimidin-4-ylamino)thiazole-5-carboxamide (BMS-354825), a dual Src/Abl kinase inhibitor with potent antitumor activity in preclinical assays." J Med Chem **47**(27): 6658-61.

Ma, G., D. Lu, *et al.* (1997). "Bcr phosphorylated on tyrosine 177 binds Grb2." Oncogene **14**(19): 2367-72.

Maguer-Satta, V., S. Burl, *et al.* (1998). "BCR-ABL accelerates C2-ceramide-induced apoptosis." Oncogene **16**(2): 237-48.

Mahon, F. X., F. Belloc, *et al.* (2003). "MDR1 gene overexpression confers resistance to imatinib mesylate in leukemia cell line models." Blood **101**(6): 2368-73.

Mahon, F. X., M. W. Deininger, *et al.* (2000). "Selection and characterization of BCR-ABL positive cell lines with differential sensitivity to the tyrosine kinase inhibitor STI571: diverse mechanisms of resistance." Blood **96**(3): 1070-9.

Maliepaard, M., G. L. Scheffer, *et al.* (2001). "Subcellular localization and distribution of the breast cancer resistance protein transporter in normal human tissues." Cancer Res **61**(8): 3458-64.

Maliepaard, M., M. A. van Gastelen, *et al.* (1999). "Overexpression of the BCRP/MXR/ABCP gene in a topotecan-selected ovarian tumor cell line." Cancer Res **59**(18): 4559-63.

Manley, P. W., S. W. Cowan-Jacob, *et al.* (2002). "Imatinib: a selective tyrosine kinase inhibitor." Eur J Cancer **38 Suppl 5**: S19-27.

Manley, P. W., S. W. Cowan-Jacob, *et al.* (2005). "Advances in the structural biology, design and clinical development of Bcr-Abl kinase inhibitors for the treatment of chronic myeloid leukaemia." Biochim Biophys Acta **1754**(1-2): 3-13.

Marin, D., J. M. Goldman, *et al.* (2003). "Transient benefit only from increasing the imatinib dose in CML patients who do not achieve complete cytogenetic remissions on conventional doses." Blood **102**(7): 2702-3; author reply 2703-4.

Marley, S. B., J. L. Lewis, *et al.* (1996). "Evaluation of "discordant maturation' in chronic myeloid leukaemia using cultures of primitive progenitor cells and their production of clonogenic progeny (CFU-GM)." Br J Haematol **95**(2): 299-305.

Mauro, M. J., B. J. Druker, *et al.* (2004). "Divergent clinical outcome in two CML patients who discontinued imatinib therapy after achieving a molecular remission." Leuk Res **28 Suppl 1**: S71-3.

Mayerhofer, M., P. Valent, *et al.* (2002). "BCR/ABL induces expression of vascular endothelial growth factor and its transcriptional activator, hypoxia inducible factor-1alpha, through a pathway involving phosphoinositide 3-kinase and the mammalian target of rapamycin." Blood **100**(10): 3767-75.

Michor, F., T. P. Hughes, *et al.* (2005). "Dynamics of chronic myeloid leukaemia." Nature **435**(7046): 1267-70.

Miller, J. S., V. McCullar, *et al.* (1999). "Single adult human CD34(+)/Lin-/CD38(-) progenitors give rise to natural killer cells, B-lineage cells, dendritic cells, and myeloid cells." Blood **93**(1): 96-106.

Mogi, M., J. Yang, *et al.* (2003). "Akt signaling regulates side population cell phenotype via Bcrp1 translocation." J Biol Chem **278**(40): 39068-75.

Montaner, S., R. Perona, *et al.* (1998). "Multiple signalling pathways lead to the activation of the nuclear factor kappaB by the Rho family of GTPases." J Biol Chem **273**(21): 12779-85.

Morrison, S. J., A. M. Wandycz, *et al.* (1997). "Identification of a lineage of multipotent hematopoietic progenitors." Development **124**(10): 1929-39.

Mukai, M., X. F. Che, *et al.* (2003). "Reversal of the resistance to STI571 in human chronic myelogenous leukemia K562 cells." Cancer Sci **94**(6): 557-63.

Muller, M. C., N. Gattermann, *et al.* (2003). "Dynamics of BCR-ABL mRNA expression in first-line therapy of chronic myelogenous leukemia patients with imatinib or interferon alpha/ara-C." Leukemia **17**(12): 2392-400.

Musto, P., L. Melillo, *et al.* (1991). "High risk of early resistant relapse for leukaemic patients with presence of multidrug resistance associated P-glycoprotein positive cells in complete remission." Br J Haematol **77**(1): 50-3.

Nakanishi, T., K. Shiozawa, *et al.* (2006). "Complex interaction of BCRP/ABCG2 and imatinib in BCR-ABL-expressing cells: BCRP-mediated resistance to imatinib is attenuated by imatinib-induced reduction of BCRP expression." Blood **108**(2): 678-84.

Nam, S., D. Kim, *et al.* (2005). "Action of the Src family kinase inhibitor, dasatinib (BMS-354825), on human prostate cancer cells." Cancer Res **65**(20): 9185-9.

Ng, I. O., K. Y. Lam, *et al.* (1998). "Expression of P-glycoprotein, a multidrug-resistance gene product, is induced by radiotherapy in patients with oral squamous cell carcinoma." Cancer **83**(5): 851-7.

O'Brien, S. G., F. Guilhot, *et al.* (2003). "Imatinib compared with interferon and low-dose cytarabine for newly diagnosed chronic-phase chronic myeloid leukemia." N Engl J Med **348**(11): 994-1004.

Oda, T., C. Heaney, *et al.* (1994). "Crkl is the major tyrosine-phosphorylated protein in neutrophils from patients with chronic myelogenous leukemia." J Biol Chem **269**(37): 22925-8.

O'Hare, T., D. K. Walters, *et al.* (2005). "In vitro activity of Bcr-Abl inhibitors AMN107 and BMS-354825 against clinically relevant imatinib-resistant Abl kinase domain mutants." Cancer Res **65**(11): 4500-5.

Okuda, K., E. Weisberg, *et al.* (2001). "ARG tyrosine kinase activity is inhibited by STI571." Blood **97**(8): 2440-8.

Ottmann, O. G. and D. Hoelzer (2002). "The ABL tyrosine kinase inhibitor STI571 (Glivec) in Philadelphia positive acute lymphoblastic leukemia - promises, pitfalls and possibilities." Hematol J **3**(1): 2-6.

Ozawa, T., Y. Natori, *et al.* (2007). "Imaging dynamics of endogenous mitochondrial RNA in single living cells." Nat Methods **4**(5): 413-9.

Pendergast, A. M., L. A. Quilliam*, et al.* (1993). "BCR-ABL-induced oncogenesis is mediated by direct interaction with the SH2 domain of the GRB-2 adaptor protein." <u>Cell</u> **75**(1): 175-85.

Peng, B., P. Lloyd*, et al.* (2005). "Clinical pharmacokinetics of imatinib." <u>Clin Pharmacokinet</u> **44**(9): 879-94.

Perez-Caro, M., N. Gutierrez-Cianca*, et al.* (2007). "Sustained leukaemic phenotype after inactivation of BCR-ABLp190 in mice." <u>Oncogene</u> **26**(12): 1702-13.

Qiao, Y., H. Molina*, et al.* (2006). "Chemical rescue of a mutant enzyme in living cells." <u>Science</u> **311**(5765): 1293-7.

Raaijmakers, M. H., E. P. de Grouw*, et al.* (2006). "ABCB1 modulation does not circumvent drug extrusion from primitive leukemic progenitor cells and may preferentially target residual normal cells in acute myelogenous leukemia." <u>Clin Cancer Res</u> **12**(11 Pt 1): 3452-8.

Rao, V. V., J. L. Dahlheimer*, et al.* (1999). "Choroid plexus epithelial expression of MDR1 P glycoprotein and multidrug resistance-associated protein contribute to the blood-cerebrospinal-fluid drug-permeability barrier." <u>Proc Natl Acad Sci U S A</u> **96**(7): 3900-5.

Rappa, G., A. Lorico*, et al.* (1997a). "Evidence that the multidrug resistance protein (MRP) functions as a co-transporter of glutathione and natural product toxins." <u>Cancer Res</u> **57**(23): 5232-7.

Rappa, G., A. Lorico*, et al.* (1997b). "Overexpression of the multidrug resistance genes mdr1, mdr3, and mrp in L1210 leukemia cells resistant to inhibitors of ribonucleotide reductase." <u>Biochem Pharmacol</u> **54**(6): 649-55.

Robey, R. W., Y. Honjo*, et al.* (2001a). "A functional assay for detection of the mitoxantrone resistance protein, MXR (ABCG2)." <u>Biochim Biophys Acta</u> **1512**(2): 171-82.

Robey, R. W., W. Y. Medina-Perez*, et al.* (2001b). "Overexpression of the ATP-binding cassette half-transporter, ABCG2 (Mxr/BCrp/ABCP1), in flavopiridol-resistant human breast cancer cells." <u>Clin Cancer Res</u> **7**(1): 145-52.

Roche-Lestienne, C., V. Soenen-Cornu*, et al.* (2002). "Several types of mutations of the Abl gene can be found in chronic myeloid leukemia patients resistant to STI571, and they can pre-exist to the onset of treatment." <u>Blood</u> **100**(3): 1014-8.

Roeder, I., M. Horn*, et al.* (2006). "Dynamic modeling of imatinib-treated chronic myeloid leukemia: functional insights and clinical implications." <u>Nat Med</u> **12**(10): 1181-4.

Rose, W. C., F. Y. Lee*, et al.* (2001). "Preclinical antitumor activity of BMS-214662, a highly apoptotic and novel farnesyltransferase inhibitor." <u>Cancer Res</u> **61**(20): 7507-17.

Ross, D. D., J. E. Karp*, et al.* (2000). "Expression of breast cancer resistance protein in blast cells from patients with acute leukemia." <u>Blood</u> **96**(1): 365-8.

Ross, D. D., W. Yang*, et al.* (1999). "Atypical multidrug resistance: breast cancer resistance protein messenger RNA expression in mitoxantrone-selected cell lines." <u>J Natl Cancer Inst</u> **91**(5): 429-33.

Rowley, J. D. (1973). "Letter: A new consistent chromosomal abnormality in chronic myelogenous leukaemia identified by quinacrine fluorescence and Giemsa staining." <u>Nature</u> **243**(5405): 290-3.

Rumpold, H., A. M. Wolf*, et al.* (2005). "RNAi-mediated knockdown of P-glycoprotein using a transposon-based vector system durably restores

imatinib sensitivity in imatinib-resistant CML cell lines." <u>Exp Hematol</u> **33**(7): 767-75.

Sargent, J. M., C. J. Williamson*, et al.* (2001). "Breast cancer resistance protein expression and resistance to daunorubicin in blast cells from patients with acute myeloid leukaemia." <u>Br J Haematol</u> **115**(2): 257-62.

Sarkadi, B., C. Ozvegy-Laczka*, et al.* (2004). "ABCG2 -- a transporter for all seasons." <u>FEBS Lett</u> **567**(1): 116-20.

Sattler, M. and R. Salgia (1998). "Role of the adapter protein CRKL in signal transduction of normal hematopoietic and BCR/ABL-transformed cells." <u>Leukemia</u> **12**(5): 637-44.

Sattler, M., R. Salgia*, et al.* (1996). "The proto-oncogene product p120CBL and the adaptor proteins CRKL and c-CRK link c-ABL, p190BCR/ABL and p210BCR/ABL to the phosphatidylinositol-3' kinase pathway." <u>Oncogene</u> **12**(4): 839-46.

Sawyers, C. L. (1999). "Chronic myeloid leukemia." <u>N Engl J Med</u> **340**(17): 1330-40.

Sawyers, C. L., J. McLaughlin*, et al.* (1995). "Genetic requirement for Ras in the transformation of fibroblasts and hematopoietic cells by the Bcr-Abl oncogene." <u>J Exp Med</u> **181**(1): 307-13.

Schindler, T., W. Bornmann*, et al.* (2000). "Structural mechanism for STI-571 inhibition of abelson tyrosine kinase." <u>Science</u> **289**(5486): 1938-42.

Schittenhelm, M. M., S. Shiraga*, et al.* (2006). "Dasatinib (BMS-354825), a dual SRC/ABL kinase inhibitor, inhibits the kinase activity of wild-type, juxtamembrane, and activation loop mutant KIT isoforms associated with human malignancies." <u>Cancer Res</u> **66**(1): 473-81.

Schneider, E., K. H. Cowan*, et al.* (1995). "Increased expression of the multidrug resistance-associated protein gene in relapsed acute leukemia." <u>Blood</u> **85**(1): 186-93.

Shah, N. P., J. M. Nicoll*, et al.* (2002). "Multiple BCR-ABL kinase domain mutations confer polyclonal resistance to the tyrosine kinase inhibitor imatinib (STI571) in chronic phase and blast crisis chronic myeloid leukemia." <u>Cancer Cell</u> **2**(2): 117-25.

Shah, N. P., C. Tran*, et al.* (2004). "Overriding imatinib resistance with a novel ABL kinase inhibitor." <u>Science</u> **305**(5682): 399-401.

Shizuru, J. A., R. S. Negrin*, et al.* (2005). "Hematopoietic stem and progenitor cells: clinical and preclinical regeneration of the hematolymphoid system." <u>Annu Rev Med</u> **56**: 509-38.

Shukla, S., Z. E. Sauna*, et al.* (2007). "Evidence for the interaction of imatinib at the transport-substrate site(s) of the multidrug-resistance-linked ABC drug transporters ABCB1 (P-glycoprotein) and ABCG2." <u>Leukemia</u>.

Singh, S. K., C. Hawkins*, et al.* (2004). "Identification of human brain tumour initiating cells." <u>Nature</u> **432**(7015): 396-401.

Smit, J. W., M. T. Huisman*, et al.* (1999). "Absence or pharmacological blocking of placental P-glycoprotein profoundly increases fetal drug exposure." <u>J Clin Invest</u> **104**(10): 1441-7.

Smyth, M. J., E. Krasovskis*, et al.* (1998). "The drug efflux protein, P-glycoprotein, additionally protects drug-resistant tumor cells from multiple forms of caspase-dependent apoptosis." <u>Proc Natl Acad Sci U S A</u> **95**(12): 7024-9.

Southgate, T. D., E. Garside*, et al.* (2006). "Dual agent chemoprotection by retroviral co-expression of either MDR1 or MRP1 with the P140K mutant of O6-methylguanine-DNA-methyl transferase." <u>J Gene Med</u> **8**(8): 972-9.

Steinbach, D., W. Sell, *et al.* (2002). "BCRP gene expression is associated with a poor response to remission induction therapy in childhood acute myeloid leukemia." <u>Leukemia</u> **16**(8): 1443-7.

Strife, A., C. Lambek, *et al.* (1988). "Discordant maturation as the primary biological defect in chronic myelogenous leukemia." <u>Cancer Res</u> **48**(4): 1035-41.

Suvannasankha, A., H. Minderman, *et al.* (2004). "Breast cancer resistance protein (BCRP/MXR/ABCG2) in acute myeloid leukemia: discordance between expression and function." <u>Leukemia</u> **18**(7): 1252-7.

Takada, T., H. Suzuki, *et al.* (2005). "Regulation of the cell surface expression of human BCRP/ABCG2 by the phosphorylation state of Akt in polarized cells." <u>Drug Metab Dispos</u> **33**(7): 905-9.

Talpaz, M., H. M. Kantarjian, *et al.* (1986). "Hematologic remission and cytogenetic improvement induced by recombinant human interferon alpha A in chronic myelogenous leukemia." <u>N Engl J Med</u> **314**(17): 1065-9.

Talpaz, M., N. P. Shah, *et al.* (2006). "Dasatinib in imatinib-resistant Philadelphia chromosome-positive leukemias." <u>N Engl J Med</u> **354**(24): 2531-41.

Talpaz, M., R. T. Silver, *et al.* (2002). "Imatinib induces durable hematologic and cytogenetic responses in patients with accelerated phase chronic myeloid leukemia: results of a phase 2 study." <u>Blood</u> **99**(6): 1928-37.

Tan, B., D. Piwnica-Worms, *et al.* (2000). "Multidrug resistance transporters and modulation." <u>Curr Opin Oncol</u> **12**(5): 450-8.

Thomas, J., L. Wang, *et al.* (2004). "Active transport of imatinib into and out of cells: implications for drug resistance." <u>Blood</u> **104**(12): 3739-45.

Trock, B. J., F. Leonessa, *et al.* (1997). "Multidrug resistance in breast cancer: a meta-analysis of MDR1/gp170 expression and its possible functional significance." <u>J Natl Cancer Inst</u> **89**(13): 917-31.

Valencia-Burton, M., R. M. McCullough, *et al.* (2007). "RNA visualization in live bacterial cells using fluorescent protein complementation." <u>Nat Methods</u> **4**(5): 421-7.

van den Heuvel-Eibrink, M. M., E. A. Wiemer, *et al.* (2002). "Increased expression of the breast cancer resistance protein (BCRP) in relapsed or refractory acute myeloid leukemia (AML)." <u>Leukemia</u> **16**(5): 833-9.

van der Holt, B., B. Lowenberg, *et al.* (2005). "The value of the MDR1 reversal agent PSC-833 in addition to daunorubicin and cytarabine in the treatment of elderly patients with previously untreated acute myeloid leukemia (AML), in relation to MDR1 status at diagnosis." <u>Blood</u> **106**(8): 2646-54.

van der Kolk, D. M., E. Vellenga, *et al.* (2002). "Expression and activity of breast cancer resistance protein (BCRP) in de novo and relapsed acute myeloid leukemia." <u>Blood</u> **99**(10): 3763-70.

van der Pol, M. A., H. J. Broxterman, *et al.* (2003). "Function of the ABC transporters, P-glycoprotein, multidrug resistance protein and breast cancer resistance protein, in minimal residual disease in acute myeloid leukemia." <u>Haematologica</u> **88**(2): 134-47.

van der Zee, A. G., H. Hollema, *et al.* (1995). "Value of P-glycoprotein, glutathione S-transferase pi, c-erbB-2, and p53 as prognostic factors in ovarian carcinomas." <u>J Clin Oncol</u> **13**(1): 70-8.

Van Etten, R. A. (1999). "Cycling, stressed-out and nervous: cellular functions of c-Abl." <u>Trends Cell Biol</u> **9**(5): 179-86.

Wang, J. C., M. Doedens, *et al.* (1997). "Primitive human hematopoietic cells are enriched in cord blood compared with adult bone marrow or mobilized

peripheral blood as measured by the quantitative in vivo SCID-repopulating cell assay." <u>Blood</u> **89**(11): 3919-24.

Wang, L., A. Giannoudis, *et al.* (2007). "Expression of the Uptake Drug Transporter hOCT1 is an Important Clinical Determinant of the Response to Imatinib in Chronic Myeloid Leukemia." <u>Clin Pharmacol Ther</u>.

Weissman, I. L. (2000). "Stem cells: units of development, units of regeneration, and units in evolution." <u>Cell</u> **100**(1): 157-68.

White, D. L., V. A. Saunders, *et al.* (2007). "Most CML patients who have a suboptimal response to imatinib have low OCT-1 activity: higher doses of imatinib may overcome the negative impact of low OCT-1 activity." <u>Blood</u> **110**(12): 4064-72.

White, D. L., V. A. Saunders, *et al.* (2006). "OCT-1-mediated influx is a key determinant of the intracellular uptake of imatinib but not nilotinib (AMN107): reduced OCT-1 activity is the cause of low in vitro sensitivity to imatinib." <u>Blood</u> **108**(2): 697-704.

Widmer, N., S. Colombo, *et al.* (2003). "Functional consequence of MDR1 expression on imatinib intracellular concentrations." <u>Blood</u> **102**(3): 1142.

Wijnholds, J., R. Evers, *et al.* (1997). "Increased sensitivity to anticancer drugs and decreased inflammatory response in mice lacking the multidrug resistance-associated protein." <u>Nat Med</u> **3**(11): 1275-9.

Yanovich, S. and R. N. Taub (1983). "Differences in daunomycin retention in sensitive and resistant P388 leukemic cells as determined by digitized video fluorescence microscopy." <u>Cancer Res</u> **43**(9): 4167-71.

Yong, A. S., R. M. Szydlo, *et al.* (2006). "Molecular profiling of CD34+ cells identifies low expression of CD7, along with high expression of proteinase 3 or elastase, as predictors of longer survival in patients with CML." <u>Blood</u> **107**(1): 205-12.

Yuen, A. R. and B. I. Sikic (1994). "Multidrug resistance in lymphomas." <u>J Clin Oncol</u> **12**(11): 2453-9.

Zhang, X. and R. Ren (1998). "Bcr-Abl efficiently induces a myeloproliferative disease and production of excess interleukin-3 and granulocyte-macrophage colony-stimulating factor in mice: a novel model for chronic myelogenous leukemia." <u>Blood</u> **92**(10): 3829-40.

Zhou, D. C., J. P. Marie, *et al.* (1992). "Relevance of mdr1 gene expression in acute myeloid leukemia and comparison of different diagnostic methods." <u>Leukemia</u> **6**(9): 879-85.

Zhou, D. C., R. Zittoun, *et al.* (1995). "Expression of multidrug resistance-associated protein (MRP) and multidrug resistance (MDR1) genes in acute myeloid leukemia." <u>Leukemia</u> **9**(10): 1661-6.

Zhou, S., J. J. Morris, *et al.* (2002). "Bcrp1 gene expression is required for normal numbers of side population stem cells in mice, and confers relative protection to mitoxantrone in hematopoietic cells in vivo." <u>Proc Natl Acad Sci U S A</u> **99**(19): 12339-44.

Zhou, S., J. D. Schuetz, *et al.* (2001). "The ABC transporter Bcrp1/ABCG2 is expressed in a wide variety of stem cells and is a molecular determinant of the side-population phenotype." <u>Nat Med</u> **7**(9): 1028-34.

Zhou, S., Y. Zong, *et al.* (2003). "Hematopoietic cells from mice that are deficient in both Bcrp1/Abcg2 and Mdr1a/1b develop normally but are sensitized to mitoxantrone." <u>Biotechniques</u> **35**(6): 1248-52.

Zonder, J. A., P. Pemberton, *et al.* (2003). "The effect of dose increase of imatinib mesylate in patients with chronic or accelerated phase chronic

myelogenous leukemia with inadequate hematologic or cytogenetic response to initial treatment." <u>Clin Cancer Res</u> **9**(6): 2092-7.

Zong, Y., S. Zhou*, et al.* (2005). "Loss of P-glycoprotein expression in hematopoietic stem cells does not improve responses to imatinib in a murine model of chronic myelogenous leukemia." <u>Leukemia</u> **19**(9): 1590-6.